KU LEUVEN

DOCTORAL SCHOOL OF BIOMEDICAL SCIENCES
Faculty of Medicine

Primary Progressive Aphasia: a language disorder studied at the behavioral, structural and molecular imaging level

Jolien Schaeverbeke

Supervisor:
Prof. dr. Rik Vandenberghe
(promotor)

Dissertation presented in partial fulfillment of the requirements for the degree of Doctor in Biomedical Sciences

19^{th} of December 2017

KU Leuven
Biomedical Sciences Group
Faculty of Medicine
Department of Neurosciences

KU LEUVEN
DOCTORAL SCHOOL
BIOMEDICAL SCIENCES

Primary Progressive Aphasia: a language disorder studied at the behavioral, structural and molecular imaging level

Jolien SCHAEVERBEKE

Examination committee:
Prof. dr. Peter Janssen, chair
Prof. dr. Rik Vandenberghe, supervisor (promotor)
Prof. dr. Mathieu Vandenbulcke
Prof. dr. Wim Van Paesschen
Prof. dr. Jason Warren (UK)
Dr. Tim Van Langenhove (UGent)

Dissertation presented in partial fulfillment of the requirements for the degree of Doctor in Biomedical Sciences

19^{th} of December 2017

© 2017 KU Leuven – Faculty of Medicine
Uitgegeven in eigen beheer, Jolien Schaeverbeke, Herestraat 49, ON-2, box 1027, 3000 Leuven, Belgium (Belgium)

Alle rechten voorbehouden. Niets uit deze uitgave mag worden vermenigvuldigd en/of openbaar gemaakt worden door middel van druk, fotokopie, microfilm, elektronisch of op welke andere wijze ook zonder voorafgaande schriftelijke toestemming van de uitgever.

All rights reserved. No part of the publication may be reproduced in any form by print, photoprint, microfilm, electronic or any other means without written permission from the publisher.

Abstract

Following the first description of a case series of patients with a 'language-predominant' dementia syndrome by Marsel Mesulam in 1982, the term primary progressive aphasia (PPA) was coined. The *primary* symptom of PPA is the loss of language, which is *progressive* in nature.
As of 2011, three clinical subtypes within the spectrum of PPA are internationally recognized: a nonfluent/agrammatic (NFV), a semantic (SV) and a logopenic variant (LV). Of the LV cases, 50-60% have underlying Alzheimer's disease (AD) pathology. In 50-88% of NFV cases the underlying cause is frontotemporal lobar degeneration (FTLD)-tauopathy (i.e. corticobasal degeneration (CBD), progressive supranuclear palsy (PSP) or Pick's disease pathology) and 69-83% of SV cases have FTLD-Transactive response DNA binding Protein 43 kDa (TDP-43) type C pathology as underlying cause. Despite gradually increasing knowledge, the pathophysiology of PPA remains still poorly understood. The general aim of this thesis was to study pathophysiological mechanisms underlying PPA at a behavioral, structural and molecular imaging level.

Using non-linguistic, acoustic stimuli devoid of meaning, we demonstrated that a subset of PPA patients were impaired in key domains of nonverbal core auditory processing. Patients with NFV PPA had the most marked deficits within the time/rhythm domain for the processing of short sequences of up to seven tones. A subset of the SV patients were also impaired, though less severely. Patients with LV PPA did not show any significant individual impairments. Our sound perception data allowed reliable discrimination of NFV from LV cases even though these contained no language stimuli and were purely based on perceptual judgment of pitch and rhythm in tone sequences. We also demonstrated that performance on a subset of the psychoacoustic tests correlated with conventional verbal repetition tests. Rhythm and time processing deficits

in NFV PPA relied on right-hemispheric brain structures including the frontal operculum and posterior insula. We postulate that auditory timing pathways are altered in NFV PPA, which are used in common for processing acoustic sequence structure in both speech output and acoustic input. The perceptual timing deficits may contribute to the speech apraxia in NFV which is characterized by abnormal duration of inter-segmental time intervals of speech among other features.

A subset of NFV PPA patients have single-word comprehension problems besides motor speech problems and/or agrammatism. These patients are considered as the fourth 'mixed' variant (MV) of PPA. Based on imaging results reported in the current thesis, MV PPA showed a tau PET pattern, measured by [^{18}F]-THK5351, which is highly similar to that observed in patients with NFV without single-word comprehension deficits (NFV-pure), namely increased [^{18}F]-THK5351 binding in the premotor cortex and supplementary motor area. The topography of [^{18}F]-THK5351 binding, but not the degree of atrophy was correlated with core clinical features of MV PPA. In MV, the atrophy pattern was more widespread and patients had a higher likelihood of underlying Alzheimer's disease pathology compared to NFV-pure PPA.

Next, we investigated in a series of PPA patients whether basal forebrain (BF) volume loss relates to cholinergic depletion and how this depends on the PPA variant. The BF is reportedly atrophic in SV and in NFV PPA, which might indicate a cholinergic deficit. Acetylcholinesterase (AChE) activity, a cholinergic system marker, was quantitatively measured in the neo- and allocortex using N-[^{11}C]-Methylpiperidin-4-yl propionate (PMP)-PET with arterial sampling and metabolite correction. In the PPA group, only LV cases showed decreases in AChE activity levels compared to controls. Surprisingly, a substantial number of SV cases showed significant AChE activity increases compared to controls. We concluded that based on our findings, BF atrophy in SV PPA does not imply cholinergic depletion.

In summary, the findings reported in this thesis shed light on the non-linguistic, acoustic processing deficits and the underlying neuronanatomical, and molecular imaging correlates which contribute to the clinical phenotype of PPA. Despite increasing knowledge, truly disease-modifying therapies are currently not available in PPA. Based on our findings, tau PET provides a direct measure of the topographic distribution of the underlying brain changes and could be of value in future trials in clinical drug development. A subset of LV cases could potentially benefit from treatment with cholinomimetic medication.

Samenvatting

De term primair progressieve afasie (PPA) werd voor het eerst gehanteerd na de beschrijving van een reeks patiënten met een taal-gerelateerd dementie syndroom door Marsel Mesulam in 1982. Het *primaire* symptoom in PPA is het verlies van taal, dat *progressief* van aard is.
Sinds 2011 worden er internationaal drie klinische subtypen binnen het spectrum van PPA erkend op basis van de kenmerkende taal-problemen van ieder subtype: een nonfluente/agrammatische (NFV), een semantische (SV) en een logopene variant (LV). Vijftig tot zestig procent van de patienten met LV hebben de ziekte van Alzheimer als onderliggende pathologische onderzaak. In 50-88 % van de NFV patienten is de onderliggende oorzaak een pathologische opstapeling van het eiwit tau van het frontotemporale lobaire degeneratie (FTLD)-type (i.e. corticobasale degeneratie (CBD), progressieve supranucleaire palsy (PSP) of de ziekte van Pick), terwijl 69-83 % van de SV patienten FTLD-Transactive response DNA-binding proteïn 43 kDa (TDP-43) type C pathologie als onderliggende oorzaak heeft. Ondanks de geleidelijk toenemende kennis is de pathofysiologie van PPA nog steeds onvolledig gekend. Het algemene doel van dit proefschrift was het bestuderen van de pathofysiologische mechanismen onderliggend aan PPA op het vlak van gedrag, structurele en moleculaire beeldvorming.

Met behulp van niet-linguïstische, akoestische stimuli zonder enige betekenis, hebben we aangetoond dat een deel van de PPA patiënten problemen heeft in verschillende domeinen betreffende niet-verbale geluidsverwerking. Patiënten met NFV PPA vertoonden de meest prominente aantasting binnen het tijds- en ritme-domein voor de verwerking van korte sequenties van maximaal zeven tonen. Een deel van de SV patiënten was ook aangetast, hoewel minder ernstig. Patiënten met LV PPA hadden geen significante afwijkingen. De psychoakoestische

taken konden op een betrouwbare manier discrimineren tussen NFV en LV patienten, hoewel deze geen taal-gerelateerde stimuli bevatten en uitsluitend gebaseerd waren op de perceptie van toonhoogte en ritme in sequenties van tonen. We hebben eveneens aangetoond dat de performantie op een deel van de psychoakoestische taken gecorreleerd was met scores op conventionele verbale woord herhalingstaken. Problemen in de verwerking van tijd en ritme in NFV PPA konden in verband gebracht worden met het afsterven van rechter-hemisferische hersengebieden, waaronder het frontale operculum en de posterieure insula. Gebaseerd op deze bevindingen, veronderstellen we dat auditieve tijds-gerelateerde 'pathways' aangetast zijn in NFV PPA, die gemeenschappelijk gebruikt worden door onze hersenen voor het verwerken van de akoestische sequentiestructuur in zowel spraakproductie als geluidsverwerking. De aantasting kan bijdragen tot de spraakapraxie in patienten met NFV PPA. Deze spraakapraxie wordt ondermeer gekenmerkt door een abnormale duur van inter-segmentale tijdsintervallen tijdens het spreken.

Een deel van de NFV PPA patiënten heeft naast spraakproblemen en/of agrammatisme ook problemen met enkelvoudig woordbegrip. Deze patiënten worden beschouwd als de vierde 'mixed' variant (MV) van PPA. Op basis van beeldvormingsresultaten die in het huidige proefschrift beschreven werden, vertoonden MV PPA patienten een tau PET patroon, gemeten door de tau PET tracer [^{18}F]-THK5351, dat sterk overeenkwam met het patroon van de NFV patienten zonder woordbegripsproblemen (NFV-pure), namelijk verhoogde [^{18}F]-THK5351 binding in de premotorische cortex- en de supplementaire moter cortex. De topografie van [^{18}F]-THK5351 binding, maar niet de mate van atrofie was gecorreleerd met de klinische kenmerken van MV PPA patienten. In vergelijking met NFV-pure PPA, was het atrofiepatroon uitgebreider in MV PPA en patiënten hadden een hogere kans op de ziekte van Alzheimer als onderliggende oorzaak.

Vervolgens hebben we in een reeks PPA-patiënten onderzocht of volumeverlies in de basale nuclei van de hersenen in verband gebracht kon worden met een defect in het cholinerge neurotransmitter systeem, en of dit mogelijks afhankelijk was van het PPA subtype. De basale nuclei zijn namelijk atrofisch in SV en in NFV PPA, wat kan wijzen op een cholinerg defect in PPA. Acetylcholinesterase (AChE) activiteit, een merker voor het cholinerge systeem, werd daarom kwantitatief onderzocht in de hersenen door middel van N-[^{11}C]-Methylpiperidin-4-yl propionaat (PMP)-PET met arteriële staalname en metabolietcorrectie. In de PPA groep bleken alleen LV patienten een verlaagde AChE-activiteit te vertonen in vergelijking met gezonde controles. Onverwachts vertoonden

een aantal SV patienten een significante stijging in AChE-activiteit in vergelijking met gezonde controles. We besloten dat op basis van onze bevindingen, atrofie van de basale nuclei in SV PPA geen cholinerg defect impliceert.

Samengevat hebben we in dit proefschrift kunnen aantonen dat er een verstoorde verwerking optreedt van niet-linguïstische, akoestische stimuli in PPA. We konden ook de onderliggende neuronanatomische en moleculaire beeldvormings correlaten zichtbaar maken die bijdragen tot het klinisch beeld van PPA. Ondanks de toenemende kennis zijn er momenteel geen medicijnen beschikbaar die PPA patienten zouden kunnen genezen. Op basis van onze bevindingen, blijk dat tau PET de onderliggende pathologie in de hersenen van PPA patienten zichtbaar kan maken. Dit kan een belangrijke toegevoegde waarde betekenen voor toekomstige klinische, farmaceutische onderzoeken. Een deel van de LV patienten zou mogelijks behandeld kunnen worden met cholinomimetische medicatie.

List of abbreviations

3R	three repeat
4R	four repeat
AAT	Akense afasie test
Aβ_{42}	amyloid-β_{42}
ACC	anterior cingulate cortex
ACh	acetylcholine
AChE	acetylcholinesterase
act	active
AD	Alzheimer's disease
AGD	argyrophilic grain disease
AOS	apraxia of speech
AST	asymmetric sampling in time
ATL	anterior temporal lobe
au	arbitrary units
aud	auditory
AVF	animal verbal fluency
BA	Brodmann area
BBB	blood-brain barrier
BChE	butyrylcholinesterase
BF	basal forebrain
BNT	Boston naming test
BORB	Birmingham object recognition battery
CAA	cerebral amyloid angiopathy
CBD	corticobasal degeneration
ChAT	choline acetyltransferase
CDR	clinical dementia rating
CERAD	consortium to establish a registry for Alzheimer's disease
compr	comprehension
CPM	colored progressive matrices
cpo	cycle per octave
cps	cycle per second
CSF	cerebrospinal fluid

CT	computed tomography
DIAS	diagnostisch instrument voor apraxie van de spraak
DLBD	diffuse Lewy body disease
DLPFC	dorsolateral prefrontal cortex
DM	dynamic modulation
DV	distribution volume
DVR	distribution volume ratio
FDG	fluoro-deoxy-glucose
FoV	field of view
FM	frequency modulation
fMRI	functional magnetic resonance imaging
FTD	frontotemporal dementia
FTLD	frontotemporal lobar degeneration
FWE	family-wise error
FWHM	full-width at half maximum
GM	gray matter
hip	hippocampus
IFG	inferior frontal gyrus
ITG	inferior temporal gyrus
LV	logopenic variant
m	modulation
mAChR	cholinergic muscarinic receptor
min	minute
MMSE	mini-mental state examination
MNI	Montreal Neurological Institute
MP4A	N-[^{11}C]-methyl-4-piperidyl acetate
MRI	magnetic resonance imaging
MRAC	MR based attenuation correction
MTG	middle temporal gyrus
MTL	medial temporal lobe
MV	mixed variant
nAChR	nicotinic acetylcholine receptors
NFTs	neurofibrillary tangles
NFV	nonfluent variant
NIA-AA	national institute on Aging-Alzheimer's association
ns	nanoseconds
olf	olfactory gyrus
p	pitch
PALPA	psychophysical assessment of language processing in aphasia
PCC	posterior cingulate cortex
PET	positron emission tomography
PGN	progranulin
phg	parahippocampal gyrus
PHF	paired helical fragments

PIB	Pittsburgh Compound-B
PMP	N-[^{11}C]-Methylpiperidin-4-yl propionate
PPA	primary progressive aphasia
PPT	pyramids and palmtrees
PSP	progressive supranuclear palsy
PT	planum temporale
PVC	partial volume correction
PVE	partial volume effects
RF	radiofrequency
RFT	random field theory
RNA	ribonucleic acid
r	rhythm
rTMS	repetitive transcranial magnetic stimulation
s	second
SD	semantic dementia
sent	sentence
SMA	supplementary motor area
SMG	supramarginal gyrus
SPM	statistical parametric mapping
Spt	sylvian parietal temporal region
STG	superior temporal gyrus
STS	superior temporal sulcus
SUVR	standardized uptake value ratio
SV	semantic variant
SVM	support vector machine
t	timbre
T	Tesla
TAC	time activity curve
TDP-43	transactive response DNA binding protein 43 kDa
TE	echo time
TI	inversion time
TMS	transcranial magnetic stimulation
tot	total region
VAChT	vesicular acetylcholine transporter
VBM	voxel-based morphometry
VLPFC	ventral prefrontal cortex
VOIs	volumes of interest
WEZT	werkwoorden en zinnentest
WP	word picture
writ	written

Contents

Abstract i

Samenvatting iii

List of abbreviations vii

Contents xi

1 Introduction 1

1.1 Oh language where art thou ? 1

1.2 Language and healthy aging 3

1.3 Language and pathological aging: primary progressive aphasia 3

1.3.1 Clinical manifestations of PPA 5

1.3.2 Nonverbal deficits in PPA 9

1.4 A focus on pathology associated with PPA 10

1.5 Multimodal imaging of pathological substrates 14

1.6 Basal forebrain nuclei and the cholinergic system 15

1.7 Aims of the thesis 18

2 Experimental techniques 20

2.1 Non-linguistic auditory tasks 20
2.2 Magnetic resonance imaging 22
2.2.1 Voxel-based morphometry 23
2.3 Positron emission tomography imaging 24
2.3.1 Quantification of PET signal 25
2.3.2 PET tracers 27
2.4 Statistical analysis of imaging data 28

3 Core auditory processing deficits in PPA **29**

3.1 Abstract 29
3.2 Introduction 31
3.3 Material and Methods 33
3.3.1 Subjects 33
3.3.2 Neuropsychological protocol 34
3.3.3 Experimental tests of acoustic processing 35
3.3.4 Volumetric MRI 40
3.3.5 Statistical analyses 40
3.4 Results 43
3.4.1 Behavioral data: psychoacoustic test scores . . . 43
3.4.2 Experimental auditory performance: group-based analysis 44
3.4.3 Experimental auditory performance: individual auditory profiles 48
3.4.4 Relationship with neuropsychological test scores 48
3.4.5 Relationship with symptom duration, hearing loss and auditory short-term memory 49
3.5 Discussion 50
3.5.1 Differences between PPA subtypes 50

3.5.2 Perceptual processing of pitch and rhythm in short tone sequences . . . 52
3.5.3 Potential study limitations . . . 53
3.6 Conclusion . . . 53

4 Neuroanatomy of time and rhythm processing deficits in primary progressive aphasia 58

4.1 Abstract . . . 58
4.2 Introduction . . . 60
4.3 Material and Methods . . . 62
4.3.1 Subjects . . . 62
4.3.2 Neuropsychological protocol . . . 64
4.3.3 Experimental tests of acoustic processing . . . 64
4.3.4 Statistical analyses . . . 67
4.4 Results . . . 69
4.4.1 Demographics . . . 69
4.4.2 Clinicoanatomical features . . . 69
4.4.3 Experimental auditory performance: group-based and individual analyses . . . 70
4.4.4 Neuroanatomic correlates of temporal processing deficits . . . 71
4.4.5 Domain-specificity of neuroanatomical correlates for temporal processing deficits . . . 74
4.5 Discussion . . . 76
4.5.1 The role of the frontal operculum and insula in timing . . . 77
4.5.2 Lateralization effects . . . 79
4.5.3 Domain-specificity of the frontal operculum for timing tasks . . . 80

4.5.4 Shared neuroanatomy for timing and speech apraxia features in NFV PPA 81
4.5.5 Potential study limitations and strengths 82
4.6 Conclusion 82

5 Single-word comprehension deficits in the nonfluent variant of primary progressive aphasia 87

5.1 Abstract 87
5.2 Introduction 88
5.3 Material and Methods 90
5.3.1 Subjects 90
5.3.2 Neuropsychological and neurolinguistic protocol . 91
5.3.3 Volumetric MRI acquisition and analysis 93
5.3.4 [^{18}F]-THK5351 PET acquisition and analysis . . 94
5.3.5 Amyloid biomarker measurement and analysis . . 94
5.3.6 Statistical analyses 95
5.4 Results 98
5.4.1 Demographics 98
5.4.2 Neuropsychological and neurolinguistic profile of individual cases 98
5.4.3 Group-based deficits in MV PPA for additional neuropsychological domains 100
5.4.4 Anatomy of atrophy 102
5.4.5 [^{18}F]-THK5351 binding pattern 102
5.4.6 Amyloid biomarker positivity 105
5.4.7 Imaging biomarkers of individual MV PPA cases 106
5.4.8 Correlation between imaging biomarkers and core clinical features 107
5.5 Discussion 108

5.5.1 MV PPA and its relation to AD 112
5.5.2 Potential study limitations 113
5.6 Conclusion 114

6 Cholinergic depletion and basal forebrain volume in primary progressive aphasia 116

6.1 Abstract 116
6.2 Introduction 117
6.3 Material and Methods 118
6.3.1 Subjects 118
6.3.2 Neuropsychological protocol 119
6.3.3 PET acquisition and analysis 119
6.3.4 MRI acquisition and analysis 121
6.3.5 Statistical analyses 123
6.4 Results 125
6.4.1 Primary outcome analyses 125
6.4.2 Secondary outcome analyses 129
6.5 Discussion 133
6.5.1 Cholinergic alterations 133
6.5.2 BF atrophy and its relation to cholinergic alterations 134
6.5.3 A cholinergic therapy for PPA ? 135
6.5.4 Potential study limitations 135
6.6 Conclusion 136

7 General discussion 138

7.1 The intersection between core auditory processing and language 140
7.2 Imaging biomarkers in PPA 143

7.2.1 Tau PET 143
7.2.2 Cholinergic PET 147
7.3 Therapeutic interventions 148

Bibliography **151**

Curriculum vitae **191**

Publications **195**

7.4 Publications in international peer-reviewed journals . . . 195
7.5 Published conference abstracts 197

A Conflict of interest statement, Personal Contribution and Acknowledgments **201**

A.1 Conflict of interest and Personal Contribution 201
A.2 Acknowledgments 203

Preface

The famous composer of Bolero, Maurice Ravel, developed an insidiously progressive language disorder accompanied by impaired musical expression in his early sixties. He complained bitterly that he had all this music in his brain but could not play it or write it down. Ravel was studied by the French neurologist Alajouanine and at that time his disorder was classified as 'Wernicke's aphasia', with prominent anomia, agraphia and alexia (for both verbal and musical material) (Warren and Rohrer, 2009). At that time, a painful procedure of injecting air into the fluid filled spaces of the brain (ventricles) provided contrast for acquiring an X-ray of his brain. This so called pneumoencephalogram showed unilateral left hemispheric atrophy, which is indicative of primary progressive aphasia (PPA) in retrospect. Researchers hypothesize that the fact he adopted different uses of timbre could be attributed to his disease (Alexoudi et al., 2016). Since 1980's, both the delineation of the syndrome of PPA, as well as the application of modern imaging techniques such as PET, CT and MRI have revolutionized the field of neuroimaging. While the true nature of Ravel's illness remains a matter of speculation, the substantial scientific progress made, enabled us to perform extensive research in PPA as described in the following pages of this PhD thesis.

Chapter 1

Introduction

1.1 Oh language where art thou ?

At this very moment, while reading the first sentence of this PhD thesis, a wonderful world of tiny neurons is being activated unconsciously. Language skills we develop through life allow us to observe these signs as words put into a syntactic structure which convey meaning to us. Language is a crucial and complex lifelong faculty, which starts to develop early in life (Shiller et al., 2010). Language evolution is viewed as a complex cultural development by some researchers (Arbib, 2005), while others consider it as an evolutionary emergence of neural structures capable of supporting abstract organizational features that are found in all human languages (Chomsky, 2017). The heart of human language is a system of representations relating forms to meaning.

Language processing shows a systematic relationship with handedness. In about 98% of right-handed individuals, the language and speech network is distributed in the left hemisphere (Mesulam et al., 2014a). This network surrounds the Sylvian fissure and encompasses the pars triangularis and pars opercularis of the inferior frontal gyrus (IFG) ('Broca's area') through the angular and supramarginal gyri into the lateral temporal cortex as well as the medial temporal lobe (MTL) including structures such as the perirhinal cortex (Scott and Wise, 2004; Hickok, 2009; Ueno et al., 2011; Bruffaerts et al., 2013; Liuzzi et al., 2015). According to contemporary concepts, the Sylvian fissure divides this network into a ventral stream centred in the temporal lobes which

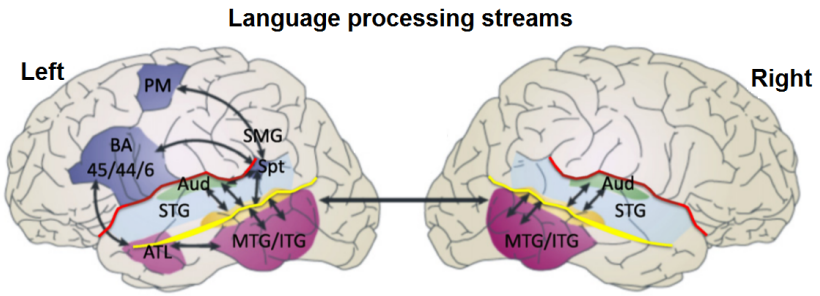


Figure 1.1: **Schematic representation of the language network**. The language network is divided by the Sylvian fissure (red line) into a ventral stream for speech comprehension centered in the temporal lobe, and a dorsal stream for sensory-motor integration which involves structures at the parietal–temporal junction and frontal lobe. ATL: anterior temporal lobe, Aud: auditory cortex (early processing stages), BA 45/44/6: Brodmann areas 45, 44, and 6, MTG/ITG: middle temporal gyrus, inferior temporal gyrus, PM: premotor, dorsal portion, SMG: supramarginal gyrus, Spt: Sylvian parietal temporal region (left only), STG: superior temporal gyrus, yellow line: superior temporal sulcus (STS). Modified with permission from Hickok (2009).

processes speech signals for comprehension (Scott and Wise, 2004; Ueno et al., 2011), and a dorsal stream, mapping acoustic speech signals to parietal and frontal lobe articulatory networks (Hickok and Poeppel, 2015) (Fig. 1.1). Both streams project into the IFG, which has a crucial role in the interaction of these two streams (Liuzzi et al., 2017). Language is however not completely lateralized to one hemisphere. The ventral stream is largely bilaterally organized but shows important computational differences between the left- and right-hemispheric language systems, while the dorsal stream is strongly lateralized to the dominant language hemisphere (Hickok and Poeppel, 2015).

The neural basis of language lateralization dates back to the notion of leftward asymmetry of the planum temporale (PT, i.e. the area behind Heschl's gyrus, the auditory cortex) in 65% of individuals and its location in auditory areas close to regions relevant for speech comprehension (a region called 'Wernicke's area') (Geschwind and Levitsky, 1968). As discussed earlier in this section, the PT is however not the sole region involved in auditory speech and language processing (Hickok and Poeppel, 2015). Moreover, based on current knowledge, the human PT is not a

dedicated language processor, but is engaged in the analysis of many types of complex sound (Griffiths and Warren, 2002). Spoken language is a highly specialized signal in acoustic, cognitive and evolutionary terms, representing a particularly significant species of complex sound (Goll et al., 2010).

1.2 Language and healthy aging

During healthy aging, most comprehension abilities remain preserved (Federmeier et al., 2003). It has been shown that vocabulary even improves across the adult life span (Shafto and Tyler, 2014). In contrast to comprehension processes, the production of language shows a substantial age-related decline (Cross and Burke, 2004). Aging leads to slower and decreased picture naming accuracy and increases in 'tip of the tongue states', in which a subject is temporarily unable to retrieve a known word. This is not due to a pathological condition such as neurodegenerative disease but caused by selective deficits in phonological access (Cross and Burke, 2004), due to a reduced integrity of brain regions involved in phonological production (i.e. the left anterior insula and the left superior longitudinal fasciculus) (Shafto et al., 2007; Stamatakis et al., 2011).

Overall, language is very much preserved compared to other cognitive functions during healthy aging (Wingfield and Grossman, 2006). This is an important consideration when discriminating language impairments due to pathological conditions from healthy aging.

1.3 Language and pathological aging: primary progressive aphasia

Damage to the language network can result in aphasia, a term which denotes a disorder in language processing. Aphasia can be present in different forms depending on the distribution of lesions in the language network (Marsh and Hillis, 2006; Gorno-Tempini et al., 2011). The greatest body of work has been based on aphasia caused by stroke (Marsh and Hillis, 2006). However, at the end of the 19^{th} century, rare cases were described by the neurologists Arnold Pick, Joseph Jules Dejerine and the psychiatrist Paul Serieux with a progressive disorder of language, which couldn't be attributed to stroke or neoplasm (for

review: Mesulam (2013a)). At pathological examination, one of these cases showed bitemporal cortical atrophy and neuronal loss. This pattern is not usually seen in stroke patients. Following the description of a series of cases studied by Marsel Mesulam in 1982 (Mesulam, 1982) with 'a slowly progressing aphasic disorder', the term 'Primary progressive aphasia' (PPA) was coined (Mesulam, 1987).

The cardinal feature of PPA is the relentless dissolution of language. A root diagnosis of PPA is justified if three criteria are fulfilled. First, a diagnosis of PPA requires the presence of word finding difficulties (anomia) which cannot be attributed purely to healthy aging. Second, the language impairment is due to underlying neurodegenerative disease, which is therefore progressive in nature. Third, the language impairment is the primary and most salient feature during the first two years of the disease, while memory, visuospatial skills and behavior remain relatively intact. Impairments in other cognitive domains can emerge after only a few years (Matias-Guiu et al., 2014). This is classified as a clinical condition which is given the term 'PPA-plus' (Dickerson, 2012). Nonetheless, the deficit in language remains the most salient feature throughout the illness and progresses more rapidly than deficits in other cognitive domains (Mesulam, 1987).

PPA is considered a form of dementia because of its gradual cognitive decline to the point where activities of daily living become compromised. It is however considered a 'language-based' dementia unlike the more prevalent 'memory-based' dementia associated with typical Alzheimer's disease (AD). In contrast to typical dementias, PPA most commonly has an early onset, i.e. in the late 50's, and an approximately equal prevalence across gender (Johnson et al., 2005; Hodges et al., 2010; Mesulam et al., 2014a). As of yet, there are no community-based surveys documenting the frequency of PPA in the population. The prevalence of PPA has been suggested to fall in the range of $1.1-6$ per 100,000 (Johnson et al., 2005).

Following the initial description of a series of PPA cases (Mesulam, 1987), patients with a selective loss of semantic memory, called semantic dementia (SD) (Warrington, 1975; Hodges et al., 1992; Neary et al., 1998) and patients with a progressive nonfluent language disorder have been described (Grossman et al., 1996; Neary et al., 1998). These phenotypes were first incorporated into diagnostic criteria for the clinical classification of frontotemporal lobar degeneration (FTLD) (Neary et al., 1998). Patients with a clinical state of fluctuating word finding deficits without the frank agrammatism of the classic nonfluent aphasias

and without a semantic impairment were labeled under the neologism 'logopenia', derived from the Greek words logos (word) and penia (deficiency) (Mesulam, 1982; Gorno-Tempini et al., 2004a, 2008; Mesulam et al., 2014a). This logopenic phenotype was however initially not recognized as a distinct clinical entity. Gradually, more evidence became available demonstrating that this logopenic phenotype was distinct from the progressive nonfluent variant (Gorno-Tempini et al., 2004a, 2008). Partly motivated by the need to consolidate the logopenic phenotype, a consensus meeting in 2011 attempted to develop and refine criteria for these three conditions (Gorno-Tempini et al., 2011).

1.3.1 Clinical manifestations of PPA

Within the spectrum of PPA, three clinical subtypes have been recognized based on the core language domains of grammatical ability, word comprehension, object naming, repetition and motor aspects of speech being affected (Gorno-Tempini et al., 2011). PPA is consequently subdivided into a nonfluent/agrammatic (NFV), a semantic (SV) and a logopenic variant (LV) (Gorno-Tempini et al., 2011) (Fig. 1.2). It is however suggested that a fourth phenotype should be added, i.e. the mixed variant (MV) of PPA (Mesulam et al., 2009, 2012)(for review: Vandenberghe (2016)).

The classification of PPA into one of these variants may occur at one of three levels: clinical, imaging-supported, or by means of a definite pathologic diagnosis (Gorno-Tempini et al., 2011). However, no agreed clinical evaluation scale on which to derive the diagnosis exists. In the next section, we will discuss each PPA variant separately and its association with characteristic patterns of brain atrophy or hypometabolism (measured with [^{18}F]-fluoro-deoxy-glucose positron emission tomography ([^{18}F]-FDG-PET)), which reflects the behavioral manifestations.

Nonfluent/agrammatic variant PPA

Clinically, NFV PPA requires the presence of one or both of two core features: speech apraxia and agrammatism, which most often occur together (Gorno-Tempini et al., 2011; Mesulam et al., 2012). Speech apraxia in NFV PPA patients is characterized by notably decreased, halting, effortful motor speech output with inconsistent speech sound errors and distortions, in particular for polysyllabic words with consonant

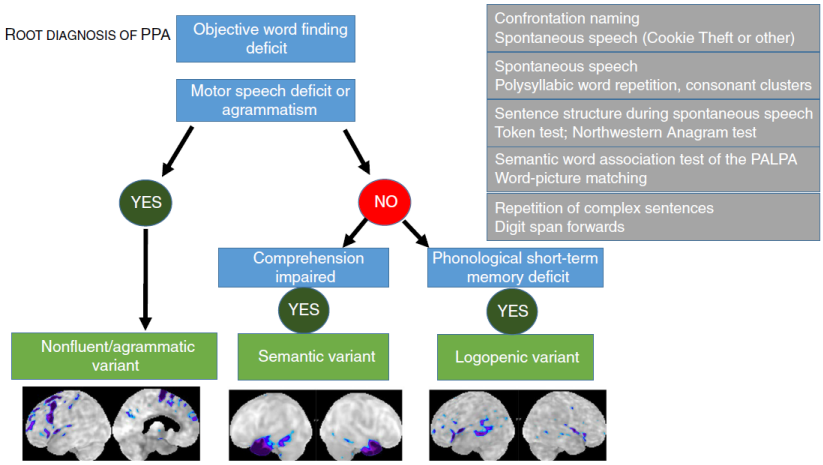


Figure 1.2: **Classification scheme for PPA**. Within the spectrum of PPA, three clinical subtypes have been recognized: a nonfluent/agrammatic, a semantic and a logopenic variant. Blue, most critical language dimension; gray, some examples of frequently used conventional neuropsychological tests; green, subtype. PALPA: Psycholinguistic Assessment of Language Processing in Aphasia. Modified from Vandenberghe (2016).

clusters (Ash et al., 2010). The changes in relative duration and intensity of vowels as well as the pauses during reading are the most distinctive characteristics (Ballard et al., 2014). Dysarthria (articulatory abnormalities) can also be present in NFV as part of the motor speech impairment.

Agrammatic features of NFV PPA include inappropriate word order, misuse of word endings, prepositions, pronouns, conjunctions, and verb tenses with a decrease in mean length of utterance and sentence complexity, which can in turn affect comprehension of syntactically complex sentences. These core features are present in the setting of preserved single-word comprehension and preserved object knowledge (Gorno-Tempini et al., 2011).

Brain areas that have been implicated in word planning, articulation and syntactic processing deficits in NFV PPA are part of the dorsal language stream (Marcotte et al., 2017) including the left IFG, (the pars opercularis and pars triangularis) (Rabinovici et al., 2008; Matías-Guiu et al., 2015b), the premotor cortex and supplementary motor area (SMA)

and the anterior insula (Mandelli et al., 2014, 2016). In particular, apraxia of speech relates to atrophy of the premotor cortex and SMA (Josephs et al., 2006a; Ogar et al., 2007; Josephs et al., 2012). The syntactic processing deficits in NFV PPA are associated with atrophy in the IFG and in the middle superior temporal sulcus (STS) (Wilson et al., 2010). Beside cortical involvement, subcortical atrophy has been reported in the caudate nucleus bilaterally extending to the left putamen (Gorno-Tempini et al., 2004a). Over time, atrophy extends into the dorsolateral and ventral prefrontal cortex (DLPFC and VLPFC), superior temporal gyrus (STG), a greater portion of temporoparietal cortex, the anterior temporal lobe (ATL) (Rogalski et al., 2011b) and to orbital and anterior cingulate regions (Grossman, 2010).

Semantic variant PPA

Patients with SV PPA show semantic processing deficits instantiated as impairments in single-word comprehension and confrontation naming as the two core clinical features (Gorno-Tempini et al., 2011). One of the following three features should also be present in SV: impaired object knowledge for low frequency items, surface dyslexia with poor reading of irregular words and/or dysgraphia (i.e. incoherent writing). Speech remains fluid without word-finding pauses albeit impoverished in meaning due to word finding difficulties and an increased use of generic as opposed to specific words (i.e. taxonomic interference). Sentence comprehension can remain relatively preserved, as long as the constituent nouns can be decoded at a generic level. During progression of the disease, spontaneous speech may become restricted to stereotyped utterances and echolalia (i.e. unsolicited repetition of verbal utterances made by another person). Progressive deterioration of semantic knowledge in SV is also apparent in production tasks, such as picture naming, verbal definitions, object drawing (Bozeat et al., 2003) and object use (Bozeat et al., 2002). Eventually, all kinds of verbal communication become compromised in SV PPA.

The atropy and hypometabolism pattern observed in SV PPA presumably compromises regions of the ventral language stream (Marcotte et al., 2017). In particular, the lateral and ventral surfaces of the left ATL are compromised early in the disease course (Mummery et al., 2000; Rabinovici et al., 2008; Rogalski et al., 2011b; Matías-Guiu et al., 2015b). Atrophy can additionally encompass the anterior IFG, the orbitofrontal cortex, anterior cingulate cortex (ACC) (Kumfor et al., 2016), anterior hippocampus (Tan et al., 2014), the anterior fusiform

region subjacent to the head and body of the hippocampus (Mion et al., 2010) and the perirhinal cortex (Hodges and Patterson, 2007). The latter region is required to bind properties of not just perceptually, but also semantically confusable objects together, enabling their disambiguation from other similar objects and thus comprehension (Kivisaari et al., 2012). Functional Magnetic Resonance Imaging (fMRI) activity patterns in the perirhinal cortex of healthy individuals, overlapping with the atrophic regions in SV, reflect semantic similarities between written words (Bruffaerts et al., 2013; Liuzzi et al., 2015).

Over time, atrophy in SV extends posteriorly and superiorly into the ipsilateral temporal lobe, and to the contralateral ATL (Avants et al., 2007; Rogalski et al., 2011b). The rate of tissue loss in the right temporal lobe overtakes the left temporal lobe as the disease evolves (Rohrer et al., 2008). As this occurs, face and object recognition can become severely compromised (Chan et al., 2009; Gefen et al., 2013; Mesulam et al., 2013). SV PPA patients with atrophy in the right temporal pole, amygdala and insula may encounter problems of emotional processing as well (Hsieh et al., 2012) and can exhibit a variety of behavioral symptoms including social disinhibition, perseverative behavior, somatization, depression and aggressive behavior (Iaccarino et al., 2015; Van Langenhove et al., 2016).

Logopenic variant PPA

A first core clinical hallmark in the diagnosis of LV PPA relates to deficient single-word retrieval in spontaneous speech and naming (nouns more than verbs). Prominent repetition problems in particular for complex sentences and phrases are considered the second core clinical hallmark of LV PPA (Gorno-Tempini et al., 2011; Leyton et al., 2014; Henry et al., 2015). This repetition deficit was not described in the first reports (Mesulam, 1982), but is currently regarded as a core clinical hallmark of LV PPA (Gorno-Tempini et al., 2004a, 2008, 2011). Hesitant spontaneous speech can be characterized by phonological paraphasias, which are abnormal utterances resembling the sound of the intended word. These core features occur in the context of relatively spared syntactic, semantic, and motor speech abilities (Gorno-Tempini et al., 2008). Comprehension of syntactically complex sentences might be compromised as the disease progresses.

In LV PPA, the left posterior temporal, supramarginal, and angular gyri as well as the left temporoparietal junction and inferior parietal lobe are typically affected (Gorno-Tempini et al., 2004a, 2008; Rabinovici et al.,

2008; Rohrer et al., 2010a, 2013; Matías-Guiu et al., 2015b). Atrophy can also include the posterior cingulate cortex (PCC), precuneus and the MTL (Rohrer et al., 2010a, 2013). Involvement of the temporoparietal junction has been linked to a disturbance in the phonological loop resulting in sentence repetition deficits (Nelissen et al., 2010). Deficient naming in LV is associated with left middle temporal gyrus (MTG) atrophy (Win et al., 2017). Atrophy in LV spreads over time into the inferior temporal lobe, the IFG, the DLPFC, the nucleus caudatus and the PCC/precuneus of the left hemisphere as well as to the temporoparietal junction of the contralateral hemisphere (Rogalski et al., 2011b; Rohrer et al., 2013; Brambati et al., 2015).

Mixed variant PPA

Patients exhibiting a combination of both single-word comprehension deficits along with speech apraxia or agrammatism, can be classified as MV PPA (Mesulam et al., 2009, 2012). However, this fourth phenotype is currently not recognized in the international consensus criteria for classification of PPA (Gorno-Tempini et al., 2011). Only limited neuroimaging data are currently available in MV PPA, revealing atrophy in the temporoparietal junction and STG (Mesulam et al., 2012; Sajjadi et al., 2014) and additional atrophy in the IFG (Mesulam et al., 2012). Atrophy involving the IFG, insula and precuneus has been shown in an independent series of MV cases (Spinelli et al., 2017).

In summary, distinctive clinical-anatomical patterns in PPA are most conspicuous in the initial stages of the disease, and reflect relatively selective damage to the language and speech network, usually located in the left hemisphere, manifestated as structural atrophy, hypoperfusion or hypometabolism. However, clinical-anatomical correlations in PPA reflect group-wide probabilities and often, individual PPA patients may show atrophy which extends to regions characteristically affected in other variants (Catani et al., 2013).

1.3.2 Nonverbal deficits in PPA

As already mentioned in the previous section, the generalized deterioration of semantic memory in SV PPA extends also to the nonverbal domain. Face and object recognition can become severely compromised, but also recognition of everyday environmental sounds (Bozeat et al., 2000; Hsieh et al., 2011) and famous tunes (Hsieh et al.,

2011) can be affected. A previous study in SV PPA demonstrated that the ability to recognize environmental sounds correlated with right-sided medial temporal structures primarily the right amygdala, while famous tunes recognition correlated with a more lateral cluster in the right temporal pole (Hsieh et al., 2011). Impaired recognition of familiar voices may also occur in SV PPA and often accompanies the development of prosopagnosia in which patients encounter difficulties in recognizing familiar faces (Gainotti et al., 2003). The neural substrates of prosopagnosia include the posterior fusiform gyrus (Hsieh et al., 2011; Kumfor et al., 2015). Processing of apperceptive (object representational) and semantic sound can be deficient in NFV and SV PPA (Goll et al., 2010), although deficits of auditory early perceptual analysis are more common in NFV PPA (Goll et al., 2010, 2011). Previous studies of our group have shown nonverbal gesture discrimination processing deficits across the spectrum of PPA, which are associated with gray matter volume loss in the left anterior inferior parietal cortex extending into the posterior STG (Nelissen et al., 2010). Nonverbal gesture discrimination deficits correlated with impairments in gesture imitation, word and pseudoword repetition, and writing-to-dictation (Nelissen et al., 2010).

While verbal impairments in PPA are extensively studied, it is clear that non-verbal impairments in PPA also contribute to the clinical phenotype. In this thesis, we will analyze whether nonverbal impairments in processing of core auditory stimuli of three different auditory domains: pitch, time/rhythm and timbre, are present in the syndrome of PPA.

1.4 A focus on pathology associated with PPA

In an era of etiology-specific treatments for neurodegenerative conditions, determining the neuropathological basis of PPA is of crucial importance. Neuropathological classification of PPA cases using immunohistochemical assessment techniques begins with the separation into FTLD or AD pathology. FTLD pathology is characterized by the presence of tau-positive inclusions or by the presence of Transactive response DNA binding Protein 43 kDa (TDP-43) proteinopathy, while AD pathology is related to tau-positive inclusions in combination with β-amyloid pathology (Grossman, 2010). Tau is a microtubule associated phosphoprotein (Weingarten et al., 1975), involved in the stabilization and assembly of microtubuli, which are in turn critical for cytoskeletal support and intracellular transport (Iqbal et al., 2015). The protein tau exists in six isoforms, categorized into two functionally different groups, depending

on the presence of three repeats (3R) or four repeats (4R) of the microtubule binding domain. Endogenous hyperphosphorylation of tau can lead to decreased microtubule binding (Maas et al., 2000). When tau is hyperphosphorylated, it will become missorted from the axon into the somatodendritic compartment by retrograde axonal transport (Li et al., 2011). As a consequence, abnormally hyperphosphorylated tau detaches from the microtubuli and aggregates. Conditions which are characterized by tau aggregates include AD, dementia with Pick bodies (Pick's disease), argyrophilic grain disease (AGD), corticobasal degeneration (CBD) and progressive supranuclear palsy (PSP) (Villemagne et al., 2015).

Tau aggregates associated with AD pathology are constituted of both 3R and 4R tau isoforms, which ultrastructurally form paired helical fragments (PHF) (Arima, 2006). Under the light microscope, tau aggregates of the AD-type manifest as neurofibrillary tangles (NFTs) in the neuronal soma, as neuropil threads in neurites, and as dystrophic neurites surrounding a β-amyloid core in neuritic plaques (Fig. 1.3A,B). This type of pathology is present in 50-100% of cases with LV PPA (Grossman, 2010; Spinelli et al., 2017).

According to the 2012 National Institute on Aging-Alzheimer's Association (NIA-AA) guidelines, AD neuropathologic changes are ranked along three parameters (Amyloid, Braak and the Consortium to Establish a Registry for Alzheimer's disease (CERAD) criteria (Mirra et al., 1991)) to obtain an 'ABC score' (Hyman et al., 2012). Standard immunohistochemical assessment of NFTs is performed using the Braak staging scheme which follows a stereotypical spatiotemporal pattern of symmetric tau distribution in the brain, starting in the entorhinal cortex and spreading to the hippocampus and neocortical regions (Braak and Braak, 1991; Braak et al., 2006a). However, in PPA due to AD, the principles of Braak staging do not apply in any strict fashion as the neocortex contains more NFTs than the entorhinal cortex and hippocampus (Mesulam et al., 2014b; Giannini et al., 2017), usually with a greater leftward asymmetry (Josephs et al., 2013a; Gefen et al., 2012). The other hallmark, β-amyloid deposition can be observed as extracellular deposits of β-amyloid (Fig. 1.3B) or as neuritic plaques (Fig. 1.3A). In the latter, a denser core of fibrillar β-amyloid is deposited at the center of a cluster of phospho-tau immunoreactive dystrophic neurites. These forms of β-amyloid are respectively assessed by Thal staging (Thal et al., 2002) or the CERAD scale (Mirra et al., 1991).

In NFV PPA patients, 50-88% of cases are associated with FTLD-tau aggregates (i.e. CBD, PSP or Pick's disease) (Grossman, 2010; Spinelli

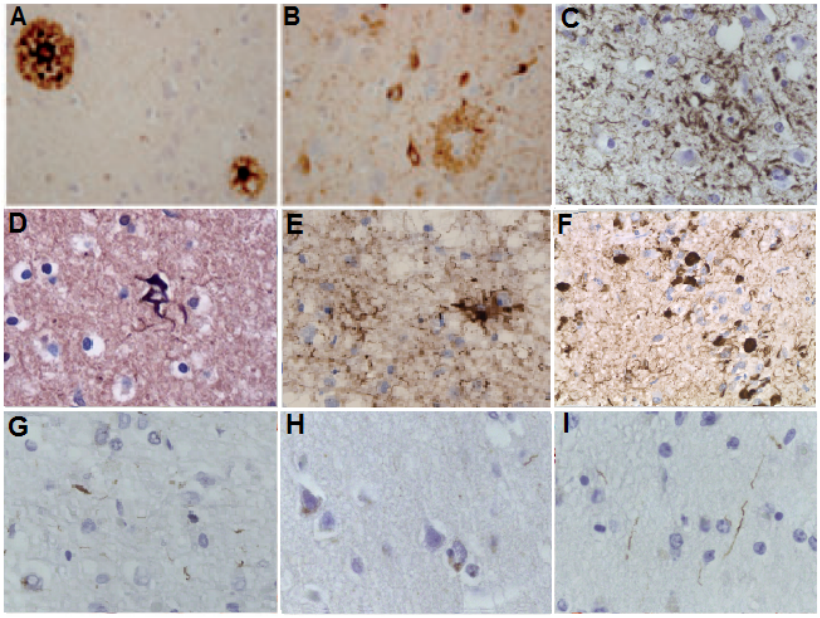


Figure 1.3: **Pathological lesions in PPA**. Immunohistochemical stainings of **(A)** a neuritic plaque, **(B)** neurofibrillary tangles and diffuse extracellular deposits of β-amyloid, **(C)** astrocytic plaques, **(D)** coiled body, **(E)** tufted astrocytes, **(F)** Pick bodies, **(G)** TDP-43 type A, **(H)** TDP-43 type B and **(I)** TDP-43 type C. Courtesy of the Pathology Department of UZ Leuven.

et al., 2017). FTLD-tau of the CBD and PSP type consist of 4R tau isoforms, which form straight filaments or twisted ribbons at the ultrastructural level. Under the light microscope, these tau aggregates can be appreciated as astrocytic plaques (Fig. 1.3C), neuropil threads and coiled bodies (Fig. 1.3D) in CBD (Kertesz and Munoz, 2004; Armstrong et al., 2013) or as globose tangles and tufted astrocytes (Fig. 1.3E) in PSP (Kertesz and Munoz, 2004). Tau isoforms exclusively constituted out of 3R tau are present in Pick bodies (Fig. 1.3F), which form the major constituents of Pick's disease pathology (Grossman, 2010).

In SV PPA, 69-83% of cases show FTLD-TDP-43 type C pathology (Fig. 1.3I) as the primary pathological substrate (Grossman, 2010; Spinelli et al., 2017). TDP-43 is a RNA-binding protein which normally resides in the nucleus (Zhang et al., 2011). In pathological conditions, cleavage

of its amino-terminal portion results in migration out of the nucleus into the cytoplasm, followed by ubiquitination and phosphorylation (Zhang et al., 2011). The nature of the TDP-43-mediated neurotoxicity is not yet understood, although protein misfolding may play a prominent role. According to the pattern of TDP-43 inclusions, several histopathological subtypes have been defined (Mackenzie et al., 2011). TDP-43 type A is associated with the presence of many neuronal cytoplasmic inclusions and short dystrophic neurites (Fig. 1.3G) and is most commonly observed in monogenic autosomal dominant cases of PPA, e.g. progranulin (GRN) mutations (Baker et al., 2006; Neumann et al., 2006). In TDP-43 type B, some neuronal cytoplasmic inclusions and rare dystrophic neurites are present (Fig. 1.3H). This type is genetically associated with a hexanucleotide repeat expansion in C9ORF72 (Mackenzie et al., 2011; Cruts et al., 2013). Type C is characterized by the presence of rare neuronal cytoplasmic inclusions and long dystrophic neurites (Fig. 1.3I) (Mackenzie et al., 2011). TDP-43 inclusions of type C are most often encountered in PPA, particularly in the SV of PPA. In rare cases, TDP-43 pathology can be present in an asymmetric fashion in PPA with a GRN mutation (Gliebus et al., 2010).

Although some concordance exists between pathology and each PPA variant, the clinical diagnosis does not provide an entirely reliable indication of the underlying pathology in individual PPA patients. This association is only a statistical likelihood and not diagnostically definitive. For instance, in NFV PPA patients, although the likelihood of a primary FTLD-tauopathy is higher, secondary AD pathology can 'contaminate' the immunohistochemical assessment (Spinelli et al., 2017). In SV PPA, secondary PSP or secondary AD pathology can also be present in addition to TDP-43 pathology (Spinelli et al., 2017). While the majority of LV PPA cases are associated with primary AD pathology, secondary Lewy Body or PSP pathology can be found (Spinelli et al., 2017). In a meta-analysis of PPA LV series from different centers, 38% were due to FTLD TDP-43, and 5-10% were caused by tau-associated FTLD (Grossman, 2010). LV can also be caused by AD combined with Lewy body pathology (Mesulam et al., 2014b; Harris et al., 2013). Regarding MV PPA, only limited cases have been assessed (Mesulam et al., 2014b; Spinelli et al., 2017). In one report, AD pathology was present in 67% of cases (four out of six), while only 17% (one out of six) had FTLD-tau (CBD) or TDP-B pathology (one out of six) (Mesulam et al., 2014b). Others demonstrated a lower percentage of underlying AD pathology in MV PPA (25%, one out of four). In one series, Pick's disease pathology was the underlying etiology in most MV cases (50%, two out of four),

although one MV case (25%, one out of four) showed TDP-43 type A pathology (Spinelli et al., 2017).

1.5 Multimodal imaging of pathological substrates

One major development in the diagnosis of the underlying pathology in PPA has been the advent of amyloid PET imaging (Klunk et al., 2004). Amyloid PET has been shown to correlate strongly with lowered cerebrospinal fluid (CSF) values of amyloid-β_{42} (Aβ_{1-42}) (Adamczuk et al., 2015). Considering PPA, amyloid PET has proven useful in the identification of AD pathology in PPA patients (Rabinovici et al., 2008; Leyton et al., 2011; Teichmann et al., 2013), confirming the higher prevalence of AD pathology in LV PPA (Matías-Guiu et al., 2015a), and the lower prevalence in the other two variants (Rabinovici et al., 2008; Leyton et al., 2011; Martersteck et al., 2015). To date, no amyloid PET imaging study in MV PPA has been published so far. Diffuse amyloid burden in PPA is generally indistinguishable from the pattern in typical AD (Rabinovici et al., 2008; Leyton et al., 2011). However, left-lateralized amyloid burden across PPA variants can be present (Martersteck et al., 2015). Regulatory approval of amyloid PET imaging ligands (for review: Vandenberghe et al. (2013)) has improved clinical diagnosis of AD-related PPA, although neuropathologically speaking, AD can only be diagnosed in case amyloid-positivity is accompanied by the presence of NFTs (Mirra et al., 1991).

The availability of tau PET ligands is currently restricted to research settings (for review: Hall et al. (2017)). [^{18}F]-AV-1451 (previously known as ([^{18}F]-T807) was the first and still most widely used tau PET ligand in the study of typical AD (Chien et al., 2013). While the diffuse distribution pattern in amyloid PET imaging failed to correlate with clinical impairment in AD, elevated [^{18}F]-AV1451 binding correlated significantly with clinical impairment (Johnson et al., 2016).
Regarding PPA, elevated left-lateralized [^{18}F]-AV-1451 PET has only been reported in LV PPA cases (Ossenkoppele et al., 2016; Nasrallah et al., 2017; Xia et al., 2017). Specifically, increased left temporoparietal [^{18}F]-AV-1451 binding has been demonstrated to be significantly associated with language impairment (Ossenkoppele et al., 2016).
However, [^{18}F]-AV-1451 is not a sole player in the tau PET imaging field. Recently, a series of THK compounds became available including the most

recent [^{18}F]-THK5351 compound ([^{18}F]-GE-216) (Harada et al., 2016). Other promising tracers include [^{11}C]-PBB3 (Maruyama et al., 2013) and [^{18}F]-MK-6240 (Walji et al., 2016). [^{18}F]-THK5351 is considered to have a high binding affinity and selectivity for tau aggegrates, over β-amyloid, α-synuclein, and TDP-43 (Harada et al., 2016). Recent studies with [^{18}F]-THK5351 PET have shown elevated binding in patients with AD (Harada et al., 2016), CBD (Kikuchi et al., 2016) and PSP (Ishiki et al., 2017) compared to healthy controls. However, it is currently unknown how this tracer regionally binds to molecular aggregates in patients with PPA and whether [^{18}F]-THK5351 PET patterns differ between PPA variants. In this thesis, we will investigate these issues.

A specific ligand for TDP-43 pathology could be extremely informative in diagnosing the underlying pathology in PPA. As of yet, TDP-43 tracers are currently under intensive investigation, but so far, no compounds entered the clinical trial phase.

1.6 Basal forebrain nuclei and the cholinergic system

Cholinergic depletion has been documented in typical AD (Kuhl et al., 1999; Bohnen et al., 2003, 2005), but it is currently unknown whether a cholinergic deficit also occurs in atypical AD presenting as PPA or in PPA due to a tauopathy or TPD-43 proteinopathy. According to MRI volumetric studies, the basal forebrain (BF) is atrophic in SV and NFV PPA (Teipel et al., 2014b, 2016), which provides a rationale for investigating cholinergic system alterations in PPA in this thesis.

The BF nuclei are part of the brain's cholinergic system, which is basically constituted by two other populations including the midpontine nuclei and a large population of striatal interneurons. The cholinergic nuclei of the BF comprise the medial septum (Ch1), the horizontal and vertical diagonal band of Broca (Ch2 and Ch3), and the nucleus basalis of Meynert (Ch4) (Mesulam, 2013b) (Fig.1.4), which in turn has six subdivisions (Teipel et al., 2014a). The midpontine nuclei are constituted of the peduncolo-pontine nucleus (Ch5), the dorsolateral tegmental nucleus (Ch6) (Fig.1.4), the medial habenular nucleus (Ch7) and the parabigeminal nucleus (Ch8) (Pepeu and Grazia Giovannini, 2017).

Moderate degenerative changes in BF nuclei occur during early adulthood

(Bigl et al., 1987; Baker-Nigh et al., 2015), and aggravate in advanced age (Bigl et al., 1987; Grothe et al., 2012). Atrophy during aging however does not primarily result from cell loss but rather from dendritic, synaptic, and axonal degeneration (Burke and Barnes, 2006). Extensive BF volume reductions are predominantly associated with pathological conditions, such as AD (Teipel et al., 2005; Grothe et al., 2012; Kilimann et al., 2014), diffuse Lewy Body disease (DLBD) (Grothe et al., 2014), CBD (Kasashima and Oda, 2003), PSP (Tagliavini et al., 1984; Kasashima and Oda, 2003) or Parkinson's disease with dementia (Whitehouse et al., 1983).

At the cellular level, BF degeneration is visible as severe cell loss in the large neurons of the nucleus basalis of Meynert (Arendt et al., 1983; Whitehouse et al., 1983). Of the brain's cholinergic system, the BF constitutes the main source of cholinergic innervation to the cortical mantle (Mesulam, 2013b), while the midpontine nuclei provide cholinergic input to the thalamus and BF (Pepeu and Grazia Giovannini, 2017).

Within the BF, Ch1 and Ch2 provide the cholinergic innervation to the hippocampal complex and the hypothalamus, Ch3 to the olfactory bulb, and Ch4 to the rest of the cerebral cortex and amygdala (Mesulam, 2013b). Two highly organized and discrete bundles of cholinergic fibres originating from Ch4, have been designated as the medial and lateral cholinergic pathways. The medial pathway joins the white matter of the gyrus rectus; curves around the rostrum of the corpus callosum; enters the cingulum bundle; and supplies the parolfactory, cingulate, and retrosplenial cortices. The lateral pathway has a capsular division traveling in the external capsule and uncinate fasciculus and a perisylvian division traveling within the claustrum and extreme capsule. Branches of the perisylvian division supply the frontoparietal operculum, insula, and STG, whereas branches of the capsular division supply the remaining parts of the frontal, parietal, and temporal neocortex (Selden et al., 1998).

The major functional components of the cholinergic system include the acetylcholine synthesizing and degrading enzymes, choline acetyltransferase (ChAT) (DeKosky et al., 2002), and acetylcholinesterase (AChE) (Kuhl et al., 1999; Bohnen et al., 2003, 2005), respectively, the vesicular acetylcholine transporter (VAChT) to transport acetylcholine into the vesicles, the cholinergic muscarinic (mAChR) and nicotinic acetylcholine receptors (nAChR) for synaptic signaling (Schliebs and Arendt, 2011).

Reductions in a number of cortical cholinergic markers such as ChAT, mAChR, and nAChR as well as reductions in acetylcholine levels are

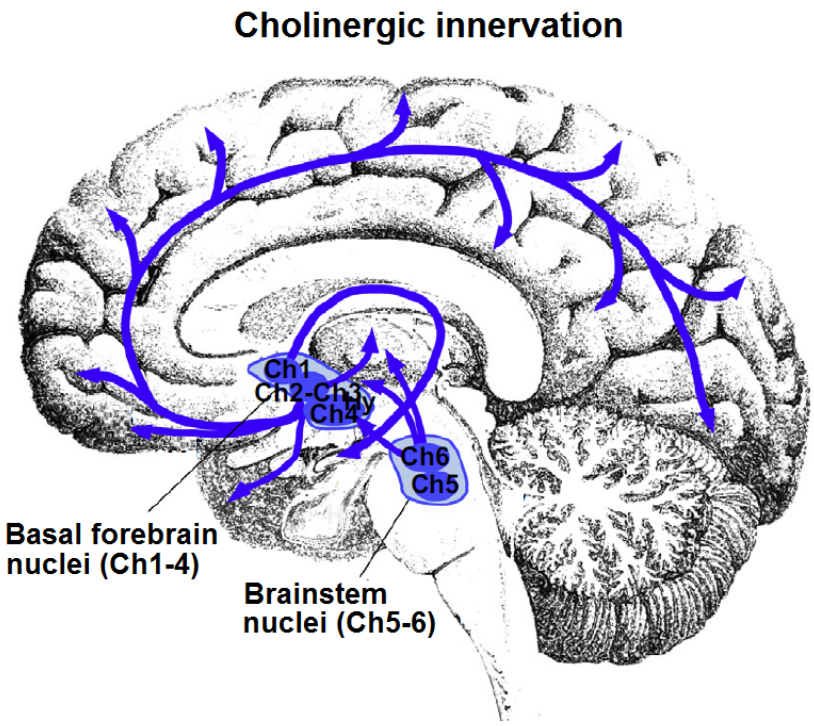


Figure 1.4: **The cholinergic system of the brain**. The cholinergic nuclei of the BF comprise the medial septum (Ch1), the horizontal and vertical diagonal band of Broca (Ch2 and Ch3), and the nucleus basalis of Meynert (Ch4) which provide the main cholinergic innervation of the cortical mantle. The midpontine nuclei are constituted of the peduncolopontine nucleus (Ch5), the dorsolateral tegmental nucleus (Ch6) and provide innervation to the thalamus among others. (Ch7-8) are not depicted. Modified with permission from Pepeu and Grazia Giovannini (2017).

correlated with clinical dementia severity (Bierer et al., 1995; Schliebs and Arendt, 2011). These findings led to the formulation of the cholinergic hypothesis of memory dysfunction in AD (Bartus, 2000). Abundant evidence showed that cholinergic dysfunction might be triggered by β-amyloid pathology (Schliebs and Arendt, 2011).

Beneficial effects of cholinomimetic medication such as AChE inhibitors or mAChR agonists on cognition have subsequently led to their regulatory approval in clinically probable AD. In DLBD (Shimada et al., 2009; Mazere et al., 2016) and PD (Hall et al., 2014), significant cholinergic dysfunction has been reported. However, regulatory approval for cholinomimetic medication has not (yet) been extended to other neurodegenerative syndromes. Moreover, it is currently unclear whether the reported BF atrophy in PPA also implies cholinergic depletion, which could potentially be treated by cholinomimetic medication.

1.7 Aims of the thesis

The general aim of this thesis is to study the syndrome of PPA at a behavioral, structural and molecular imaging level.

More specifically, in **chapter 3** we assessed how non-verbal processing of auditory stimuli across the domains of pitch, time/rhythm and timbre relates to specific aspects of speech and language in PPA. We also assessed whether performance on a subset of these auditory domains correlated with conventional language tests.

In **chapter 4**, the neural correlates accounting for deficient processing of nonlinguistic acoustic stimuli were determined by means of voxel-based morphometry (VBM) on high-resolution T_1-weighted structural magnetic resonance imaging (MRI) scans of a larger group of PPA patients.

In **chapter 5**, we examined the prevalence and nature of single-word comprehension problems in individual PPA patients with speech apraxia and/or agrammatism. We also assessed how these patients differed based on their atrophy pattern as well as on [^{11}C]-Pittsburgh Compound B ([^{11}C]-PIB) and [^{18}F]-THK5351 PET binding from healthy controls and other PPA variants. Neuropsychological performance in domains apart from single-word comprehension, motor speech and grammatical processing was also assessed and compared between groups.

In **chapter 6**, we tested the hypothesis that a cholinergic deficit may

exist in specific PPA variants given the BF atrophy reported in PPA (Teipel et al., 2014b, 2016). Cholinergic denervation estimated by AChE activity levels, was quantitatively measured in the neo- and allocortex using N-[^{11}C]-Methylpiperidin-4-yl propionate (PMP)-PET with arterial sampling and metabolite correction. Whole-brain and BF volumes were quantified using VBM.

Chapter 2

Experimental techniques

2.1 Non-linguistic auditory tasks

Non-linguistic auditory stimuli of three different auditory domains: pitch, time/rhythm and timbre/modulation were used in this PhD project. Here, we will briefly discuss the underlying rationale during the design of these particular tasks. The abbreviations used in this section: pitch (p), time/rhythm (r) and timbre/modulation (m) refer to the twelve tasks, of which a more detailed description will be provided in chapter 3 of this thesis. All tasks were designed to have structure that is relevant to speech. Speech has a complex acoustic structure based on spectro-temporal patterns at multiple time scales ranging from tens of milliseconds at the segmental level to the suprasegmental level of phrases and sentences spanning several seconds.

If we consider the auditory domain of pitch, its perception depends on the neural representation of the spectral (frequency) and temporal structure of acoustic stimuli. Complex patterns of pitch changes are embodied in spoken language. These pitch pattern changes establish stress locations and are used for segmentation of the speech stream (Foxton et al., 2003). Spoken language processing as well as reading depends critically more on global pitch pattern perception than on perception of absolute pitch values (Foxton et al., 2003). With this in mind, tasks were administrated during this PhD work which assessed fine-grained perception of pitch changes (p1) and recognition of change in pitch direction (p2) as well as discrimination of more complex patterns of local (p3) or global (p4)

pitch changes (Foxton et al., 2004). Measures of phonological skill have been associated with discrimination of more complex patterns of pitch changes (Grube et al., 2013).

In the time/rhythm domain, phonological skill has been associated with discrimination of single time-intervals (r1) (Grube et al., 2013) and with processing of short isochronous sequences (isochrony deviation detection, r2) (Grube et al., 2012). The flow of speech is commonly perceived as having a particular rhythmic pattern. Rhythm is a pivotal structuring element of speech which is crucially involved in segmentation processes, subserving language comprehension and acquisition (Geiser et al., 2008). To this end, our test battery also included a metrical pattern discrimination task (Grube and Griffiths, 2009), with either a strongly (r3) or a weakly (r4) metrical beat. Metrical pattern discrimination has been shown to correlate with poem reading skills (Grube et al., 2013).

As a third auditory domain, we investigated timbre processing. Timbre is defined operationally as the property that distinguishes two sounds of identical pitch, duration, and intensity (Warren et al., 2005). In the timbre/modulation domain, frequency modulation (FM) and more complex spectro-temporal modulation patterns (Dynamic Modulation: DM, expressed as spectral (cycles/octave, cpo) and temporal rate (cycles/sec, cps) (Chi et al., 1999)) are relevant to speech perception (Drullman, 1995; Shannon et al., 1995; Boemio et al., 2005; Giraud and Poeppel, 2012). Auditory FM sensitivity has been shown to correlate with phonological skill in young children (Talcott et al., 2000). Specifically, 2 Hz FM (m1) corresponds to a temporal window relevant to slow, prosodic variations and 40 Hz FM (m2) to fast phonemic variations. DM underlying timbre in speech is necessary for comprehension by human listeners and for vocal gender identification (Elliott and Theunissen, 2009). The DM tasks used during this PhD work (DM detection (m3) and DM discrimination (m4)), assess mechanisms relevant to the processing of complex spectral patterns that change over time, like formant changes in speech perception (Chi et al., 1999; Elliott and Theunissen, 2009). DM detection (m3) has previously been shown to relate to speech comprehension in acquired Wernicke's aphasia (Robson et al., 2013) and DM discrimination (m4) scores correlated with speech and language skills in children with dyslexic traits (Grube et al., 2014).

These stimuli have previously been intensively investigated in a wide range of behavioral studies in children and young adults with typical and atyical language development (Foxton et al., 2003; Grube et al., 2012, 2013, 2014), patients with congenital amusia (Foxton et al., 2004),

Wernicke's aphasia (Robson et al., 2013) and patients with cerebellar degeneration or basal ganglia dysfunction (Grube et al., 2010; Cope et al., 2014) or in experiments using continuous transcranial magnetic theta-burst stimulation over the medial cerebellum in healthy individuals (Grube et al., 2010). In this thesis, we will apply the same psychoacoustic battery in PPA patients and matched healthy control subjects.

2.2 Magnetic resonance imaging

Magnetic resonance imaging (MRI) is a powerful non-invasive imaging technique to visualize anatomy and physiology of the human body (Grover et al., 2015). In the study of neurodegenerative diseases such as AD, MRI is the most widely used imaging modality. It is based on the physical principle that hydrogen atoms (protons), which are abundantly present in human tissue, possess a nuclear spin which can be manipulated by external magnetic fields. In the absence of an external magnetic field, the direction of these spins is random and therefore the net magnetization will approach zero. When a subject moves into an MRI scanner, the nuclear spins align with the external magnetic field (B0) (usually 1.5 or 3 Tesla (T)) and precess around an axis parallel to the direction of B0 (the z-axis). The precession frequency (i.e. the Larmor frequency) is proportional to the main magnetic field strength. This results in a net magnetization proportional to the strength of B0. If a perpendicular radiofrequency (RF) pulse at the same frequency as the Larmor frequency is given in the plane perpendicular to B0 (xy plane) at a certain flipping angle, the spins tilt away and enter an excitation state (high energy state). Hence the longitudinal magnetization (z-axis) decreases and the transverse magnetization (xy plane) increases. As soon as the RF pulse is terminated, the spins will gradually return to the earlier equilibrium state (low energy state) parallel to B0 by means of two relaxation phenomena. In one of these relaxation phenomena, spins release their energy to the surrounding lattice as they return to their low energy state. As a result, the longitudinal magnetization (z-axis) recovers in an exponential way, which can be characterized by the time constant T_1. This is the time point at which the longitudinal magnetization (z-axis) has reached 63% of its original value again. The second type of relaxation is the spin-spin relaxation, whereby each spin experiences a slightly different magnetic field due to differences in their chemical environment. This results in spins obtaining slightly different precession frequencies which causes an overall loss of phase coherence. This process

is characterized by the time constant T_2, which describes how much time it takes for the transverse magnetization (xy plane) to drop to 63% of the original signal. The fact that these time constants are tissue specific, is exploited by weighting the MRI acquisition sequences more heavily to these effects in order to generate contrast between tissues.

In order to spatially localize the protons, the measured signal is encoded by three small linear magnetic gradients superimposed on the external magnetic field B0. Usually, a first gradient is applied during the RF pulse to select the slice or volume to be measured: the applied pulse frequency will only excite those spins with the same precession frequency, i.e. at a known location in the magnetic field. A phase-encoding gradient is briefly applied to cause a position-dependent shift of the signal in time: spins will dephase faster where a higher gradient strength is applied. Finally, during read-out, a frequency-encoding gradient is applied, altering the precession frequency based on field strength. The transverse magnetization induces an alternating current in the receiver RF coils around the subject's head placed along the xy plane. This produces the imaging signal: a sum of sine waves where each combination of phase and frequency identifies a given spatial location. By applying an inverse Fourier transformation, this signal can be decomposed from the frequency domain back to the spatial domain (Grover et al., 2015), which results in a visual interpretable MRI image.

2.2.1 Voxel-based morphometry

As described in the previous section, a T_1-weighted structural MRI gives optimal contrast between gray and white matter. This makes it ideally suited for voxel-based morphometry (VBM) (Ashburner and Friston, 2000). VBM is a technique which can be used to quantify gray matter volumes. A first step in this procedure involves removal of MRI inhomogeneities and noise, followed by segmenting the T_1-weighted structural MRI. Segmentation allows characterizing the intensity distributions of tissue classes including gray matter, white matter and cerebrospinal fluid (CSF). Every voxel in the image is assigned a probability of belonging to each of those classes based on its intensity and its spatial location. First, a voxel's intensity is compared to a Gaussian mixture model where the intensity distribution of each tissue class is modelled by a Gaussian function. Second, the spatial location of a voxel can be taken into account after the subject's image has been normalized to a standard space (usually Montreal Neurological Institute

(MNI) space) which holds *a priori* tissue probability maps. The high-dimensional normalization process involves an affine step which includes translation, rotation, scaling, shearing and a non-linear warping step.

To compensate for volumetric differences introduced by the spatial normalization process, voxel values in the segmented image can be multiplied by the local value in the deformation field obtained form the normalization process. This basically weighs (modulates) the intensity of a voxel by the amount of volume change applied to it, resulting in modulated gray matter volume images which can be used for gray matter volume quantification. Besides the application of VBM, automated techniques that have been used to study neurodegeneration in PPA include cortical thickness mapping (Rogalski et al., 2011b) and tensor-based morphometry (Brambati et al., 2007).

2.3 Positron emission tomography imaging

PET is a minimally invasive imaging technique which enables the study of biologic function by spatially detecting radionuclides incorporated in a PET tracer which has a biological target (Lameka et al., 2016).
Proton-rich radionuclides produced in a cyclotron, such as ^{18}Fluor or ^{11}Carbon, contain an unstable nucleus, which make these atoms prone to decay into a more stable nucleus. During this decay, a proton is converted into a neutron while releasing a positron. This positron will react almost immediately with its antiparticle, an electron. During the annihilation process, the mass of the two particles is transformed into two photons of 511 keV, emitted in opposite directions at approximately 180 degrees between each other. Simultaneous detection of these two photons by detectors in the PET scanner (i.e. scintillator crystals) is interpreted as one annihilation event. Subsequently, photomultiplier tubes connected to the scintillator crystals transform the signal of these photons into an electric current, which is further amplified to produce a measurable signal. An electronic coincidence circuit evaluates the timing of the absorbed photons and only the pairs of photons which are detected nearly simultaneously (within 10 ns) along the line connecting the two detectors of the PET scanner in space, are passed through. The measured coincidence events (annihilations) can be stacked into 2D projection images called sinograms, which show the number of coincidence events across each line for a given angle.

Photons can however be attenuated and scattered by travelling through

the subject's tissue. Prior to reconstruction, the data are therefore first preprocessed to correct for attenuation, random occurrences, and scatter. The attenuating properties of the tissues are measured, usually by a low dose CT scan *prior* to the PET scan (in case of a PET/CT scanner) in order to estimate the fraction of lost signal. In case of the GE Signa 3T PET/MR scanner (GE Healthcare, Chicago, USA) described in chapter 5 of this thesis, attenuation correction is based on an attenuation map representing the linear attenuation coefficient. For each PET bed, an MRAC (MRI based Attenuation Correction) scan is acquired based on Lava-Flex axial images. The MRAC processing exists of the reconstruction of both the *in vivo* (patient) attenuation map and the *ex vivo* (non-patient objects) attention map. The latter takes into account hardware such as the patient cradle and the RF coils, and are generated based on templates stored in the database which are constructed based on CT images. In the head region, the attenuation map is constructed based on the segmentation of the MRI image into four tissues (air, lung, fat, tissue). The attenuation for the skull bone is included based on an atlas-based approach. This method has been validated against PET/CT data.
After correction has been applied to account for lost signal, sinograms are reconstructed to visually interpretable PET images by means of 'back-projecting' the data: i.e. assigning the value measured on a particular line to that entire line, for each angle. This is usually done in an iterative way by expectation-maximization algorithms which optimize the likelihood that the given data points are generated by a model of which the parameters are continually refined. The resulting PET image reflects the binding pattern of the PET tracer to its molecular target.

2.3.1 Quantification of PET signal

To date, only visual assessment of amyloid PET scans is currently approved by the health authorities (Vandenberghe et al., 2013). Quantification based methods such as compartment kinetic models, distribution volume ratio (DVR) or standardized uptake value ratio (SUVR) calculations are however also appropriate methods to assess PET tracer binding.

Kinetic models involve fitting the observed data to mathematical models of tracer behaviour. For novel tracers, the comprehensive mathematical model includes all variables that could be relevant. A comprehensive model requires a long dynamic scan starting at the time of bolus injection

to chart tracer uptake and clearance over time in the brain (i.e. used for fitting time activity curves (TAC)), as well as an estimate of the plasma input function. This plasma input function is derived from the measured radioactivity concentration in arterial blood samples taken at various time intervals after tracer injection. When radiolabelled metabolites are present that do not pass the blood-brain barrier (BBB), the radioactivity associated with these metabolites must first be determined. This can be achieved by separating metabolites from intact tracer by high performance liquid chromatography. The plasma input function should consequently be corrected for metabolites by applying a constrained Hill model as metabolite correction function (metabolite-corrected plasma input TAC). With the metabolite-corrected plasma TACs as input, regional brain TACs are fitted to a theoretical comprehensive mathematical model, which is characterized by different rate constants including one for influx (K_1, min^{-1}) and efflux (k_2, min^{-1}) across the blood-brain barrier, depending on the compartment kinetic model used (Koeppe et al., 1999).

A drawback of these models is that they rely on arterial sampling, which is burdensome to the patient. For this reason, alternative methods such as the reference tissue model are preferred. This method allows quantification of tracer kinetics without measuring the arterial input function, thus avoiding arterial cannulation and time-consuming metabolite measurements (Salinas et al., 2015). A reference region devoid of the biological target of interest can also be applied in Logan graphical analysis (Logan et al., 1996). Logan graphical analysis compares an input function to a TAC using a non-iterative solution to a multi-compartmental model for tracer behavior. The result is a 'slope' that is equal to the tracer distribution volume (DV) in the tissue of interest when compared to the input function from this reference region. For [^{11}C]-PIB PET analyses, the cerebellar cortex is usually used as a reference region (Mintun et al., 2006), resulting in parametric DVR images. A further simplification can be to calculate SUVR images based on the static images at later timepoints, in which the PET tracer reached a steady state (plateau phase), divided by the uptake in a reference region (e.g. the cerebellar cortex).

An important confound in quantification of PET images are partial volume effects (PVE) (Rousset et al., 2007). These effects occur when the tissue of interest (e.g. gray matter) is smaller than the sampling resolution of the imaging technique (about 4 to 8 mm Full-Width at Half Maximum (FWHM) for PET). The measured signal results in an averaging of effects in the tissue of interest and surrounding tissues within

an image voxel. PVE has the net effect of making small objects appear larger but less intense, since the total number of counts is preserved. This especially poses a problem when the effect of interest involves assessing decreases of tracer binding (e.g. hypometabolism measured with [^{18}F]-FDG-PET). In such cases, a decreased PET signal could result from a genuine decrease in tracer binding, from atrophy or from a mixture of both. To disentangle these effects, partial volume correction (PVC) algorithms are applied which attempt to correct the measured PET signal by modelling it as a combination of effects in the various tissue classes (usually gray matter and white matter derived from the MRI segmentations) taking into account the proportion of those tissue classes (Müller-Gärtner et al., 1992).

2.3.2 PET tracers

In this PhD project three different PET tracers have been used:

1. [^{11}C]-Pittsburgh Compound B ([^{11}C]-PIB) (N-methyl-[^{11}C]2-(4'-methylaminophenyl)-6-hydroxybenzothiazole)
2. [^{18}F]-THK5351 (6-[(3-[^{18}F]-2- hydroxy)propoxy]-2-(4-methylaminopyridyl) quinoline)
3. [^{11}C]PMP (N-[^{11}C]-Methylpiperidin-4-yl propionate)

[^{11}C]-PIB is a thioflavin T derived PET tracer (Klunk et al., 2004) with high affinity for β-amyloid (K_d = 1-3 nM,), over α-synuclein, and posphotau. Direct comparison to *post mortem* tissue within the same subjects has shown that the [^{11}C]-PIB PET signal mainly reflects specific binding to neuritic plaques and to depositions in blood vessel walls (cerebral amyloid angiopathy, CAA). Binding to diffuse plaques was much less prominent (Klunk et al., 2004).

[^{18}F]-THK5351 is considered to have a high binding affinity for PHF tau aggegrates (K_d = 2.9 nM), over β-amyloid, α-synuclein, and TDP-43 (Harada et al., 2016). Recent PET-imaging studies with [^{18}F]-THK5351 have shown elevated binding in disease-specific regions in AD, CBD and PSP patients compared to controls (Harada et al., 2016; Kikuchi et al., 2016; Ishiki et al., 2017).

[^{11}C]PMP is a lipophilic analog of ACh which diffuses into the brain and becomes metabolized by AChE into a hydrophilic metabolite, which is trapped at the site of its production (Irie et al., 1996). Based on a comprehensive kinetic model, the rate of ACh hydrolysis can be calculated and this provides an index of AChE activity (Irie et al., 1996). [^{11}C]PMP

has been shown to be selective for AChE over butyrylcholinesterase (BChE) (Kuhl et al., 1999).

2.4 Statistical analysis of imaging data

Prior to statistical analysis, images are spatially smoothed with FWHM Gaussian kernels in order to enhance the signal-to-noise ratio, to compensate for residual anatomical variability due to registration errors and inter-subject differences, and to allow the use of Gaussian Random Field Theory (RFT). Statistical inference about images can be made either by volume of interest (VOI) based approaches or whole-brain voxel-based analysis. The latter is usually preferred because of its unbiased nature, since it is independent of VOI definitions. Within the framework of Statistical Parametric Mapping (SPM, Wellcome Trust Centre for Neuroimaging, London, UK), parametric statistics are performed in every voxel. Due to the large set of voxels contained in an image, a correction for multiple comparisons is needed to account for the number of false positive incidences. Since neighbouring voxels, and therefore the statistical tests, are not independent, a Bonferroni correction would be too conservative. A commonly used alternative method, which has been implemented in SPM, is the family-wise error (FWE) correction based on Gaussian RFT. The FWE gives the likelihood that we are accepting that the observed set (family) of voxels has arisen by chance only, taking into account the number of 'independent observations'. In the case of SPM, this number is smaller than the actual number of voxels and is determined based on Gaussian RFT, a mathematical approach to define theoretical results for smooth statistical maps. More specifically, the smoothness of the statistical map is estimated, taking into account both its inherent and applied smoothness. This is used to determine the number of resels (resolution elements) in the image, whereby a resel is simply defined as a volume of voxels of the same size as the FWHM of the smoothness of the image. FWE corrected p-values can be generated for peak height (highest Z value) and cluster extent (number of contiguous voxels above a given Z value). These two measures are often combined to assess the significance of a result. Cluster-level inferences are generally more sensitive than peak-level inferences but at the expense of reduced localizing power. In this thesis the default statistical threshold for all voxelwise statistical analyses was set at voxel-level uncorrected $p < 0.001$, with a cluster-level FWE-corrected threshold $p < 0.05$ (Poline et al., 1997).

Chapter 3

Core auditory processing deficits in PPA

This study is published as a shared first author paper:

Grube,M*, Bruffaerts,R*, Schaeverbeke,J*, Neyens,V, De Weer,AS, Seghers,A, Bergmans,B, Dries,E, Griffiths,TD, Vandenberghe,R (2016). Core auditory processing deficits in primary progressive, Brain 139(6), 1817-1829.

* = *first authors*

3.1 Abstract

The extent to which non-linguistic auditory processing deficits may contribute to the phenomenology of primary progressive aphasia (PPA) is not established. Using non-linguistic stimuli devoid of meaning we assessed three key domains of auditory processing (pitch, time/rhythm, and timbre) in a consecutive series of 18 patients with PPA (eight with semantic variant (SV), six with nonfluent/agrammatic variant (NFV) and four with logopenic variant (LV)), as well as 28 age-matched healthy controls. We examined whether performance on the psychoacoustic tasks in the three domains related to the patients' speech and language profile.

At the group level, patients were significantly impaired in the three domains. Patients had the most marked deficits within the rhythm domain for the processing of short sequences of up to seven tones. Patients with NFV showed the most pronounced deficits at the group and the individual level. A subset of the SV patients were also impaired, though less severely. Patients with LV did not show any significant individual impairments. Significant deficits remained after partialling out effects of executive dysfunction. Performance on a subset of the psychoacoustic tests correlated with conventional verbal repetition tests. A core central auditory impairment exists in PPA for nonlinguistic stimuli. While NFV PPA is clinically characterized by a motor speech deficit (output problem), perceptual processing of tone sequences is clearly deficient. This may indicate the co-occurrence in the NFV of a deficit in working memory for auditory objects. Parsimoniously we propose that auditory time processing pathways are altered which are used in common for processing acoustic sequence structure in both speech output and acoustic input.

3.2 Introduction

Primary progressive aphasia (PPA) is characterized by progressive word finding difficulties caused by selective neurodegeneration of the language and speech network (Mesulam et al., 2014b). Depending on the subtype (Gorno-Tempini et al., 2011), the word finding problems may be accompanied by word comprehension and object recognition deficits, as in the semantic variant (SV) (Hodges et al., 1992); speech apraxia or agrammatism may be most prominent, as in the nonfluent/agrammatic variant (NFV) (Grossman, 2012); or phonological working memory deficits may cause deficits repeating series of numbers and complex sentences, as in the logopenic variant (LV) (Gorno-Tempini et al., 2004b, 2008; Mesulam et al., 2012). While the core clinical phenotype in PPA is by definition dominated by the verbal communication difficulties, the concomitance of nonverbal deficits of object recognition and object knowledge are a well-documented and defining feature of SV (Hodges et al., 1992; Gorno-Tempini et al., 2011). In subtypes distinct from SV, experimental studies have unveiled deficits in nonverbal domains e.g. related to ideomotor praxis (Adeli et al., 2013) and gesture discrimination (Nelissen et al., 2010). The study of combined verbal and nonverbal deficits may yield a unique view on ontogenetic and neuroanatomical bonds between language and specific nonverbal processes in the intact brain and inform hypotheses about the pathogenesis of the language dysfunction.

The purpose of the current study was twofold: at the basic neuroscience level to evaluate how language and speech relate to core auditory analysis of pitch, time/rhythm and timbre, and at the clinical level, to examine how deficits in nonverbal sound processing relate to the pathogenesis of clinical symptoms in PPA.

For pitch (Patterson et al., 2002), time/rhythm (Teki et al., 2011) and timbre (Overath et al., 2008, 2010), extensive processing occurs in areas beyond primary auditory cortex, especially at higher levels of complexity or longer temporal windows of integration. Compared to earlier studies (Bozeat et al., 2000; Warren et al., 2005; Goll et al., 2010, 2011; Hailstone et al., 2011; Hsieh et al., 2011, 2012; Omar et al., 2011; Rohrer et al., 2012; Fletcher et al., 2013a), our approach was unique in the systematic nature of the investigation of the three domains within the same patients across the range of PPA subtypes. Moreover, we focused entirely on auditory processing levels of non-linguistic stimuli preceding the association with meaning (be it verbal meaning, emotional content or identity). As a

third important distinction from previous work, we assessed pitch and time judgments for sequences of tones up to seven tones while previous paradigms when using non-linguistic stimuli focused on single tones or pairs of tones. The tasks and stimuli we used have been previously applied in children and young adults with typical and atypical language development (Foxton et al., 2003; Grube et al., 2013, 2014), patients with congenital amusia (Foxton et al., 2004), patients with Wernicke's aphasia (Robson et al., 2013) and patients with cerebellar degeneration or basal ganglia dysfunction (Grube et al., 2010; Cope et al., 2014). The non-linguistic acoustic stimuli used were designed to have structure that is relevant to speech and language processing at different levels from individual phonemes to sentences. In the pitch and time domain, the structure varied between single pitch or time intervals and sequences of pitch or time intervals. In the timbre domain, we also changed features over different timescales that correlate with phoneme or sentence-level analysis. In both domains of pitch and time/rhythm, sequence processing has been related to prosodic processing and segmentation processes in speech and to language skills in children (Grube et al., 2012) and young adults (Foxton et al., 2003; Grube et al., 2013). In the timbre domain, Frequency Modulation (FM) and more complex spectro-temporal modulation patterns (Dynamic Modulation: DM) are relevant to speech perception (Drullman, 1995; Shannon et al., 1995; Boemio et al., 2005; Giraud and Poeppel, 2012). Specifically, 2 Hz FM corresponds to a temporal window relevant to slow, prosodic variations and 40 Hz FM to fast phonemic variations. The DM tasks assess mechanisms relevant to the processing of complex spectral patterns that change over time, like formant changes in speech perception (Chi et al., 1999; Elliott and Theunissen, 2009). DM detection has been previously shown to relate to speech comprehension in acquired Wernicke's aphasia (Robson et al., 2013) and DM discrimination scores correlate with speech and language skills in children with dyslexic traits (Grube et al., 2013).

We assessed how auditory perception across the domains of pitch, time/rhythm and timbre relates to specific aspects of speech and language skill in PPA.

3.3 Material and Methods

3.3.1 Subjects

The study was approved by the Ethics Committee, University Hospitals Leuven. All participants provided written informed consent in accordance with the Declaration of Helsinki. PPA patients were recruited via the memory clinic University Hospitals Leuven (Table 3.1). A consecutive series of 23 patients who fulfilled the international consensus criteria for PPA (Gorno-Tempini et al., 2011) enrolled for the experiment (Table 3.1). Five of the subjects had to be excluded for the following reasons: peripheral hearing loss (one); lack of ability to perform the experimental tasks according to practice runs due to disease severity (two); lack of cooperation (one); unique phenotype (foreign accent syndrome). The remaining 18 participants were able and sufficiently cooperative to undergo the extensive psychoacoustic testing and produce reliable data. Before study participation, each PPA patient was classified according to the Gorno-Tempini et al. (2011) recommendations. The classification relied on the clinical evaluation by an experienced neurologist, in combination with neurolinguistic assessment and clinical MRI, as well as, where available, [^{18}F]-fluoro-deoxy-glucose positron emission tomography ([^{18}F]-FDG-PET), cerebrospinal fluid (CSF) AD biomarkers and [^{11}C]-PIB amyloid PET (Table 3.1). Eight cases were classified as SV, six as NFV, and four as LV PPA (Table 3.1) (Gorno-Tempini et al., 2011). The SV and LV groups each showed a relatively homogeneous classical phenotype (Gorno-Tempini et al., 2011). All NFV cases had speech apraxia with buccolingual apraxia. In one NFV (running case number 6), speech apraxia was by far the most prominent clinical abnormality, with no apparent agrammatism and preserved comprehension. According to the Josephs et al. (2013b) terminology, this case could also possibly be classified as primary progressive apraxia of speech (PPAOS or AOS), at least during the initial disease phase when she underwent the experimental tests. NFV case numbers 13 and 15 had agrammatism in addition to speech apraxia. Cases 20-22 also had word comprehension deficits on detailed testing besides agrammatism and speech apraxia, with, in addition, object recognition problems in case 21 and 22 (Table 3.1). While we included these subjects in the NFV group, the latter three cases would also fit into the recently defined 'mixed' subtype (Mesulam et al., 2012, 2014b). An [^{18}F]-FDG-PET scan was available in fifteen of the cases and a volumetric MRI in seventeen cases (case 10 had claustrophobia and received [^{18}F]-FDG-PET only). The NFV group

showed volume loss and hypometabolism in the left frontal opercular, left anterior insular and left supplementary motor area (SMA) (Fig. 3.2A). The SV cases showed anterior temporal and orbitofrontal abnormalities, strictly conforming to the expected pattern Gorno-Tempini et al. (2011) (Fig. 3.2B). The LV group showed a more heterogeneous pattern, with clear posterior temporal hypometabolism in case 9, premotor involvement in case 11 and ventral temporal hypometabolism in case 4.

Twenty-eight age- and education-matched cognitively intact controls (half of them male, age range 51 to 76 years, mean 62.2, SD 7.8 years; education range 9 to 22 years, mean 14.0, SD 2.8 years) completed the same experimental psychoacoustic test battery as the PPA patients. All subjects also underwent a full neuropsychological assessment.

For the purpose of comparing brain volume in the PPA subtypes with that of a normal control group, we made use of a large group of 86 healthy age- and gender-matched controls subjects (47 male; age range 53-76 years, mean 64.9, SD 5.9 years, Mini-mental state examination (MMSE) score > 27 and Clinical Dementia Rating scale (CDR) $= 0$). This normative MRI cohort included, among others, 22 of the controls from the psychoacoustic experiment (the remaining six controls refused MRI or had a medical contraindication).

Hearing sensitivity was measured in all participants using a clinical Bekesy-type audiometer for frequencies of 0.5, 1, 2, 4, and 8 kHz, on the left and right ear, respectively. In the pure-tone audiograms, all subjects were able to detect stimuli of up to 1000 Hz below a Hearing Level of 30 dB on at least one side. There were no significant differences between left and right ear hearing levels (two-tailed t-test, $p = 0.14$).

3.3.2 Neuropsychological protocol

Confrontation naming was assessed by means of the Dutch version of the Boston Naming Test (BNT) (Mariën et al., 1998). Single-word comprehension, sentence comprehension and repetition were evaluated by means of tests selected from the Psycholinguistic Assessment of Language Processing in Aphasia (PALPA) and the Akense Afasie test (AAT). Nonverbal executive functioning and fluid intelligence was evaluated by means of the Raven's Coloured Progressive Matrices (CPM). The Birmingham Object Recognition Battery (BORB) test (easy (B) and hard (A)) was used as a measure of object identification. The verbal associative-semantic test of the PALPA (PALPA subtest 49) and the

picture-version of the Pyramids and Palm trees test (PPT) was used to measure semantic-associative capacity (Table 3.1). Although it was not part of the neuropsychological protocol of the study, we retrieved the digit span forward scores from the clinical patient files where available (Table 3.1).

3.3.3 Experimental tests of acoustic processing

The psychoacoustic battery consisted of four pre-existing tasks of pitch, time/rhythm and timbre each (Grube et al., 2012, 2014). Sound was generated by means of a Roland UA-4FX audio/MIDI interface with Sennheiser HD linear 250-II/280 headphones. Sound intensity was adjusted individually from a fixed value to a comfortable level where needed, within a range of 65 to 80 dB Sound Pressure Level. The tasks were implemented in Matlab (version 7.2.0, Mathworks, Natick, MA, USA).

A schematic representation of all tasks is provided in Figure 3.1. Depending on preference and ability, subjects responded verbally, by pressing keys on the keyboard, or by pointing to the corresponding interval on a graphical scheme reflecting the trial structure in front of them (a piece of paper in front of the subjects showing two or three circles, depending on the task assessed). Each subject responded using a same response modality for all tasks. Prior to each task, we explained to the subject which auditory domain was being probed. The instructions were repeated to the subject as needed until he or she confirmed to fully understand the task. We presented the instructions verbally, and also in a graphical way and by simple examples.

Before acquisition of each psychoacoustic task, subjects had to pass a number of practice trials of that task (minimum five). The difficulty level of the practice trials was the same for all subjects at the start for each task. If an incorrect response was given on a practice trial, the subject received feedback on the nature of the error. Practice trials and instructions were repeated until five consecutive correct responses were recorded. If needed, the starting level was decreased in difficulty level. The difficulty level at the start of the test trials was the same as in the practice trials. If the subject indicated during the test trials that they had forgotten the instructions, the task was aborted, the instructions repeated, practice trials run again and the test phase then re-started.

Adaptive tracking procedure and threshold estimation

Two tasks (see below: p3, p4) used a same-different paradigm with fixed difficulty levels (Foxton et al., 2003), with the score correct as the outcome measure. The remaining 10 tasks used a two-alternative forced-choice adaptive paradigm following a two-down, one-up algorithm (difficulty level increased after 2 consecutive correct responses and decreased after every incorrect one). A larger step size was used up to the fourth reversal and after that a smaller one. The outcome measure was the perceptual threshold, calculated as the mean over the last six reversals measured with the small step size, estimating the 70.9%-correct point of the psychometric function (Levitt, 1971). A high perceptual threshold indicated impairment on that task.

Pitch

The basic change in pitch detection task (p1; 50 trials) (Fig. 3.1A) required pure tones to be discriminated based on their frequency. On each trial, the subject was presented with two pairs of tones with a tone duration of 250 ms and an interval of 2000 ms between pairs. The target pair contained a change in frequency (up or down), the reference did not. The centre frequencies for the two pairs were roved independently in the range of 500 Hz $\pm$ 3 semitones in a pseudo-randomized, fixed order. The magnitude of the change in frequency within the target pair had a default starting value of five semitones, adaptively adjusted in steps of 0.8 and 0.2. The task of the subject was to identify the pair that included the change in frequency. The outcome measure was the perceptual threshold obtained by adaptively adjusting the size of the change in frequency.

The pitch change direction discrimination task (p2; 50 trials) (Fig. 3.1A) required two pairs of pure tones to be judged as 'same' or 'different' based on the direction of the changes in frequency within the pairs (same-different judgement). The frequency within either pair could either go 'up' or 'down', and the two pairs could thus either have the 'same' or 'different' directions. The combination of directions was pseudo-randomized in a balanced, fixed order across trials, with equal numbers of 'same' and 'different' pairs going 'up' and 'down'. The centre frequencies for the two pairs were in the range of 500 Hz $\pm$ 3 semitones, roved between trials and pairs. The change in frequency within pairs had a default starting value of five semitones, adaptively adjusted in steps of 0.8 and 0.2. The

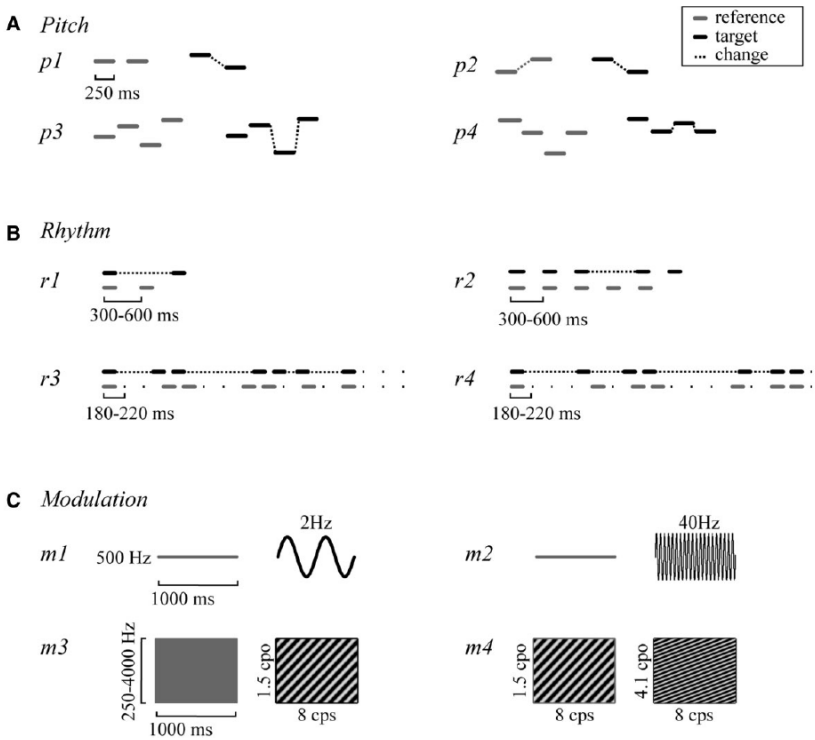


Figure 3.1: **Schematic illustration of experimental tasks, with one reference and one target example depicted per task**. **(A)** Pitch: basic change detection (p1), change-direction discrimination (p2), detection of a local change in pitch sequence (p3), detection of a global change in pitch sequence (p4). **(B)** Rhythm and timing: single time-interval discrimination (r1), isochrony deviation detection (r2), metrical pattern discrimination for a strongly (r3) and a weakly metrical sequence (r4). **(C)** Modulation (timbre): 2 Hz frequency modulation (FM) detection (m1), 40 Hz FM detection (m2), dynamic modulation (DM) detection (m3), dynamic modulation discrimination (m4). Note: x- and y-axes correspond to time and frequency throughout, but scales vary and are in part arbitrary.

outcome measure was the perceptual threshold obtained by adaptively adjusting the size of the change in frequency.

The local and global change in pitch detection tasks (p3, p4; 40 trials) (Fig. 3.1A) used pitch sequences of five tones each with a duration of 250 ms, separated by an inter-stimulus-interval of 2000 ms (in-between sequences) and required the subject to indicate whether two sequences were 'the same' or 'different' (adapted from Foxton et al. (2003)) (same-different judgement). In the local change detection task (p3), in the 'different' pairs, there was one change in frequency in the third or fourth note in the second sequence compared to the first, but the patterns of 'ups and downs' remained preserved. In the global change detection task (p4) in contrast, the change in frequency in the third or fourth tone caused a change also in the global contour, i.e. in the pattern of 'ups and downs'. Each task contained 40 trials, including 20 'same' and 20 'different', with each reference sequence occurring once in a 'same' and once in a 'different' trial, in a pseudo-randomized fixed order. The outcome measure was the score correct (a low score indicated impairment).

Rhythm and timing

All four rhythm and timing tasks (Fig. 3.1B) used 500 Hz, 100 ms pure-tones. The basic single time-interval duration discrimination task (r1; 50 trials) (Grube et al., 2010) required subjects to indicate which of two tone pairs comprised the 'longer gap' than the reference of varying duration with inter-onset interval of 300 to 600 ms (roved in 60 ms steps, in pseudo-randomized, fixed order). The initial default difference in the target being longer was by 90% of the reference inter-onset-interval, and adaptively adjusted in steps of 12% and 6%.

In the isochrony deviation detection task (r2; 50 trials) (Grube et al., 2012), subjects were required to indicate which of two otherwise isochronous five-tone sequences contained a lengthening or 'extra gap'. The target pair had one lengthened inter-onset-interval between the 3rd and 4th tone, the reference sequence had an isochronous inter-onset interval ranging from 300 to 600 ms (roved in 60 ms steps), and the target had one lengthened interval after the 3rd tone. The initial default value of the lengthening was 60% of the inter-onset-interval, adaptively adjusted in steps of 6% and 2%.

In the metrical pattern discrimination tasks (r3, r4; 50 trials) (Grube and Griffiths, 2009), subjects were required to decide which of three

rhythmic sequences of seven tones each sounded 'different', or 'wrong', based on a distortion (or change) in the rhythm. The reference sequence had a strongly (r3) or a weakly (r4) metrical beat of four evoked by the temporal spacing of the tones over 16 time units of 180-220 ms each (roved between stimuli). In the strongly metrical sequence, accented tones occurred every four units, in the weakly metrical sequence, two of those were silent (for more details see Grube and Griffiths (2009)). The default initial distortion in pattern (a change in the long compared to the short intervals) was 65%, adaptively adjusted in steps of 12% and 6%. The outcome measure for each of the tasks was the perceptual threshold obtained by adaptively adjusting the difference between reference and target stimuli. The difference was measured relative (in percent) to the duration or tempo of the reference.

Timbre/Modulation

The four tasks of timbre (modulation) perception (Fig. 3.1C) (Grube et al., 2012) included two frequency-modulation (FM) detection tasks (m1 and m2), one spectro-temporal, dynamic modulation (DM) detection (m3) and one DM discrimination (m4) task, testing the processing of modulations thought to be relevant to speech (Witton et al., 1998; Chi et al., 1999; Talcott et al., 2000; Schönwiesner and Zatorre, 2009; Grube et al., 2012; Robson et al., 2013).

In the two FM detection tasks (m1, m2; 50 trials) (Grube et al., 2012), subjects were required to identify a tone (duration 1000 ms) modulated at a rate of 2 Hz (sounding 'ringing or wobbly') and 40 Hz (sounding 'rough'), respectively, against a 'flat-sounding' unmodulated 500 Hz reference. The initial magnitude of modulation, expressed by the modulation index (MI: ratio of maximum frequency deviation to modulation frequency) was 3.5 for the 2 Hz FM (equalling $\pm$ 7 Hz maximum deviation from the carrier frequency of 500 Hz), adapted in steps of 0.39 and 0.13. For the 40 Hz FM, the default initial MI was 0.16 (equalling $\pm$ 6.4 Hz maximum frequency deviation for the carrier), adapted in steps of 0.13 and 0.06.

The DM detection task (m3; 50 trials) (Grube et al., 2012) required the discrimination of a modulated ('alien or laser-like') target sound against an unmodulated reference. The stimuli consisted of 400 components, logarithmically spaced across four octaves from 250 to 4000 Hz (Robson et al., 2013). Components' amplitudes were sinusoidally modulated in frequency (spectral) and time (temporal) with a rate of 1.5 cycles per octave (cpo) and 8 cycles per second (Hz), respectively. These rates also

occur in speech (Chi et al., 1999), but the sounds have no resemblance to any natural speech sounds. All stimuli had an upward drift in spectral peaks over time. Default initial modulation depth was 0.75, adaptively adjusted in steps of 0.075 and 0.025. On each trial, two 1000 ms sounds were presented and subjects had to identify the modulated one.

The DM discrimination task (m4; 50 trials) (Grube et al., 2012) required the discrimination of such spectro-temporal modulation sounds based on a difference in spectral modulation rate density. Dynamic modulations in the target stimuli may result in perceived differences in loudness compared with unmodulated reference stimuli and therefore stimulus intensities were pseudo-randomly varied to prevent this as an extraneous cue (Robson et al., 2013). Reference stimuli had a spectral rate of 1.5 cpo and a temporal rate of 8 Hz, the target a higher spectral rate. The default initial difference in spectral modulation rate was 3.6 cpo, adapted in steps of 0.4 and 0.2. The outcome measure for each of these tasks was the perceptual threshold obtained by adaptively adjusting the amount or difference in modulation.

3.3.4 Volumetric MRI

All patients, except case 10 (claustrophobia), and 86 healthy controls received a high resolution T_1-weighted structural MRI on a 3T Philips Intera system equipped with an 8-channel receive-only head coil (Philips SENSitivity Encoding head coil), using a 3D turbo field echo sequence (coronal inversion recovery prepared 3D gradient-echo images, inversion time (TI) 900 ms, shot interval = 3000 ms, echo time (TE) = 4.6 ms, flip angle 8 degrees, field of view (FoV) = 250×250 mm, 182 slices, voxel size 0.98× 0.98×1.2 mm^3).

3.3.5 Statistical analyses

Behavioral data

All psychoacoustic group data were tested for normality with the Lilliefors version of the Kolmogorov-Smirnoff test for composite normality. In cases where the outcome measure for a given task in its original format deviated from normality in controls or in patients, we log-transformed the data for both groups and used these as outcome measures in order to allow for parametric analyses at the group level.

At the group level, the psychoacoustic data were compared between the PPA group and the healthy controls using a one-sided independent-samples t-test with the threshold for significance set at $p < 0.05$, Bonferroni-corrected for multiple comparisons by the number of tests performed (n = 12). We compared the psychoacoustic test scores between the subtypes (SV, NFV and LV) using Kruskal-Wallis followed by *post hoc* Tukey-Kramer pairwise comparison of subtypes ($p < 0.05$).

At the individual level, each PPA patient's performance was analyzed in comparison to the group by using a modified t-test based on Crawford and Howell (1998). For the comparison between each individual patient and the controls, to facilitate comparison between tasks and to enable Bonferroni correction, the exact p values (estimated percentiles) calculated according to Crawford and Howell (1998)) were transformed into normalized Z scores using the standard normal cumulative distribution function. The significance threshold was set to $Z = 2.64$ equalling a one-tailed significance level of $p < 0.05$, Bonferroni-corrected for the number of tests (n = 12).

The individual level of impairment was also verified with adjustment for potential contributing factors such as age or general cognitive capacity (as measured by CPM) following the procedure developed by Crawford and Garthwaite (2006). As a first step, we performed a multiple linear regression analysis in the healthy controls for each of the psychoacoustic tests, with as outcome variable the psychoacoustic test score and as independent variables age and executive function. Variables that had a significant effect on any of the test scores in these multiple regression analyses in normal controls were used as covariates for which we adjusted when comparing the individual's patient scores with the normal control group. Note that if a covariate had a significant effect on any of the 12 tests, it was included as a covariate in the regression equation for each of the 12 tests when comparing individual patients with controls.

Furthermore, we examined how accurately a machine learning classifier could assign an individual case to one of the three clinical subtype groups (three classes: NFV, SV and LV) based on the set of 12 psychoacoustic test scores, regardless of any other behavioral or imaging information, and which of the psychoacoustic tests were most discriminative in that respect. We used a linear support vector machine (SVM) approach (C = Inf, $\alpha = 0$) as implemented in Spider (version 1.71 (http://people.kyb.tuebingen.mpg.de/spider/, Weston J., Elisseef A, BakIr G., and Sinz F., Max Planck Institute for Biological Cybernetics, Tübingen, Germany, running under Matlab version 2011b) for pairwise

classification into every possible pair of subtypes (NFV-LV, NFV-SV, LV-SV). Half of the data of every subtype was used for training the classifier, while the other half was used as a test set to determine the performance of the classifier (two-fold cross-validation). Multiple repeats (n = 1,400) were performed in a way so that each possible combination of training and test data was used. Next, we calculated if the performance of the classifier was better than expected by chance, using random permutation labelling. For this purpose, PPA subtype labels were randomly assigned and the classification procedure was run 1,000 times as described above. Finally, we determined the feature weights for each psychoacoustic test. The feature weight of a psychoacoustic test is the component of the normal vector of the hyperplane along that test's dimension. Feature weights indicate how much a particular test contributes to the classification.

We further tested for a relationship between the psychoacoustic test scores and conventional neuropsychological measures. Given the relatively large number of the conventional neuropsychological tests administered and the potential correlations between scores on these conventional tests, we first conducted a factor analysis (SPSS Statistics 22, IBM) on the full neuropsychological dataset to reduce the number of correlations to be performed with the psychoacoustic scores. The dataset included the conventional neuropsychological test scores (Table 3.1) from all PPA patients, plus the 28 age-matched controls who had undergone the same neuropsychological battery. The factor analysis procedure was identical to that used in previous studies (Vandenbulcke et al., 2005; Molenberghs et al., 2009; Nelissen et al., 2010). Factors were extracted consecutively and orthogonalized to each other. Only factors with an eigenvalue $>$ 1 were retained (Kaiser criterion). A variance maximizing (varimax) rotation of the original variable space was used to obtain an interpretable pattern of factor loadings while preserving factor orthogonality. Factor scores for every subject were derived from these loadings and indicate how well a subject performed on the neuropsychological tests subsumed under a given factor. Individual factor scores were calculated per factor. Normality of the factor scores was tested using the Lilliefors version of the Kolmogorov-Smirnov Test for Composite Normality. The individual factor scores of the PPA cases were correlated with their scores on the psychoacoustic tasks using the Pearson correlation method throughout. The significance threshold was set at one-tailed $p < 0.05$, Bonferroni-corrected for multiple comparison by the number of tests (n = 12 times the number of factors).

Finally, we performed within the PPA group a Pearson regression analysis for each of the psychoacoustic test scores with symptom duration as the

independent variable, and a similar analysis with audiometric hearing levels as the independent variable. We also performed a Spearman regression analysis for each of the psychoacoustic test scores with digit span forward as independent variable (from the patients in whom it was available; Table 3.1). The significance threshold was set at $p < 0.05$ corrected for the number of psychoacoustic tests (n = 12).

MRI analysis

All procedures were carried out with Statistical Parametric Mapping 8 (SPM8, Wellcome Trust Centre for Neuroimaging, London, UK, http://www.fil.ion.ucl.ac.uk/spm) and the Voxel-Based Morphometry 8 toolbox (VBM8, http://dbm.neuro.uni-jena.de/vbm). High-resolution T_1-weighted MRI images were registered to Montreal Neurological Institute (MNI) space and segmented into gray matter, white matter, and CSF (Ashburner and Friston, 2000). An erosion/dilatation procedure with thorough cleaning removed most of the extracerebral voxels. Misclassified voxels were manually removed and T_1-weighted MRI images were reentered into the VBM routine. The normalized gray matter partitions were weighted ('modulated') to account for non-linear volume changes resulting from the normalization process. 'Non-linear modulation only' was chosen to account for differences in total intracranial volume. All preprocessed gray matter maps passed visual inspection for overall segmentation and normalization accuracy. For subsequent voxelwise statistical comparisons, gray matter maps were smoothed with an 8 mm isotropic Full-width Half Maximum (FWHM) Gaussian 3D kernel. The absolute intensity threshold was set at 0.1 (Ridgway et al., 2009).

We compared gray matter volume between PPA subtypes and controls by means of a voxelwise ANCOVA with gray matter volume as dependent variable and four subgroups (NFV, SV, LV and controls) as between-subjects factor and age and gender as a nuisance variables (Fig. 3.2A-B).

3.4 Results

3.4.1 Behavioral data: psychoacoustic test scores

All patients were able to perform the psychoacoustic tasks and produce informative results. Figure 3.3 provides overlay plots of the patients' individual staircase tracks for the adaptive tasks, and of the cumulative

percentage of the correct responses for the fixed-difficulty level tasks p3 and p4. Thresholds could be reliably measured in the adaptive tasks, as demonstrated by the graphs leveling off gradually and reaching a plateau, typically from trial 25 onward. In the two pitch sequence tasks (p3, p4), the constant, steady increase over the course of the tasks (40 trials) evidence the reliable measurement of discrimination ability also for these two tasks.

All outcome measures were normally distributed in both the controls and the patients in either their original form, or else after log-transformation (for p1, r1, r2, m2 and m3), except one minor deviation in the patient group for r2 ($p = 0.018$).

In the healthy controls, a multiple linear regression analysis with age and CPM scores as independent variables and psychoacoustic test scores as outcome variable, indicated a significant correlation between CPM scores and scores on discrimination of direction of change in pitch (p2) ($\rho = 0.45$, $p = 0.019$) but not with any of the other tasks ($p > 0.17$). There was no correlation with age.

3.4.2 Experimental auditory performance: group-based analysis

Performance in the PPA group was significantly poorer than in the control group for all pitch tasks (p1-4), the discrimination of strongly metrical patterns (r3), and FM detection at 40 Hz (m2) (Fig. 3.4A). When each of the subgroups was compared to the control group, discrimination of weakly metrical sequences (r4) was significantly impaired in NFV (corrected $p < 0.05$) (Fig. 3.4C).

We directly compared the psychoacoustic measures between the three clinical subtype groups (SV, NFV, LV) by means of the Kruskal-Wallis. This revealed a significant between-subtype difference for the detection of local (p3: $\text{chi}^2(2) = 6.03$, $p = 0.049$) and global changes in pitch sequences (p4: $\text{chi}^2(2) = 6.01$, $p = 0.049$) and for the discrimination of weakly metrical sequences (r4: $\text{chi}^2(2) = 9.36$, $p = 0.009$). *Post hoc* comparisons revealed a significant difference between NFV and LV and between NFV and SV for discrimination of weakly metrical sequences (r4), with scores in NFV being more affected than in the two other subtypes (Tukey-Kramer $p < 0.05$).

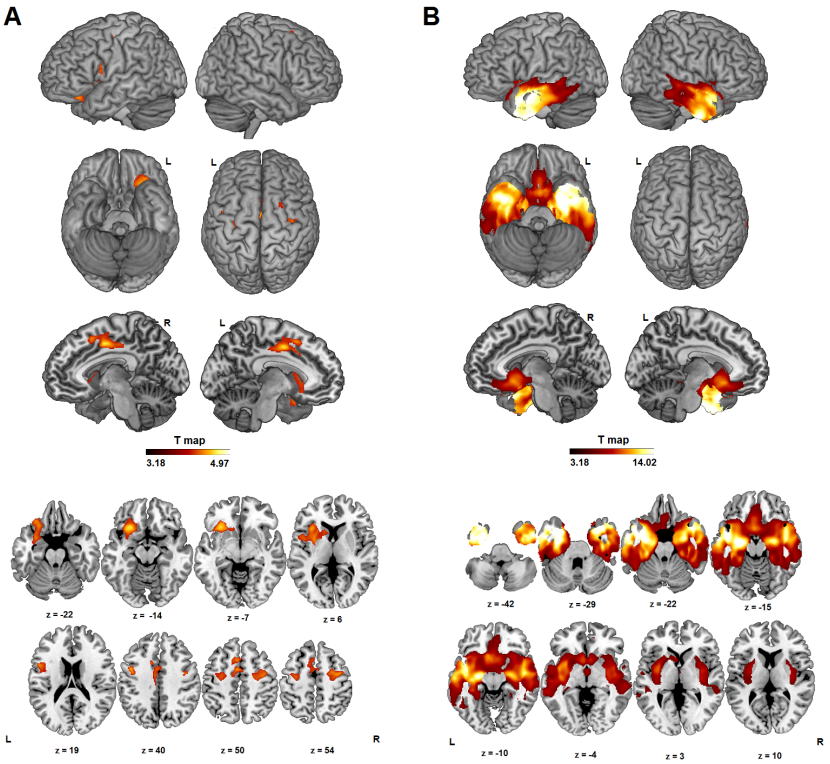


Figure 3.2: **Volumetric comparison between PPA subtypes and controls**. Results are based on a one-way ANCOVA with gray matter volume as dependent variable and four subgroups (six NFV, seven SV, four LV and 86 controls) as between-subjects factor, corrected for age and gender. **(A)** Atrophy in the NFV group compared to controls, **(B)** Atrophy in the SV group compared to controls. T-maps are projected on a rendered brain template and slices (Rorden et al., 2007) at a voxel-level uncorrected $p<0.001$, with a cluster-level family wise error (FWE)-corrected threshold $p<0.05$.

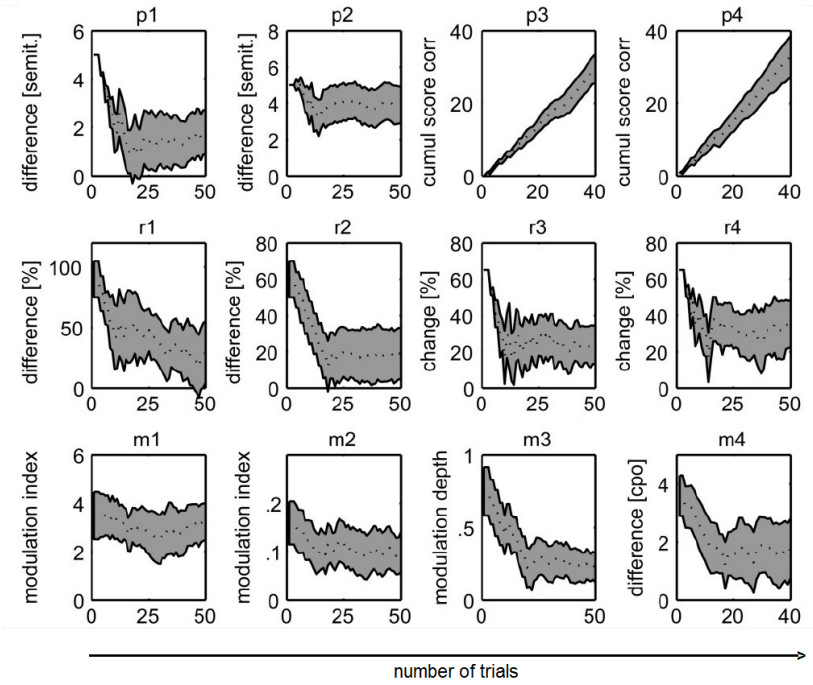


Figure 3.3: **Illustration of overall reliability of the 12 psychoacoustic experimental tasks**. Depicted is the course of all patients' individual responses as a function of trial number. The dotted line and grey shaded area depict the median response course ± the mean absolute difference from that for all patients. For the 10 adaptively controlled tasks (all except the pitch local (p3) and global (p4) sequence tasks), the graphs demonstrate the reliable course with a general decrease of respective difference between reference and target (ordinate: in pitch, or time, or modulation), and the reaching of a plateau, typically from trial 25 onward. For the two non-adaptive tasks of local and global change in pitch detection (top right), the graphs demonstrate the steady increase of correct responses from the first to the last trial.

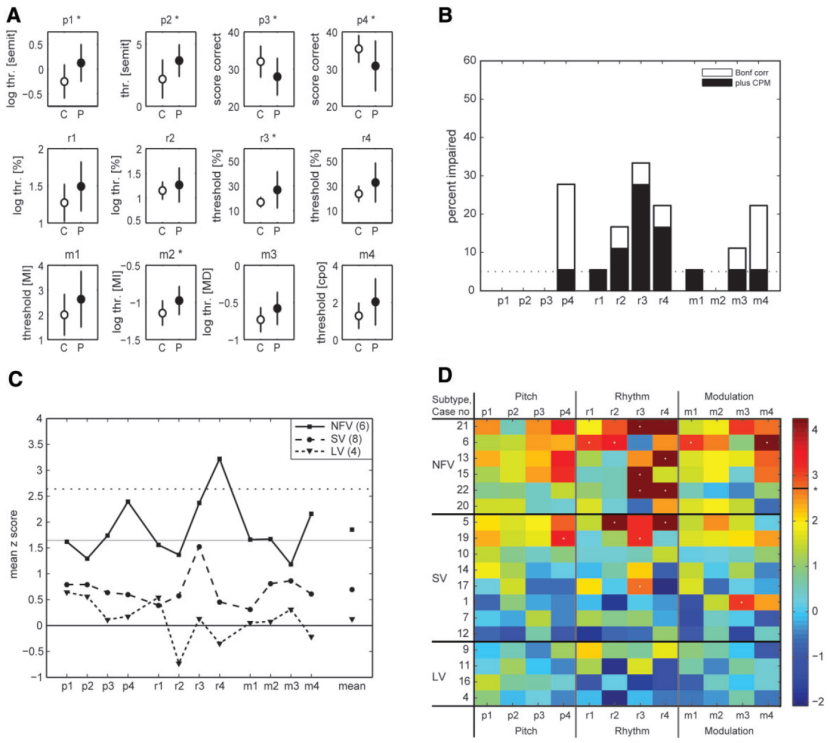


Figure 3.4: **Patients' psychoacoustic data in comparison to controls.** **(A)** Group comparison of psychoacoustic scores between the PPA group and controls. Asterisks denote a significant difference (p = 0.05, Bonferroni-corrected). **(B)** Percentage of all PPA patients (n = 18) who exhibited a significant impairment, plotted for each of the 12 tests. White boxes indicate percentage of deficits at the individual deficits (Crawford t-test, Bonferroni-corrected), black boxes indicate the percentage that remains significant after regressing out the effect of Coloured Progressive Matrices (CPM) scores as a measure of fluid intelligence. **(C)** Mean Z scores across patients within the three clinical subtype groups. Mean Z scores are plotted for each task, and in addition the overall mean across tasks (far right). Gray line corresponds to the uncorrected p of 0.05, the dotted line to the Bonferroni-corrected p. **(D)** All 18 individual patients' performance in comparison to controls, in the order of severity (measured by the individual mean Z score across tasks) within each clinical subtype. The color scale reflects the Crawford based Z scores derived from the modified t-test. The deficits that persist after adjustment for CPM scores are marked with a white dot at the centre.

3.4.3 Experimental auditory performance: individual auditory profiles

Based on the psychoacoustic test scores, the SVM classifier was able to correctly assign individual cases to the NFV versus LV class in 77.6% ($p = 0.026$). This means that out of the 10 cases (NFV plus LV), two or three were misclassified per iteration. Classification between other subtypes was not possible ($p > 0.13$). The vector weights used for the classification between NFV and LV were highest for the detection of local changes in pitch sequences (p3) and for the discrimination of a weakly metrical pattern (r4) (Table 3.2).

Significant impairments after correction for the number of tasks performed ($Z > 2.64$) were observed at the individual level mainly for global change in pitch detection (p4; 3 NFV, 2 SV cases), isochrony deviation (r2; 2 NFV, 1 SV), strongly metrical pattern discrimination (r3; 3 NFV, 3 SV), weakly metrical pattern discrimination (r4; NFV, 1SV) and DM detection (m3, 4 NFV) (Fig. 3.4D). After also adjusting for CPM scores (Crawford and Garthwaite, 2006), significant individual impairments remained mostly for the isochrony deviation task (r2) and the metrical pattern discrimination tasks (r3-4) (Fig. 3.4D, marked with the white dot): Three out of 6 NFV cases were significantly impaired on weakly metrical pattern discrimination (r4) and three on strongly metrical pattern discrimination (r3). Two SV cases were significantly impaired on strongly metrical pattern discrimination (r3) (Fig. 3.4D).

3.4.4 Relationship with neuropsychological test scores

Factor analysis of the neuropsychological test battery yielded two factors, together explaining 75.7% of the variance (Table 3.3). The first factor clustered naming, comprehension, object identification and semantic test scores. The second factor clustered PALPA pseudoword and word repetition scores, AAT total repetition scores and the CPM (Table 3.3). The outcome of this factor analysis was in line with that obtained in previous PPA studies using a similar neuropsychological protocol in independent patient groups (Vandenbulcke et al., 2005; Nelissen et al., 2010). We did not find significant correlations between any of the psychoacoustic measures and individual scores on factor 1. Individual scores on factor 2 (the 'repetition factor') correlated with scores on the detection of a local change in pitch sequence (p3: ρ = -0.66, corrected $p = 0.024$). There were trends in the same direction for detection of a

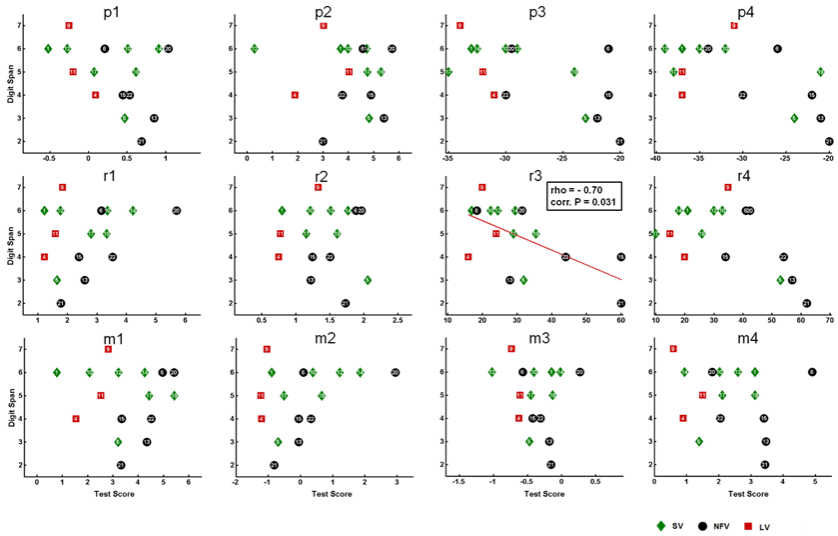


Figure 3.5: **Relationship between auditory short-term memory and psychoacoustic task performance**. Regression plots for each of the psychoacoustic test scores (on the abscissa) and the digit span forward score (on the ordinate). At a corrected p level, the correlation is significant only for metrical pattern discrimination with a strongly metrical beat (r3).

global change in pitch sequence (p4, uncorrected $p = 0.008$), metrical pattern discrimination (r3-4, uncorrected $p < 0.01$) and three of the timbre processing tasks (m2-4, uncorrected $p < 0.02$).

3.4.5 Relationship with symptom duration, hearing loss and auditory short-term memory

Symptom duration did not correlate with any of the psychoacoustic test scores ($p > 0.12$) in this sample. No correlations were found between scores on any of the psychoacoustic tests and the patients' hearing levels derived from the audiogram ($p > 0.13$). Digit span forward scores correlated significantly with the scores for metrical pattern discrimination with a strongly metrical beat (r3, ρ = -0.70, corrected $p = 0.031$). At an uncorrected $p < 0.05$, correlations were also present for basic change in pitch detection (p1, ρ = -0.50, uncorrected $p = 0.048$), local and global

change in pitch detection (p3, ρ = -0.53, uncorrected $p = 0.035$; p4, ρ = -0.53, uncorrected $p = 0.042$ (Fig. 3.5).

3.5 Discussion

Using non-linguistic stimuli we performed a systematic investigation of auditory processing in the pitch, time/rhythm and timbre domain in PPA at a level of processing that does not depend on any association with long-term memory, emotion or meaning. In a substantial number of PPA patients, in particular those suffering from NFV, processing of short sequences (five to seven tones) of non-linguistic stimuli was found to be significantly impaired (Fig. 3.4C,D). This is remarkable as the clinical phenotype in NFV is dominated by speech output problems and our tests assessed the cerebral processing of auditory input.

3.5.1 Differences between PPA subtypes

The NFV PPA patients (Fig. 3.4C,D) showed the most pronounced impairment in processing rhythm of tone sequences among the three subtypes. Within the PPA NFV subgroup, considerable phenotypical heterogeneity existed. In some NFV cases (such as case 6) speech apraxia dominated the clinical picture (Josephs et al., 2013b). Other NFV patients showed prominent agrammatism in addition to speech apraxia, and yet others had single-word comprehension deficits in addition to the speech apraxia and agrammatism (Table 1) (Mesulam et al., 2012, 2014b). Regardless of this clinical variability, the psychoacoustic deficits were found across the spectrum of NFV. The psychoacoustic profile of the cases that could be classified as 'mixed variant' did not differ from the other NFV cases (Fig 4D).
Only relatively recently was the LV subtype formally set apart from the NFV subtype (Gorno-Tempini et al., 2004a, 2011): the most characteristic deficit in LV is abnormal repetition of complex sentences while the most characteristic deficit in NFV is motor speech apraxia and/or agrammatism. Our sound perception data allowed reliable discrimination of NFV from LV cases even though these contained no language stimuli and were purely based on perceptual judgment of pitch and rhythm in tone sequences. The language deficit in LV has been attributed to a deficit in the phonological loop implicated in models of working memory (Gorno-Tempini et al., 2008; Foxe et al.,

2013). The relative preservation of processing of tone sequences in LV underscores the distinction between phonological working memory and the type of auditory working memory required to process nonverbal sounds and sequences of those. In this respect it is worth noting that in a previous study of intonation discrimination (Rohrer et al., 2012) LV performed worse than NFV. Discrimination of pitch, duration and intensity of syllable pairs and contour discrimination of four-syllable sequences was impaired in both subtypes (Rohrer et al., 2012) leading to linguistic and emotional receptive dysprosody (Rohrer et al., 2012) and impaired judgments of accents (Fletcher et al., 2013a). These tasks all used linguistic stimuli (syllables) and this could potentially explain the difference in outcome with our study.

Previous studies have probed some of the same processes we studied but mainly in isolation, mostly with the goal of understanding higher-level processing deficits (Warren et al., 2005; Goll et al., 2010, 2011). Discrimination of spectral shapes is impaired in NFV (Goll et al., 2010, 2011). In our study, the most discriminative feature between NFV versus the other subtypes came from the pitch and rhythm tasks using sequences of five to seven tones, a type of task that had not been reported on before in PPA. To the best of our knowledge, our study is the first to reveal abnormalities in pitch and rhythm processing in PPA using strictly nonlinguistic stimuli. Across the entire PPA group, the factor analysis did not indicate any relationship between the psychoacoustic test scores and anomia or tests of semantic processing. We interpret this as evidence that the processes underlying the auditory deficits are more related to a dorsal processing route, which mediates repetition of pseudowords among other tasks, than to a ventral processing route that mediates intelligibility of speech (Ueno et al., 2011). This conforms with the primary aim of the study, which was to study auditory processing at a level independent of higher-level associations. At an associative level of auditory processing, the SV PPA has previously been associated with deficits in the recognition of environmental sounds (Bozeat et al., 2000), famous tunes (Hsieh et al., 2011), and emotions in music (Hsieh et al., 2012). In our study a subset of SV PPA cases had significantly abnormal scores on the psychoacoustic tests for pitch, rhythm and timbre depending on the individual level. Given that the stimuli used here did not convey any meaning or emotion, it cannot be said that psychoacoustic processing of non-linguistic, non-musical stimuli was entirely preserved in SV PPA.

3.5.2 Perceptual processing of pitch and rhythm in short tone sequences

The most pronounced deficits within the pitch and time domain were seen when sequences were used, and mostly so in NFV, in particular in the time domain. These striking deficits are remarkable in that the clinical picture in NFV is characterized by speech output problems and these subjects showed the most prominent perceptual deficits. A precedent for deficits in auditory analysis associated with deficits in vocal output is provided by the cortical disorder of tone deafness (Griffiths, 2008). This is recognised as an output disorder (for singing) but has been characterized as a disorder of musical analysis that can be defined by abnormal pitch-sequence perception associated with cortical pathology within a temporofrontal network for pitch working memory (Griffiths, 2008). Among the diagnostic characteristics of speech apraxia in NFV, are the abnormal lengthening of vowels and of inter-segmental intervals (with segments referring to syllables or words) as well as the unevenness in pitch (Josephs et al., 2012; Ballard et al., 2014). We see a striking parity between these prominent clinical speech output characteristics and the pitch, duration and timing judgment errors during the perceptual tasks we applied. Because of this apparent similarity, we favor a unifying explanation for both the speech production problem and the acoustic perceptual abnormalities. The clinically prominent motor speech problems and the subclinical auditory deficit for timing and pitch could be related via a common 'temporal scaffolding' of processing of acoustic structure over time, used for auditory input up to speech output (Grube et al., 2013). In a broader theoretical sense, auditory perceptual processing is considered fundamental to normal speech production in several models, such as the sensory theory of speech production (Giraud and Poeppel, 2012). The sequences did not contain linguistic stimuli and therefore relied on working memory for auditory objects rather than phonological working memory. A verbal short-term memory deficit, as measured by means of digit span forward, is present in NFV, and principally so in cases with agrammatism with or without apraxia of speech (Rohrer et al., 2010b). The sequence processing deficit in our study could be caused by an auditory working memory deficit distinct from phonological working memory, an observation that has not been reported before to our knowledge. We however consider it unlikely that an auditory working memory problem could explain the motor speech deficits in NFV but it could play a role in agrammatism (Grossman and Ash, 2004; Rohrer et al., 2010b). The motor speech deficit may co-occur with the nonverbal auditory working memory deficit because

both rely on nearby anatomical regions. Auditory working memory relies on the inferior frontal gyrus and sulcus and premotor cortex (Smith and Jonides, 1999), regions of predilection in NFV.

3.5.3 Potential study limitations

PPA is relatively rare and patients can only reliably fulfill demanding psychophysical tasks of this kind when they are in a fairly early stage. Statistical comparisons between subgroups or negative findings within subgroups (such as LV) must be interpreted with caution given the relatively low sample size per subgroup. Potential differences in stage or severity of the disease may also play a role when comparing between subtypes. Inclusion criteria were, among others, relatively preserved hearing levels as well as proof of proper understanding and execution of the tasks during practice trials. The psychoacoustic tasks have been designed to avoid as much as possible interference from language production or comprehension deficits. Reliable results were obtained, as illustrated by the adaptive threshold tracking staircase plots and the cumulative increase in correct scores for the tasks with fixed-difficulty levels (Fig. 3.3). Significant deficits remained after adjustment for general cognitive capacity (executive function or nonverbal fluid intelligence), as measured with Raven's CPM.

Our battery did not include a formal speech apraxia assessment. The repetition tests require subjects to repeat phonemes, consonant-vowel (CV) combinations, words, pseudowords and sentences. The pronunciation is scored in fine detail, so that patients with motor speech deficits will be impaired to varying degree on these tests (Sajjadi et al., 2012; Leyton et al., 2014) (Table 3.1). Finally, it is inherent to this type of correlational study that we cannot establish a causal link between e.g. the perceptual deficit and the motor speech deficit as this would logically require an effective intervention.

3.6 Conclusion

While PPA NFV is clinically characterized by a motor speech output deficit, our findings clearly indicate a concomitant problem with perceptual processing of timing of tone sequences. We therefore argue that accurate sequence processing of timing is necessary for both motor speech and perceptual judgments of tone sequences. Both the motor and

the perceptual parts may rely on a common 'scaffolding' of processing of acoustic structure over time, used for auditory input up to speech output (Grube et al., 2013).

Table 3.1: Demographics and neuropsychological assessment

Case nr.	1	5	7	10	12	14	17	19	6	13	15	20	21	22	4	9	11	16
Age	76	70	61	64	64	48		69	52	79	71	78	72	63	57	64	62	71
Gender	m	f	m	f	m	f	f	f	f	f	m	m	f	f	f	m	f	m
Education	14	12	17	12	8	12	10	7	17	8	15	17	12	15	15	17	15	15
Variant	SV	SV	SV	SV	SV	SV	SV	SV	NFV	NFV	NFV	NFV	NFV	NFV	LV	LV	LV	LV
Symptom dur.	6	1.5	3	3	3	6	2	5	2	5	1.5	2.5	2.5	5	0.5	3	1.5	1
MRI	+	+	+	-	+	+	+	+	+	+	+	+	+	+	+	+	+	+
FDG PET	+	+	+	+	+	+	+	+	-	+	+	+	-	+	+	+	+	-
PIB SUVR	1.15	-	-	-	-	-	-	-	1.2	-	-		-		1.85	2.24	-	-
CSF Aβ_{42}	-	1330	-	-	-	-	-	733	-	1028	-	816	1060	865	664	-	516	-
CSF t-tau	-	269	-	-	-	-	-	262	-	312	-	195	424	183	183	-	>1200	-
BNT /60	**34**	**22**	**7**	**10**	**20**	**12**	**35**	**16**	58	48	55	48	**30**	**41**	56	**41**	53	53
PALPA comprehension																		
aud. WP /40	**38**	**36**	**31**	**29**	**31**	**27**	40	**30**	40	40	**37**	39	**36**	**38**	40	40	40	40
assoc.-sem. /30	27	**17**	**18**	**22**	**14**	**24**	27	**21**	28	**22**	28	26	29	25	28	**23**	27	28
AAT comprehension																		
aud. word /30	**19**	**15**	**11**	**19**	**19**	**11**	**21**	**14**	30	27	27	**24**	**20**	**21**	30	29	25	28
aud. sent. /30	26	**20**	25	**19**	**20**	25	**21**	**24**	30	**24**	25	**12**	**23**	25	30	27	25	30
writ. word /30	**20**	**18**	**13**	**11**	**13**	**19**	**24**	**14**	30	30	**25**	**23**	**21**	28	30	30	**26**	30
writ. sent. /30	25	**21**	**24**	**23**	**22**	27	27	30	30	**24**	**25**	18	**21**	30	30	28	30	30
PALPA repetition																		
single-word /80	72	78	78	79	71	79	76	78	76	74	74	74	69	80	80	80	77	80
pseudoword /80	**55**	71	74	65	**56**	80	72	77	**55**	59	**40**	**54**	**30**	79	74	69	79	63
AAT repetition																		
phoneme /30	30	**28**	29	30	**28**	30	30	30	**28**	29	30	29	**26**	30	30	**28**	30	**27**
single-word /30	**27**	29	29	30	**27**	30	**28**	**26**	**24**	**21**	30	**28**	30	30	30	29	30	30
cognates /30	30	30	30	30	30	30	30	29	**28**	**22**	29	**28**	**24**	30	30	30	30	29
composed /30	30	30	**28**	30	29	30	**28**	30	**26**	**23**	**25**	29	**18**	30	29	30	30	**27**
sent. /30	30	28	**25**	30	29	30	30	29	**26**	**27**	**18**	28	**11**	28	28	28	30	**27**
BORB B /32	**23**	**18**	**20**	**21**	**26**	**26**	31	**23**	31	30	31	**26**	**18**	**22**	29	31	31	31
BORB A /32	**20**	**20**	**18**	**18**	**18**	**17**	27	**17**	26	25	26	29	**21**	28	25	25	24	26
PPT /52	**37**	**39**	**40**	**35**	**40**	**46**	50	**43**	52	51	50	**47**	**46**	**48**	51	51	52	50
CPM /36	29	**24**	36	31	29	35	36	34	31	**24**	**24**	30	**12**	32	33	35	31	33
Digit Span Forward	6	3	-	6	6	6	5	5	6	3	4	6	2	4	-	4	7	5

Abbreviations: AAT: Akense Afasie Test, Assoc.-sem: associative semantic, aud.: auditory, BNT: Boston Naming test, BORB: Birmingham Object recognition battery B (easy) and A (hard), CPM: Coloured Progressive Matrices, CSF: cerebrospinal fluid (pg/ml), PIB SUVR, Pittsburgh Compound-B PET standardized uptake value ratio in a composite cortical volume of interest (Adamczuk et al., 2013), PPT: Pyramids and Palm trees test with pictures, sent.: sentence, symptom dur.: duration (years), WP: word-picture; writ: written. '-': means that data were not acquired. Age, education and symptom duration are expressed in years. Bold: Significantly different from controls based on Crawford and Garthwaite (2006) or Crawford and Howell (1998) statistical procedures.

Table 3.2: Support Vector Machine results

Feature weights	NFV vs.LV
p1	0.0053
p2	0.0192
p3	0.0612
p4	0.0006
r1	-0.0004
r2	0.0005
r3	-0.0067
r4	0.0898
m1	0.0100
m2	0.0028
m3	0.0023
m4	0.0104

Feature weights of Support Vector Machine used for classification between NFV versus LV. SVM was able to discriminate between NFV and LV, with highest feature weights for detection of a local change in pitch sequences (p3) and for discrimination of weakly metrical sequences (r4).

Table 3.3: Factoranalysis

Factor	1	2
Eigenvalue	7.938	2.656
variance explained	56.701	18.969
AAT written word comprehension	**0.903**	0.187
Boston Naming Test	**0.921**	0.100
AAT auditory word comprehension	**0.889**	0.132
PPT	**0.873**	0.163
PALPA auditory word-picture matching	**0.859**	0.051
Object Recognition A Hard	**0.794**	0.156
PALPA associative-semantic task	**0.739**	0.371
Object Recognition B Easy	**0.729**	0.288
AAT written sentence comprehension	0.565	0.568
AAT auditory sentence comprehension	0.592	0.394
PALPA pseudoword repetition	0.134	**0.912**
AAT repetition	0.047	**0.863**
CPM	0.174	**0.799**
PALPA word repetition	0.247	**0.774**

The neuropsychological test score loadings onto two factors. The first column shows the naming and comprehension factor (Factor 1) and the second column the repetition factor (Factor 2). Loadings > 0.70 are indicated in bold. AAT: Akense aphasie test, CPM: Colored Progressive Matrices, PPT: Pyramids and Palm trees test.

Chapter 4

Neuroanatomy of time and rhythm processing deficits in primary progressive aphasia

This study has been prepared for publication:

Schaeverbeke,J, Grube,M, Bruffaerts,R, Gabel,S, Meersmans,K, Van Bouwel,K, Dries,E, Jamoulle,T, Neyens,V, Sieben,A, Pijnenburg,Y, Peeters,R, Van Laere,K, Dupont,P, Griffiths,TD, Vandenberghe,R. Neuroanatomy of time and rhythm processing deficits in primary progressive aphasia.

4.1 Abstract

A subset of patients with primary progressive aphasia (PPA), a neurodegenerative syndrome characterized by atrophy in the language and speech network, have a core central auditory impairment. The non-fluent variant of PPA in particular shows deficient perceptual processing of rhythm and timing of nonverbal tone sequences. Its underlying

anatomical underpinnings remain unclear. We therefore aimed to assess the neuroanatomical basis of rhythm and time processing deficits in the syndrome of PPA. Domain-specificity was assessed by comparing results with those obtained for the domains of pitch and timbre processing. Perceptual thresholds were acquired in a consecutive memory-clinic recruited series of 27 patients with PPA (12 with the semantic variant, nine with the non-fluent/agrammatic variant, and six with the logopenic variant) and 28 age-matched healthy controls for four non-linguistic rhythm and timing tasks. Two absolute time duration discrimination tasks were performed, namely a single time-interval discrimination, and isochrony deviation detection task and two tasks assessing strongly and weakly metrical pattern discrimination, respectively. The domain-specificity of the findings was ascertained by means of four tasks probing pitch processing and four tasks probing timbre processing. High-resolution T_1-weighted structural magnetic resonance imaging (MRI) scans were processed using voxel-based morphometry (VBM) and entered in whole-brain voxel-wise linear regression analyses between gray matter volume maps and test performance.

Across the PPA group, higher perceptual thresholds on single time-interval duration discrimination were associated with atrophy in the right frontal operculum and higher isochrony deviation thresholds were associated with atrophy in the right posterior insula. The correlations remained significant when analyses were performed within the NFV PPA group. Two other clusters were obtained in the insula bilaterally for frequency modulation detection at 40 Hz, which overlapped to a minor extent with the frontal opercular cluster derived from the correlation with single time-interval duration discrimination deficits.

Rhythm and time processing deficits in the syndrome of PPA reflect right-hemispheric involvement of the frontal operculum and posterior insula. We propose that the perceptual timing deficits may contribute to the speech apraxia in NFV which is characterized by abnormal duration and inter-segmental time intervals of speech.

4.2 Introduction

Primary progressive aphasia (PPA) is classified into a nonfluent/agramatic (NFV), a semantic (SV) and a logopenic variant (LV) PPA (Gorno-Tempini et al., 2011). While the clinical phenotype in PPA is by definition dominated by the verbal communication difficulties, deficits of nonverbal auditory sound processing occur in all PPA subtypes (Bozeat et al., 2000; Uttner et al., 2006; Goll et al., 2010, 2011; Hailstone et al., 2011; Hsieh et al., 2011, 2012; Omar et al., 2011; Rohrer et al., 2012; Fletcher et al., 2013a, 2015; Golden et al., 2016). More specifically, non-linguistic auditory processing deficits of sound across the domains of pitch, time/rhythm and timbre (modulation) are present in PPA (Grube et al., 2016; Golden et al., 2016). The most consistent and profound deficits are observed in the time and rhythm domain, with the highest degree of impairment found in NFV PPA (Grube et al., 2016). A subset of SV PPA patients are also impaired, though less severely, while LV PPA patients do not exhibit any significant impairments (Grube et al., 2016). Deficits in time and rhythm processing may contribute to the prominent motor speech impairment in NFV PPA, in particular, the prolongation of inter-segmental time-intervals during spontaneous speech and prolongation of vowels (Ballard et al., 2014). The prolongation of vowel duration in polysyllabic words has been shown to covary with gray matter volume loss in the bilateral precentral gyrus, supplementary motor area (SMA) and pars opercularis of the inferior frontal gyrus (IFG) (Ballard et al., 2014). These regions might also be involved in the rhythm and timing deficits for non-linguistic auditory stimuli in NFV PPA (Grube et al., 2016). However, the neuroanatomical basis of these deficits is unclear. Impaired processing of temporal regularity in speech signals in NFV correlates with atrophy of the left SMA and right caudate nucleus (Hardy et al., 2017b). These regions might also be involved in the rhythm and timing deficits for non-linguistic auditory stimuli in NFV PPA (Grube et al., 2016).

The tasks used in the current study have previously been applied in patients with multiple system atrophy and Huntington's disease (Cope et al., 2014). The basal ganglia have an essential role in the perception of both absolute, duration-based timing as well as relative, beat-based timing (Teki et al., 2011; Grahn and Rowe, 2013; Cope et al., 2014). The basal ganglia can be atrophic in NFV PPA (Rogalski et al., 2011a; Brambati et al., 2015; Mandelli et al., 2015, 2016). Other areas of atrophy in NFV PPA include the left IFG, premotor cortex, SMA, frontal operculum and insular cortex, which are regions relevant for speech

production (Rogalski et al., 2011a; Brambati et al., 2015; Mandelli et al., 2015, 2016). A task-based functional magnetic resonance imaging (fMRI) study demonstrated that deficits of temporal irregularity processing of spoken syllable sequences in NFV PPA were associated with reduced activation of the anterior cingulate cortex (ACC) and SMA (Hardy et al., 2017a).
In the healthy brain, time estimation involves a distributed network consisting of the dorsolateral prefrontal cortex (DLPFC), pre-SMA/SMA, the anterior insula, the dorsal striata, and the right frontal operculum among other regions (Morillon et al., 2009). Perception of auditory simple metric rhythms relies on the basal ganglia as well as the anterior STG, left IFG, and the pre-SMA/SMA according to task-based fMRI studies (Grahn and Brett, 2007). The most consistent activations are located in the pre-SMA/SMA, which plays a role in sequence predictability for both motor tasks (Lang et al., 1990; Gerloff et al., 1997) as well as auditory tasks (Grahn and Brett, 2007; Chen et al., 2008; Bengtsson et al., 2009). Processing of more complex metric and non-metric rhythms additionally activates higher-level cortical areas such as the superior prefrontal cortex (Bengtsson et al., 2009).

It has been suggested that processing of time duration as well as processing of pitch sequences in natural segmented sounds are both localized to a right-hemispheric network including the posterior IFG, cerebellum and posterior STG (Griffiths et al., 1999). Activations in the superior temporal lobe are not unique to timing but are also present during pitch processing tasks (Patterson et al., 2002; Warren et al., 2003, 2005; Stewart et al., 2008). The STG is activated bilaterally during a passive listening task in both pitch and timbre conditions (Allen et al., 2017). The acoustic correlates of timbre have been linked to the STG (Allen et al., 2017), but also to the mid-portion of the right STS (Menon et al., 2002; Allen et al., 2017), extending into the circular insular sulcus (Menon et al., 2002).

As a primary objective, we aimed to establish the neural correlates of rhythm and timing processing deficits in PPA (Grube et al., 2016). As a secondary objective, the domain-specificity of rhythm and timing processing deficits was assessed using pitch and timbre processing as control conditions. Based on the non-linguistic origin of the stimuli, we expected the rhythm and timing processing deficits would not necessarily correlate with atrophy in the language-dominant hemisphere, but might involve bilateral or right-hemispheric regions. Considering the regions that are typically atrophic in NFV PPA (Grossman, 2010; Rogalski et al., 2011b; Mandelli et al., 2016; Spinelli et al., 2017), we hypothesized

involvement of the frontal operculum, insula and basal ganglia in the absolute time duration discrimination tasks, while metrical pattern discrimination deficits would be related to atrophy of key structures for rhythm perception such as the dorsal premotor cortex and pre-SMA/SMA (Grahn and Brett, 2007; Chen et al., 2008; Teki et al., 2011).

4.3 Material and Methods

4.3.1 Subjects

A consecutive series of 32 PPA patients were recruited at the memory clinic University Hospitals Leuven. Each PPA case was diagnosed according to international consensus recommendations (Gorno-Tempini et al., 2011). This classification relied on the clinical evaluation by an experienced neurologist in combination with the results from the clinical MRI and [^{18}F]-fluoro-deoxy-glucose positron emission tomography ([^{18}F]-FDG-PET) scan. Cerebrospinal fluid (CSF) AD biomarkers or amyloid PET were also acquired in a subset of PPA patients. Four of the PPA patients had to be excluded *a priori* based on their inability to perform the practice runs of the psychoacoustic experiments. One patient was excluded from our analyses due to an atypical presentation of PPA (foreign accent), which did not fit any of the phenotypes described in the international consensus recommendations (Gorno-Tempini et al., 2011). A total of 27 PPA patients were retained in the study. Twelve patients were classified *a priori* as SV, nine as NFV and six as LV. Eighteen PPA patients (cases 1-22) were included in a previous paper of nonverbal acoustic processing in PPA (Grube et al., 2016), described in the previous chapter. Nine additional PPA patients were recruited between 2016-2017 (cases 23-32). Positivity on AD biomarkers was present in none of the NFV or SV cases and in five out of six LV cases. One SV case was diagnosed *post mortem* with TDP-43 type C and secondary AD pathology (case 1). The SV and LV groups showed a relatively homogeneous classical phenotype (Table. 4.1, Table. 4.3). All NFV cases had speech apraxia with buccolingual apraxia (Table. 4.2). In one NFV case (case 6), speech apraxia was by far the most prominent clinical abnormality. NFV cases 13, 15, 23 and 25 had prominent agrammatism in addition to speech apraxia. Cases 20-23 and 31 also had single-word comprehension deficits on detailed testing besides agrammatism and speech apraxia with, in addition, object recognition problems in cases 21 and 23. While we included these subjects in the NFV group, these

cases would also fit into the recently defined 'mixed' subtype of PPA (Mesulam et al., 2009, 2012; Vandenberghe, 2016)(Table. 4.2). All cases except NFV running case 23 were right-handed.

Healthy control subjects were recruited through advertisement in local newspapers or internet asking for volunteers above the age of 55 years for participation in a scientific study. Control participants did not have any subjective memory or visual complaints or any history of significant neurological, hearing or psychiatric illness. None of the control participants took any psychotropic or vasoactive medication. Twenty-eight age- and education-matched cognitively intact control subjects (15 male; age range 51-76 years, mean 62.2, standard deviation (SD) 7.8; education range 9-22 years, mean 14.0, SD 2.8; Mini-mental state examination (MMSE) > 27; Clinical Dementia Rating scale (CDR) $= 0$) completed the experimental psychoacoustic and the neuropsychological test battery of which 22 received an MRI scan (the remaining six controls refused MRI or had a medical contraindication). For the purpose of comparing gray matter volume in the PPA subtypes with that of a normal control group, we additionally added MRI scans from 52 matched controls (23 male; age range 57-83 years, mean 69.8, SD 6.6; CDR $= 0$) (Adamczuk et al., 2013) to reach a total of 74 MRI scans.
Neurolinguistic and neuropsychological data from 67 cognitively intact control subjects (including the 28 controls who underwent the experimental psychoacoustic tests and 22 out of 52 who were added for the volumetric comparison)(32 male; age range 53-89 years, mean 67.1, SD 7.4; education range 8-22 years, mean 13.6, SD 2.8; CDR $= 0$) were used to calculate whether the performance of an individual PPA patient was within norms (Nelissen et al., 2007; Grube et al., 2016).

All PPA patients completed the experimental psychoacoustic and the neuropsychological test battery. Peripheral hearing sensitivity was measured in all participants prior to participation in the psychoacoustic experiment using a clinical Bekesy-type audiometer for frequencies of 0.5, 1, 2, 4, and 8 kHz, on the left and right ear, respectively. In the pure tone audiograms, all subjects were able to detect stimuli of up to 1000 Hz below a hearing level of 30 dB on at least one ear. There were no significant differences between left and right ear hearing levels (two-tailed t-test, $p = 0.15$).

The study was approved by the Ethics Committee, University Hospitals Leuven. After receiving a complete description of the study protocol, all participants or their spouses provided written informed consent in accordance with the Declaration of Helsinki.

4.3.2 Neuropsychological protocol

Confrontation naming was assessed by means of the Dutch version of the Boston Naming Test (BNT) (Mariën et al., 1998). Single-word comprehension and repetition were evaluated by means of tests selected from the Psycholinguistic Assessment of Language Processing in Aphasia (PALPA) and the Akense Afasie test (AAT). Nonverbal executive functioning and fluid intelligence was evaluated by means of the Raven's Coloured Progressive Matrices (CPM). The Birmingham Object Recognition Battery (BORB) test (easy (B) and hard (A)) was used as a measure of object identification. The verbal associative-semantic test of the PALPA (PALPA subtest 49) and the picture-version of the Pyramids and Palm trees test (PPT) was used to measure semantic-associative capacity (Table. 4.1, Table. 4.2, and Table. 4.3).

4.3.3 Experimental tests of acoustic processing

The psychoacoustic battery consisted of four pre-existing tasks of pitch, time/rhythm and timbre each (Grube et al., 2012, 2014), which are explained in detail in the previous chapter. A schematic representation of all tasks is provided in Figure 4.1. Before acquisition of each psychoacoustic task, subjects had to pass a number of practice trials of that task (minimum five).

Adaptive tracking procedure and threshold estimation

Two tasks (see below: p3, p4) used a same-different paradigm with fixed difficulty levels (Foxton et al., 2003), with the score correct as the outcome measure. The remaining 10 tasks used a two-alternative forced-choice adaptive paradigm following a two-down, one-up algorithm (difficulty increasing after 2 consecutive correct responses and decreasing after every incorrect one). The outcome measure was the perceptual threshold, calculated as the mean over the last six reversals measured with the small step size, estimating the 70.9%-correct point of the psychometric function (Levitt, 1971).

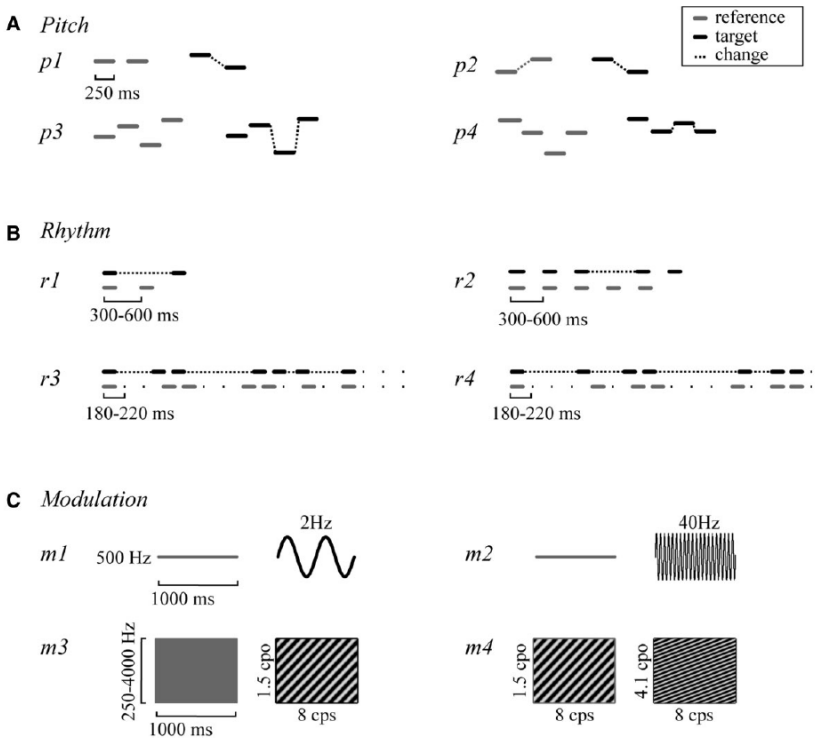


Figure 4.1: **Schematic illustration of experimental tasks, with one reference and one target example depicted per task**. **(A)** Pitch: basic change detection (p1), change-direction discrimination (p2), detection of a local change in pitch sequence (p3), detection of a global change in pitch sequence (p4). **(B)** Rhythm and timing: single time-interval discrimination (r1), isochrony deviation detection (r2), metrical pattern discrimination for a strongly (r3) and a weakly metrical sequence (r4). **(C)** Modulation (timbre): 2 Hz frequency modulation (FM) detection (m1); 40 Hz FM detection (m2), dynamic modulation (DM) detection (m3), dynamic modulation discrimination (m4). Note: x- and y-axes correspond to time and frequency throughout, but scales vary and are in part arbitrary.

Rhythm and timing

All four rhythm and timing tasks (Fig. 4.1B) used 500 Hz, 100 ms pure-tones. The basic single time-interval duration discrimination task (r1; 50 trials) (Grube et al., 2010) required subjects to indicate which of two tone pairs comprised the 'longer gap' than the reference. In the isochrony deviation detection task (r2; 50 trials) (Grube et al., 2012), subjects were required to indicate which of two otherwise isochronous five-tone sequences contained a lengthening or 'extra gap'. In the metrical pattern discrimination tasks (r3, r4; 50 trials) (Grube and Griffiths, 2009), subjects were required to decide which of three rhythmic sequences of seven tones each sounded 'different', or 'wrong', based on a distortion (or change) in the rhythm. The reference sequence had a strongly (r3) or a weakly (r4) metrical beat of four (for more details see Grube and Griffiths (2009)). The outcome measure for each of the tasks was the threshold obtained by adaptively adjusting the difference between reference and target stimuli. The difference was measured relative (in percent) to the duration or tempo of the reference.

Pitch and Timbre control tasks

The basic change in pitch detection task (p1; 50 trials), the pitch change direction discrimination task (p2; 50 trials), and local and global change in pitch detection tasks (p3, p4; 40 trials) (Fig. 4.1A) along with four tasks of timbre (modulation) perception (Fig. 4.1C) (Grube et al., 2012) including two frequency-modulation (FM) detection tasks (m1 and m2), one spectro-temporal, dynamic modulation (DM) detection (m3) and one DM discrimination (m4) task were applied as control conditions. For a detailed description of these tasks, we refer to the previous chapter of this thesis.

Volumetric MRI acquisition and analysis

Twenty-six patients (case 10 was excluded due to claustrophobia) and 22 healthy control subjects who participated in the psychoacoustic experiment received a T_1-weighted structural MRI on a 3T Philips Intera system equipped with an 8-channel receive-only head coil (Philips SENSitivity Encoding head coil), using a 3D turbo field echo sequence (coronal inversion recovery prepared 3D gradient-echo images, inversion time (TI) 900 ms, shot interval = 3000 ms, echo time (TE) = 4.6

ms, flip angle 8 degrees, field of view (FoV) = 250×250 mm, 182 slices, voxel size 0.98× 0.98×1.2 mm^3). Nine patients and 52 healthy control subjects received a T_1-weighted structural MRI scan on a 3T Philips Achieva dstream scanner equipped with a 32-channel head volume coil, using a 3D turbo field echo sequence (coronal inversion recovery prepared 3D gradient-echo images, TI 900 ms, shot interval = 3000 ms, TE = 4.6 ms, TR = 9.6 ms, flip angle 8°, FoV = 250×250 mm, 182 slices, slice thickness = 1.2 mm, voxel size 0.98×0.98×1.2 mm^3). Preprocessing of the T_1-weighted MRI images was performed with voxel-based morphometry (VBM8, http://dbm.neuro.uni-jena.de/vbm) running on Statistical Parametric Mapping (SPM8, Wellcome Trust Centre for Neuroimaging, London, UK) (Ashburner and Friston, 2000) implemented in Matlab R2012b (Mathworks, Natick, MA, USA) as described previously (Gillebert et al., 2015; Schaeverbeke et al., 2017). The resulting gray matter volumes have been adjusted for overall brain size (total intracranial volume) by using the 'nonlinear only' component in the spatial normalization process for modulation of gray matter voxel intensities (Barnes et al., 2010). For subsequent voxelwise statistical comparisons, gray matter maps were smoothed with an 8 mm isotropic Full-Width Half Maximum (FWHM) Gaussian 3D kernel.

4.3.4 Statistical analyses

Voxel-based analyses

Psychoacoustic test scores which deviated in their original format from normality in controls or in patients, were log-transformed for both groups to fulfill the assumptions of normality for SPM analyses. Before voxelwise statistical analysis were performed, psychoacoustic scores were checked for outliers using the Grubbs' test: Z scores higher than three standard deviations were classified as outliers.

As primary outcome analysis, for each of the four time and rhythm tasks, a voxelwise linear regression analysis was performed between modulated gray matter volume maps as dependent variable and the psychoacoustic test scores as independent variable, with age, gender and scanner site as nuisance variables (Barnes et al., 2010). We also performed voxelwise linear regression analyses within the PPA subtype groups separately.

As a first secondary outcome analysis, for each of the other two domains (pitch and timbre), a voxelwise linear regression analysis was performed between modulated gray matter volume maps as dependent variable and

the psychoacoustic test scores as independent variable, with age, gender and scanner site as nuisance variables (Barnes et al., 2010). The domain-specificity of our findings was analyzed by calculating the percentage of overlap between clusters obtained for rhythm and timing and clusters obtained in the pitch and timbre tasks at a significance threshold of voxel-level uncorrected $p < 0.001$, with a cluster-level family wise error (FWE)-corrected threshold $p < 0.05$ (Poline et al., 1997). In case a significant correlation was found, we calculated the mean gray matter volume in these clusters obtained in the voxelwise linear regression analyses to visualize the correlation in a scatterplot.

For all voxelwise analyses, the default significance threshold was set at voxel-level uncorrected $p < 0.001$, with a cluster-level family wise error (FWE)-corrected threshold $p < 0.05$ (Poline et al., 1997). In the correlational analyses with psychoacoustic task performance, a correction for the number of regressions (n = 12) was applied on top of the cluster-level FWE-corrected threshold (= $p_{corr.}$).

Behavioral and neuropsychological analyses

Standard statistical analyses were performed in Statistics Software Package for the Social Sciences (version 24, IBM Statistics, Armonk, USA). Demographic data were statistically assessed using Kruskal-Wallis, followed by two-tailed Mann-Whitney *U post hoc* analyses for continuous measures and with Pearson chi^2 tests for categorical measures.

Psychoacoustic task performance was statistically compared between the PPA group (n = 27) and the healthy control group (n = 28) using one-sided Kruskal-Wallis at a Bonferonni corrected $p < 0.05$, correcting for the number of tasks (n = 12). *Post hoc* two-tailed Mann-Whitney *U* tests were applied to assess differences between each PPA subgroup and the healthy controls, and across the PPA subgroups at a Bonferonni corrected $p < 0.05$, correcting for the number of tasks (n = 12).

At the individual patient level, psychoacoustic task performance of each PPA patient against the control group was expressed as a one-tailed t value, converted into a z score using a multiple single case series methodology (Crawford and Howell, 1998). The Z score cut-off was derived from the modified t-test procedure for which the Bonferroni-corrected $p = 0.05$ corresponds to a Z score of 2.64.

The individuals' neuropsychological test scores were statistically contrasted with an extended group of matched healthy controls (n = 67,

described in the Methods section) following the procedure developed by Crawford and Garthwaite (2006). As a first step, we performed for each task a hierarchical multiple linear regression analysis in the healthy control group, with as outcome variable the neuropsychological test scores and as predictor variables age and education. Variables that had a significant effect on any of the test scores in the healthy controls were included as predictor variables in the regression equation: there was a statistically significant correlation of education with the hard BORB object recognition task (R^2 adjusted = 0.054, $p = 0.034$), and with the CPM task (R^2 adjusted = 0.075, $p = 0.016$). Age had a significant effect on performance on the BNT (R^2 adjusted = 0.048, $p = 0.042$), AAT repetition of single words (R^2 adjusted = 0.065, $p = 0.043$), cognates (R^2 adjusted = 0.15, $p = 0.003$) and concatenated words (R^2 adjusted = 0.11, $p = 0.011$). Consequently, when assessing the individual patient's scores, education or age, respectively, were entered as predictor variables and the test score of the individual patient as dependent variable in the regression equation derived from the control group. The discrepancy between the predicted score and the observed score was expressed as a Z-score, which was considered abnormal at 1.9. Individual performance on the other tasks was statistically compared with the control group based on a modified t-test (Crawford and Howell, 1998)

4.4 Results

4.4.1 Demographics

Within the PPA group, PPA variants did not differ in age ($\text{chi}^2(2) = 0.92$, $p = 0.63$), education ($\text{chi}^2(2) = 1.87$, $p = 0.39$) or gender ($\text{chi}^2(2) = 2.15$, $p = 0.34$). Symptom duration, as approximated by information derived from the patient, reliable informants and medical records, was not significantly different between PPA variants ($\text{chi}^2(2) = 0.60$, $p = 0.74$).

4.4.2 Clinicoanatomical features

NFV patients exhibited atrophy of the bilateral frontal lobe including the pars opercularis and pars triangularis, the premotor cortex, SMA and anterior insula. Atrophy in the left hemisphere of NFV PPA additionally encompassed the DLPFC, STG, and parts of the temporoparietal cortex

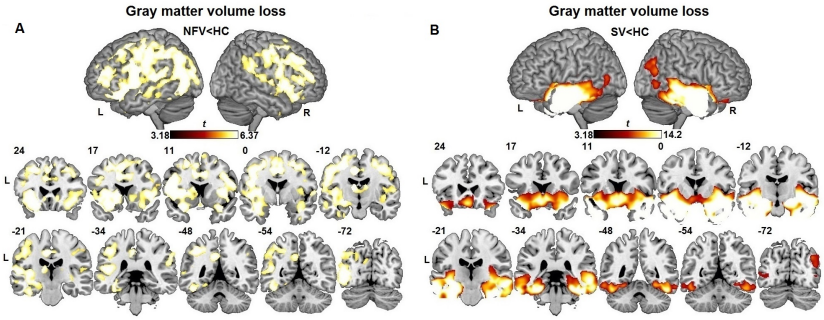


Figure 4.2: **Volumetric comparison between PPA subtypes and controls**. Results are based on a one-way ANCOVA with gray matter volume as dependent variable and four subgroups (nine NFV, eleven SV, six LV and 74 controls) as between-subjects factor, corrected for age, gender and scanner site. **(A)** Atrophy in the NFV group compared to controls, **(B)** Atrophy in the SV group compared to controls. *T*-maps are projected on a rendered MNI template brain and corresponding slices (Rorden et al., 2007) at a voxel-level uncorrected $p<0.001$, with a cluster-level family wise error (FWE)-corrected threshold $p<0.05$.

(Fig. 4.2A). SV patients showed severe atrophy of the bilateral anterior temporal lobe, including the amygdala and hippocampus, and perirhinal cortex among other structures (Fig. 4.2B). Atrophy in LV PPA was only significant at a voxel-level uncorrected threshold of $p<0.001$ without FWE-correction and was restricted to the left posterior third of the left MTG, the precuneus and left fusiform gyrus as well as the right STG/STS.

4.4.3 Experimental auditory performance: group-based and individual analyses

All 27 patients were able to perform the psychoacoustic tasks and produce informative results (Fig. 4.3A).

At the group-level, performance in the total PPA group was significantly poorer than in the control group for discrimination of weakly metrical patterns (r4, $\text{chi}^2(3) = 15.3$, $p_{corr.} = 0.009$).
Post hoc analyses showed deficits in the NFV PPA group but not in the other variants compared to controls on weakly metrical pattern

discrimination (r4, $U = 13$, $p_{corr.} = 0.001$). A direct comparison of the psychoacoustic measures between the three clinical subtype groups did not reveal any significant differences ($p_{corr.} > 0.092$) in the rhythm domain.

Performance in the total PPA group on the control tasks (pitch and timbre) was significantly poorer than in the control group, for pitch change detection (p1, $chi^2(2) = 12.4$, $p_{corr.} = 0.037$) and frequency detection at 40 Hz (m2, $chi^2(2) = 13.4$, $p_{corr.} = 0.023$). *Post hoc* analyses showed deficits in the NFV PPA group but not in the other variants compared to controls on pitch change detection (p1, $U = 36.5$, $p_{corr.} = 0.009$) and on FM detection at 40 Hz (m2, $U = 17.5$, $p_{corr.} = 0.002$). A direct comparison of the control tasks between the three clinical subtype groups did not reveal any significant differences ($p_{corr.} > 0.26$).

Psychoacoustic impairments at the individual patient level are shown in Figure 4.3B.

4.4.4 Neuroanatomic correlates of temporal processing deficits

Single time-interval duration discrimination (r1) performance correlated with gray matter volume loss in the right frontal operculum (pFWE-corrected plus corrected for the number of tests (n = 12), $p_{corr.} = 0.036$, 1398 voxels, $Z = 4.12$; peak coordinate: 51, 18, 0) (Fig. 4.4A-B). When the voxelwise correlational analysis was performed within the group of NFV PPA patients at a significance threshold of p uncorrected < 0.005, there was a cluster in the right frontal operculum ($p_{uncorr.} = 0.001$, 541 voxels, $Z = 3.64$; 48, 8, 22). No correlations were found in the right frontal operculum within the LV or SV groups.

Impaired isochrony deviation detection (r2) performance correlated significantly with gray matter volume loss in the right posterior insula ($p_{corr.}= 0.024$, 1501 voxels, $Z = 4.57$; 41, -31, 18) (Fig. 4.4C-D). When the voxelwise correlational analysis was performed within the group of NFV PPA patients at a significance threshold of p uncorrected < 0.005, there was a cluster in the right insula ($p_{uncorr.} = 0.011$, 260 voxels, $Z = 3.62$; 39, -18, -3). The cluster in the right insula did not overlap with the right inferior frontal opercular cluster obtained for single time-interval duration discrimination (r1). No significant correlations were found in

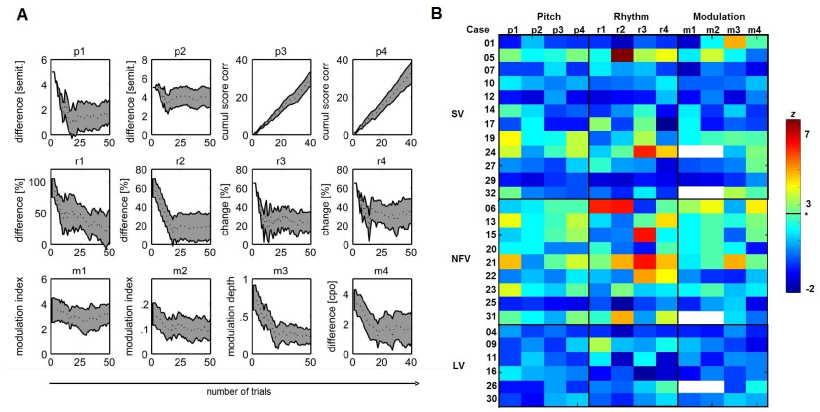


Figure 4.3: **Illustration of overall reliability and Z scores for the 12 psychoacoustic experimental tasks**. **(A)** Depicted is the course of all patients' individual responses as a function of trial number. The dotted line and grey shaded area depict the median response course ± the mean absolute difference from that for all patients. For the 10 adaptively controlled tasks (all except the pitch local and global sequence tasks), the graphs demonstrate the reliable course with a general decrease of respective difference between reference and target (ordinate: in pitch, or time, or modulation), and the reaching of a plateau, typically from trial 25 onward. For the two non-adaptive tasks of local and global change in pitch detection (top right), the graphs demonstrate the steady increase of the score correct from the first to the last trial. **(B)** All 27 individual patients' performance in comparison to controls. The color scale reflects the Crawford-based Z scores derived from the modified t-test (line and asterisk indicate Bonferroni-corrected p of 0.05 ($Z > 2.64$)). White: no data recorded for that particular task.

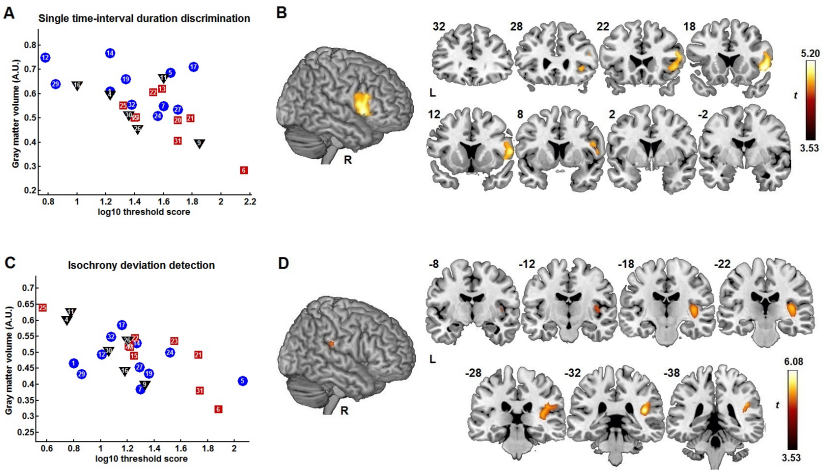


Figure 4.4: **Neuroanatomic correlates of temporal processing deficits, corrected for age, gender and scanner site**.
(A) Scatterplot demonstrating the correlation between gray matter volume and single time-interval duration discrimination threshold scores, **(B)** T maps of the latter correlation, **(C)** Scatterplot demonstrating the correlation between gray matter volume and isochrony deviation detection, **(D)** T maps of the latter correlation. Threshold scores are plotted on the abscissa and extracted modulated gray matter volumes (arbitrary units) on the ordinate of the scatterplot. Black triangles: LV, red squares: NFV, blue circles: SV PPA patients. T maps are projected on an MNI template brain rendering and on coronal slices with corresponding MNI coordinates in the left upper corner at a voxel-level uncorrected $p<0.001$, with a cluster-level family wise error (FWE)-corrected threshold $p<0.05$, plus corrected for the number of tests (n = 12).

the right insula within the LV or SV groups using the same significance threshold.

At voxel-level uncorrected $p<0.001$, strongly metrical pattern discrimination (r3) deficits were associated with gray matter volume loss in the right superior frontal cortex including the premotor cortex ($p_{uncorr.} = 0.050$, 328 voxels, $Z = 3.77$; 17, 29, 57). There was also a borderline significant cluster in the left SMA ($p_{uncorr.} = 0.064$, 287 voxels, $Z = 4.59$; -20, 3, 63). When the voxelwise correlational analysis was performed within the group of NFV PPA patients at a significance threshold of p uncorrected < 0.005, there was a cluster in the left SMA ($p_{uncorr.} < 0.001$, 756 voxels, $Z = 3.34$; -5, 21, 58).
No voxelwise correlations were obtained between gray matter volume loss and weakly metrical pattern discrimination (r4).

We investigated whether a laterality effect existed by flipping the VOIs, derived from the voxelwise regression analysis described in the previous section, around the anteroposterior axis and assessed the correlation with the psychoacoustic test scores. Performance on single time-interval duration discrimination (r1) was correlated with a homotopic cluster in the left frontal operculum ($\rho(24) = -0.57$, $p = 0.001$) (Fig. 4.5A). Gray matter volume of the left frontal operculum of PPA patients was significantly lower than gray matter volume in the right frontal operculum ($t = -4.05$, $p < 0.001$).

There was no association between symptom duration and gray matter atrophy in the left or right frontal operculum ($p > 0.24$). Impaired isochrony deviation detection (r2) performance did not correlate with left posterior insular atrophy ($\rho(24) = -0.25$, $p = 0.11$) (Fig. 4.5B).

4.4.5 Domain-specificity of neuroanatomical correlates for temporal processing deficits

In the pitch domain, no significant correlations were found in the right frontal operculum or right insular cortex. In the timbre domain, deficits on frequency modulation detection at a rate of 40 Hz (m2) were associated with gray matter volume loss in the insular cortex bilaterally (to the left: $p_{corr.} = 0.002$, 2086 voxels, $Z = 4.48$; -35, 5, 12 (Fig. 4.6A,C) and to the right, including the frontal operculum: $p_{corr.} = 0.002$, 2078 voxels, $Z = 4.14$; 47, 26, -2) (Fig. 4.6B,C). The right frontal opercular part of this cluster overlapped for 8.5% (177 voxels) with the cluster obtained for single time-interval duration discrimination (r1) (Fig. 4.7). No other

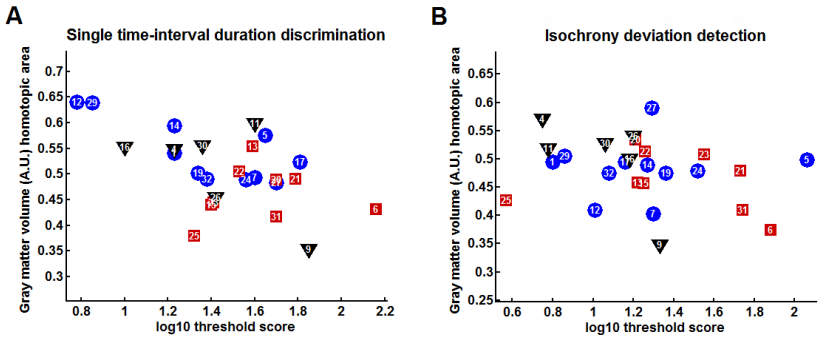


Figure 4.5: **Laterality effects of temporal processing deficits**. **(A)** Scatterplot demonstrating the correlation between gray matter volume in the left frontal operculum and single time-interval duration discrimination threshold scores, **(B)** the relationship between gray matter volume in the left insula and isochrony deviation detection scores. Threshold scores are plotted on the abscissa and extracted modulated gray matter volumes (arbitrary units) on the ordinate of the scatterplot. Black triangles: LV, red squares: NFV, blue circles: SV PPA patients.

timbre tasks were associated with right frontal opercular or right insular atrophy.

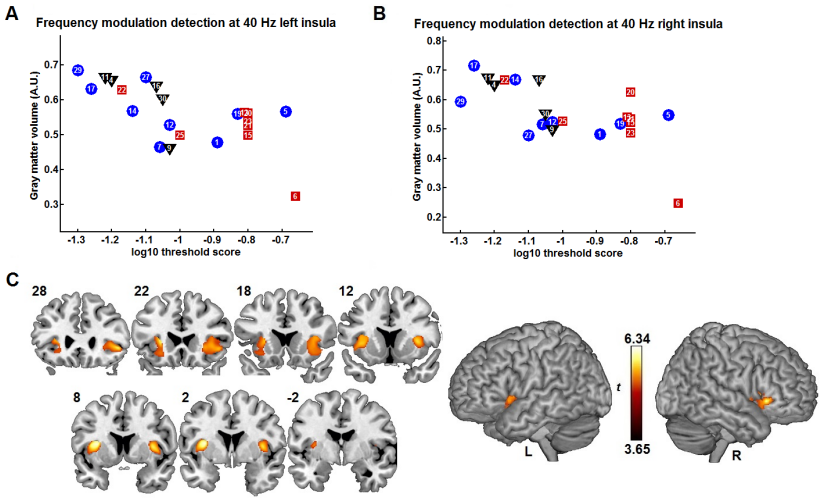


Figure 4.6: **Neuroanatomic correlates of deficits on frequency modulation detection at 40 Hz, corrected for age, gender and scanner site**. **(A)-(B)** Scatterplots with threshold scores are plotted on the abscissa and extracted modulated gray matter volumes for the left and right insula (arbitrary units) on the ordinate. Black triangles: LV, red squares: NFV, blue circles: SV PPA patients. **(C)** T maps are projected on an MNI template brain rendering and on coronal slices with the corresponding MNI coordinates in the left upper corner at a voxel-level uncorrected $p<0.001$, with a cluster-level family wise error (FWE)-corrected threshold $p<0.05$, plus corrected for the number of tests (n = 12).

4.5 Discussion

Deficits on single time-interval duration discrimination (r1) were associated with atrophy in the right frontal operculum. Isochrony deviation detection (r2) deficits were associated with right insular atrophy. When the analysis was performed within the NFV PPA patients, these correlations remained significant. In the timbre domain, impairment on frequency modulation detection at 40 Hz (m2) was associated with atrophy in the bilateral insular cortex including the right frontal operculum. This right frontal opercular part overlapped to a minor degree with the right frontal opercular cluster derived from the single time-interval duration discrimination (r1) task.

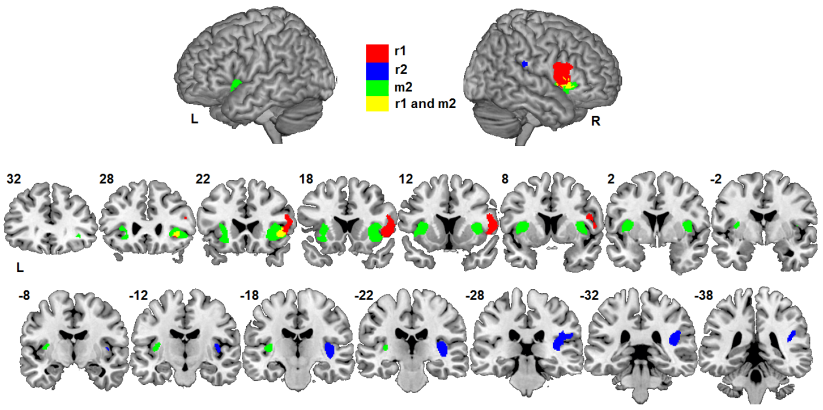


Figure 4.7: **Domain-specificity of neuroanatomical correlates for temporal processing deficits, corrected for age, gender and scanner site**.
T maps are projected on an MNI template brain rendering and on coronal slices with the corresponding MNI coordinates in the left upper corner at a voxel-level uncorrected $p<0.001$, with a cluster-level family wise error (FWE)-corrected threshold $p<0.05$, plus corrected for the number of tests (n = 12). Red: atrophy cluster obtained for single time-interval duration discrimination (r1), blue: atrophy cluster obtained for isochrony deviation detection (r2), green: atrophy cluster obtained for frequency modulation detection at 40 Hz (m2).

4.5.1 The role of the frontal operculum and insula in timing

The insula has well-developed connections with the auditory cortex (Bamiou et al., 2003) and shows responsiveness during auditory evoked potentials (Sudakov et al., 1971). Previous auditory task-based experiments, in which subjects had to discriminate between the duration of two tone pairs, reported activations localized to the right frontal operculum and the right insula (Rao et al., 2001). Another study using a similar task as in Rao et al. (2001), reported activations in the anterior insula bilaterally with a right-hemispheric predominance (Nenadic et al., 2003). These findings are consistent with our results.
Timing-related activations in the right frontal operculum or insular cortex are however not unique to the auditory modality but occur cross-modally (Lejeune et al., 1997; Rao et al., 2001; Ferrandez et al., 2003; Pastor et al., 2006; Marchant and Driver, 2013). In an audiovisual activation study

for instance, visual isochrony activated a timing-related brain network similar to the auditory timing network, with the strongest activations located in the right anterior insula (Marchant and Driver, 2013). It has been shown that the right insula is crucial for the detection of temporally coincident boundaries of perceptual objects both in the auditory as well as in the visual domain (Herdener et al., 2009). Purely visual duration discrimination, assessed by a timing task using subsecond to multisecond time-intervals, also showed activations in a similar network including the bilateral insula (Lewis and Miall, 2003; Morillon et al., 2009). Using a similar task, others have shown timing-related activations in the right insula (Ferrandez et al., 2003). Further evidence demonstrating a link between the insula and timing originates from patients with insular stroke (Bamiou et al., 2006). These patients exhibit deficits on duration discrimination tasks, in which they had to differentiate between shorter and longer duration of stimuli (Bamiou et al., 2006).
The frontal operculum shows significantly greater activity during measurement of short time-intervals (Lewis and Miall, 2003) and activates strongly during interval information processing of visual stimuli (Schubotz and von Cramon, 2001). Altough these findings relate to the visual modality, we demonstrated that the structural integrity of the frontal operculum also plays a role in single time-interval discrimination in the auditory modality. Overall, the aforementioned studies show that the human insula as well as the frontal operculum are multimodally responsive areas that integrate information from visual and auditory sensory modalities (Bamiou et al., 2003). More specifically, there is an evolving view that these regions may be crucial in processing and estimating time, which is supported by our results.

During timing-related processing, the insula and frontal operculum are however not uniquely activated, but a widespread 'timing network', which is cross-modally present, is involved (Nenadic et al., 2003; Grahn and Brett, 2007; Chen et al., 2008; Morillon et al., 2009; Teki et al., 2011; Grahn and Rowe, 2013). Increasing the task difficulty of an auditory timing task recruits the insula/operculum together with the SMA, DLPFC, thalamus and the striatum (Tregellas et al., 2006). Based on previous work, it has been suggested that the pre-SMA and frontal operculum form key components of a cortico-striatal functional network for selectively attending to, and estimating time, independent of stimulus-modality (Schubotz and von Cramon, 2001; Ferrandez et al., 2003; Lewis and Miall, 2003; Coull, 2004). Not only functionally, but also structurally, the SMA is strongly connected through the aslant tract with the pars opercularis and with the insular cortex (Catani et al., 2013;

Mandelli et al., 2014, 2016). Compelling evidence shows that the SMA is not only involved in core time perception but also mediates temporal regularity perception in auditory and motor sequences (Grahn and Brett, 2007; Chen et al., 2008; Teki et al., 2011). We therefore hypothesized involvement of the pre-SMA/SMA and dorsal premotor cortex in deficits on the strongly metrical pattern discrimination task (r3), as these regions are typically atrophic in NFV PPA (Grossman, 2010; Rogalski et al., 2011b; Mandelli et al., 2016; Spinelli et al., 2017). In line with our expectations, we demonstrated a correlation at a reduced significance threshold between metrical pattern discrimination performance (r3) and gray matter volume loss in the right dorsal premotor cortex and borderline significant with gray matter volume of the left pre-SMA/SMA. When the analysis was restricted to NFV patients, metrical pattern discrimination performance correlated with atrophy in the left SMA. This is consistent with a previous study demonstrating that impaired processing of temporal regularity in speech signals in NFV correlates with atrophy of the left SMA (Hardy et al., 2017b).

4.5.2 Lateralization effects

In the whole-brain voxelwise correlational analysis at a predefined significance threshold, single time-interval discrimination (r1) correlated with a cluster in the right but not in the left frontal operculum. We demonstrated that gray matter volume loss in the left homotopic region also showed a significant effect on single time-interval discrimination (r1) deficits. Our findings are in accordance with previous studies, which show a strong effect in the right hemisphere for time discrimination tasks consisting of two tone pairs (Rao et al., 2001; Nenadic et al., 2003). However, this left-hemispheric effect was depended on the significance threshold used. Lowering the significance threshold to voxel-level uncorrected $p < 0.001$ revealed a cluster in the left-hemispheric homotopic area (data not shown).

In the total group of PPA patients, the left frontal operculum was more atrophic compared to the right frontal operculum. The voxelwise volumetric group-comparisons of all three PPA variants showed besides left-hemispheric atrophy, involvement of homotopical regions of the right hemisphere which might be due to disease progression (Grossman, 2010; Rogalski et al., 2011b; Ballard et al., 2014; Mandelli et al., 2016; Spinelli et al., 2017). No effect of symptom duration was found on gray matter volume loss in the left or right frontal opercular cluster. This should

however be considered with caution as symptom duration does not entirely capture disease severity or rate of atrophy progression.

The contribution of selective right-hemispheric atrophy to isochrony deviation detection (r2) deficits was fairly robust, as significant effects in the left homotopic area were absent, both at a VOI-level and at a whole-brain level even if the significance threshold was lowered to voxel-level uncorrected $p < 0.001$. Functional lateralization effects in temporal auditory processing of speech or music have been reported in the insula before: the left insula is hypothesized to process segmental information, while the right insula processes intonation contours of verbal utterances and musical melodies (Meyer et al., 2002; Ackermann and Riecker, 2004).

4.5.3 Domain-specificity of the frontal operculum for timing tasks

Impairment on frequency modulation detection at 40 Hz (m2) was associated with atrophy in the insular cortex bilaterally. This cluster partly overlapped with the right frontal operculum cluster associated with single time-interval duration discrimination (r1). However, the percentage of overlap was rather low, which indicates that the clusters are located in separate regions of the insula/frontal operculum. Our findings are in agreement with a previous study demonstrating involvement of the insular cortex in timbre processing (Menon et al., 2002; Reiterer et al., 2008). However, other studies found an association between timbre and the mid-portion of the right STS and bilateral STS/STG (Warren et al., 2005; Allen et al., 2017). A case study of a patient with a right hemisphere infarction involving the insula reported spared timbre judgement for a frequency modulation task at 40 Hz, albeit with significantly lower perceptual thresholds than controls (Griffiths et al., 1997). To date, there is only limited knowledge regarding the neural correlates of timbre processing (Platel et al., 1997; Menon et al., 2002; Allen et al., 2017). Differences in task design may account for the heterogeneous results regarding the neuroanatomical underpinnings. Moreover, a recent study demonstrated that timbre processing does not rely on an unique brain region but overlaps with regions involved in pitch processing (Allen et al., 2017).

We also obtained a cluster in left insula for performance on frequency modulation detection at 40 Hz (m2). It has been proposed that during timbre processing, spectral cues (harmonic structure) are linked to the right hemisphere and temporal cues (i.e. attack-decay dynamics) are

linked to the left hemisphere (Reiterer et al., 2008). Both cues are present in the frequency modulation detection task, which can explain the bilateral effect. This bilateral effect might also be explained by the 'asymmetric sampling in time' (AST) hypothesis (Poeppel, 2003). Basically, the AST suggests that perception of rapidly changing cues (around 40 Hz) preferentially drives the left hemisphere, whereas the right auditory cortex is better adapted at processing slowly changing acoustic cues (around 4 Hz).

4.5.4 Shared neuroanatomy for timing and speech apraxia features in NFV PPA

The right-hemispheric correlations for single time-interval duration discrimination (r1) and isochrony deviation detection (r2) deficits were also significant when we performed the analyses within the NFV PPA group. Consequently, we hypothesize that deficits on these tasks might be associated with the clinical phenotype of motor speech deficits in NFV PPA.

The role of the frontal operculum is well-documented in studies assessing language (Poldrack et al., 1999, 2001; Meyer et al., 2002; Ballard et al., 2014; Zaccarella and Friederici, 2015). Patients with fronto-opercular lesions show strikingly preserved word reading but are less accurate at reading non-words (Poldrack et al., 1999; Fiez et al., 2006). These findings might indicate that the frontal operculum is important in analyzing sequential information over time (Tillmann et al., 2006; Geiser et al., 2008), regardless of semantic content.
Accurate timing is also of great importance in execution of motor programs of speech. Right frontal opercular and right insular atrophy in patients with NFV PPA has been related to more silence time during reading and lower contrastiveness of vowel duration in polysyllabic words with weak-strong stress (Ballard et al., 2014). An independent study also showed that motor speech deficits are strongly associated with lesions in the IFG (pars opercularis) and in the premotor cortex (Josephs et al., 2013b). These regions are considered to be centrally involved in the development and refinement of speech motor programs specifying temporally and spatially coordinated multi-articulator movements for syllable production (Bohland and Guenther, 2006).

4.5.5 Potential study limitations and strengths

Patients that could not reliably perform the practice tasks were excluded of any further analysis. Musical training or expertise were very unlikely to drive performance (Ono et al., 2011), as none of the participants were professional musicians. However, the effect of working memory impairments could have influenced task performance, in particular for tasks which used long sequences of tones. Of note is that the sequences did not contain linguistic stimuli and therefore our tasks relied on working memory for auditory objects rather than on phonological working memory. The relative preservation of processing of tone sequences in LV underscores the distinction between phonological working memory and the type of auditory working memory required to process nonverbal sounds and sequences of those. The phonological working memory impairment in LV does not affect processing of short term memory of tones (Foxe et al., 2016). Some studies demonstrated that the opercular region of the inferior frontal gyrus is necessary for the normal operation of phonologically based working memory mechanisms (Nixon et al., 2004). This overlaps with the brain basis for auditory working memory including the insula bilaterally as well as the auditory cortex, hippocampus and IFG (Kumar et al., 2016). We cannot exclude the contribution of impaired auditory working memory to performance on single time-interval duration discrimination (r1) or isochrony devation detection (r2), especially as these tasks rely on shared neuroanatomical substrates. We however consider it unlikely that an auditory working memory problem could explain the motor speech deficits in NFV but it could play a role in agrammatism (Grossman and Ash, 2004; Rohrer et al., 2010b). Previous studies demonstrated a distributed network underlying rhythm and timing processing rather than single structures being involved (Grahn and Brett, 2007). The use of morphometry in this study instead of fMRI precludes to make assumptions on the network-based connectivity of these regions.

4.6 Conclusion

Rhythm and timing processing deficits in the syndrome of PPA are associated with right-hemispheric atrophy of the frontal operculum and posterior insula. The right frontal operculum was however not uniquely involved in timing but had an additional role in timbre processing. We

propose that the perceptual timing deficits contribute to the motor speech problem associated with NFV PPA.

Table 4.1: Demographics and neuropsychological assessment of SV PPA

Case nr.	1	5	7	10	12	14	17	19	24	27	29	32
Age	76	70	61	64	64	48	58	69	73	63	55	70
Gender	m	f	m	f	m	f	f	f	f	f	m	f
Education	14	12	17	12	8	12	10	7	14	13	14	17
Variant	SV	SV	SV	SV	SV	SV	SV	SV	SV	SV	SV	SV
Symptom dur.	6	1.5	3	3	3	6	2	5	1.5	1	0.5	5
MRI	+	+	+	-	+	+	+	+	+	+	+	+
FDG PET	+	+	+	+	+	+	+	+	+	+	+	+
PIB SUVR	1.15	-	-	-	-	-	-	-	-	1.12	1.2	-
CSF $A\beta_{42}$	-	1330	-	-	-	-	-	733	1558	-	-	-
CSF t-tau	-	269	-	-	-	-	-	262	428	-	-	-
BNT /60	**34**	**22**	**7**	**10**	**20**	**12**	**35**	**16**	**11**	**17**	**33**	**4**
PALPA comprehension												
aud. WP /40	**38**	**36**	**31**	**29**	**31**	**27**	40	**30**	**26**	**26**	39	**33**
assoc.-sem. /30	27	**17**	**18**	**22**	**14**	**24**	27	**21**	**12**	**22**	**14**	**15**
AAT comprehension												
aud. word /30	**19**	**15**	**11**	**19**	**19**	**11**	**21**	**14**	**14**	**22**	28	**16**
aud. sent. /30	26	**20**	25	**19**	**20**	25	**21**	**24**	**24**	**23**	30	**24**
writ. word /30	**20**	**18**	**13**	**11**	**13**	**19**	**24**	**14**	**17**	**17**	30	**18**
writ. sent. /30	25	**21**	**24**	**23**	**22**	27	27	30	25	**22**	30	**22**
PALPA repetition												
single-word /80	72	78	78	79	71	79	76	78	79	77	79	80
pseudoword /80	**55**	71	74	65	**56**	80	72	77	77	67	77	71
AAT repetition												
phoneme /30	30	**28**	29	30	**28**	30	30	30	30	30	30	30
single-word /30	**27**	29	29	30	**27**	30	30	**28**	29	**27**	30	26
cognates /30	30	30	30	30	30	30	30	29	30	**28**	30	30
composed /30	30	30	**28**	30	29	30	**28**	30	30	**28**	30	30
sent. /30	30	28	**25**	30	29	30	30	29	29	30	30	28
BORB B /32	**23**	**18**	**20**	**21**	**26**	**26**	31	**23**	**22**	**22**	**25**	**19**
BORB A /32	**20**	**20**	**18**	**18**	**18**	**17**	27	**17**	**17**	**22**	26	**22**
PPT /52	**37**	**39**	**40**	**35**	**40**	**46**	50	**43**	**31**	**38**	**47**	**41**
CPM /36	29	**24**	36	31	29	35	36	34	28	34	34	35

Abbreviations: AAT: Akense Afasie Test, Assoc.-sem: associative semantic, aud.: auditory, BNT: Boston Naming test, BORB: Birmingham Object recognition battery B (easy) and A (hard), CPM: Coloured Progressive Matrices, CSF: cerebrospinal fluid (pg/ml), PIB SUVR, Pittsburgh Compound-B PET standardized uptake value ratio in a composite cortical volume of interest (Adamczuk et al., 2013), PPT: Pyramids and Palm trees test with pictures, sent.: sentence, symptom dur.: duration (years), WP: word-picture; writ: written. '-': means that data were not acquired. Age, education and symptom duration are expressed in years. Bold: Significantly different from controls based on Crawford and Garthwaite (2006) or Crawford and Howell (1998) statistical procedures.

Table 4.2: Demographics and neuropsychological assessment of NFV PPA

Case nr.	6	13	15	20	21	22	23	25	31
Age	52	79	71	78	72	63	62	57	70
Gender	f	f	m	m	f	f	f	f	m
Education	17	8	15	17	12	15	12	10	18
Variant	NFV	NFV	NFV	NFV	NFV	NFV	NFV	NFV	NFV
Symptom dur.	2	5	1.5	2.5	2.5	5	1	3.5	3
MRI	+	+	+	+	+	+	+	+	+
FDG PET	-	+	+	+	-	+	+	+	+
PIB SUVR	1.2	-	-		-		1.26	-	1.35
CSF $A\beta_{42}$	-	1028	-	816	1060	865	-	1057	-
CSF t-tau	-	312	-	195	424	183	-	247	-
BNT /60	58	48	55	48	**30**	**41**	**46**	**7**	**41**
PALPA comprehension									
aud. WP /40	40	40	**37**	39	**36**	**38**	39	**37**	39
assoc.-sem. /30	28	**22**	28	**23**	**19**	**24**	26	29	25
AAT comprehension									
aud. word /30	30	27	27	**24**	**20**	**21**	26	26	**23**
aud. sent. /30	30	**24**	25	**12**	**23**	25	**19**	26	**21**
writ. word /30	30	30	**25**	**23**	**21**	28	**23**	30	**19**
writ. sent. /30	30	**24**	**25**	18	**21**	30	**24**	**23**	**22**
PALPA repetition									
single-word /80	76	74	74	74	69	80	80	76	77
pseudoword /80	**55**	59	**40**	**54**	**30**	79	72	63	57
AAT repetition									
phoneme /30	**28**	29	30	29	**26**	30	**28**	**27**	**20**
single-word /30	**26**	**24**	**21**	30	**28**	30	30	29	30
cognates /30	**28**	**22**	29	**28**	**24**	30	30	**28**	29
composed /30	**26**	**23**	**25**	29	**18**	30	29	**15**	29
sent. /30	**26**	**27**	**18**	28	**11**	28	28	**17**	28
BORB B /32	31	30	31	**26**	**18**	**22**	**25**	28	31
BORB A /32	26	25	26	29	**21**	28	**19**	31	24
PPT /52	52	51	50	**47**	**46**	**48**	**47**	**47**	**47**
CPM /36	31	**24**	**24**	30	**12**	32	31	-	**29**

Abbreviations: AAT: Akense Afasie Test, Assoc.-sem: associative semantic, aud.: auditory, BNT: Boston Naming test, BORB: Birmingham Object recognition battery B (easy) and A (hard), CPM: Coloured Progressive Matrices, CSF: cerebrospinal fluid (pg/ml), PIB SUVR, Pittsburgh Compound-B PET standardized uptake value ratio in a composite cortical volume of interest (Adamczuk et al., 2013), PPT: Pyramids and Palm trees test with pictures, sent.: sentence, symptom dur.: duration (years), WP: word-picture; writ: written. '-': means that data were not acquired. Age, education and symptom duration are expressed in years. Bold: Significantly different from controls based on Crawford and Garthwaite (2006) or Crawford and Howell (1998) statistical procedures.

Table 4.3: Demographics and neuropsychological assessment of LV PPA

Case nr.	4	9	11	16	26	30
Age	57	64	62	71	77	74
Gender	f	m	f	m	m	m
Education	15	17	15	15	10	18
Variant	LV	LV	LV	LV	LV	LV
Symptom dur.	6 0.5	3	1.5	1	5.0	4
MRI	+	+	+	+	+	+
FDG PET	+	+	+	-	+	+
PIB SUVR	1.85	2.24	-	-	-	-
CSF Aβ_{42}	664	-	516	-	564	321
CSF t-tau	183	-	>1200	-	407	858
BNT /60	56	**41**	53	53	46	**24**
PALPA comprehension						
aud. WP /40	40	40	40	40	**38**	**38**
assoc.-sem. /30	28	**23**	27	28	28	27
AAT comprehension						
aud. word /30	30	29	25	28	26	25
aud. sent. /30	30	27	25	30	26	25
writ. word /30	30	30	**26**	30	27	**25**
writ. sent. /30	30	28	30	30	**22**	26
PALPA repetition						
single-word /80	80	77	80	80	79	80
pseudoword /80	74	69	79	63	66	**56**
AAT repetition						
phoneme /30	30	**28**	30	**27**	30	29
single-word /30	30	29	30	30	30	29
cognates /30	30	30	30	29	30	30
composed /30	29	30	30	**27**	**15**	30
sent. /30	28	28	30	**27**	**13**	**24**
BORB B /32	29	31	31	31	28	**26**
BORB A /32	25	25	24	26	23	**21**
PPT /52	51	51	52	50	49	**45**
CPM /36	33	35	31	33	32	**12**

Abbreviations: AAT: Akense Afasie Test, Assoc.-sem: associative semantic, aud.: auditory, BNT: Boston Naming test, BORB: Birmingham Object recognition battery B (easy) and A (hard), CPM: Coloured Progressive Matrices, CSF: cerebrospinal fluid (pg/ml), PIB SUVR, Pittsburgh Compound-B PET standardized uptake value ratio in a composite cortical volume of interest (Adamczuk et al., 2013), PPT: Pyramids and Palm trees test with pictures, sent.: sentence, symptom dur.: duration (years), WP: word-picture; writ: written. '-': means that data were not acquired. Age, education and symptom duration are expressed in years. Bold: Significantly different from controls based on Crawford and Garthwaite (2006) or Crawford and Howell (1998) statistical procedures.

Chapter 5

Single-word comprehension deficits in the nonfluent variant of primary progressive aphasia

This study has been prepared for publication:

Schaeverbeke,J, Gabel,S, Meersmans,K, Evenepoel,C, Bruffaerts,R, Van Bouwel,K, Dries,E, Sieben,A, Pijnenburg,Y, Peeters,R, Bormans,G, Van Laere,K, Koole,M, Dupont,P, Vandenberghe,R. Single-word comprehension deficits in the nonfluent variant of primary progressive aphasia.

5.1 Abstract

According to the current recommendations for primary progressive aphasia (PPA) classification, single-word comprehension is typically spared in patients with the nonfluent/agrammatic variant (NFV-pure) of PPA. When single-word comprehension deficits occur in combination with speech apraxia and/or agrammatism, this has sometimes been referred to as the mixed variant (MV) of PPA.

In a consecutive series of PPA patients, we examined the prevalence and nature of word comprehension problems in individual PPA patients with speech apraxia and/or agrammatism. We also assessed how these patients differed based on their atrophy pattern as well as on [^{11}C]-PIB and [^{18}F]-THK5351 PET binding from controls and other PPA variants. Neuropsychological performance in domains apart from single-word comprehension, motor speech and grammatical processing was also assessed and compared to controls and other PPA variants.
Six out of 10 cases who had been classified *a priori* as NFV PPA had deficits on conventional single-word comprehension tests along with speech apraxia. In these patients, object knowledge and object recognition were also affected, although to a lesser degree than in the semantic variant (SV) of PPA. Atrophy in MV PPA was present in frontal and temporoparietal regions, while atrophy in NFV-pure PPA was localized to frontal regions. [^{18}F]-THK5351 binding in MV was highest in the left upper premotor cortex and supplementary motor area (SMA) and the pattern overlapped with that seen in NFV-pure in the SMA. At the individual patient level, this particular [^{18}F]-THK5351 binding pattern was present in five out of six MV cases. Elevated [^{18}F]-THK5351 binding was also present in four of these five cases in the basal ganglia and in the midbrain including the substantia nigra. [^{18}F]-THK5351 binding, but not gray matter volume loss, correlated with core clinical features of MV PPA. Regarding amyloid burden, two out of six MV PPA cases were amyloid biomarker-positive compared to none of the NFV-pure cases. As a group, elevated [^{11}C]-PIB binding in MV PPA was localized to the orbitofrontal cortex and precuneus.

In patients with motor speech problems and/or agrammatism who have concomitant single-word comprehension problems (MV PPA), the topographical distribution of [^{18}F]-THK5351 binding is highly similar to that observed in NFV-pure, but atrophy is more widespread in MV PPA. The topography of [^{18}F]-THK5351 binding, but not the degree of atrophy was correlated with core clinical features of MV PPA. MV PPA may have possibly a higher likelihood of amyloid-positivity compared to NFV-pure PPA.

5.2 Introduction

Primary progressive aphasia (PPA) is a neurodegenerative syndrome, characterized by an isolated language impairment with relative sparing of other cognitive domains (Gorno-Tempini et al., 2011). Depending

on its clinical presentation, three variants are currently recognized: a logopenic (LV), a nonfluent/agrammatic (NFV) and a semantic variant (SV) of PPA (Gorno-Tempini et al., 2011). LV PPA show hesitant speech, phonemic paraphasias and repetition problems in particular for complex sentences. The clinical diagnosis of NFV PPA is based on the presence of two core clinical features: speech apraxia and/or agrammatism, and at least two of the following three features: impaired comprehension of syntactically complex sentences, spared single-word comprehension, or spared object knowledge (Gorno-Tempini et al., 2011). Problems of sentence comprehension may occur as a part of the agrammatism. Cases who have purely speech apraxia without clear agrammatism are sometimes classified as apraxia of speech (AOS) (Josephs et al., 2006b, 2012, 2013b; Whitwell et al., 2017a). AOS is a disorder of speech motor planning and/or programming that has been set apart from PPA according to some researchers (Josephs et al., 2006b, 2012, 2013b; Whitwell et al., 2017a). Preservation of single-word comprehension or object knowledge in NFV is in line with the classical localization of these functions in the ventral language processing stream (Hickok and Poeppel, 2015). By contrast, in NFV PPA the dorsal language stream is typically affected (Mandelli et al., 2016; Marcotte et al., 2017). This contrasts with SV PPA where impaired single-word comprehension is a core clinical feature along with confrontation naming deficits (Gorno-Tempini et al., 2011). One of the following three features should also be present in SV: impaired object knowledge for low frequency items, surface dyslexia with poor reading of irregular words and/or dysgraphia (Gorno-Tempini et al., 2011).

The combination of motor speech problems and/or agrammatism together with single-word comprehension deficits has previously been proposed in a few studies to constitute a fourth, mixed variant (MV) of PPA (Mesulam et al., 2009, 2012; Sajjadi et al., 2014)(for review: Vandenberghe (2016)). However, this PPA variant is not formally recognized in the current classification criteria (Gorno-Tempini et al., 2011). Some studies report that 15-30% of PPA patients remain unclassified as they fit criteria for more than one PPA variant (Mesulam et al., 2012; Martersteck et al., 2015). It has been shown that inclusion of a mixed phenotype into the list of variants raises the comprehensiveness of the classification from 80% to nearly 90% of PPA cases (Mesulam et al., 2012). To date, only limited neuroimaging data are available in MV PPA. Based on structural magnetic resonance imaging (MRI), atrophy is confined to frontotemporal regions with a left-hemispheric predominance (Mesulam et al., 2012; Spinelli et al., 2017). At pathological examination, MV PPA

is more likely associated with Alzheimer's disease (AD) pathology, being present in 25%-67% of cases (Mesulam et al., 2014b; Spinelli et al., 2017), or with Pick's disease pathology (50%) (Spinelli et al., 2017).

The primary objective was to assess the prevalence and nature of single-word comprehension problems in individual PPA patients with speech apraxia and/or agrammatism. We also assessed how these patients differed based on their atrophy pattern as well as on [^{11}C] Pittsburgh Compound B ([^{11}C]-PIB) and [^{18}F]-THK5351 positron emission tomography (PET) binding compared to controls, NFV-pure, SV and LV PPA. [^{11}C]-PIB has high affinity and selectivity for β-amyloid plaques (Klunk et al., 2004) and [^{18}F]-THK5351 is considered to have high binding affinity and selectivity for tau aggegrates (Harada et al., 2016). As a secondary objective, neuropsychological performance in domains apart from the defining domains of single-word comprehension or speech apraxia and/or agrammatism was compared to controls, NFV-pure, SV and LV PPA.

5.3 Material and Methods

5.3.1 Subjects

A consecutive series of 19 patients who fulfilled the international consensus criteria for PPA (Gorno-Tempini et al., 2011) enrolled. Seventeen patients were recruited through the memory clinic University Hospitals Leuven, case 3 was referred for the study by the Free University Amsterdam and case 17 by the University Hospital Ghent. One case (case 15) had to be excluded due to a subarachnoid cyst anterior to the left temporal lobe. Classification of patients relied on the clinical evaluation by an experienced neurologist in combination with the results from the clinical MRI and [^{18}F]-fluoro-deoxy-glucose ([^{18}F]-FDG-PET) scan. None of the cases could be considered as progressive AOS (Josephs et al., 2006b, 2012, 2013b; Whitwell et al., 2017a) as agrammatism was present in all patients that concomitantly exhibited motor speech problems. A subset of PPA patients (n = 11) had had a CSF AD biomarker measurement (INNOTEST ELISA for amyloid-β_{42} (Aβ_{42}) (cut-off = 745 pg/ml, (Adamczuk et al., 2015)), total-tau, and phospho$_{181}$-tau, Fujirebio Europe, Ghent, Belgium), which was performed at the Laboratory of Medical analysis, Medicine Department of UZ Leuven, Belgium, as part of the clinical work-up (Table 5.1). In PPA patients who

had not previously received a clinical CSF test for Aβ_{42}, [^{11}C]-PIB PET was acquired (the cut-off for amyloid-positivity was based on a modified t-test, comparing each individual patient with a matched control group (Crawford and Howell, 1998)).

Neurolinguistic and neuropsychological data from 67 cognitively intact control subjects (32 male; age range 53-89 years, mean 67.1, standard deviation (SD) 7.4; education range 8-22 years, mean 13.6, SD 2.8; Mini-mental state examination (MMSE) score $>$ 27 and Clinical Dementia Rating scale (CDR) = 0) (Nelissen et al., 2007; Grube et al., 2016) were used to calculate whether the performance of an individual PPA patient was within norms. Of these 67 control subjects, 22 underwent a high resolution T_1-weighted structural MRI on the same scanner as the 18 PPA patients, 20 a [^{18}F]-THK5351 PET scan, and 16 of these 20 subjects also underwent a [^{11}C]-PIB PET scan as part of the study protocol. For the purpose of comparing brain volume in the PPA variants with that of a matched cognitively intact control group, high resolution T_1-weighted structural MRI scans of 30 additional matched cognitively intact controls scanned on the same MRI scanner were used (14 male; age range 59-83 years, mean 71.7, SD 5.4; MMSE score $>$ 27; CDR = 0) (Adamczuk et al., 2014). For the purpose of comparing amyloid load between groups, [^{11}C]-PIB scans of 19 matched amyloid-negative controls (13 male; age range 68-80 years, mean 73.7, SD 3.3; MMSE score $>$ 27; CDR = 0) were used (Adamczuk et al., 2016).

The study was approved by the Ethics Committee, University Hospitals Leuven (s56920, EC approval 22/09/2014). After receiving a complete description of the study protocol, all participants or their spouses provided written informed consent in accordance with the Declaration of Helsinki.

5.3.2 Neuropsychological and neurolinguistic protocol

General cognitive functioning was assessed by the CDR and the MMSE. Colored Progressive Matrices (CPM) was used to assess nonverbal fluid intelligence. Confrontation naming was assessed by means of the Boston Naming Test (BNT) (Mariën et al., 1998). Verbal fluency was assessed by the 1-minute Animal Verbal Fluency test.

The main aim of this study was to detect single-word comprehension problems in patients with motor speech problems and/or agrammatism. Single-word comprehension was assessed using the sum of the Akense

Afasie test (AAT) auditory and written single-word comprehension scores (20 trials). In the auditory and written word comprehension subtests of the AAT, 10 words are presented per modality. One target picture and three distracter pictures are presented simultaneously and subjects have to indicate the picture that corresponds to the word. One distracter picture is semantically related to the target picture. The performance of individual patients on the sum of the AAT auditory and written single-word comprehension test was statistically compared with the control group based on a modified t-test (Crawford and Howell, 1998) (Table 5.1) (see Statistical analyses).

The Psycholinguistic Assessment of Language Processing in Aphasia (PALPA) auditory word-picture matching test (PALPA subtest 45) was additionally used to assess word comprehension deficits. In this task (40 trials), a concrete noun is presented auditorily together with a target picture and four distractors. Two distractors are semantically related to the target, a third is perceptually similar and the fourth picture is unrelated. Subjects were asked to point to the target.

Associative-semantic memory was assessed by the picture-version of the Pyramids and Palm trees test (PPT)(52 trials) which relies on the capability to make semantic associations between two pictures.

The Birmingham Object Recognition Battery (BORB) (easy (B) and hard (A), 32 trials each) was used as a measure of object identification. In this task, subjects have to indicate whether an animal or tool depicted in a line drawing exists in real life.

In the PALPA associative-semantic task (PALPA subtest 49), a noun is presented visually together with four choice noun stimuli (a target noun, a noun that is semantically related to the target, and two unrelated nouns). Subjects have to underline or circle the noun that matches the sample stimulus most closely in meaning, for a total of 15 word series with high imageability and 15 with low imageability.

Verb comprehension and grammaticality were assessed by the Werkwoorden en Zinnentest (WEZT). Grammaticality was quantified using both the WEZT auditory sentence comprehension test (40 trails) as well as the WEZT sentence anagram test (20 trials). During administration of the WEZT sentence anagram test, the patient is asked to put single words printed on separate cards into a syntactic structure which describes the action depicted in a target picture. Sentences can occur in the active or passive tense, of which half represent reversible actions and half represent irreversible actions.

In the AAT repetition task, the examiner pronounces 10 phonemes, 10 monosyllabic words, 10 foreign words, 10 composed words and 10 sentences of increasing length which the subject has to repeat.

In the PALPA word repetition task (PALPA subtest 9), the examiner who is sitting in front of the subject, pronounces 80 nouns and 80 pseudowords which the subject has to repeat.
Diagnostisch Instrument voor apraxie van de Spraak (DIAS) was used to assess consonant and vowel repetition (15 each, sum = DIAS severity score) as well as diadochokinesis. The diadochokinesis task was used to assess the ability to make antagonistic movements using different parts of the mouth, tongue, and soft palate in quick succession. During this task, the examiner first reads three successive sounds or tokens aloud, e.g. alternating task: 'pa ta ka' or the sequential task: 'pa pa pa' and asks the patient to repeat these once. If the patient was able to repeat this sequence correctly, he/she is asked to repeat it as many times as possible during a period of eight seconds. In total, the patient has to repeat six alternating and six sequential sounds (Table 5.1).

5.3.3 Volumetric MRI acquisition and analysis

Study participants were scanned on the same day as the acquisition of the neuropsychological test battery. All subjects received a high resolution T_1-weighted structural MRI on a 3T Philips Achieva dstream equipped with a 32-channel head volume coil, using a 3D turbo field echo sequence (coronal inversion recovery prepared 3D gradient-echo images, inversion time (TI) 900 ms, shot interval = 3000 ms, echo time (TE) = 4.6 ms, repetition time (TR) = 9.6 ms, flip angle 8°, field of view (FoV) = 250×250 mm, 182 slices, slice thickness = 1.2 mm, voxel size 0.98×0.98×1.2 mm^3). Preprocessing of the T_1-weighted images was performed with Voxel-based morphometry (VBM8, http://dbm.neuro.uni-jena.de/vbm) running on Statistical Parametric Mapping (SPM8) (Ashburner and Friston, 2000) implemented in Matlab R2012b (Mathworks, Natick, MA, USA) as described previously (Gillebert et al., 2015; Schaeverbeke et al., 2017). The resulting gray matter volumes were adjusted for overall brain size (total intracranial volume) by using the 'nonlinear only' component in the spatial normalization process for modulation of gray matter voxel intensities (Barnes et al., 2010). For subsequent voxel-based statistical analyses, gray matter maps were smoothed with an 8 mm isotropic Full-Width Half Maximum (FWHM) Gaussian 3D kernel.

5.3.4 [^{18}F]-THK5351 PET acquisition and analysis

[^{18}F]-THK5351 PET scans were acquired on a 16-slice Siemens Biograph PET/CT scanner (Siemens Medical Solutions, Erlangen, Germany). After bolus injection of [^{18}F]-THK5351 (mean dose 185.2 MBq, SD 5.7 MBq, range 178.7-191.0 MBq) in an antecubital vein, five control subjects were scanned dynamically with arterial sampling between 0-100 min post-injection to assess the optimal PET imaging window. The remaining controls and all PPA patients were scanned between 50-80 min *post* injection with [^{18}F]-THK5351 (mean dose 184.1 MBq, SD 8.5 MBq, range 165.8-196.0 MBq in controls, mean dose 181.8 MBq, SD 6.8 MBq, range 164.9-192.3 MBq in patients). A low dose CT scan was acquired for attenuation correction purposes prior to PET scan acquisition. PET emission images were acquired in 3D mode and subsequently reconstructed as six 300 s frames using 3D-filtered back-projection, corrected for random events, scatter, photon attenuation and decay using the manufacturer's software (ordered-subsets expectation maximization with 16 subsets and 4 iterations).

Individual [^{18}F]-THK5351 PET emission frames were realigned, summed and rigidly co-registered to the subjects T_1-weighted MRI scan. Both the summed PET images as well as the T_1-weighted MRI segmentations were normalized to Montreal Neurological Institute (MNI) template space. The normalized [^{18}F]-THK5351 PET scans were subsequently corrected for partial volume effects using the modified Müller-Gärtner method (Müller-Gärtner et al., 1992). Partial volume corrected (PVC) standardized uptake volume ratio (SUVR) images with the subject-specific cerebellar gray matter as reference region were created. For voxel-based statistical analyses, PVC [^{18}F]-THK5351 SUVR images were smoothed with an isotropic 8 mm FWHM Gaussian kernel.

[^{18}F]-THK5351 PET data were obtained within 2-182 days from the [^{11}C]-PIB PET scan (mean 82 days in controls; mean 19 days in PPA patients).

5.3.5 Amyloid biomarker measurement and analysis

[^{11}C]-PIB PET scans were acquired on a GE Signa 3T PET/MR scanner (GE Healthcare, Chicago, USA) operating in 3D mode to estimate amyloid burden. For normative reasons, sixteen controls also received a [^{11}C]-PIB PET scan on the same scanner. The [^{11}C]-PIB PET scans of two controls needed to be excluded based on abortion of scanning

due to claustrophobia. [^{11}C]-PIB was injected intravenously as a bolus (mean dose 270.5 MBq, SD 26.2 MBq, range 230.6-316.4 MBq in patients and mean dose 267.8 MBq, SD 51 MBq, range 197.5-364.9 MBq in controls) in an antecubital vein. Dynamic images were acquired during a 70 min period and reconstructed using an atlas-based approach based on the manufacturer's software. Two patients received a 30 min [^{11}C]-PIB PET scan between 40 and 70 min *post* injection on a Siemens Biograph PET/CT scanner (Siemens Medical Solutions, Erlangen, Germany) in a clinical context. For normative reasons as well as to account for possible scanner site effects, [^{11}C]-PIB scans of 19 matched amyloid-negative controls acquired on the same Siemens Biograph PET/CT scanner were used (Adamczuk et al., 2016).

Processing of [^{11}C]-PIB PET images was done as previously described (Adamczuk et al., 2013, 2016). Briefly, individual PET emission frames were realigned, summed and rigidly co-registered to the subjects T_1-weighted MRI scan. Both the summed PET images as well as the T_1-weighted MRI segmentations were normalized to MNI template space. The normalized [^{11}C]-PIB PET scans were subsequently corrected for partial volume effects using the modified Müller-Gärtner method (Müller-Gärtner et al., 1992). [^{11}C]-PIB PET SUVR images with the subject-specific cerebellar gray matter as reference region were created as previously described (Adamczuk et al., 2013, 2016).

Our primary PET outcome measure was the mean [^{11}C]-PIB PET SUVR in a composite cortical volume of interest (VOI). The composite VOI consisted of five bilateral cortical areas (Adamczuk et al., 2013). Neocortical [^{11}C]-PIB PET SUVR values were considered positive if they were significantly elevated compared to the matched healthy control group based on a modified *t*-test (Crawford and Howell, 1998). For voxel-based statistical analyses, PVC [^{11}C]-PIB SUVR images were smoothed with an isotropic 6 mm^3 FWHM Gaussian kernel.

5.3.6 Statistical analyses

Standard statistical analyses were performed in Statistics Software Package for the Social Sciences (version 24, IBM Statistics, Armonk, USA). Demographic data were statistically assessed using Kruskal-Wallis for continuous variables, followed by two-tailed Mann-Whitney *U post hoc* tests and with Pearson chi^2 tests for categorical variables. Neuropsychological test scores were checked for outliers using the Grubbs'

test: Z scores higher than three standard deviations were classified as outliers. Outliers were removed when performing correlational analyses.

A first objective was to assess the prevalence of deficits on single-word comprehension tests in individual PPA patients with speech apraxia and/or agrammatism. The individuals' neuropsychological test scores were statistically contrasted with an extended group of healthy controls (n = 67) (described in the Methods section) following the procedure developed by Crawford and Garthwaite (2006). As a first step, we performed for each task a hierarchical multiple linear regression analysis in the healthy control group, with as outcome variable the neuropsychological test scores and as predictor variables age and education. Variables that had a significant effect on any of the test scores in the healthy controls were included as predictor variables in the regression equation: there was a statistically significant effect of education on the hard BORB object recognition task (R^2 adjusted = 0.054, $p = 0.034$), and on the CPM task (R^2 adjusted = 0.075, $p = 0.016$). Age had a significant effect on performance on the AVF (R^2 adjusted = 0.14, $p = 0.012$), BNT (R^2 adjusted = 0.048, $p = 0.042$), AAT repetition of single words (R^2 adjusted = 0.065, $p = 0.043$), cognates (R^2 adjusted = 0.15, $p = 0.003$) and concatenated words (R^2 adjusted = 0.11, $p = 0.011$). Consequently, when assessing the individual patient's scores, education or age, respectively, were entered as predictor variables and the test score of the individual patient as dependent variable in the regression equation derived from the control group. The discrepancy between the predicted score and the observed score was expressed as a Z-score, which was considered abnormal at 1.9. Individual performance on the other tasks was statistically compared with the control group based on a modified t-test (Crawford and Howell, 1998) (Table 5.1).

The nature of the single-word comprehension deficit in MV PPA was analyzed in detail by assessing the influence of word frequency. Word frequency was retrieved using the SUBTLEX-NL database (http://crr.ugent.be/programs-data/subtitle-frequencies/subtlex-nl) for the dominant meaning of words (Keuleers et al., 2010). However, in 11 out of 20 trials of the AAT auditory and written single-word comprehension test, the non-dominant meaning of a word with multiple meanings (i.e. a homonym) is targeted. For instance, in case the word 'star' was presented to the patient, the target picture depicted a 'popstar' and the distractor picture depicted a 'sun', which was semantically related to the dominant meaning but not to the non-dominant meaning of 'star'. In order to estimate the relative meaning frequencies of each meaning of a homonym, we made use of lexical

associations, as described in Armstrong et al. (2012). Associations of the words used in the AAT single-word comprehension task were taken from the Small World of Words Project (De Deyne et al., 2013) (https://smallworldofwords.org/nl/project/explore). The estimated frequency of the non-dominant meaning of a word was calculated by multiplying the relative frequency with the frequency retrieved from the SUBTLEX-NL database. The frequency of the words assessed in the PALPA word-picture matching task (PALPA subtest 45) were directly taken from the SUBTLEX-NL database, as only the dominant meaning of words was targeted in this test. In total, we were able to retrieve the frequency for 53 out of 60 words from the pooled AAT and PALPA word comprehension tasks.

As a second objective, the T_1-weighted structural MRI, [^{18}F]-THK5351 and [^{11}C]-PIB PET SUVR images of MV PPA patients were compared to controls, NFV-pure, SV and LV PPA patients (= between-subjects factor) using a whole-brain voxelwise analysis of covariance (ANCOVA) with two-tailed *post hoc* *t*-tests in SPM12 running on Matlab R2014b (Mathworks, Natick, MA, USA) with age and gender as nuisance variables. For the ANCOVA with [^{11}C]-PIB PET SUVR images, scanner type was added as a nuisance variable.

Imaging data of individual patients were statistically contrasted to images of the control group for each modality, using a voxelwise modified *t*-test (Crawford and Howell, 1998) at voxel-level uncorrected $p<0.001$.

We also performed voxelwise linear regression analyses across the NFV-pure and MV groups with modulated gray matter volume maps or PVC [^{18}F]-THK5351 PET SUVR images as dependent variable and the test scores on the defining domains of grammatical processing, motor speech or single-word comprehension as independent variable, and age and gender as nuisance variables (Barnes et al., 2010). The absolute intensity threshold was set at 0.1 (Ridgway et al., 2009). Test scores which deviated in their original format from normality, were log-transformed to fulfill the assumptions of normality for SPM analyses. In case a significant correlation was found, we calculated the mean gray matter volume or mean [^{18}F]-THK5351 SUVR signal intensity in these clusters obtained in the voxelwise linear regression analyses to visualize the correlation in a scatterplot.

For all group-based voxelwise analyses, the default significance threshold was set at voxel-level uncorrected $p < 0.001$, with a cluster-level family wise error (FWE)-corrected threshold $p < 0.05$ (Poline et al., 1997).

As a secondary objective, neuropsychological performance in domains apart from the defining domains of grammatical processing, motor speech or single-word comprehension was compared to controls, NFV-pure, SV and LV PPA using Kruskal-Wallis, followed by two-tailed Mann-Whitney *U post hoc* tests, uncorrected for the number of comparisons due to the small sample size of each group.

5.4 Results

5.4.1 Demographics

PPA variants did not differ in terms of age ($\text{chi}^2(3) = 2.05$, $p = 0.56$), education ($\text{chi}^2(3) = 0.063$, $p = 0.996$), gender ($\text{chi}^2(3) = 3.6$, $p = 0.31$) or symptom duration ($\text{chi}^2(3) = 4.66$, $p = 0.199$).

5.4.2 Neuropsychological and neurolinguistic profile of individual cases

Significant deficits at the individual patient level are shown in bold in Table 5.1.

Ten cases fulfilled *a priori* core clinical criteria for NFV PPA encompassing agrammatism in language production and AOS presenting as effortful, halting speech with inconsistent speech sound errors and distortions (Gorno-Tempini et al., 2011) as measured by the AAT repetition test, PALPA subtest 9 repetition of words and pseudowords along with the DIAS and WEZT. In one NFV case (running case 14), agrammatism was by far the most prominent clinical abnormality without AOS. In these ten NFV PPA cases, syntactic comprehension measured with the WEZT auditory sentence comprehension test was additionally affected and object identification measured with the BORB object recognition test was preserved (fulfilling two out of three ancillary features) (Gorno-Tempini et al., 2011).

Six out of these 10 cases classified *a priori* as NFV PPA had concomitant single-word comprehension problems as measured with the sum of the AAT auditory and written word comprehension test (Table 5.1). Hence, these patients did not strictly fulfill criteria for NFV-pure nor for any of the other PPA variants. This phenotype is in accordance with a diagnosis of MV PPA (Mesulam et al., 2009, 2012).

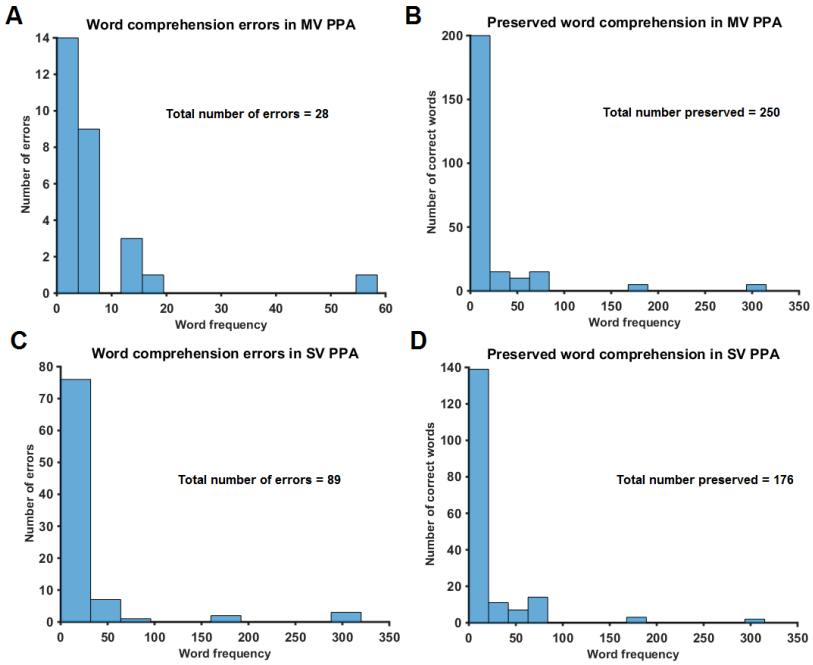


Figure 5.1: **Error typing of word comprehension in MV PPA for word frequency distribution**. Word frequency is plotted on the abscissa and number of errors on the ordinate for **(A)** word errors in MV PPA, **(B)** preserved word comprehension in MV PPA, **(C)** word errors in SV PPA, **(D)** preserved word comprehension in SV PPA. In MV PPA case 18, word frequency data were only available for the AAT comprehension task (20 words), explaining the difference in the total number of scores compared to SV PPA. Note that the scale of the x-axis and y-axis differs between panels.

We analyzed the nature of single-word comprehension problems for words present in the auditory and written AAT single-word comprehension and PALPA word-picture matching tasks. The frequency distribution of the words used in these task is plotted in Figure 5.1. MV PPA patients showed errors on low frequency words, but much less so on high frequency words (Fig. 5.1A). SV PPA patients showed besides errors on low frequency words, also errors on high frequency words (Fig. 5.1C). Regardless of word frequency, errors in SV PPA were more prevalent than in MV PPA (31% more errors) (Fig. 5.1C). The number of words preserved in MV PPA was also higher than in SV PPA (30% more words correct) (Fig. 5.1B,D). A detailed assessment of the type of word comprehension deficits in MV PPA patients, revealed that errors were presumably made on trials assessing the non-dominant meaning of a homonym, which is associated with a lower meaning frequency than the dominant meaning. Consequently, the errors made on low frequency words (Fig. 5.1A) were attributable to the non-dominant meaning of these words. In these trials, patients were not able to retrieve the non-dominant meaning of the word but usually pointed to the distracter picture which was semantically related to the dominant meaning of that word.

5.4.3 Group-based deficits in MV PPA for additional neuropsychological domains

If we considered the six MV PPA cases as a group, deficits were present in other neuropsychological domains apart from grammatical, motor speech or single-word comprehension tasks.

Scores on the PALPA verbal associative-semantic task were significantly lower in MV PPA compared to controls for words with low ($U = 40.5$, $p = 0.010$) and high imageability ($U = 57.5$, $p = 0.026$), but did not differ compared to the other variants ($p > 0.055$) (Fig. 5.2A,B). Scores on the picture-version of the PPT were significantly lower in MV PPA compared to controls ($U = 5$, $p < 0.001$) and compared to NFV-pure PPA ($U = 2$, $p = 0.031$), but did not differ compared to LV PPA ($p = 0.43$). Performance on the PPT was significantly better for MV PPA than for SV PPA ($U = 18$, $p = 0.034$)(Fig. 5.2C).
Scores on the BORB object recognition task were significantly lower in MV PPA compared to controls for the easy task ($U = 74$, $p = 0.040$) and for the hard task ($U = 27.5$, $p = 0.002$) (Fig. 5.2D,E). MV PPA patients scored better than SV PPA on the easy ($U = 0.5$, $p = 0.011$)

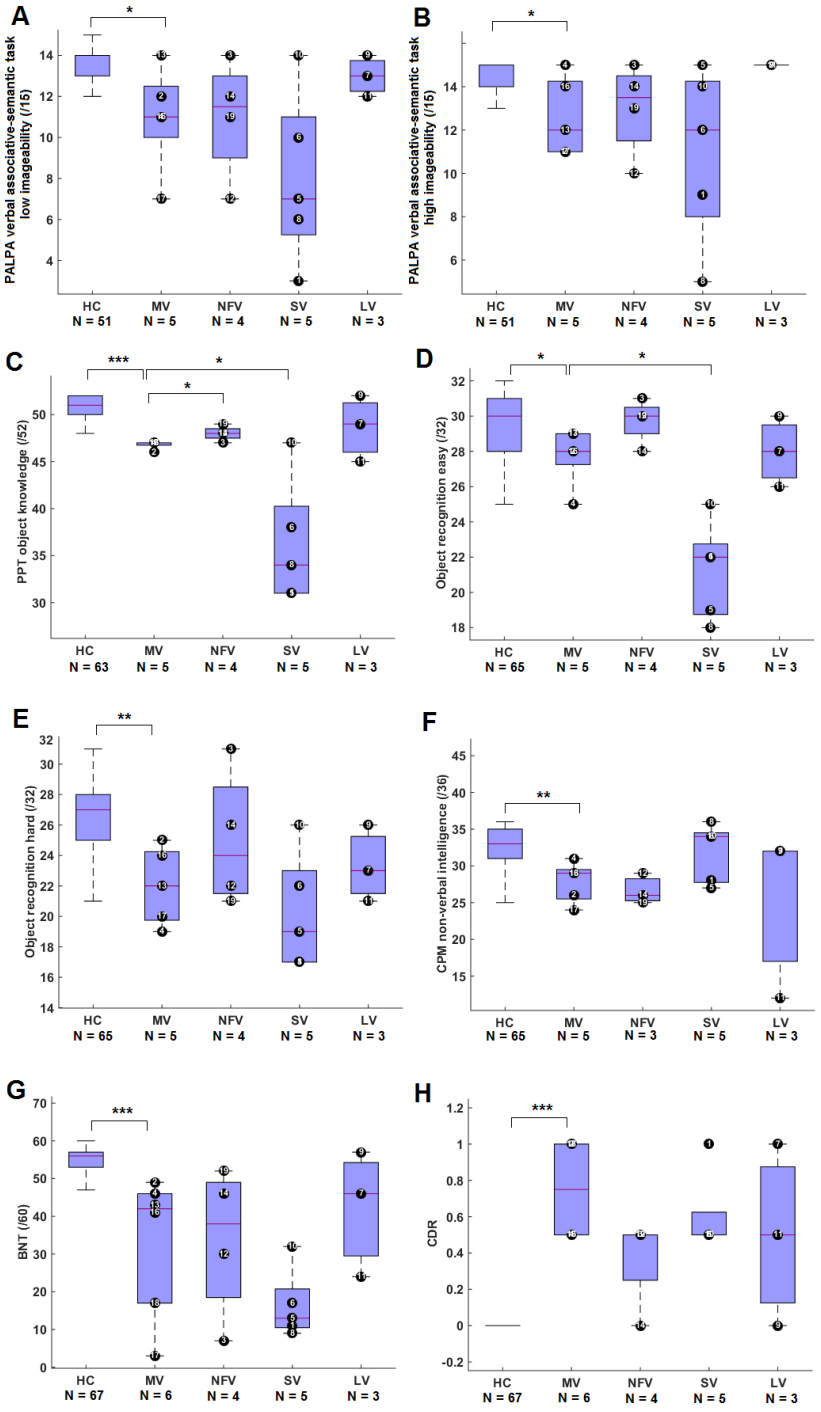


Figure 5.2: **Neuropsychological performance in MV PPA**. Only statistics of direct group-comparisons between MV and the other groups (controls, NFV-pure, SV and LV) are depicted. **(A)** and **(B)** PALPA, **(C)** PPT, **(D)** and **(E)** BORB, **(F)** CPM, **(G)** BNT, **(H)** CDR. Boxplot: minimum, first quartile, median (red line), third quartile, and maximum. $*p < 0.05$, $**p < 0.01$, $***p < 0.001$.

(Fig. 5.2D), but not on the hard BORB object recognition task ($p = 0.34$) (Fig. 5.2E). No differences were found between MV and NFV-pure and LV on the BORB object recognition test ($p > 0.079$) (Fig. 5.2D,E). Compared to controls, MV PPA had significantly lower scores on nonverbal fluid intelligence measured by the CPM ($U = 39.5$, $p = 0.005$). No differences were found compared to the other variants ($p > 0.17$) (Fig. 5.2F). Scores on the BNT were significantly lower in MV PPA compared to controls ($U = 10.0$, $p < 0.001$), but did not differ compared to the other variants ($p > 0.12$) (Fig. 5.2G). The CDR score was significantly higher in MV PPA compared to controls, although no differences in CDR were observed compared to the other variants ($p > 0.067$) (Fig. 5.2H).

5.4.4 Anatomy of atrophy

Atrophy in the MV PPA group was relatively widespread and compromised mainly left-hemispheric frontal and temporoparietal regions (Fig. 5.3A). The left inferior parietal lobule, superior temporal gyrus (STG), posterior aspect of the middle temporal gyrus (MTG) as well as the left insular cortex, dorsolateral prefrontal cortex (DLPFC), premotor cortex, supplementary motor area (SMA), and the left hippocampus and perirhinal cortex (Liuzzi et al., 2015) were atrophic compared to the control group. The precuneus, cingulate cortex and the frontal operculum were atrophic bilaterally (Fig. 5.3A). Compared to SV, volume differences were localized to the left premotor cortex and to the left inferior frontal sulcus in MV PPA (Fig. 5.3B). Compared to LV, atrophy in MV PPA was confined to the bilateral caudate nuclei extending into the left putamen and the left insula (Fig. 5.3C). There were no differences between MV and NFV-pure PPA at the pre-set threshold. At a lower significance threshold, atrophy in the NFV-pure group compared to controls, was localized to the left postcentral gyrus and pars orbitalis of the inferior frontal gyrus (IFG) (Fig. 5.3D).

5.4.5 [^{18}F]-THK5351 binding pattern

[^{18}F]-THK5351 binding in MV PPA was higher in the left precentral gyrus, the left premotor cortex and bilateral SMA compared to controls (Fig. 5.4A). An almost identical pattern was present when MV PPA was compared to SV PPA (Fig. 5.4B). At a lower significance threshold, MV PPA showed additional elevated [^{18}F]-THK5351 binding in the left STG

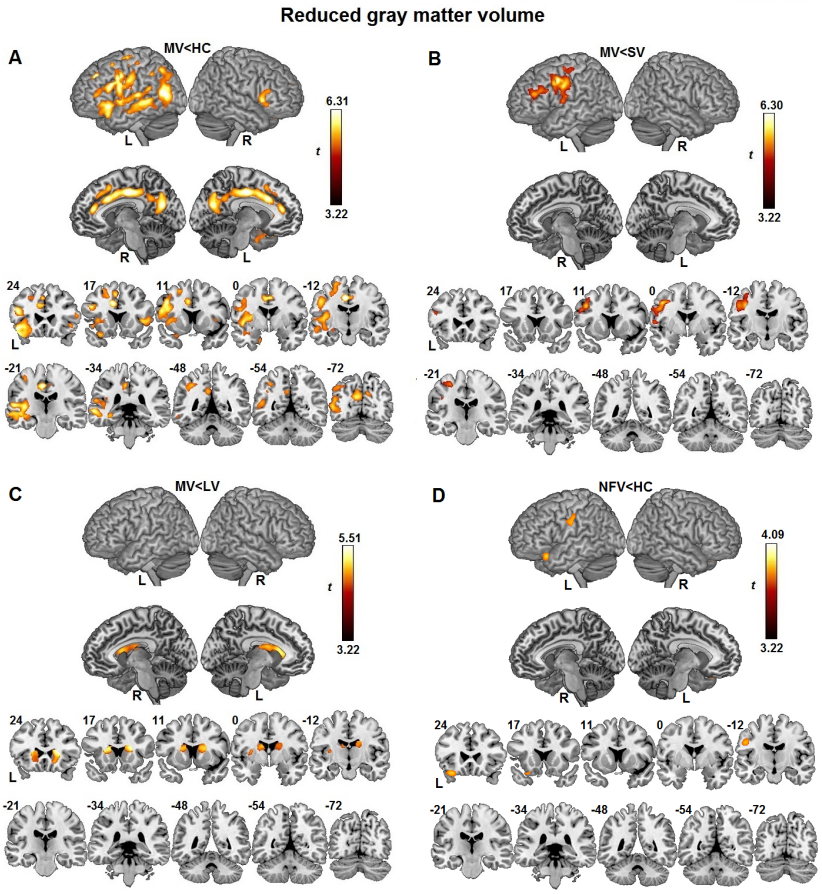


Figure 5.3: **Reduced gray matter volume**. Reduced gray matter volume based on a voxelwise ANCOVA, depicted by a one-sided T map on an MNI template brain rendering and on coronal slices in **(A)** MV PPA compared to controls, **(B)** MV PPA compared to SV PPA, **(C)** MV PPA compared to LV PPA, **(D)** NFV-pure PPA compared to controls. The significance threshold was set at voxel-level uncorrected $p<0.001$ with cluster-level family wise error (FWE)-corrected threshold $p<0.05$ but lowered to voxel-level uncorrected $p<0.001$ for NFV-pure compared to controls.

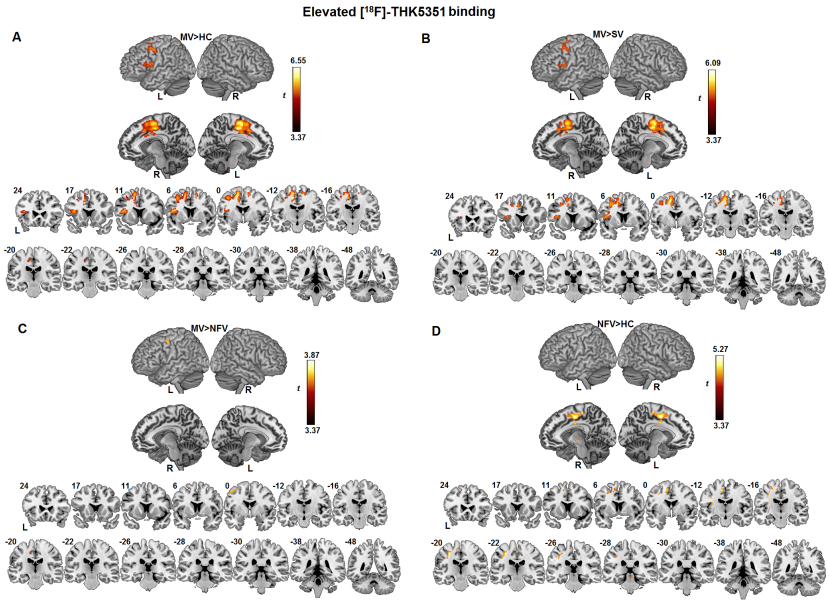


Figure 5.4: **Elevated [^{18}F]-THK5351 binding**. Elevated [^{18}F]-THK5351 binding was measured on PVC SUVR images, statistically contrasted using a voxelwise ANCOVA, depicted by a one-sided T map on an MNI template brain rendering and on coronal slices. **(A)** Higher binding in MV PPA compared to controls, **(B)** compared to SV PPA, **(C)** and compared to NFV PPA, **(D)** higher binding in NFV-pure compared to controls. The significance threshold was set at voxel-level uncorrected $p<0.001$ with cluster-level family wise error (FWE)-corrected threshold $p<0.05$, but lowered to voxel-level uncorrected $p<0.001$ for NFV-pure compared to controls.

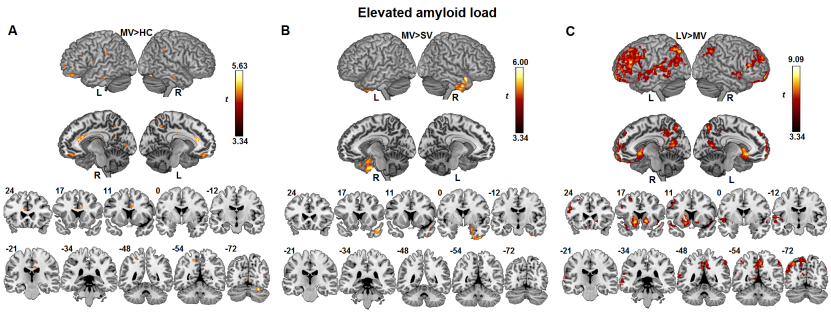


Figure 5.5: **Elevated amyloid load**. Elevated amyloid load was measured on PVC [^{11}C]-PIB PET SUVR images, statistically contrasted using a voxelwise ANCOVA, depicted by a one-sided T map on an MNI template brain rendering in **(A)** the MV PPA group compared to 33 controls, **(B)** MV PPA compared to SV PPA, **(C)** MV PPA compared to LV PPA. The significance threshold was set at voxel-level uncorrected $p<0.001$ with cluster-level family wise error (FWE)-corrected threshold $p<0.05$, but lowered to voxel-level uncorrected $p<0.001$ for MV PPA compared to controls.

compared to controls. Compared to NFV-pure, MV PPA showed more [^{18}F]-THK5351 binding in the left premotor cortex (Fig. 5.4C). Elevated [^{18}F]-THK5351 binding in the NFV-pure group compared to controls was present in the SMA bilaterally (Fig. 5.4D).

5.4.6 Amyloid biomarker positivity

As a group, MV PPA patients showed elevated [^{11}C]-PIB binding in the bilateral orbitofrontal cortex, the anterior cingulate cortex (ACC) and in the precuneus/posterior cingulate cortex (PCC) compared to controls (Fig. 5.5A). Higher [^{11}C]-PIB binding in MV PPA was present in the right anterior temporal lobe extending medially into the hippocampal complex, compared to SV PPA (Fig. 5.5B). Compared to MV, LV PPA showed higher [^{11}C]-PIB binding distributed across frontotemporal regions and in the bilateral striatum with relative sparing of primary visual and sensorimotor cortices (Fig. 5.5C). No differences were found between MV and NFV-pure PPA in terms of [^{11}C]-PIB binding.

At the individual level, two out of six MV PPA cases (case 13, 76 years; and case 17, 65 years) were amyloid-positive based on either neocortical

[^{11}C]-PIB PET SUVR values or on CSF Aβ_{42} values (Table 5.1). In the LV group, all three cases were amyloid-positive (Table 5.1). By contrast, none of the NFV-pure or SV cases were amyloid-positive (Table 5.1).

5.4.7 Imaging biomarkers of individual MV PPA cases

Individual atrophy maps (red) and elevated [^{18}F]-THK5351 binding maps (blue) of all MV PPA patients are shown in Figure 5.6 (panels A-F). All MV PPA cases showed elevated [^{18}F]-THK5351 binding in the medial frontal cortex. More specifically, elevated [^{18}F]-THK5351 binding was present in five out of six cases in the SMA (Fig. 5.6B-F, blue). These cases also showed elevated binding in the premotor cortex (blue), which overlapped in most cases with the atrophy pattern (violet). In most cases, elevated [^{18}F]-THK5351 binding was also present in the STG, although to a lesser degree (blue dots). Four of the five cases who showed elevated [^{18}F]-THK5351 binding in the SMA/premotor cortex, also showed elevated binding in the basal ganglia and in the midbrain including the substantia nigra (Fig. 5.6B-E, blue).

Binding in the basal ganglia, cingulum and midbrain without SMA/premotor cortical involvement was present in one case (Fig. 5.6A, blue). Another MV case showed only elevated [^{18}F]-THK5351 binding in cortical regions but not in subcortical regions (Fig. 5.6F, blue). The latter case (Fig. 5.6F, blue), together with case 17 (Fig. 5.6E, blue) showed extensive [^{18}F]-THK5351 binding, encompassing almost the entire temporal lobe with a left-hemispheric asymmetry. This pattern overlapped with the atrophy pattern of these patients (Fig. 5.6E-F, red). In three out of six cases, atrophy was also present in the left IFG, without overlap with [^{18}F]-THK5351 binding (Fig. 5.6B-D, red). Three cases showed atrophy in the pons which did not overlap with elevated [^{18}F]-THK5351 binding (Fig. 5.6A,B,E, red).

[^{11}C]-PIB PET was available in four out of the six MV PPA cases (running case nr. 4, 13, 16 and 17, Table 5.1). Two of these cases showed significantly elevated [^{11}C]-PIB binding unilaterally (Fig. 5.6G), while in MV case 17, [^{11}C]-PIB binding was more prominent in the right frontotemporal cortex (Fig. 5.6H). MV case 4 and case 16 did not show any elevated [^{11}C]-PIB binding, neither did MV case 2 and 18 show positivity on CSF AD biomarkers (Table 5.1).

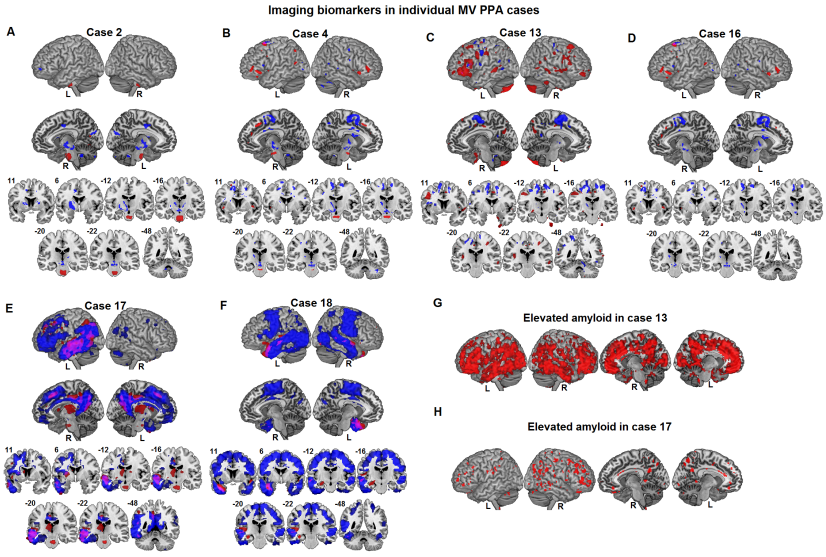


Figure 5.6: **Imaging biomarkers in individual MV PPA cases**. **(A)**-**(F)**: T maps represent atrophy (red) compared to 52 controls and elevated PVC [^{18}F]-THK5351 binding (blue) based on SUVR images of each individual MV PPA case contrasted to 20 controls. **(G)**-**(H)**: T maps representing elevated amyloid load based on PVC [^{11}C]-PIB SUVR images contrasted to 14 controls for case 13 and case 17.

5.4.8 Correlation between imaging biomarkers and core clinical features

In the pooled MV and NFV-pure group, lower scores on the AAT phoneme repetition test, indicative of AOS, correlated with higher [^{18}F]-THK5351 binding in the premotor cortex and SMA bilaterally (Fig. 5.7A,B). There was also a cluster in the right temporo-occipital junction, the right insula and in the hippocampus (Fig. 5.7A,B).

Elevated [^{18}F]-THK5351 binding and deficits on the sum of the AAT single-word comprehension test showed a significant correlation in the right basal ganglia extending to the right frontal operculum (Fig. 5.7C,D). No significant correlations were obtained for tests on agrammatism. No significant correlations were obtained between any of these tests and gray matter volume loss.

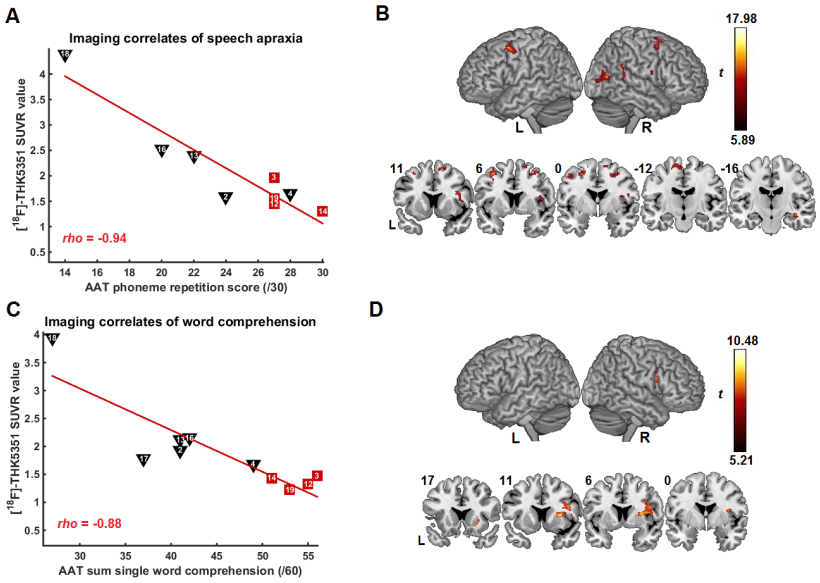


Figure 5.7: **Correlation between [^{18}F]-THK5351 binding and core clinical features, corrected for age and gender**. Scatterplots demonstrating the correlation between elevated partial volume corrected [^{18}F]-THK5351 SUVR binding extracted form the clusters derived in the voxelwise correlations with test scores on **(A)** the AAT phoneme repetition test, **(C)** the sum of the AAT single-word comprehension test, with corresponding T maps of the correlations **(B,D)** projected on a template brain and on slices with the corresponding MNI coordinates.

5.5 Discussion

The presence of single-word comprehension difficulties in 60% of PPA patients with motor speech deficits and/or agrammatism was more frequent than expected. Object knowledge and object recognition were also affected, although to a lesser degree than SV PPA.
Atrophy in the MV PPA group encompassed left frontal and temporoparietal regions, affecting both ventral and dorsal language pathways. The topographical distribution of [^{18}F]-THK5351 binding in MV was highly similar to NFV-pure in the SMA. Although in the premotor cortex, [^{18}F]-THK5351 binding was significantly higher in MV compared to NFV-pure. This [^{18}F]-THK5351 binding pattern was present in five out of six MV PPA patients and also extended to subcortical structures in

four MV cases. [^{18}F]-THK5351 binding in these regions, but not gray matter volume loss, was associated with core clinical features of MV PPA. Based on amyloid biomarkers, MV PPA patients were more likely to be amyloid-positive compared to patients with the NFV-pure phenotype of PPA.

Data-driven mathematical analyses of neurolinguistic data in PPA broadly confirm the presence of separate clusters corresponding to the three variants but also leave 15-30% unclassified (Vandenberghe, 2016). Of these unclassifiable cases, several might be fitting into the MV phenotype of PPA, although the current classification criteria proposed by Gorno-Tempini et al. (2011) do not include this phenotype as a separate variant. In a cohort of PPA cases with mild and early disease, the inclusion of a MV PPA phenotype into the list of variants raised the comprehensiveness of the classification from 80% to nearly 90% (Mesulam et al., 2012).
In accordance with these previous reports, all MV PPA patients in the current study had single-word comprehension problems along with agrammatism. The single-word comprehension deficits were more often present for the non-dominant meaning of words than for high frequency words. We therefore hypothesize that single-word comprehension deficits in MV PPA patients are due to impaired semantic control mechanisms rather than impaired semantic retrieval, as occurs in SV PPA (Jefferies and Lambon Ralph, 2006). A task-based activation study in healthy individuals, associated meaning dominance effects with the left MTG and STG, left precentral gyrus and superior frontal gyrus, and right subcortical areas, including the globus pallidus and putamen (Grindrod et al., 2014). The latter regions were typically affected by atrophy or showed elevated [^{18}F]-THK5351 binding in individual MV cases (Fig. 5.6). Moreover, elevated [^{18}F]-THK5351 binding in the right basal ganglia correlated with deficits on the sum of the AAT single-word comprehension test across MV and NFV PPA patients. It is appealing to assume that this finding could explain the deficits on meaning dominance effects (Grindrod et al., 2014). However, the correlation was based on nine patients and therefore, it should be considered with caution.

In contrast to the group-based atrophy pattern obtained in MV PPA (Fig. 5.3), previous studies of MV PPA (Mesulam et al., 2012; Spinelli et al., 2017) showed also atrophy in the ATL besides atrophy in the temporoparietal junction, the STG (Mesulam et al., 2012; Sajjadi et al., 2014), the IFG (Mesulam et al., 2012; Spinelli et al., 2017), the insula and the precuneus (Spinelli et al., 2017). Inter-individual differences due to low sample sizes, i.e. two cases in Mesulam et al. (2012), 4

cases in Spinelli et al. (2017) and 14 cases in Sajjadi et al. (2014) may have contributed to these differences in atrophy patterns. Basically, the ATL is not considered part of the classic language and speech network (Hickok and Poeppel, 2015). Nonetheless, observations in SV PPA and healthy individuals indicate that the left ATL has a critical role in honing the acuity of object naming and word comprehension (Mesulam et al., 2013; Jackson et al., 2016). In line with these studies, the MV PPA cases exhibiting the lowest score on the sum of the AAT single-word comprehension task (case 17 and 18)(Table 5.1), also showed left ATL atrophy (Fig. 5.6E,F).

All MV PPA cases suffered from motor speech impairments instantiated as effortful spontaneous speech, impaired antagonistic movements during the DIAS diadochokinesis task and problems with repetition of consonants and phonemes (Table 5.1). Based on previous studies, it has been shown that agrammatism and motor speech deficits occur most often together, at least in NFV-pure PPA (Mesulam et al., 2012). The NFV-pure PPA group showed atrophy confined to the dorsal language pathway (including the left IFG), which is in line with previous studies (Rogalski et al., 2011a; Mandelli et al., 2014, 2016). This pattern was highly similar to MV PPA, but the latter group also showed atrophy in the left posterior temporal gyrus and temporoparietal junction. The occurence of prominent agrammatism has typically been linked with loss of structural integrity in these regions along with atrophy in the left IFG, middle frontal gyri (MFG), insula and caudate nucleus (Amici et al., 2007; Wilson et al., 2010; Josephs et al., 2013b; Whitwell et al., 2013). Speech apraxia, another clinical feature of all MV PPA cases in this cohort, correlated with elevated [^{18}F]-THK5351 binding in the superior lateral premotor cortex and SMA bilaterally. Atrophy of the SMA has consistently been associated with AOS (Josephs et al., 2012, 2013b). Apart from its function in speech motor control (Alario et al., 2006), the SMA is connected to the IFG through the aslant tract (Catani et al., 2013; Mandelli et al., 2014, 2016), which plays a crucial role in articulation and, in NFV-pure PPA, its integrity correlates with the amount of distortion errors that patients made in spontaneous speech (Mandelli et al., 2014) and with motor control necessary for word production (Alario et al., 2006). Consistent with our findings, previous studies have demonstrated an association between the severity of AOS and premotor cortical involvement (Whitwell et al., 2013). AOS features in the current cohort of MV cases would be categorized as the 'phonetic type' of AOS (type 1), predominated by sound distortions and distorted sound substitutions (Josephs et al., 2012, 2013b; Whitwell et al., 2017a).

While AOS is not included in the proposed diagnostic criteria for MV PPA (Mesulam et al., 2012), all MV PPA cases in Spinelli et al. (2017) also showed AOS accompanied by both agrammatism and single-word comprehension deficits. In that study (Spinelli et al., 2017), atrophy of the premotor cortex was also observed in MV PPA, which is consistent with our findings.

Elevated [^{18}F]-THK5351 binding in the SMA was also present in NFV-pure PPA. NFV PPA is in 50-88% of cases associated with frontotemporal lobar (FTLD)-tau aggregates of the corticobasal degeneration (CBD) type or progressive supranuclear palsy (PSP) type at pathological examination (Grossman, 2010; Spinelli et al., 2017). The [^{18}F]-THK5351 ligand has been shown to bind in corticobasal syndrome to the globus pallidus, precentral, postcentral, superior frontal, superior parietal cortex, and PCC (Kikuchi et al., 2016), as well as in PSP patients in the globus pallidus and in the midbrain (Ishiki et al., 2017). Another tau PET tracer, [^{18}F]-AV-1451 has shown elevated binding in the precentral gray and white matter and in the midbrain, putamen, globus pallidus, and thalamus in patients with corticobasal syndrome (Cho et al., 2017). In our study, elevated [^{18}F]-THK5351 in superior frontal regions (SMA/premotor cortex) was present in five out of six MV PPA cases and in the midbrain (substantia nigra) in four out of six MV PPA cases. The group-based topographic distribution of [^{18}F]-THK5351 binding in MV PPA is similar to regions most vulnerable to CBD pathology (Dickson et al., 2002). The striatum and subthalamic nucleus are involved early in the disease course of typical CBD, while the substantia nigra is usually involved in later stages of the disease (Dickson et al., 2002). [^{18}F]-THK5351 binding in the midbrain nuclei may however also reflect possible underlying PSP tau pathology in some MV PPA cases (Dickson, 1999; Ishiki et al., 2017; Passamonti et al., 2017). Besides binding to CBD and PSP pathology, [^{18}F]-THK5351 also binds to tau pathology of the AD type (Harada et al., 2016). Although the observed [^{18}F]-THK5351 binding pattern in MV PPA dissociates from the tau pattern observed in typical AD, which primarily occurs first in the temporal lobe structures (Braak et al., 2006b; Johnson et al., 2016). It also dissociates from the tau PET binding pattern in left temporoparietal regions in LV PPA (Ossenkoppele et al., 2016).

Atrophy in MV PPA was more widespread than [^{18}F]-THK5351 binding and also included temporal lobe structures. We could not find differences in age or symptom duration which could possibly explain the more widespread atrophy pattern expanding into the temporal lobes. Disease severity would be reflected in more severe deficits on neuropsychological

and neurolinguistic test scores. If we correlated test performance with [^{18}F]-THK5351 binding or atrophy, only [^{18}F]-THK5351 binding showed correlations with core clinical features in MV PPA. This might indicate that [^{18}F]-THK5351 binding is specific for regions which have increased vulnerability in MV PPA. However due to the low sample size, this should be considered only as preliminary evidence. Our results are consistent with a study demonstrating generally stronger group effect sizes with tau PET compared to MRI volumetry when patients with non-amnestic AD (including patients with LV PPA) were contrasted to amnestic AD (Nasrallah et al., 2017).

5.5.1 MV PPA and its relation to AD

In the MV PPA group, the precuneus was involved in atrophy and in amyloid deposition. The precuneus is usually not affected in patients with SV PPA or NFV-pure PPA (Rogalski et al., 2011a). By contrast, the precuneus might be atrophic in LV PPA (Schaeverbeke et al., 2017), most often in LV cases who have underlying AD pathology (Spinelli et al., 2017). This is in line with observations made early in the disease course of typical AD (Villain et al., 2012). Involvement of the precuneus might point to underlying AD pathology. In this study, two out of six MV PPA cases showed amyloid-positivity (33%) based on [^{11}C]-PIB PET as well as on CSF AD biomarkers (Table 5.1). This percentage is higher than what has been observed in studies assessing amyloid PET-positivity in patients with NVF-pure (16-25%) or SV PPA (0-20%), but lower than the percentage of amyloid-positivity in LV PPA patients (78-100%) (Rabinovici et al., 2008; Leyton et al., 2011; Martersteck et al., 2015). An important consideration when assessing the prevalence of amyloid-positivy, is that the likelihood of being amyloid-positive increases with older age (Ossenkoppele et al., 2015). There were however no differences in age between MV and NFV-pure PPA which could explain the higher prevalence of amyloid-positivity in the MV cases. A remarkable high degree of amyloid-positivity has been found in 'unclassifiable' cases (for example 80%, four out of five cases in Martersteck et al. (2015)). Similarly, cases labeled clinically as 'unclassifiable' were shown to be more likely to have an AD CSF biomarker profile (Gil-Navarro et al., 2013). It might well be that a subset of these 'unclassifiable' cases can be assigned to the MV subtype of PPA. *Post mortem* evaluation confirms the higher prevalence of AD pathology in MV PPA (67% of cases, four out of six) (Mesulam et al., 2014b). In the latter MV PPA cohort, 17% (one out of six) had FTLD-tau (CBD) or TDP-B pathology (one

out of six) (Mesulam et al., 2014b). In other series, the percentage of AD pathology was lower in MV PPA (25%, one out of four). In one series, Pick's disease pathology was the most prevalent etiology in MV PPA (50%, two out of four cases) although one MV PPA case showed FTLD TDP-43 type A pathology (Spinelli et al., 2017). As we have demonstrated here, *in vivo* imaging might suggest an earlier diagnosis of underlying AD in cases with MV PPA. However, our study limits any firm conclusions regarding the histopathological basis of MV PPA.

5.5.2 Potential study limitations

A potential drawback of using [^{18}F]-THK5351 PET is the non-specific binding to an undefined molecular substrate in the basal ganglia (Harada et al., 2016; Ng et al., 2017). Moreover, *in vivo* experiments in patients with AD or PSP using deprenyl displacement suggested that [^{18}F]-THK5351 may bind to MAO-B (Ng et al., 2017). Regardless of the issue of non-specificity, elevated [^{18}F]-THK5351 binding is present in regions which are known to be associated with conditions in which a tauopathy is the underlying neuropathological cause namely the SMA, premotor cortex, basal ganglia and midbrain. However, no firm conclusions regarding the underlying type of tauopathy can be drawn as this study is limited by the lack of *post mortem* confirmation.

The total number of PPA patients included is rather small, which is partly inherent to the relatively low prevalence of the disease. The imaging and neuropsychological test protocol used in this study is burdensome, which makes it only suitable for mildly affected patients. In case 17 and 18 the severity of speech apraxia precluded the application of the full neuropsychological test battery. Moreover, not all patients received a [^{11}C]-PIB PET scan, either to reduce burden to the patient or due to the already available CSF AD biomarkers. The differences in sample size might have contributed to different effect sizes when comparing cases to controls based on [^{11}C]-PIB or [^{18}F]-THK5351 data. We applied PVC to correct for atrophy which might influence quantification of [^{11}C]-PIB PET or [^{18}F]-THK5351 PET data. Due to the low resolution of PET, it is difficult to reliably assess tracer uptake in small regions such as the nuclei of the midbrain, even after coregistration and PVC with MRI data of the subject. We therefore did not discriminate between the different nuclei of the midbrain but considered it as a single structure.

5.6 Conclusion

In patients with motor speech problems and/or agrammatism who have concomitant single-word comprehension problems (MV PPA), the topographical distribution of [^{18}F]-THK5351 binding is highly similar to that observed in NFV-pure, but atrophy is more widespread in MV PPA. The topography of [^{18}F]-THK5351 binding, but not the degree of atrophy was correlated with core clinical features of MV PPA. These patients have possibly a higher likelihood of amyloid-positivity compared to NFV-pure PPA.

Table 5.1: Demographics and neuropsychological assessment

Case	2	4	13	16	17	18	3	12	14	19	1	5	6	8	10	7	9	11
PPA variant	MV	MV	MV	MV	MV	MV	NFV	NFV	NFV	NFV	SV	SV	SV	SV	SV	LV	LV	LV
Age (years)	80	62	76	70	65	49	57	68	66	63	73	71	63	52	55	77	63	74
Gender	M	F	M	M	M	F	F	F	F	M	F	F	F	F	M	M	F	M
Education (years)	17	12	12	18	19	10	10	10	15	10	14	8	13	13	14	10	12	18
Handedness	R	L	R	R	R	R	R	R	R	R	R	R	R	R	R	R	R	R
Symptom duration (months)	33	16	37	39	40	53	43	60	74	29	19	44	11	131	6	59	95	48
PIB SUVR	/	1.26	**2.1**	1.35	**1.57**	/	/	/	1.16	1.37	/	/	1.12	1.14	1.2	/	**1.81**	/
CSF Aβ_{42} (pg/ml)	816	/	**477**	/	759	1077	1057	832	/	/	1558	733	/	/	/	**564**	**664**	**321**
CSF t-tau (pg/ml)	195	/	442	/	744	231	247	320	/	/	428	262	/	/	/	407	/	858
CSF p-tau (pg/ml)	42	/	59.6	/	87.1	31	34	43	/	/	52	36.3	/	/	/	65.7	/	95
CDR	1	0.5	0.5	0.5	1	1	0.5	0.5	0	0.5	1	0.5	0.5	0.5	0.5	1	0	0.5
AAT sum single word compr. (/60)	**41**	**49**	**41**	**42**	**37**	**27**	56	55	51	53	**31**	**32**	**39**	**35**	58	53	54	**50**
AAT written words compr. (/30)	**19**	**23**	**21**	**19**	**24**	**19**	30	30	27	30	**17**	**16**	**17**	**16**	30	27	28	**25**
AAT aud. words compr. (/30)	**22**	**19**	28	26	26	25	**22**	26	**20**	**23**	**13**	**8**	26	25	**24**	**23**	**14**	**16**
PALPA aud. word picture (/40)	40	39	39	39	**38**	/	**37**	39	**38**	40	**26**	**27**	**26**	**21**	39	**38**	39	38
WEZT aud. sentences compr. (/40)	**36**	**36**	**33**	**31**	**12**	/	**29**	**26**	**35**	**33**	**37**	**33**	38	38	39	**27**	40	**37**
WEZT act. sent. anagram (/10)	10	10	**9**	10	**5**	/	10	**9**	10	10	10	10	10	10	10	10	10	10
WEZT pas. sent. anagram (/10)	10	**9**	**9**	**5**	**5**	/	10	**6**	10	10	10	**9**	10	**9**	10	10	10	10
WEZT Verb compr. (/60)	**56**	**45**	**55**	**52**	**42**	/	60	**40**	**42**	58	**43**	**32**	**51**	**48**	58	57	57	**53**
AAT Written sentence compr. (/30)	**20**	**24**	**19**	**22**	**23**	/	**23**	**20**	26	**23**	25	**21**	**22**	**24**	30	**22**	30	26
AAT phoneme rep. (/30)	**24**	**28**	**22**	**20**	/	**14**	**27**	**27**	30	**27**	30	29	30	30	30	30	30	29
AAT single word rep. (/30)	28	30	**19**	30	/	**19**	29	30	30	**24**	29	**28**	**27**	30	30	30	30	29
AAT concatenated word rep. (/30)	**27**	29	**23**	29	/	**1**	**15**	29	30	**26**	30	29	**28**	**26**	30	**15**	29	30
AAT sent. rep. (/30)	**27**	28	28	28	/	**0**	**17**	**24**	28	**25**	29	29	30	**27**	30	**13**	**26**	**24**
DIAS severity score (/30)	**28**	**24**	**12**	**27**	**11**	/	**28**	**20**	30	30	**27**	**24**	30	30	30	30	30	**29**
DIAS diadochok.	103	**50**	**42**	115	75	/	**24**	**51**	77	79	**50**	70	147	125	80	77	114	117
BNT (/60)	**7**	**30**	**46**	52	**11**	**13**	**17**	**9**	**32**	**46**	57	**24**	49	**46**	**43**	**41**	**3**	**17**
PALPA Verbal assoc.-sem. HI (/15)	**11**	15	12	14	**11**	/	15	**10**	14	13	**9**	15	12	**5**	14	15	15	15
PALPA Verbal assoc.-sem. LI (/15)	12	**11**	14	**11**	**7**	/	14	**7**	12	**11**	**3**	**7**	**10**	**6**	14	13	14	12
PPT (/52)	**46**	**47**	**47**	**47**	**47**	/	**47**	**48**	**48**	49	**31**	**31**	**38**	**34**	**47**	49	52	**45**
BORB easy B (/32)	28	**25**	29	28	29	/	31	30	28	30	**22**	**19**	**22**	**18**	**25**	28	30	**26**
BORB hard A (/32)	**25**	**19**	**22**	**24**	**20**	/	31	**22**	**26**	**21**	**17**	**19**	**22**	**17**	**26**	**23**	**26**	**21**
CPM (/36)	**26**	31	29	29	**24**	/	/	29	**26**	**25**	28	27	34	36	34	32	32	**12**

Abbreviations: AAT: Akense Afasie Test, act.: active; Assoc.-sem: associative semantic, aud.: auditory, BNT: Boston Naming test, BORB: Birmingham Object recognition task, CPM: Colored Progressive Matrices, compr.: comprehension, CSF: cerebrospinal fluid, diadochok.: diadochokinesis, DIAS: Diagnostisch Instrument voor Apraxie van de Spraak, HI: high imageability, LI: low imageability, MMSE: mini-mental state examination, pas.: passive, PIB SUVR: [^{11}C]-Pittsburgh Compound-B PET standardized uptake value ratio in the composite cortical volume of interest, PPT: Pyramids and Palm trees test, rep.: repetition, sent.: sentence, WEZT: Werkwoorden en Zinnentest. /: no data collected. Bold: Significantly different from controls based on Crawford and Garthwaite (2006) or Crawford and Howell (1998) statistical procedures.

Chapter 6

Cholinergic depletion and basal forebrain volume in primary progressive aphasia

This study is published as:

Schaeverbeke,J, Evenepoel,C, Bruffaerts,R, Van Laere,K, Bormans,G, Dries,E, Tousseyn,T, Nelissen,N, Peeters,R, Vandenbulcke,M, Dupont,P, Vandenberghe,R (2017). Cholinergic depletion and basal forebrain volume in primary progressive aphasia, NeuroImage Clinical 13, 271-279. (Schaeverbeke et al., 2017)

6.1 Abstract

Primary progressive aphasia (PPA) is a heterogeneous syndrome with various neuropathological causes for which no medical treatment with proven efficacy exists. Basal forebrain (BF) volume loss has been reported in PPA but its relation to cholinergic depletion is still unclear.
The primary objective of this study was to investigate whether cholinergic alterations occur in PPA variants and how this relates to BF volume loss. An academic memory clinic based consecutive series of 11 PPA patients (five with the semantic variant (SV), four with the logopenic variant (LV) and two with the nonfluent variant (NFV)) participated in

this cross-sectional *in vivo* PET imaging study together with 10 healthy control subjects. Acetylcholinesterase (AChE) activity was quantitatively measured in the neo- and allocortex using N-[^{11}C]-Methylpiperidin-4-yl propionate (PMP)-PET with arterial sampling and metabolite correction. Whole brain and BF volumes were quantified using voxel-based morphometry on high-resolution magnetic resonance imaging (MRI) scans.
In the PPA group, only LV cases showed decreases in AChE activity levels compared to controls. Surprisingly, a substantial number of SV cases showed significant AChE activity increases compared to controls. BF volume did not correlate with AChE activity levels in PPA. To conclude, in our sample of PPA patients, LV but not SV was associated with cholinergic depletion. BF atrophy in PPA does not imply cholinergic depletion.

6.2 Introduction

Primary progressive aphasia (PPA) is characterized by an isolated language impairment and is divided clinically into the subtypes of logopenic (LV), nonfluent (NFV) and semantic variant (SV) aphasia (Gorno-Tempini et al., 2011; Vandenberghe, 2016). Of the LV cases, 50-60% have underlying Alzheimer's disease (AD) pathology. In 50-88% of NFV cases the underlying cause is frontotemporal lobar degeneration (FTLD)-tauopathy (i.e. corticobasal degeneration (CBD), progressive supranuclear palsy (PSP) or Pick's disease pathology) and 69-83% of SV cases have FTLD-Transactive response DNA binding Protein 43 kDa (TDP-43) type C pathology (Grossman, 2010) (for review: Vandenberghe (2016)).

Cholinergic depletion has been documented in typical AD (Kuhl et al., 1999; Bohnen et al., 2003, 2005), but it is currently unknown whether a cholinergic deficit also occurs in atypical AD presenting as PPA or in PPA due to a tauopathy or TPD-43 proteinopathy. According to magnetic resonance imaging (MRI) volumetric studies, the basal forebrain (BF) is atrophic in PPA SV and NFV (Teipel et al., 2014b, 2016) and mainly so the posterior part of the nucleus basalis (Ch4) and nucleus subputaminalis (NSP). The BF is the primary source of cholinergic transmission to the neo- and allocortex (Zaborszky et al., 2015), hence the hypothesis that a cholinergic deficit may also exist in non-AD cases of PPA. *Post mortem* morphometric studies of the BF have mainly focused on AD or on FTLD-tau. In AD, severe degeneration of the BF, mainly

the posterior part of Ch4, has been reported (Teipel et al., 2005; Grothe et al., 2014; Baker-Nigh et al., 2015; Kerbler et al., 2015). In FTLD-tau, Ch4 degeneration has been shown in PSP (Tagliavini et al., 1984; Kasashima and Oda, 2003), whereas both degeneration (Kasashima and Oda, 2003) and preservation (Dickson, 1999) of Ch4 have been reported in CBD.

Cholinergic denervation resulting from BF volume loss may be reflected in altered AChE activity levels. AChE activity levels can be mapped *in vivo* using N-[^{11}C]-Methyl-4-piperidyl acetate ([^{11}C]MP4A)- or N-[^{11}C]-Methylpiperidin-4-yl propionate [^{11}C]PMP (Irie et al., 1996). The rate-dependent enzyme for acetylcholine (ACh) degradation i.e. acetylcholinesterase (AChE) is present at pre- and postsynaptic neurons (Wevers, 2011) and in a soluble form at the synaptic cleft (Schegg et al., 1992). Studies using [^{11}C]MP4A and [^{11}C]PMP have shown thalamic cholinergic depletion in PSP (Shinotoh et al., 1999; Hirano et al., 2010) and cortical cholinergic depletion in CBD (Shinotoh, 2007) and typical AD. Reduced AChE levels, as measured with [^{11}C]PMP-positron emission tomography (PET), have also been found in the neocortex and thalamus in two patients with FTDP-17 mutations (Hirano et al., 2006).

To date, no PET study investigated the cholinergic system in PPA exclusively. The primary objective of this study was to investigate whether cholinergic alterations occur in PPA and how this depends on the variant.
Cholinergic activity is crucial for several cognitive processes (Wevers, 2011) and plays a hypothetical role in language (Simić et al., 1999; Boban et al., 2006). As a consequence, a cholinergic deficit in PPA may have implications for therapeutic interventions.

6.3 Material and Methods

6.3.1 Subjects

Patients were recruited between 2004-2006 and between 2009-2015 at the memory clinic University Hospitals Leuven. Each PPA case was diagnosed according to Gorno-Tempini et al. (2011) recommendations. Healthy control subjects were recruited through advertisement in local newspapers or internet. Eleven patients with PPA (five SV, four LV and two NFV) (Table 6.1) participated as well as 10 control subjects. Three patients received a neuropathological examination (interval from

[^{11}C]PMP-PET till death: 6.00 ± 3.61 years). LV case 8 received a diagnosis of pathologically definite AD 3 years *post* [^{11}C]PMP-PET, NFV case 1 a diagnosis of pathologically definite CBD 5 years *post* [^{11}C]PMP-PET and SV case 9 a diagnosis of pathologically definite FTLD with TDP-43 inclusions type C pathology 10 years *post* [^{11}C]PMP-PET. There was no significant history of stroke, psychiatric illness or vascular disease in study participants. Patients had not been previously exposed to cholinesterase inhibitors and none of the study participants took anticholinergic medication. All subjects received a [^{11}C]PMP-PET scan along with a volumetric MRI scan. For MRI volumetric comparisons, we included an additional set of 24 healthy controls (age 67.3 ± 8.83 years), scanned on the same scanner, as well as 17 additional PPA patients (4 LV, 6 NFV and 7 SV) (Table 6.1) (Grube et al., 2016) and 77 additional controls (age 64.6 ± 5.86 years) who were scanned on a different scanner (see MRI acquisition and analysis).

The study was approved by the Ethics Committee, University Hospitals Leuven. All participants provided written informed consent in accordance with the Declaration of Helsinki.

6.3.2 Neuropsychological protocol

All subjects underwent extensive neuropsychological testing. Global cognitive functioning was assessed by the Clinical Dementia Rating scale (CDR). Language was assessed by means of the 60-item version of the Boston Naming test (BNT), the validated Dutch version of the Akense Afasie test (AAT) and the verbal semantic association test of the psycholinguistic assessment of language processing in aphasia (PALPA subtest 49). Visual recognition of objects was assessed by the object decision test of the Birmingham Object Recognition Battery (BORB) hard (A) and easy (B). Nonverbal fluid intelligence and reasoning ability were quantified by the Raven's Colored Progressive Matrices (CPM).

6.3.3 PET acquisition and analysis

[^{11}C]PMP was synthesized as described previously (Snyder et al., 1998). The injected activity was 261.3 ± 28.31 MBq in control subjects and 290.3 ± 62.6 MBq in PPA patients. Dynamic PET data were acquired in 3D mode during 60 minutes (rebinned in 4×15 s, 4×1 min, 2×2.5 min, 10×5 min) on a Siemens/ECAT EXACT HR+ PET scanner (CTI PET

System, Inc., Knoxville, TN 37932, USA). Data were reconstructed using 3D-filtered back-projection with a Hanning filter with cut-off frequency of 0.5 of the Nyquist frequency, corrected for random, scatter, attenuation and decay and smoothed with a 6 mm isotropic Full-Width at Half Maximum (FWHM) Gaussian 3D kernel.

For each subject 19 arterial samples were collected during the scan period to determine the individual plasma time activity curve (TAC). Seven additional samples were used for metabolite correction.
One LV PPA patient (case 6) (Table 6.1) and one control subject had to be excluded due to arterial sampling problems. One control subject was excluded based on excessive movement during PET scan acquisition. The remaining eight control subjects and 10 PPA patients were included in our PET-based analyses.

Blood samples were centrifuged, and the radioactive plasma was subsequently eluted on high-performance liquid chromatography and counted in a gamma counter. The intact fractions of tracer over time were fitted using a constrained Hill model as metabolite correction function and this function was used to correct the plasma input function.

PET images were processed using Statistical Parametric Mapping 8 (SPM8, Wellcome Trust Centre for Neuroimaging, London, UK). For each subject, subject-specific volumes of interest (VOI) were calculated by intersecting the subjects normalized gray matter (GM) map (thresholded at > 0.25) with each automatic anatomic labeling (AAL) (Tzourio-Mazoyer et al., 2002) VOI. With the metabolite-corrected plasma TACs as input, regional brain TACs were fitted to the theoretical two-tissue three-rate constant compartment model including a cerebral blood volume fraction (V_b). This model characterizes rate constants for influx (K_1, min^{-1}) and efflux (k_2, min^{-1}) across the blood-brain barrier (first tissue compartment) and the rate of hydrolysis (k_3, min^{-1}) of [^{11}C]PMP (second tissue compartment) (Koeppe et al., 1999). The k_3 values were calculated for each subject-specific VOI (Illustrated in Figure 6.3). These k_3 values are a proxy for AChE activity levels in the brain (Koeppe et al., 1999). Left and right hemispheres were analyzed separately.
To reduce spillover from high uptake regions to regions with low or moderate uptake, we additionally applied a masking in VOIs with low or moderate uptake. This mask contained all voxels with high uptake values across all control subjects and as a result, it excluded these voxels within VOIs with low or moderate uptake (spill-over correction). We then calculated a weighted mean k_3 value by taking into account the size of each subject-specific VOI of the left and right neocortex (including

frontal, parietal, temporal and occipital neocortical VOIs) and left and right allocortex (including olfactory gyrus, amygdala, hippocampus and parahippocampal gyrus VOIs) to obtain weighted mean k_3 values in known projection regions of the BF (Mesulam, 2013b).

6.3.4 MRI acquisition and analysis

The 11 PPA and 10 HC received a T_1-weighted structural MRI on a 1.5T Siemens Sonata system (Siemens Medical Solutions, Erlangen, Germany) and eight-channel head coil (coronal inversion recovery prepared 3D gradient-echo images; inversion time (TI) 800 milliseconds (ms), echo time (TE) = 3.93 ms, voxel size ($1\times1\times1$) mm^3).

Preprocessing of the T_1-weighted MRI scans was performed with Voxel-Based Morphometry 8 (VBM8) (Ashburner and Friston, 2000), implemented in Matlab R2012b (Mathworks, Natick, MA, USA) as described previously (Gillebert et al., 2015). This procedure generated non-linear only modulated GM maps, corrected for total intracranial volumetric differences. These GM maps were used to obtain mean BF GM volumes by averaging the unsmoothed modulated warped GM voxel values within the BF mask (Kilimann et al., 2014). All BF volumes have been adjusted for overall brain size by using only the nonlinear component of the spatial normalization for modulation of GM voxel intensities. The BF mask was designed by Kilimann et al. (2014); Teipel et al. (2014b) using histopathological localization of the different BF nuclei of a single patient and manual transformation to the MRI scan of the dehydrated brain. The latter scan was subsequently spatially realigned to the MRI scan of the initial MRI scan of the *in cranio* brain and finally brought to MNI space. The combined transformation parameters were applied to the BF nuclei to obtain a mask in MNI standard space (Fig. 6.1).

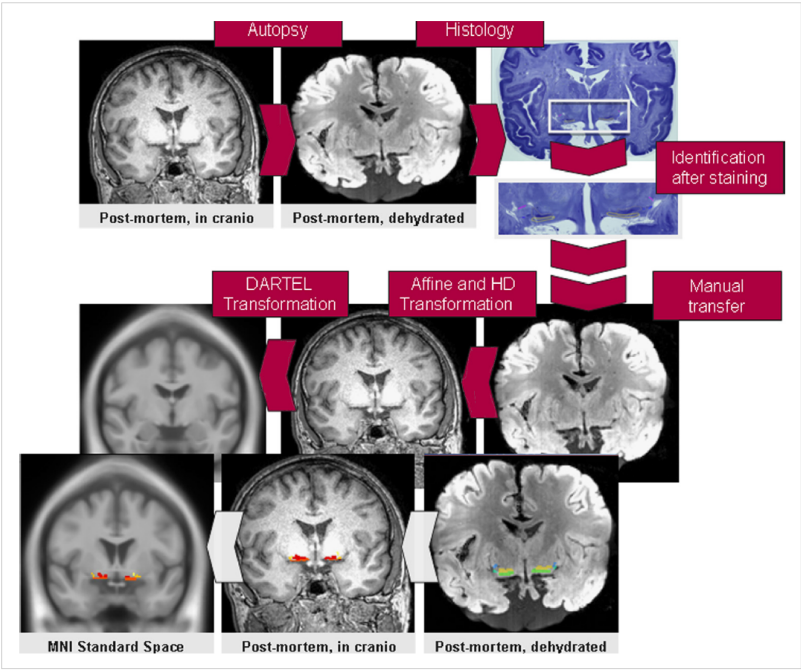


Figure 6.1: **Development of the basal forebrain mask.** The brain of a 56-years-old man was scanned using MRI *post-mortem in cranio* and after alcohol dehydratation; thereafter, it was histologically stained to define the localization of basal forebrain cholinergic nuclei (first row). The histologically stained localizations of the cholinergic nuclei were manually transferred to the corresponding MRI sections from the dehydrated brain (last row, right image). Using 12-parameter affine and high dimensional (HD) nonlinear normalization, the MRI in alcohol space was spatially realigned to the brain in *in cranio* space (middle row, middle image). The *in cranio* MRI again was spatially normalized to MNI space using DARTEL (middle row, left image). The combined transformation parameters from alcohol to *in cranio* space and from *in cranio* to MNI space were applied to the cholinergic basal forebrain mask to obtain a mask in MNI standard space (last row, middle and right image). Modified with permission from Teipel et al. (2014b).

In order to determine whether any AChE changes occurred specifically in regions that were typically affected in a particular subtype, an extended sample of PPA and controls were analyzed to determine the regions of

subtype-specific atrophy with high sensitivity. In addition to the initial sample of 11 PPA and 10 control subjects, this extended sample contained 24 additional controls who had undergone a volumetric research MRI on the same scanner using the same sequence as mentioned above as well as 17 additional PPA (4 LV, 6 NFV and 7 SV) (Grube et al., 2016) and 77 additional controls who had undergone a T_1-weighted structural MRI on a 3T Philips Intera system and an eight-channel head coil (coronal inversion recovery prepared 3D gradient-echo images; TI 900 ms, TE = 4.6 ms, voxel size ($0.98\times0.98\times1.2$) mm^3).

To identify subtype-specific atrophy, we contrasted the group of 28 PPA cases to the 111 controls in a voxelwise ANCOVA in SPM8 with smoothed modulated GM volume maps as dependent variables, group (4 levels: LV, SV, NFV, healthy controls) as between-subjects factor and age, gender and scanner site as nuisance variables. Results were considered significant at voxel-level uncorrected $p< 0.001$ combined with cluster-level family-wise error (FWE)-corrected $p< 0.05$ (Poline et al., 1997). For voxelwise statistical comparisons, GM maps were smoothed with an 8 mm isotropic FWHM Gaussian 3D kernel.

6.3.5 Statistical analyses

Standard statistical analyses were performed in Statistics Software Package for the Social Sciences (version 23, IBM Statistics, Armonk, USA). BF volumes and AChE activity levels were checked for outliers using the Grubbs' test: Z scores higher than three standard deviations were classified as outliers. The individuals' neuropsychological test scores were compared to controls using a modified t-test (Crawford and Howell, 1998) (Table 6.1). Differences in age between PPA patients and control subjects were assessed using Kruskal-Wallis and with Pearson chi^2 tests for gender.

Primary outcome analyses

Given the relatively limited sample size, the primary analysis was based on a multiple single case series methodology. Differences of AChE activity levels in global neo- and the global allocortical VOIs in the left and right hemisphere were assessed in each individual patient in comparison to the eight controls using a modified t-test (Crawford and Howell, 1998). As a second primary outcome analysis, a Spearman or Pearson correlational analysis was performed between AChE activity levels

averaged over left and right allo- and neocortex, and BF volume, depending on normality of the data.

Secondary outcome analyses

Secondary outcome analyses aimed to evaluate effects at the overall group and at the subgroup level, to examine the relationship between AChE activity levels and structural changes, and to test the replicability of the BF atrophy in PPA reported previously (Teipel et al., 2014b, 2016).

1. Differences in AChE activity were assessed at the group level (PPA versus controls) using Kruskal-Wallis and with *post hoc* Mann-Whitney U tests for differences between subgroups (uncorrected, two-tailed p values).

2. In order to evaluate the relationship between AChE activity levels and structural atrophy, AChE activity levels were calculated in each individual patient compared to controls in the regions that were characteristically atrophic for the subtype to which the case belonged (LV, NFV or SV) (VOIs are based on figure 6.5). In order to determine whether AChE activity levels were specifically lower in the atrophic regions, AChE activity levels were also evaluated in cortical regions falling outside subtype-specific regions of atrophy. The latter region was determined by subtracting the region of characteristic atrophy from the subjects normalized GM map (thresholded at > 0.25). For each individual patient, differences in AChE levels compared to controls were assessed using a modified t-test (Crawford and Howell, 1998).

3. In order to evaluate whether BF volume decreases that have previously been reported (Teipel et al., 2014b, 2016) could be replicated, a BF volume analysis was performed in the extended sample of 28 PPA and 111 control subjects. By means of an ANCOVA model, BF volumes were assessed at the group level in controls, LV, NFV and SV PPA with scanner type as nuisance variable, and *post hoc* Bonferroni correction for the number of comparisons at $\alpha = 0.05$.

4. Finally, we determined the effects of symptom duration, age, and gender on AChE activity levels by means of Spearman or Pearson correlational analyses or Mann Whitney U tests (two-tailed).

6.4 Results

6.4.1 Primary outcome analyses

AChE activity levels in PPA patients

Two out of three LV patients showed significantly lower neocortical AChE activity levels than controls in the left (case 7: t = -2.68, p = 0.016 and case 8: t = -4.12, p = 0.002) (Fig. 6.2A) and in the right hemisphere (case 7: t = -3.17, p = 0.008 and case 8: t = -5.59, $p < 0.001$) (Fig. 6.2B). No differences were found in NFV or SV cases compared to controls (all $p > 0.13$) (Fig. 6.2A, B).

In two out of three LV patients, left allocortical AChE activity levels were significantly lower than in controls (case 7: t = -1.93, p = 0.047 and case 8: t = -2.70, p = 0.015)(Fig. 6.2C). In one of these cases, right-hemispheric allocortical AChE activity levels were also lower compared to controls (case 8: t = -4.20, p = 0.002) (Fig. 6.2D). Four out of five SV patients showed significantly elevated right allocortical AChE activity levels (case 3: t = 3.39, p = 0.006; case 4: t = 4.57,p = 0.0013; case 9: t =2.26, p = 0.03; case 10: t =3.28, p = 0.007) (Fig. 6.2D). In one of these cases, left allocortical AChE activity levels were significantly higher than in controls (case 10: t=2.0, p= 0.042) (Fig. 6.2C). No significant differences compared to controls were found in NFV patients (all $p >$ 0.37).

In order to gain further insight in the elevation of allocortical AChE activity levels in SV cases, we analyzed each of the four subVOIs of which the allocortical VOI was composed. The elevation of AChE activity was mainly seen in the subVOI corresponding to the right parahippocampal gyrus (case 3: t =3.72, p = 0.004, case 4: t =5.22, $p < 0.001$, case 9: t = 2.11, p = 0.036 and case 10: t = 3.93, p = 0.003) and least so in the subVOI corresponding to the olfactory gyrus (case 9: t = 1.95, p = 0.046)(Fig. 6.2C, D).

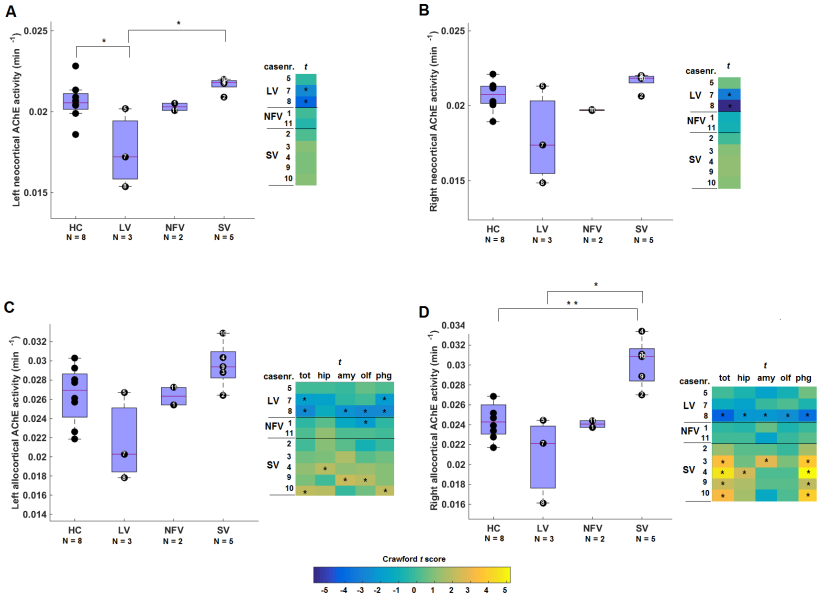


Figure 6.2: **Acetylcholinesterase activity levels.** AChE activity levels are plotted for **(A)** left and **(B)** right neocortex and for **(C)** left and **(D)** right allocortex. Boxplot: minimum, first quartile, median (red line), third quartile, and maximum. Color bar: t scores for individual AChE activity levels based on a modified t test with a threshold of $\alpha = 0.05$. Patients who significantly differed from controls based on the modified t test are indicated with an asterisk on the colorbar. For group based comparisons: $^*p < 0.05$, $^{**}p < 0.01$. Abbreviations: amy: amygdala, HC: healthy controls, hip: hippocampus, LV: logopenic variant, NFV: nonfluent variant, olf: olfactory gyrus, phg: parahippocampal gyrus, SV: semantic variant PPA patients, tot: total region.

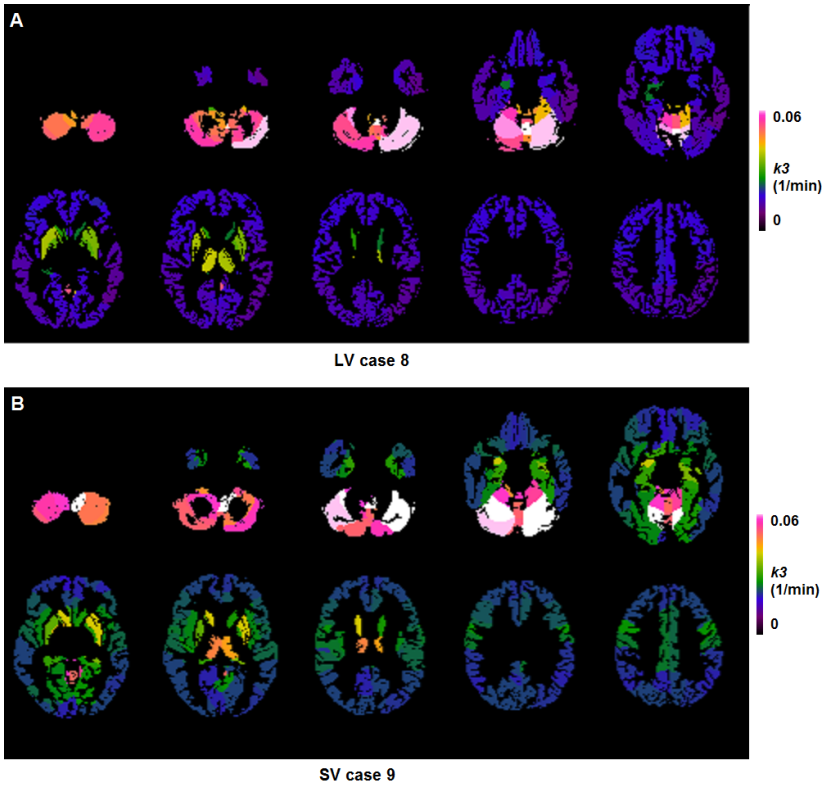


Figure 6.3: **Illustration of AChE activity levels (k_3 values)**. The colorscale represents k_3 values as an index for AChE activity levels: **(A)** reduced k_3 values in the necortex of LV case 8, **(B)** elevated k_3 values in the allocortex of SV case 9. Case numbers correspond to Table 6.1.

Correlation between BF volume and AChE activity levels

BF volume in PPA patients did not correlate with AChE activity levels in the left (ρ = 0.16, p = 0.65) or right neocortex (ρ = -0.37, p = 0.29) (Fig. 6.4A,B), nor in the left (ρ = -0.24, p = 0.51) or right allocortex (ρ = 0.28, p = 0.43) (Fig. 6.4C,D).

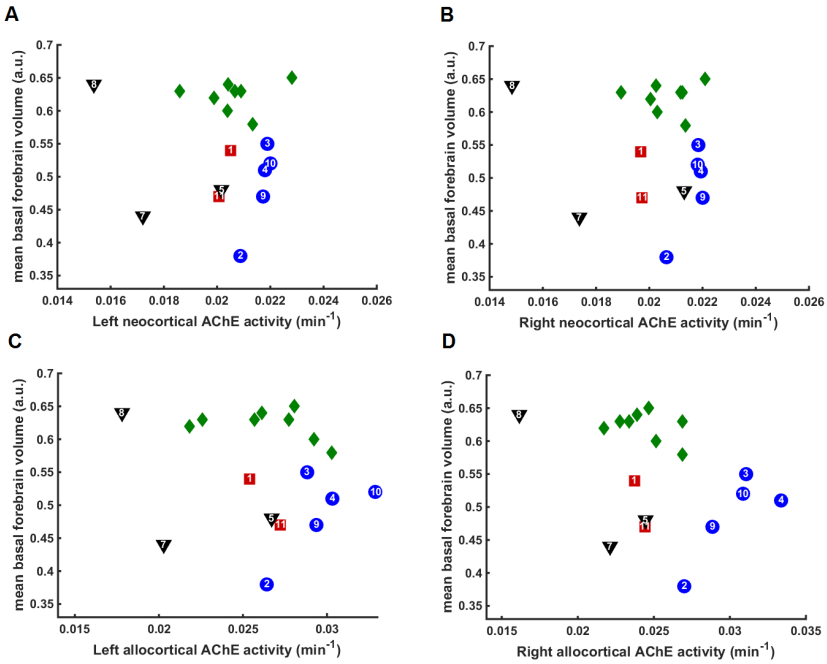


Figure 6.4: **Basal forebrain volume and AChE activity levels**. AChE activity levels of **(A)** left and **(B)** right neocortex and **(C)** left and **(D)** right allocortex on the abscissa (min^{-1}) and mean basal forebrain volumes (arbitrary units) on the ordinate. Green diamonds: HC: healthy controls, black triangles: LV: logopenic variant, red squares: NFV: nonfluent variant, blue circles: SV: semantic variant PPA patients. Case numbers correspond to Table 6.1.

6.4.2 Secondary outcome analyses

Group-based comparisons of AChE activity levels in neo- and allocortex

Left neocortical AChE activity differed significantly between groups ($chi^2(3) = 9.5$, $p= 0.024$). Only LV patients showed significantly lower left neocortical AChE activity levels compared to controls ($U = 2$, $p = 0.041$) and compared to SV patients ($U = 0$, $p = 0.025$). No differences were found between other subgroups (all $p > 0.053$) (Fig. 6.2A, B).
Right allocortical AChE activity levels were significantly different between groups ($chi^2(3) = 11.3$, $p = 0.010$) (Fig. 6.2D). SV patients had significantly elevated right allocortical AChE activity levels compared to controls ($U = 0$, $p = 0.003$) and compared to LV ($U = 0$, $p = 0.025$). No significant differences were found between other subgroups (all $p > 0.053$)(Fig. 6.2C, D).

Definition of PPA atrophic regions

In the extended sample of PPA patients and controls, LV patients showed atrophy restricted to the left posterior third of the left middle temporal gyrus (MTG), extending towards the temporoparietal junction as well as bilateral atrophy of the precuneus (Fig. 6.5A). NFV patients exhibited atrophy of the bilateral supplementary motor area (SMA) and cingulum, together with left inferior and middle frontal lobe atrophy extending towards the left insula (Fig. 6.5B). SV patients showed severe atrophy of the bilateral anterior temporal lobe (ATL), including the anterior fusiform gyri, as well as atrophy of the amygdalae, hippocampi and insulae (Fig. 6.5C). Overall, there was predominant left hemispheric atrophy independently of PPA subtype.

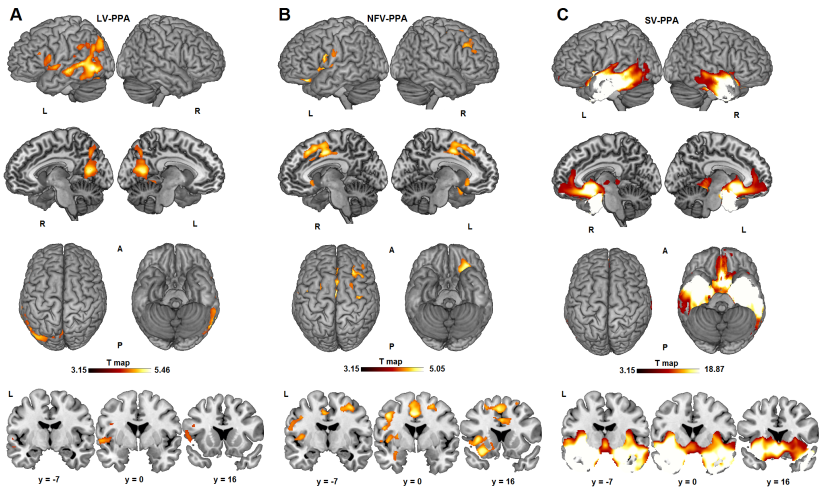


Figure 6.5: **Cortical atrophy patterns in PPA**. T-maps, generated by contrasting each PPA subgroup (total n = 28) versus controls (n = 111) in SPM8, are projected onto a surface rendering of a template brain and on coronal slices with corresponding MNI coordinates. Threshold: voxel-level uncorrected $p < 0.001$ combined with cluster-level FWE-corrected $p < 0.05$. T-maps depict brain regions of reduced gray matter volume in **(A)** logopenic variant (LV), **(B)** nonfluent variant (NFV), and **(C)** semantic variant (SV) PPA patients.

AChE activity levels in the PPA atrophic and preserved neocortical regions

At the individual patient level, two out of three LV patients showed lower AChE activity levels compared to controls in brain regions typically atrophic in LV PPA (case 7: t = -2.65, p = 0.016 and case 8: t = -6.20, $p < 0.001$)(Fig. 6.6A). These two LV patients showed also lower AChE activity levels (case 7: t = -3.04, p = 0.009 and case 8: t = -4.73, p = 0.001) compared to controls outside the regions that were typically atrophic in LV PPA (Fig. 6.6B). This suggests that the reduction in AChE activity levels is not restricted to the regions of characteristic atrophy in LV but is more diffuse. Compared to controls, two of the five SV patients showed elevated AChE activity levels in regions typically atrophic in SV PPA (case 9: t = 2.09, p = 0.038; case 10: t = 1.88, p = 0.05) (Fig. 6.6A). SV patients did not show abnormal AChE activity levels outside the SV atrophic regions (Fig. 6.6B). This may suggest that

the increase in AChE activity levels in SV could potentially be most pronounced in those regions that are also most affected structurally. No significant differences were found for NFV patients compared to controls (all $p > 0.31$).

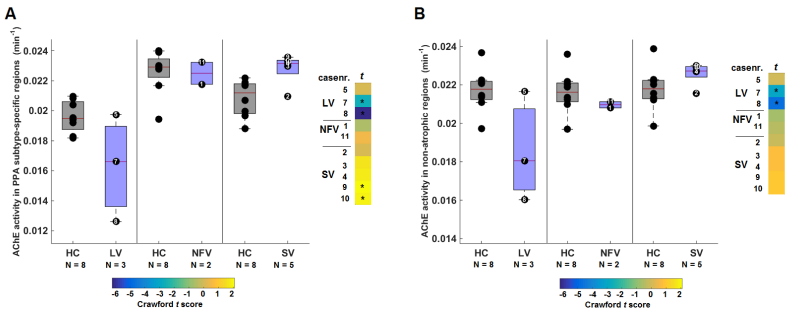


Figure 6.6: **AChE activity levels in subtype-specific PPA atrophic regions**. AChE activity based on a modified t-test with a threshold of $\alpha = 0.05$ in **(A)** subtype-specific atrophy in PPA and **(B)** complementary non-atrophic brain regions. Note that the subtype-specific regions differed depending on the variant and that the values plotted for each subtype are obtained in the regions that are atrophic for that particular subtype. Accordingly, the corresponding values in the controls were obtained in that same subtype-specific region. Patients that significantly differed from controls are indicated with an asterisk on the color bar. Abbreviations: LV: logopenic variant, HC: healthy controls, NFV: nonfluent variant, SV: semantic variant. Case numbers correspond to Table 6.1.

BF volumetry in the extended PPA sample

In the entire group of PPA patients, BF volume was reduced in three out of eight LV (case 5: t =-1.75, $p = 0.042$, case 7: t = -2.41, $p = 0.009$ and case 17: t =-2.00, $p = 0.023$), one out of eight NFV (case 11: t = -1.91, $p = 0.029$) and five out of 12 SV patients (case 2, t = -3.42, $p <$ 0.001, case 9: t = -1.91, $p = 0.029$, case 14: t = -2.45, $p = 0.008$, case 19: t = -2.56, $p = 0.006$ and case 25: t = -3.07, $p = 0.001$) compared to controls (Fig. 6.7).
There was a significant overall effect of group on BF volume (F (3,134) = 11.8, $p < 0.001$). *Post hoc* tests revealed that BF volume was most reduced in SV compared to controls (-17.2 ± 11%, $p = 0.001$). No

significant differences were found in LV (-7.3 ± 13%, $p = 0.40$) or NFV (-9.6 ± 7.8%, $p = 0.07$) patients compared to controls. No significant differences of BF volume were found between PPA variants ($p > 0.1$) (Fig. 6.7).

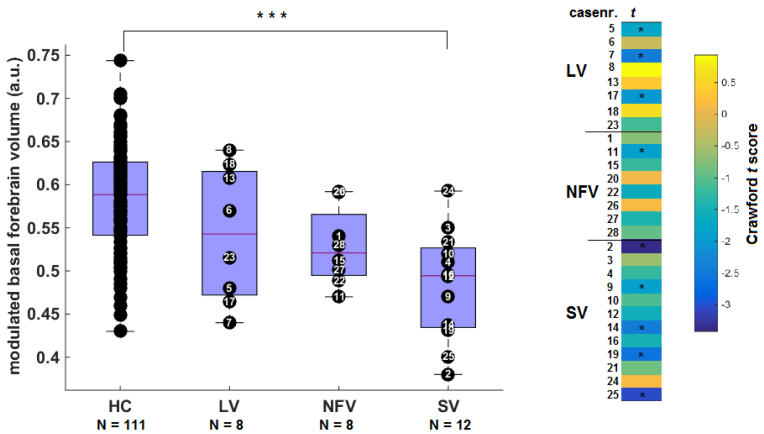


Figure 6.7: **Basal forebrain volume in PPA subtypes**. Boxplot with BF volumes: minimum, first quartile, median (red line), third quartile, and maximum and color bar: t scores for individual BF volume based on a modified t test with a threshold of $\alpha = 0.05$. Patients that significantly differed from controls are indicated with an asterisk on the color bar. For group based comparisons: $^{***}p < 0.001$. Abbreviations: HC: healthy controls, LV: logopenic variant, NFV: nonfluent variant, SV: semantic variant PPA patients. Case numbers correspond to Table 6.1.

Effects of age, gender and symptom duration on AChE activity

In the current PPA sample, there were no effects of symptom duration on AChE activity levels in the left or right neo- or allocortical region ($p > 0.30$) and no effects of age ($p > 0.098$) or gender ($p > 0.57$) on AChE activity levels.

6.5 Discussion

The current findings demonstrate that BF atrophy does not imply cholinergic depletion. The presence of BF atrophy in SV was replicated, however this was not associated with a cholinergic deficit. Instead AChE activity in SV was increased. Cholinergic depletion was only seen in LV cases, both within and outside the neocortical regions of characteristic atrophy.

6.5.1 Cholinergic alterations

The LV with pathologically definite AD (case 8) showed the strongest reductions in AChE activity levels. LV PPA can occur as an atypical variant of AD and 50-60% of cases show AD pathology (Matías-Guiu et al., 2015a). Loss of the cholinergic systems integrity is among the earliest events in the pathogenesis of typical AD: several studies have shown reduced AChE activity in typical AD patients using [^{11}C]PMP-PET (Kuhl et al., 1999; Bohnen et al., 2003, 2005). The current study shows that this finding can be extended to a subset of LV PPA cases.
The reduction in AChE activity did not appear to be limited to regions typically affected by volume loss in LV PPA. AChE activity reductions were seen also outside regions of typical atrophy. If AChE activity reductions in LV are a consequence of neuronal loss in diffusely projecting subcortical nuclei such as Ch4, one would expect that the PET measure would not strictly overlap with the measure of regional volume loss.

Unexpectedly, despite the BF volume loss, SV PPA was associated with an increase in AChE activity levels. This increase was most pronounced in regions of maximal volume loss, both in the neocortical and in the allocortical regions such as the parahippocampal gyrus. The colocalisation between AChE activity increases and structural volume loss could possibly suggest that AChE activity increases are a compensatory mechanism and a reaction to neuronal loss in SV PPA. This increase was only observed in SV cases and the vast majority of SV PPA is caused by a TDP-43 proteinopathy (Josephs et al., 2009; Grossman, 2010). In the current study, SV case 9 received a diagnosis of pathologically definite FTLD with TDP-43 inclusions subtype C.
A previous expression study in transgenic mice (Tg-VLW) expressing human tau mutations, suggested that tauopathy may be associated with AChE activity increases (Silveyra et al., 2012). This is the first study which showed AChE increases in a case with proven TDP-43

proteinopathy. It may be worth investigating how specific types of proteinopathy differentially affect neurotransmitter systems and the regional specificity of such effects.

Neuropathological examinations of other cholinergic biomarkers in semantic dementia showed that there is an increase in the proportion of cholinergic M2 muscarinic receptors compared to controls, with a decrease in the proportion of cholinergic M1 muscarinic receptors (Odawara et al., 2003). The increase in M2 receptors found by Odawara as well as the increase in AChE activity levels in the current study are possibly suggesting a compensatory reaction to the neurodegenerative neuronal loss. Elevated AChE activity levels as measured with PET have previously been reported in FTD, although non-significantly and restricted to the thalamus (Hirano et al., 2010). However, most studies on FTD failed to show any abnormalities in cholinergic system markers, be it *post mortem* (Procter et al., 1999) or at the level of cerebrospinal fluid (CSF) (Wallin et al., 2003).

6.5.2 BF atrophy and its relation to cholinergic alterations

The BF receives afferents from the amygdala and hippocampus (Aggleton et al., 1987). On their turn, cholinergic pathways arising from the BF project among others to the temporal lobe and the parahippocampal gyrus (Selden et al., 1998). These regions are typically affected in SV PPA in cross-sectional (Mummery et al., 2000; Rosen et al., 2002; Whitwell et al., 2005) and longitudinal studies of the disease (Brambati et al., 2007). However, BF volume loss in SV was not associated with cholinergic depletion.
The neuronal, glial and interstitial compartments that contribute to MRI measures of BF are far broader than the cholinergic neuronal cell population. For instance, cholinergic neurons are typically found intermingled with inhibitory interneurons, the second most important BF cell types (Mesulam, 2013b).

Our data caution against inferences based upon MRI BF volume measures with regards to cholinergic status in PPA.

6.5.3 A cholinergic therapy for PPA ?

There are currently no medications approved by the US Food and Drug Administration (FDA) to treat PPA. Language regions contain a relatively high density of AChE-containing neurons (Hutsler and Gazzaniga, 1991), which may suggest a rational basis for cholinergic treatment in PPA. Cholinergic therapy improves language in various disorders affecting the language network (Tanaka et al., 1997; Berthier et al., 2006; Ferris and Farlow, 2013; Yoon et al., 2015), although regulatory approval is restricted to clinically probable AD. To date, only one study with an open-label period of 18 weeks and a randomized, placebo-controlled phase for eight weeks with galantamine included PPA patients ((Kertesz et al., 2008). The overall language performance showed a trend towards stabilization over a total duration of eight weeks. A randomized, placebo-controlled study with memantine showed general good tolerance, however there were more frequent cognitive adverse events (Boxer et al., 2013). A therapeutic trial of donepezil in FTD failed to show any efficacy and a subgroup of patients experienced worsening of symptoms (Mendez, 2009).
Currently, cholinergic medication may be prescribed off-label in clinical practice for PPA patients who are amyloid-positive (amyloid-PET or CSF amyloid/tau). AChE-PET allows one to directly discriminate PPA cases with a cholinergic deficit from those without a cholinergic deficit. This distinction could possibly predict a therapeutic response, but this remains to be demonstrated. The cholinergic deficit in LV in the current study provide a potential rationale for off-label use of AChE inhibitors (AChEI) in LV PPA due to underlying AD pathology. However our findings do not provide direct support for the use of AChEI in SV PPA, since AChE activity appears to be already naturally increased in this subtype compared to healthy controls.

6.5.4 Potential study limitations

The number of PPA patients included is small. This is inherent to the relatively high demands of the scanning procedures, in particular for dynamic PET acquisition with arterial sampling, and the relatively low prevalence of PPA (Gorno-Tempini et al., 2011). We calculated k_3 as index for AChE activity based on the well-established theoretical two-tissue three-rate constant compartment model with a cerebral blood volume fraction (Koeppe et al., 1999). Cerebral atrophy does not influence the rate constants including k_3, nor does k_3 depend on blood

flow or aging (Kuhl et al., 1999). Based on the compartment model used, partial volume effects on k_3 are negligible if spillover from neighboring regions can be neglected (Koeppe et al., 1999; Kuhl et al., 1999). The effects of butyrylcholinesterase (BChE), which has been shown to increase in the course of neurodegenerative diseases (Nordberg et al., 2013), on the k_3 values are also negligible (Kuhl et al., 1999).
The diffuse structure of the BF itself may cause difficulties to reliably delineate its borders on MRI. We therefore used the BF mask obtained with a procedure of Kilimann (2014) based on histological staining of post mortem brain sections which were subsequently transferred to MNI space (Kilimann et al., 2014). Given the small volume of each subnucleus, we decided to assess the BF volume as one single volume as this provided a more robust estimation. The distribution of the current BF mask used in this study was compared to two previous masks, one based on a single subject (Teipel et al., 2005), and one probabilistic map based on 10 subjects (Zaborszky et al., 2008) in a study of Teipel and colleagues (Teipel et al., 2016). There was a high general agreement between all three masks. These findings suggest that the anatomy of the BF nuclei delineated by means of this procedure is relatively stable across subjects.

6.6 Conclusion

We established involvement of the cholinergic system in PPA, both at the structural and functional level. The observed cholinergic deficit further encourages development of cholinergic PPA treatments in LV, possibly in NFV but not in SV PPA cases.

Table 6.1: Demographics and neuropsychological characteristics

Casenr.	PPA variant	Postmortem	Age (y)	Disease dur. (y)	Gender	CDR	BNT (/60)	PALPA (/30)	AAT (/120)	BORB-A	BORB-B	CPM
5†	LV	/	59	2.5	m	2	/	**15**	**83**	**21**	**27**	**20**
6†	LV	/	77	2	m	1	**39**	25	**102**	**22**	30	29
7†	LV	/	66	3	m	1	**35**	27	**94**	**23**	32	**23**
8†	LV	AD	72	2.5	f	1	**24**	26	**83**	25	29	17
13	LV	/	57	0.5	f	0.5	56	28	120	25	29	35
17	LV	/	64	3	m	0.5	**41**	**23**	114	25	31	33
23	LV	/	71	1	m	0	53	28	118	26	31	33
18	LV	/	62	1.5	f	1	53	27	106	24	31	31
1†	NFV	CBD	77	3	m	1	**43**	25	105	**21**	30	**24**
11†	NFV	/	71	2.5	m	1	**45**	29	112	27	30	**21**
15	NFV	/	52	2	f	2	58	28	120	26	31	31
20	NFV	/	79	5	f	1	48	**22**	105	25	30	**24**
22	NFV	/	71	1.5	m	0.5	55	28	**102**	26	31	**24**
26	NFV	/	78	2.5	m	1	48	**23**	**77**	26	29	30
27	NFV	/	72	2.5	f	1	**30**	**19**	**85**	**21**	**18**	**12**
28	NFV	/	63	5	f	0	**41**	**24**	**104**	**22**	28	32
2†	SV	/	59	4	m	1	**36**	**22**	**78**	**17**	**23**	**21**
3†	SV	/	63	3	f	1	**14**	**24**	**95**	**22**	**25**	**23**
4†	SV	/	71	6	m	1	**13**	**22**	**95**	24	28	**17**
9†	SV	TDP	52	1.5	f	1	/	**17**	**62**	**21**	**23**	36
10†	SV	/	57	2	m	1	**14**	**22**	**87**	**19**	**26**	34
12	SV	/	76	6	m	1	**34**	27	**90**	**20**	**23**	29
14	SV	/	70	1.5	f	1	**22**	**17**	**74**	**20**	**18**	**24**
16	SV	/	61	3	m	2	**7**	**18**	**73**	**18**	**20**	36
19	SV	/	64	3	m	1	**20**	**14**	**74**	**18**	**26**	29
21	SV	/	48	6	f	1	**12**	**24**	**82**	**17**	**26**	35
24	SV	/	58	2	f	1	**35**	27	**93**	27	31	36
25	SV	/	68	5	f	1	**16**	**23**	114	25	31	34
Groupdata	PPA	Mean (SD)	65.8(8.5)	2.96(1.5)	13f/15m	0.89	34.3(15.7)	23.4(4.2)	94.5(16.1)	22.6(3.1)	27.4(4.1)	27.6(6.7)
	controls	Mean (SD)	65.4(6.7)	/	48f/63m	0	53.7 (4.7)	27.6(1.8)	114.8(4.8)	27.2(1.97)	29.8(1.5)	32.2(3.2)
		P	0.7	/	0.92	<0.001	<0.001	<0.001	<0.001	<0.001	0.01	0.005

Abbreviations: AAT: Akense afasie test comprehension scores, BORB-hard(A)/-easy(B): Birmingham object recognition battery, BNT: Boston naming test, CBD: corticobasal degeneration, CDR: Clinical dementia rating scale, CPM: colored progressive matrices, dur.: duration, PALPA: Psycholinguistic assessment of language in aphasia, subtest 49: associative-semantic task for words. PPA variants: LV: logopenic variant, NFV: nonfluent variant, SV: semantic variant PPA patients. Bold: scores which are significantly different compared to controls based on a Crawford modified *t*-test (Crawford and Howell, 1998), †Patients who received [^{11}C]PMP-PET.

Chapter 7

General discussion

Following the first description of primary progressive aphasia (PPA) by Marsel Mesulam in 1982 (Mesulam, 1982), gradually increasing knowledge regarding its diverse clinical and pathological manifestations became available (Gorno-Tempini et al., 2011). However, as of yet, the pathophysiology of PPA remains still poorly understood. The general aim of this thesis was to study pathophysiological mechanisms underlying PPA at a behavioral, structural and molecular imaging level.

In chapter 3 of this thesis, using non-linguistic, acoustic stimuli devoid of meaning we demonstrated that PPA patients (n = 18) were significantly impaired in the three key domains of auditory processing (pitch, time/rhytm, and timbre) compared to healthy controls. Patients with NFV PPA had the most marked deficits within the time/rhythm domain for the processing of short sequences of up to seven tones. A subset of SV PPA patients were also impaired, though less severely. Patients with LV PPA did not show any significant individual impairments. Significant deficits remained after partialling out effects of executive dysfunction. Our sound perception data allowed reliable discrimination of NFV from LV cases even though these contained no language stimuli and were purely based on perceptual judgment of pitch and rhythm in tone sequences. We also demonstrated that performance on a subset of the psychoacoustic tests correlated with conventional verbal repetition tests.

In chapter 4, in a larger group of PPA patients (n = 27, 18 of these patients participated in the psychoacoustic study described in chapter 3) (Fig.7.1A), the most marked deficits in patients with NFV PPA were

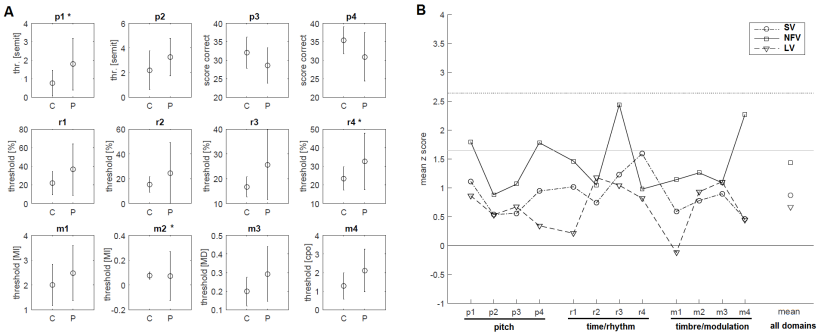


Figure 7.1: **Patients' psychoacoustic data in comparison to controls. (A)** Group comparison of psychoacoustic scores between the PPA group and controls. Pitch: basic change detection (p1), change-direction discrimination (p2), detection of a local change in pitch sequence (p3); detection of a global change in pitch sequence (p4). Time and rhythm: single time-interval discrimination (r1), isochrony deviation detection (r2), metrical pattern discrimination for a strongly (r3) and a weakly metrical sequence (r4). Timbre and modulation: 2 Hz frequency modulation (FM) detection (m1), 40 Hz FM detection (m2), dynamic modulation (DM) detection (m3), dynamic modulation discrimination (m4). Asterisks denote a significant difference ($p = 0.05$, Bonferroni-corrected (n = 12)). **(B)** Mean Z scores across patients within the three clinical subtype groups. Mean Z scores are plotted for each task, and in addition the overall mean across tasks (far right). Gray line corresponds to the uncorrected p of 0.05, the dotted line to $p = 0.05$, Bonferroni-corrected (n = 12).

found within the time/rhythm domain, followed by significant deficits in timbre and pitch processing deficits (Fig.7.1B). Patients with SV were affected to a lesser degree, with most pronounced impairments in the time/rhythm domain, while LV did not show significant abnormalities (Fig.7.1B). Voxel-based morphometry (VBM) was applied on high-resolution T_1-weighted structural magnetic resonance imaging (MRI) scans. Whole-brain voxel-wise linear regression analyses between gray matter volume maps and test performance revealed that rhythm and time processing deficits correlated with right-hemispheric involvement of the frontal operculum and posterior insula. These deficits remained when analyses were performed within the NFV PPA patients. Based on these findings, we postulate that auditory timing pathways are altered in NFV PPA, which are used in common for processing acoustic sequence

structure in both speech output and acoustic input. We propose that the perceptual timing deficits may contribute to the speech apraxia in NFV, which is characterized by abnormal duration and inter-segmental time intervals of speech, among other features.

In chapter 5, we examined the prevalence and nature of single-word comprehension problems in individual PPA patients with speech apraxia and/or agrammatism. We also assessed how these patients differed from controls and other PPA variants based on their atrophy pattern as well as on [^{11}C]-PIB and [^{18}F]-THK5351 PET binding pattern. Neuropsychological performance in domains apart from single-word comprehension, motor speech and grammatical processing was also assessed and compared between groups. In patients with motor speech problems and/or agrammatism who have concomitant single-word comprehension problems (MV PPA), the topographical distribution of [^{18}F]-THK5351 binding is highly similar to that observed in NFV-pure, but atrophy is more widespread in MV PPA. The topography of [^{18}F]-THK5351 binding, but not the degree of atrophy was correlated with core clinical features of MV PPA. MV PPA had a higher likelihood of amyloid-positivity compared to NFV-pure PPA.

Given the finding that the basal forebrain (BF) is atrophic in SV and NFV PPA according to MRI volumetric studies (Teipel et al., 2014b, 2016), we investigated in chapter 6 in a series of 11 PPA patients whether BF volume loss relates to cholinergic depletion and how this depends on the PPA variant. Acetylcholinesterase (AChE) activity was quantitatively measured in the neo- and allocortex using N-[^{11}C]-Methylpiperidin-4-yl propionate (PMP)-PET with arterial sampling and metabolite correction. Whole brain and BF volumes were quantified using VBM. In the PPA group, only LV cases showed decreases in AChE activity levels compared to controls. Surprisingly, a substantial number of SV cases showed significant AChE activity increases compared to controls, while BF volume was reduced in SV. We conclude that based on our findings, BF atrophy in SV PPA does not imply cholinergic depletion.

7.1 The intersection between core auditory processing and language

In a broad sense, auditory perceptual processing is considered fundamental to normal speech production based on several findings from studies assessing language acquisition (Shiller et al., 2010; Guenther and Hickok,

2015), as well as studies investigating the relationship between language and musical skills in children (Jentschke et al., 2005; Degé and Schwarzer, 2011; Gordon et al., 2015) and studies in patient populations (Griffiths et al., 1997; Kumral et al., 2004; Griffiths, 2008; Maruta et al., 2014).

During the development of a child's sound inventory and lexicon (Shiller et al., 2010), it has been shown that perception of complex sound, is an essential contributor to shape and fine-tune motor speech output (Guenther and Hickok, 2015). The term 'complex sound' contains a wide variety of sound, including music. If we consider musical sounds, the structure of music and language is strikingly similar. Both involve sequences of sound with specific rhythmic and melodic patterns constituting basic elements (e.g. phonemes/morphemes and notes/chords). These basic elements evolve over time according to specific rules (e.g. syntax/grammar and key/harmonic structures) that convey higher-order meaningful structures (e.g. sentences or melodies). It has been shown that musical skills training in children enhances the development of language skills such as reading and phonological awareness (Degé and Schwarzer, 2011). Conversely, children with deficits in syntactic processing tend to experience difficulties in processing musical irregularities in chord sequences (Jentschke et al., 2005). Especially rhythm perception is associated with morpho-syntactic production skills in children with typical language development (Gordon et al., 2015). Performance on temporal processing tasks has been shown to improve in particular between the age of 7-13 years till adulthood (Walker et al., 2006), with higher levels of rhythmic complexity and language skill emerging in early adulthood (Grube et al., 2013). In line with these findings, performance on metrical pattern discrimination has also been shown to correlate significantly with poem reading skills in young adults (Grube et al., 2013). Taken together, core auditory processing seems to be essential for the development of linguistic skills.

Evidence linking auditory input to motor output can also be found in patients with tone deafness (congenital amusia) (Griffiths, 2008). Although this disorder is recognized as an output disorder (for singing), changes are observed within a right-hemispheric network including the STG as well as the IFG for pitch pattern analysis and working memory for pitch (Griffiths, 2008). Furthermore, patients with stroke might have besides motor speech problems, concomitant auditory processing deficits, providing a possible link between these two processes (Griffiths et al., 1997; Kumral et al., 2004). It has been proposed that the motor speech problems in NFV PPA may reflect distorted speech input signal processing (Maruta et al., 2014). This disordered sensori-motor

integration is hypothesized to impact on motor speech output via the dorsal language pathway (Maruta et al., 2014).

Although we formulated a clear hypothesis regarding the underlying neural correlates of rhythm and timing deficits based on previous timing-related studies in healthy controls (Nenadic et al., 2003; Grahn and Brett, 2007; Chen et al., 2008; Morillon et al., 2009; Teki et al., 2011; Grahn and Rowe, 2013), we did not restrict our analyses to predefined VOIs. By employing whole-brain voxel-based analyses, we avoid potential statistical bias in the reported regions. Especially in small groups, the use of specific VOIs on the basis of previously published papers may lead to inflated type I errors (Poldrack et al., 2017). The obtained candidate regions are biologically plausible substrates for two reasons: (1) their established involvement in timing-related processes and (2) their disease-specific vulnerability in NFV PPA.

First, based on studies in healthy individuals, time estimation involves a distributed network consisting of the pre-SMA/SMA, the anterior insula, and the right frontal operculum among other regions (Morillon et al., 2009; Teki et al., 2011). These regions are multimodally responsive areas which may be crucial in processing and estimation of time (Schubotz and von Cramon, 2001; Ferrandez et al., 2003; Lewis and Miall, 2003; Coull, 2004). In particular, discrimination between the duration of two tone pairs involves the right frontal operculum and the right insula (Rao et al., 2001; Nenadic et al., 2003), while metricality perception relies more on the pre-SMA/SMA (Grahn and Brett, 2007; Chen et al., 2008; Bengtsson et al., 2009; Hardy et al., 2017b).
The insula has well-developed connections with the primary and secondary auditory cortex (Bamiou et al., 2003) and mainly the posterior part shows responsiveness during auditory evoked potentials (Sudakov et al., 1971). The SMA is strongly connected at the structural and functional level with both the insular cortex and the frontal operculum (Coull, 2004; Catani et al., 2013; Mandelli et al., 2014, 2016). We should however consider the possibility that the observed rhythm and timing deficits in NFV PPA can be caused by the netto effect of network disintegration (Catani and Ffytche, 2005). Individual regions of the timing network such as the pre-SMA/SMA might get disconnected, so that the correlation in the insula and frontal operculum could be an indirect effect. Although we found some evidence which supports a functional role of the insula and frontal operculum in timing-related processes, verification of true involvement can be achieved by applying a 'virtual lesion' in these regions in healthy individuals using transcranial magnetic stimulation (TMS).

Second, in NFV PPA, the IFG and in particular the frontal operculum is considered the syndrome-specific epicentre (Mandelli et al., 2016). Atrophy involving the frontal operculum and SMA correlates with the degree of motor speech impairment characterized by prolongation of vowel duration in polysyllabic words in NFV PPA (Ballard et al., 2014). Apart from its function in speech motor control (Alario et al., 2006), the SMA is connected to the IFG through the aslant tract (Catani et al., 2013; Mandelli et al., 2014, 2016). The structural integrity of this tract correlates with the amount of distortion errors that NFV patients make in spontaneous speech (Mandelli et al., 2014). Apart from studies in NFV PPA, the role of the frontal operculum is well-documented in studies assessing language in healthy individuals (Poldrack et al., 1999, 2001; Meyer et al., 2002; Zaccarella and Friederici, 2015). Likewise, the SMA has a proven role in language processing, more specifically related to speech motor control and speech initiation (Alario et al., 2006). The role of the insula in language and speech has been well established in patients with insular stroke (Dronkers, 1996; Kumral et al., 2004), who show phonemic disintegration and reduced verbal fluency, resulting in apraxia of speech and transcortical motor aphasia (Kumral et al., 2004). Apraxia of speech (AOS) has also been described in patients with atrophy in the premotor cortex and SMA, in which the degree of atrophy in these regions correlated with the degree of AOS (Josephs et al., 2012, 2013b; Whitwell et al., 2013).

Ultimately, a direct comparison of linguistic and non-linguistic 'carrier' signals in substantially large cohorts will be needed to properly interpret the role and nature of generic auditory deficits in PPA and their link to language skills.

7.2 Imaging biomarkers in PPA

7.2.1 Tau PET

A biomarker showing focal neurodegeneration is included in the current diagnostic criteria for the clinical diagnosis of PPA (Gorno-Tempini et al., 2011). In a clinical setting, the pattern of focal neurodegeneration is most often assessed with MRI or [^{18}F]-FDG-PET. Using MRI, one study reported a specificity of diagnosis into one of three variants above 90% for all three PPA variants. The sensitivity of MRI visual assessment in SV PPA was 92%, while sensitivity for NFV and LV PPA was only

21% and 43%, respectively (Sajjadi et al., 2017). Based on MRI alone it might be difficult to make an accurate diagnosis.
[^{18}F]-FDG-PET imaging is common practice in memory clinics and has as benefit over MRI that it can visualize neuronal dysfunction *prior* to atrophy. Visual ratings based on [^{18}F]-FDG-PET show a sensitivity and specificity of respectively, 62.5% and 96.2% for SV, 65% and 98.5% for NFV, and 89.4% and 86% for LV PPA (Matias-Guiu et al., 2017). In a previous report, agreement between readers was however more problematic for visual analysis of [^{18}F]-FDG PET in NFV PPA patients (Matías-Guiu et al., 2015b). In this perspective and for several other reasons, tau PET imaging might be of added value in diagnosing NFV PPA.
First, tau PET imaging provides additional information about the underlying pathology while [^{18}F]-FDG PET or MRI do not. Second, tau PET might show a positive signal early in the disease course, which would not yet have been captured with [^{18}F]-FDG PET or MRI alone (Ossenkoppele et al., 2016; Nasrallah et al., 2017; Phillips et al., 2017). Third, recent studies demonstrate that elevated binding on tau PET scans correlates with cognitive impairment in different patient populations including patients with PPA (Ossenkoppele et al., 2016; Xia et al., 2017; Nasrallah et al., 2017; Phillips et al., 2017). The latter finding contrasts with amyloid PET imaging, which does not correlate with (cross-sectional) measures of cognition (for review: (Vandenberghe et al., 2013)).

In NFV PPA patients, the underlying pathology is in 50-88% of cases associated with FTLD-tau aggregates (i.e. CBD, PSP or Pick's disease) (Grossman, 2010; Spinelli et al., 2017). While conflicting results have been published regarding binding of the tau PET tracer [^{18}F]-AV-1451 to FTLD-tau aggregates (Lowe et al., 2016; Cho et al., 2017; Smith et al., 2017; Whitwell et al., 2017b), autoradiographic analyses have shown that the THK5351 ligand binds to both AD- as well as FTLD-tau pathology (Harada et al., 2016; Kikuchi et al., 2016; Ishiki et al., 2017). More specifically, [^{3}H]-THK5351 binding on brain sections highly overlapped with tau lesions identified by immunohistochemistry in a PSP patient (Ishiki et al., 2017) as well as in a CBD patient (Kikuchi et al., 2016). Furthermore, fluorescent staining with THK-5351 overlaps with tau lesions detected with Gallyas-Braak staining in the striatum of a PSP case (Ishiki et al., 2017). This is an important difference compared to the first THK compound, i.e. THK523, which did not show binding to FTLD-tauopathies (Fodero-Tavoletti et al., 2014). Slight modifications in the chemical structure of the THK compound enabled

affinity for both 4R and 3R tauopathies. At the imaging level, several studies demonstrated elevated [^{18}F]-THK5351 binding in disease-specific regions in AD, PSP, and CBD (Harada et al., 2016; Kikuchi et al., 2016; Ishiki et al., 2017). However, no guidelines for visual interpretation of tau PET images have been defined yet. At this point, besides promising results in different patient populations, tau PET imaging has not yet been approved for clinical use. Before regulatory approval of a PET tracer, high numbers of patients need to be scanned in an open-label, nonrandomized, multicenter study with monitoring of adverse events. Furthermore, a comparison between *in vivo* PET imaging with *post mortem* histopathology in end-of life patients needs to be performed (Sabri et al., 2015). In this way, sensitivity and specificity values against clinical or *post mortem* diagnosis as standard-of-truth can be established. Once tau PET becomes clinically approved, an interesting alternative approach for visual interpretation would be to apply support vector machines to classify subjects automatically into a high or low uptake group based on their tau PET uptake pattern (Passamonti et al., 2017). To this end, a classifier must first be trained to extract the discriminating features by using a large dataset of independent cases. This step might however raise some problems due to the low prevalence of PPA in the general population (Johnson et al., 2005). Nonetheless, once a sufficient number of scans can be reached, the classifier can be used to assess subsequent images of individual PPA patients without the subjective interpretation of a human observer, offering a potential aid in an unbiased diagnosis.

An important issue regarding the current generation of tau PET tracers remains: non-specific binding. [^{18}F]-AV-1451, but not [^{18}F]-THK5351, binds to the choroid plexus (Ikonomovic et al., 2016), which complicates visual assessment of neighboring areas such as the hippocampal complex (Johnson et al., 2016). High binding in the basal ganglia, which is present in all tau PET tracers including [^{18}F]-AV-1451 (Marquié et al., 2015; Lowe et al., 2016; Passamonti et al., 2017) and [^{18}F]-THK5351 (Harada et al., 2016) keeps researchers puzzled. Similar to these previous reports, we observed high [^{18}F]-THK5351 binding in the basal ganglia in all groups (Fig. 7.2A). However, age correlated only in the control group with a cluster localized to the basal ganglia and the anterior and posterior hippocampus including the entorhinal cortex (Fig. 7.2B,C). Binding to the latter region is in accordance with *post mortem* studies in which tau accumulation associated with aging is observed in the entorhinal cortex (Price and Morris, 1999). The binding pattern in the basal ganglia has been attributed by some studies to neuromelanin rather than to age-related tauopathy (Marquié et al., 2015; Lowe et al., 2016).

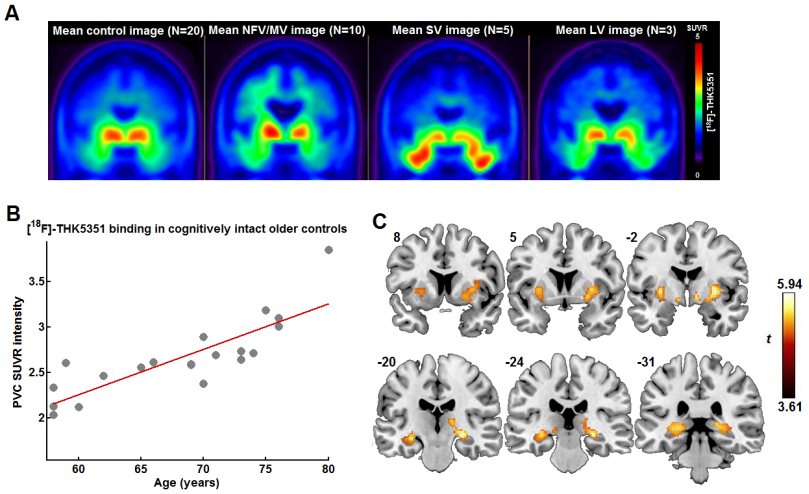


Figure 7.2: **Non-specific and age-related binding of [^{18}F]-THK5351**.
(A) Non-specific binding in the basal ganglia is present in all groups, **(B)** Correlation between age on the abscissa and [^{18}F]-THK5351 binding expressed as partial volume corrected (PVC) SUVR intensity values in the basal ganglia/hippocampus on the ordinate, **(C)** T maps of the correlation between age and [^{18}F]-THK5351 binding are projected on coronal slices (Rorden et al., 2007) with corresponding MNI coordinates in the left upper corner at a voxel-level uncorrected $p<0.001$, with a cluster-level family wise error (FWE)-corrected threshold $p<0.05$. LV: logopenic variant, MV: mixed variant, NFV: nonfluent variant, SV: semantic variant PPA patients.

This hypothesis has however been questioned by a recent study, which showed absence of neuromelanin-containing cells in the basal ganglia, indicating that off-target binding to neuromelanin is an insufficient explanation of tau PET tracer binding in this region (Passamonti et al., 2017). It has also been suggested that off-target binding might be predominantly associated with TDP-43 pathology which has been observed in SV PPA (Bevan-Jones et al., 2017). To date, no similar *ex vivo* study has been published regarding the characterization of [^{18}F]-THK5351 off-target binding. Furthermore, the [^{18}F]-THK5351 binding patterns shown in the present study do not necessarily generalize to other radioligands.

Consistent with previous tau PET studies (Ossenkoppele et al., 2016; Xia et al., 2017; Nasrallah et al., 2017; Phillips et al., 2017), we demonstrated in chapter 5 that increased [^{18}F]-THK5351 binding was associated with core clinical features of MV PPA. Interestingly, this correlation was only present for [^{18}F]-THK5351 PET binding but not for atrophy. More specifically, speech apraxia measures correlated with elevated [^{18}F]-THK5351 binding in the premotor cortex and SMA, which are regions associated with AOS (Josephs et al., 2012, 2013b). The severity of AOS has been linked with premotor cortical involvement (Whitwell et al., 2013). The single-word comprehension deficits were correlated with [^{18}F]-THK5351 binding in the basal ganglia. This region would mainly relate to a particular aspect of single-word comprehension deficits, i.e. involving meaning dominance effects (Grindrod et al., 2014). A role of the basal ganglia (left head of caudate) has been demonstrated in suppressing irrelevant words (Ali et al., 2010). Other studies suggest a circumscribed deficit in the selective attentional engagement of the semantic network on the basis of meaning frequency, possibly implicating a disturbance of frontal-subcortical systems influencing inhibitory semantic mechanisms (Copland, 2003). The single-word comprehension deficit in MV PPA might also be due to impaired semantic control resulting from tau burden or atrophy in the MTG (Adamczuk et al., 2014) or IFG (Liuzzi et al., 2017). The latter region is connected through the uncinate fascicle with the ATL, which is involved in the 'storage' of semantic knowledge (Jefferies and Lambon Ralph, 2006; Jackson et al., 2016). Another possible interpretation is that single-word comprehension deficits in MV PPA may partly be due to tau-related damage to white matter tracts, which contribute to functional effects at a distance.

Longitudinal follow-up and further validation against the gold standard of *post mortem* examination are needed to assess the sensitivity and specificity of tau PET. The application of PET scans is a high-cost investigation, and it is therefore important to clearly demonstrate its accuracy and to standardize the process of diagnostic modality prior to clinical availability. One of the newer tau PET ligands, [^{18}F]-MK-6240 (Walji et al., 2016), shows no off-target binding in the basal ganglia, which makes it one of the most promising tracers at the moment.

7.2.2 Cholinergic PET

Among all PPA variants, LV PPA showed the strongest reduction in AChE in the neocortex, although we did not find a correlation with

BF volume loss. Theoretically speaking, given that the midpontine nuclei are an alternative source of acetycholine (Pepeu and Grazia Giovannini, 2017), degeneration of these nuclei could possibly account for the observed cholinergic depletion in LV. We consider this however unlikely as the group-based contrasts between LV PPA and controls did not reveal atrophy of midpontine cholinergic nuclei, consistent with previous findings in typical AD (Woolf et al., 1989). This can be a genuine finding or due to the lower sensitivity of the T_1-weighted structural MRI sequence in that region. Moreover, cholinergic depletion was mainly present in neocortical regions, which suggests no or only a minor contribution from efferents originating from the midpontine cholinergic nuclei as these nuclei project to the thalamus, hypothalamus, globus pallidus and the BF (Hallanger and Wainer, 1988).

BF volume loss in SV PPA was not associated with cholinergic depletion. We hypothesize that at the microscopic level, the nuclei and neuronal populations that are affected in SV PPA in this region differ from those affected in AD, in which BF volume loss is associated with cholinergic depletion (Wood et al., 1983). An investigation at the pathological level will provide the necessary resolution to test this hypothesis. If we consider patients with mild cognitive impairment (DeKosky et al., 2002), it has been suggested that the upregulation of hippocampal ChAT may be due to the replacement of denervated glutamatergic synapses by cholinergic input arising from the septum (Mufson et al., 2008). This is emphasized by animal experimental studies demonstrating reactive sprouting in the hippocampus following perforant path transsections in rats (Savaskan and Nitsch, 2001). We hypothesize that a similar compensatory mechanism may occur in SV PPA in the amygdaloid complex and hippocampus (Tan et al., 2014).

7.3 Therapeutic interventions

The data presented in chapter 3 and 4 of this thesis together with other recent acoustic studies in PPA (Fletcher et al., 2013b, 2015; Golden et al., 2016; Hardy et al., 2017b) give grounds for a more general, systematic and principled re-examination of sound-based therapies for PPA. If we consider studies in nonfluent aphasia due to stroke, these patients show benefits of singing including strengthened breathing and vocal ability, improved articulation and prosody of speech, and increased verbal and nonverbal communicative behaviors (Tomaino, 2012). Singing activates right-lateralized regions including the STG, inferior central

operculum, and IFG (Özdemir et al., 2006). These right-hemispheric regions are initially spared in NFV PPA but might be affected as the disease progresses (Rogalski et al., 2011b). Patients with nonfluent aphasia due to stroke show some recovery due to the brains potential of neuroplasticity (Marsh and Hillis, 2006). In NFV PPA, due to its progressive neurodegenerative nature, neuroplasticity ultimately fails to compensate for the structural changes (Vandenbulcke et al., 2005). Therefore, musical therapy is predicted to be only partly beneficial, at least when applied early in the disease course. Of note is that one study reported that NFV PPA patients show decreased musical activity (Midorikawa et al., 2017), which makes musical therapy challenging in some cases. By contrast, patients with SV PPA show increased craving for music (i.e. musicophilia) (Fletcher et al., 2015).
Repetitive transcranial magnetic stimulation (rTMS) might be an alternative therapeutic approach to ameliorate language and speech in PPA. rTMS improved naming accuracy (Small and Llano, 2009) and when delivered over the DLPFC, it could improve language in PPA by enhancing long-term potentiation and synaptic plasticity within the stimulated and interconnected areas involved in the language and speech network (Trebbastoni et al., 2013). Another stimulation technique, transcranial direct current stimulation (tDCS) applied in patients with PPA showed improvements in global language performance, grammatical comprehension and semantic processing (McConathey et al., 2017). Sustained improvements in naming accuracy suggest that the current intervention approach is viable (Hung et al., 2017). Based on our findings, stimulation over the frontal operculum may potentially improve the clinical symptoms in NFV PPA.

In chapter 6, we showed that in a subset of LV, there is a rationale for cholinomimetic treatment. One study in PPA with an open-label period of 18 weeks and a randomized, placebo-controlled phase for eight weeks with galantamine (Kertesz et al., 2008) reported that overall language performance showed a trend towards stabilization over a total duration of eight weeks. Another randomized, placebo-controlled study with memantine showed general good tolerance (Boxer et al., 2013). By contrast, one study of donepezil treatment in FTD patients, failed to show any efficacy and a subgroup of patients experienced worsening of symptoms (Mendez, 2009).
Currently, cholinesterase inhibitors (e.g., galantamine, rivastigmine, and donepezil) and memantine may be prescribed off-label in clinical practice for PPA patients who are amyloid-positive. AChE-PET allows one to directly discriminate PPA cases with a cholinergic deficit from those

without a cholinergic deficit. This distinction could possibly predict a therapeutic response, but this remains to be demonstrated.

Lessons from clinical trials with amyloid-lowering drugs have demonstrated the importance of amyloid PET imaging in patient selection and monitoring of drug target engagement (Vandenberghe et al., 2013, 2016). Likewise, tau PET tracers including those discussed in this thesis, may also prove to be of great utility in clinical therapeutic trial design of disease-modifying treatments targeting tau aggregates. As long as a TDP-43 tracer is lacking, highly specific tau PET tracers might help to discriminate underlying tauopathy from TDP-43 in patients with PPA. Currently, ongoing preclinical and clinical therapeutic trials assessing tau-modifying compounds show great promise (for review: Tsai and Boxer (2014)) and encourage further research on truly-disease modifying therapeutics for PPA.

Bibliography

Ackermann, H. and Riecker, A. (2004). The contribution of the insula to motor aspects of speech production: a review and a hypothesis. *Brain and language*, 89(2):320–8.

Adamczuk, K., a. S. De Weer, Nelissen, N., Dupont, P., Sunaert, S., Bettens, K., Sleegers, K., Van Broeckhoven, C., Van Laere, K., and Vandenberghe, R. (2014). Functional Changes in the Language Network in Response to Increased Amyloid Deposition in Cognitively Intact Older Adults. *Cerebral Cortex*, pages 1–16.

Adamczuk, K., De Weer, A. S., Nelissen, N., Chen, K., Sleegers, K., Bettens, K., Van Broeckhoven, C., Vandenbulcke, M., Thiyyagura, P., Dupont, P., Van Laere, K., Reiman, E. M., and Vandenberghe, R. (2013). Polymorphism of brain derived neurotrophic factor influences ?? amyloid load in cognitively intact apolipoprotein e ??4 carriers. *NeuroImage: Clinical*, 2:512–520.

Adamczuk, K., Schaeverbeke, J., Nelissen, N., Neyens, V., Vandenbulcke, M., Goffin, K., Lilja, J., Hilven, K., Dupont, P., Van Laere, K., and Vandenberghe, R. (2016). Amyloid imaging in cognitively normal older adults: comparison between 18F-flutemetamol and 11C-Pittsburgh compound B. *European Journal of Nuclear Medicine and Molecular Imaging*, 43(1):142–151.

Adamczuk, K., Schaeverbeke, J., Vanderstichele, H. M. J., Lilja, J., Nelissen, N., Van Laere, K., Dupont, P., Hilven, K., Poesen, K., and Vandenberghe, R. (2015). Diagnostic value of cerebrospinal fluid A? ratios in preclinical Alzheimer?s disease. *Alzheimer's Research & Therapy*, 7(1):75.

Adeli, A., Whitwell, J. L., Duffy, J. R., Strand, E. A., and Josephs, K. A. (2013). Ideomotor apraxia in agrammatic and logopenic variants of primary progressive aphasia. *Journal of neurology*, 260(6):1594–600.

Aggleton, J. P., Friedman, D. P., and Mishkin, M. (1987). A comparison between the connections of the amygdala and hippocampus with the basal forebrain in the macaque. *Experimental brain research*, 67(3):556–68.

Alario, F.-X., Chainay, H., Lehericy, S., and Cohen, L. (2006). The role of the supplementary motor area (SMA) in word production. *Brain research*, 1076(1):129–43.

Alexoudi, A., Sakas, D., and Gatzonis, S. (2016). The "Ravel issue" and possible implications. *Dementia (London, England)*.

Ali, N., Green, D. W., Kherif, F., Devlin, J. T., and Price, C. J. (2010). The Role of the Left Head of Caudate in Suppressing Irrelevant Words. *Journal of Cognitive Neuroscience*, 22(10):2369–2386.

Allen, E. J., Burton, P. C., Olman, C. A., and Oxenham, A. J. (2017). Representations of Pitch and Timbre Variation in Human Auditory Cortex. *The Journal of Neuroscience*, 37(5):1284–1293.

Amici, S., Ogar, J., Brambati, S. M., Miller, B. L., Neuhaus, J., Dronkers, N. L., and Gorno-Tempini, M. L. (2007). Performance in specific language tasks correlates with regional volume changes in progressive aphasia. *Cognitive and behavioral neurology : official journal of the Society for Behavioral and Cognitive Neurology*, 20(4):203–11.

Arbib, M. A. (2005). From monkey-like action recognition to human language: an evolutionary framework for neurolinguistics. *The Behavioral and brain sciences*, 28(2):105–24; discussion 125–67.

Arendt, T., Bigl, V., Arendt, A., and Tennstedt, A. (1983). Loss of neurons in the nucleus basalis of Meynert in Alzheimer's disease, paralysis agitans and Korsakoff's Disease. *Acta neuropathologica*, 61(2):101–8.

Arima, K. (2006). Ultrastructural characteristics of tau filaments in tauopathies: immuno-electron microscopic demonstration of tau filaments in tauopathies. *Neuropathology : official journal of the Japanese Society of Neuropathology*, 26(5):475–83.

Armstrong, B. C., Tokowicz, N., and Plaut, D. C. (2012). eDom: norming software and relative meaning frequencies for 544 English homonyms. *Behavior research methods*, 44(4):1015–27.

Armstrong, M. J., Litvan, I., Lang, A. E., Bak, T. H., Bhatia, K. P., Borroni, B., Boxer, A. L., Dickson, D. W., Grossman, M., Hallett, M.,

Josephs, K. A., Kertesz, A., Lee, S. E., Miller, B. L., Reich, S. G., Riley, D. E., Tolosa, E., Troster, A. I., Vidailhet, M., and Weiner, W. J. (2013). Criteria for the diagnosis of corticobasal degeneration. *Neurology*, 80(5):496–503.

Ash, S., McMillan, C., Gunawardena, D., Avants, B., Morgan, B., Khan, A., Moore, P., Gee, J., and Grossman, M. (2010). Speech errors in progressive non-fluent aphasia. *Brain and Language*, 113(1):13–20.

Ashburner, J. and Friston, K. J. (2000). Voxel-based morphometry–the methods. *NeuroImage*, 11(6 Pt 1):805–21.

Avants, B., Anderson, C., Grossman, M., and Gee, J. C. (2007). Spatiotemporal normalization for longitudinal analysis of gray matter atrophy in frontotemporal dementia. *Medical image computing and computer-assisted intervention : MICCAI ... International Conference on Medical Image Computing and Computer-Assisted Intervention*, 10(Pt 2):303–10.

Baker, M., Mackenzie, I. R., Pickering-Brown, S. M., Gass, J., Rademakers, R., Lindholm, C., Snowden, J., Adamson, J., Sadovnick, A. D., Rollinson, S., Cannon, A., Dwosh, E., Neary, D., Melquist, S., Richardson, A., Dickson, D., Berger, Z., Eriksen, J., Robinson, T., Zehr, C., Dickey, C. A., Crook, R., McGowan, E., Mann, D., Boeve, B., Feldman, H., and Hutton, M. (2006). Mutations in progranulin cause tau-negative frontotemporal dementia linked to chromosome 17. *Nature*, 442(7105):916–919.

Baker-Nigh, A., Vahedi, S., oetz Davis, E. G., Weintraub, S., Bigio, E. H., Klein, W. L., and Geula, C. (2015). Neuronal amyloid-?? accumulation within cholinergic basal forebrain in ageing and Alzheimer's disease. *Brain : a journal of neurology*, 138:1722–1737.

Ballard, K. J., Savage, S., Leyton, C. E., Vogel, A. P., Hornberger, M., and Hodges, J. R. (2014). Logopenic and nonfluent variants of primary progressive aphasia are differentiated by acoustic measures of speech production. *PloS one*, 9(2):e89864.

Bamiou, D. E., Musiek, F. E., and Luxon, L. M. (2003). The insula (Island of Reil) and its role in auditory processing: Literature review. *Brain Research Reviews*, 42:143–154.

Bamiou, D. E., Musiek, F. E., Stow, I., Stevens, J., Cipolotti, L., Brown, M. M., and Luxon, L. M. (2006). Auditory temporal processing deficits in patients with insular stroke. *Neurology*, 67(4):614–619.

Barnes, J., Ridgway, G. R., Bartlett, J., Henley, S. M. D., Lehmann, M., Hobbs, N., Clarkson, M. J., MacManus, D. G., Ourselin, S., and Fox, N. C. (2010). Head size, age and gender adjustment in MRI studies: a necessary nuisance? *NeuroImage*, 53(4):1244–55.

Bartus, R. T. (2000). On neurodegenerative diseases, models, and treatment strategies: lessons learned and lessons forgotten a generation following the cholinergic hypothesis. *Experimental neurology*, 163(2):495–529.

Bengtsson, S. L., Ullén, F., Ehrsson, H. H., Hashimoto, T., Kito, T., Naito, E., Forssberg, H., and Sadato, N. (2009). Listening to rhythms activates motor and premotor cortices. *Cortex; a journal devoted to the study of the nervous system and behavior*, 45(1):62–71.

Berthier, M. L., Green, C., Higueras, C., Fernández, I., Hinojosa, J., and Martín, M. C. (2006). A randomized, placebo-controlled study of donepezil in poststroke aphasia. *Neurology*, 67(9):1687–9.

Bevan-Jones, W. R., Cope, T. E., Jones, P. S., Passamonti, L., Hong, Y. T., Fryer, T. D., Arnold, R., Allinson, K. S. J., Coles, J. P., Aigbirhio, F. I., Patterson, K., O'Brien, J. T., and Rowe, J. B. (2017). [¹⁸ F]AV-1451 binding in vivo mirrors the expected distribution of TDP-43 pathology in the semantic variant of primary progressive aphasia. *Journal of Neurology, Neurosurgery & Psychiatry*, pages jnnp–2017–316402.

Bierer, L. M., Haroutunian, V., Gabriel, S., Knott, P. J., Carlin, L. S., Purohit, D. P., Perl, D. P., Schmeidler, J., Kanof, P., and Davis, K. L. (1995). Neurochemical correlates of dementia severity in Alzheimer's disease: relative importance of the cholinergic deficits. *Journal of neurochemistry*, 64(2):749–60.

Bigl, V., Arendt, T., Fischer, S., Fischer, S., Werner, M., and Arendt, A. (1987). The cholinergic system in aging. *Gerontology*, 33(3-4):172–80.

Boban, M., Kostovic, I., and Simic, G. (2006). Nucleus subputaminalis: Neglected part of the basal nucleus of Meynert [1]. *Brain*, 129:2005–2006.

Boemio, A., Fromm, S., Braun, A., and Poeppel, D. (2005). Hierarchical and asymmetric temporal sensitivity in human auditory cortices. *Nature neuroscience*, 8(3):389–95.

Bohland, J. W. and Guenther, F. H. (2006). An fMRI investigation of syllable sequence production. *NeuroImage*, 32(2):821–841.

Bohnen, N. I., Kaufer, D. I., Hendrickson, R., Ivanco, L. S., Lopresti, B., Davis, J. G., Constantine, G., Mathis, C. A., Moore, R. Y., and DeKosky, S. T. (2005). Cognitive correlates of alterations in acetylcholinesterase in Alzheimer's disease. *Neuroscience letters*, 380(1-2):127–32.

Bohnen, N. I., Kaufer, D. I., Ivanco, L. S., Lopresti, B., Koeppe, R. A., Davis, J. G., Mathis, C. A., Moore, R. Y., and DeKosky, S. T. (2003). Cortical cholinergic function is more severely affected in parkinsonian dementia than in Alzheimer disease: an in vivo positron emission tomographic study. *Archives of neurology*, 60(12):1745–8.

Boxer, A. L., Knopman, D. S., Kaufer, D. I., Grossman, M., Onyike, C., Graf-Radford, N., Mendez, M., Kerwin, D., Lerner, A., Wu, C.-K., Koestler, M., Shapira, J., Sullivan, K., Klepac, K., Lipowski, K., Ullah, J., Fields, S., Kramer, J. H., Merrilees, J., Neuhaus, J., Mesulam, M. M., and Miller, B. L. (2013). Memantine in patients with frontotemporal lobar degeneration: a multicentre, randomised, double-blind, placebo-controlled trial. *The Lancet Neurology*, 12(2):149–156.

Bozeat, S., Lambon Ralph, M. A., Patterson, K., Garrard, P., and Hodges, J. R. (2000). Non-verbal semantic impairment in semantic dementia. *Neuropsychologia*, 38(9):1207–15.

Bozeat, S., Lambon Ralph, M. A., Patterson, K., and Hodges, J. R. (2002). When objects lose their meaning: what happens to their use? *Cognitive, affective & behavioral neuroscience*, 2(3):236–51.

Bozeat, S., Ralph, M. A. L., Graham, K. S., Patterson, K., Wilkin, H., Rowland, J., Rogers, T. T., and Hodges, J. R. (2003). A duck with four legs: Investigating the structure of conceptual knowledge using picture drawing in semantic dementia. *Cognitive neuropsychology*, 20(1):27–47.

Braak, H., Alafuzoff, I., Arzberger, T., Kretzschmar, H., and Del Tredici, K. (2006a). Staging of Alzheimer disease-associated neurofibrillary pathology using paraffin sections and immunocytochemistry. *Acta neuropathologica*, 112(4):389–404.

Braak, H. and Braak, E. (1991). Neuropathological stageing of Alzheimer-related changes. *Acta neuropathologica*, 82(4):239–59.

Braak, H., Rüb, U., Schultz, C., and Del Tredici, K. (2006b). Vulnerability of cortical neurons to Alzheimer's and Parkinson's diseases. *Journal of Alzheimer's disease : JAD*, 9(3 Suppl):35–44.

Brambati, S. M., Amici, S., Racine, C. A., Neuhaus, J., Miller, Z., Ogar, J., Dronkers, N., Miller, B. L., Rosen, H., and Gorno-Tempini, M. L. (2015). Longitudinal gray matter contraction in three variants of primary progressive aphasia: A tenser-based morphometry study. *NeuroImage. Clinical*, 8:345–55.

Brambati, S. M., Renda, N. C., Rankin, K. P., Rosen, H. J., Seeley, W. W., Ashburner, J., Weiner, M. W., Miller, B. L., and Gorno-Tempini, M. L. (2007). A tensor based morphometry study of longitudinal gray matter contraction in FTD. *NeuroImage*, 35(3):998–1003.

Bruffaerts, R., Dupont, P., Peeters, R., De Deyne, S., Storms, G., and Vandenberghe, R. (2013). Similarity of fMRI activity patterns in left perirhinal cortex reflects semantic similarity between words. *The Journal of neuroscience : the official journal of the Society for Neuroscience*, 33(47):18597–607.

Burke, S. N. and Barnes, C. A. (2006). Neural plasticity in the ageing brain. *Nature reviews. Neuroscience*, 7(1):30–40.

Catani, M. and Ffytche, D. H. (2005). The rises and falls of disconnection syndromes. *Brain : a journal of neurology*, 128(Pt 10):2224–39.

Catani, M., Mesulam, M. M., Jakobsen, E., Malik, F., Martersteck, A., Wieneke, C., Thompson, C. K., Thiebaut De Schotten, M., Dell'Acqua, F., Weintraub, S., and Rogalski, E. (2013). A novel frontal pathway underlies verbal fluency in primary progressive aphasia. *Brain*, 136:2619–2628.

Chan, D., Anderson, V., Pijnenburg, Y., Whitwell, J., Barnes, J., Scahill, R., Stevens, J. M., Barkhof, F., Scheltens, P., Rossor, M. N., and Fox, N. C. (2009). The clinical profile of right temporal lobe atrophy. *Brain*, 132(5):1287–1298.

Chen, J. L., Penhune, V. B., and Zatorre, R. J. (2008). Listening to Musical Rhythms Recruits Motor Regions of the Brain. *Cerebral Cortex*, 18(12):2844–2854.

Chi, T., Gao, Y., Guyton, M. C., Ru, P., and Shamma, S. (1999). Spectro-temporal modulation transfer functions and speech intelligibility. *The Journal of the Acoustical Society of America*, 106(5):2719–32.

Chien, D. T., Bahri, S., Szardenings, A. K., Walsh, J. C., Mu, F., Su, M. Y., Shankle, W. R., Elizarov, A., and Kolb, H. C. (2013). Early

Clinical PET Imaging Results with the Novel PHF-Tau Radioligand [F-18]-T807. *Journal of Alzheimer's Disease*, 34(2):457–468.

Cho, H., Baek, M. S., Choi, J. Y., Lee, S. H., Kim, J. S., Ryu, Y. H., Lee, M. S., and Lyoo, C. H. (2017). ¹⁸ F-AV-1451 binds to motor-related subcortical gray and white matter in corticobasal syndrome. *Neurology*, 89(11):1170–1178.

Chomsky, N. (2017). Language architecture and its import for evolution. *Neuroscience & Biobehavioral Reviews*.

Cope, T. E., Grube, M., Singh, B., Burn, D. J., and Griffiths, T. D. (2014). The basal ganglia in perceptual timing: timing performance in Multiple System Atrophy and Huntington's disease. *Neuropsychologia*, 52:73–81.

Copland, D. (2003). The basal ganglia and semantic engagement: Potential insights from semantic priming in individuals with subcortical vascular lesions, Parkinson's disease, and cortical lesions. *Journal of the International Neuropsychological Society*, 9(07):1041–52.

Coull, J. T. (2004). fMRI studies of temporal attention: allocating attention within, or towards, time. *Cognitive Brain Research*, 21(2):216–226.

Crawford, J. R. and Garthwaite, P. H. (2006). Comparing patients' predicted test scores from a regression equation with their obtained scores: a significance test and point estimate of abnormality with accompanying confidence limits. *Neuropsychology*, 20(3):259–71.

Crawford, J. R. and Howell, D. C. (1998). Comparing an Individual ' s Test Score Against Norms Derived from Small Samples. *Clinical Neuropsychologist*, 12(February 2014):482–486.

Cross, E. S. and Burke, D. M. (2004). Do alternative names block young and older adults' retrieval of proper names? *Brain and Language*, 89(1):174–181.

Cruts, M., Gijselinck, I., Van Langenhove, T., van der Zee, J., and Van Broeckhoven, C. (2013). Current insights into the C9orf72 repeat expansion diseases of the FTLD/ALS spectrum. *Trends in Neurosciences*, 36(8):450–459.

De Deyne, S., Navarro, D. J., and Storms, G. (2013). Better explanations of lexical and semantic cognition using networks derived from continued rather than single-word associations. *Behavior research methods*, 45(2):480–98.

Degé, F. and Schwarzer, G. (2011). The Effect of a Music Program on Phonological Awareness in Preschoolers. *Frontiers in Psychology*, 2:124.

DeKosky, S. T., Ikonomovic, M. D., Styren, S. D., Beckett, L., Wisniewski, S., Bennett, D. A., Cochran, E. J., Kordower, J. H., and Mufson, E. J. (2002). Upregulation of choline acetyltransferase activity in hippocampus and frontal cortex of elderly subjects with mild cognitive impairment. *Annals of neurology*, 51(2):145–55.

Dickerson, B. C. (2012). Quantitating Severity and Progression in Primary Progressive Aphasia. *Journal of Molecular Neuroscience*, 45(3):618–628.

Dickson, D. W. (1999). Neuropathologic differentiation of progressive supranuclear palsy and corticobasal degeneration. *Journal of neurology*, 246 Suppl:II6–15.

Dickson, D. W., Bergeron, C., Chin, S. S., Duyckaerts, C., Horoupian, D., Ikeda, K., Jellinger, K., Lantos, P. L., Lippa, C. F., Mirra, S. S., Tabaton, M., Vonsattel, J. P., Wakabayashi, K., and Litvan, I. (2002). Office of Rare Diseases neuropathologic criteria for corticobasal degeneration. *Journal of neuropathology and experimental neurology*, 61(11):935–46.

Dronkers, N. F. (1996). A new brain region for coordinating speech articulation. *Nature*, 384(6605):159–61.

Drullman, R. (1995). Temporal envelope and fine structure cues for speech intelligibility. *The Journal of the Acoustical Society of America*, 97(1):585–92.

Elliott, T. M. and Theunissen, F. E. (2009). The modulation transfer function for speech intelligibility. *PLoS computational biology*, 5(3):e1000302.

Federmeier, K. D., Van Petten, C., Schwartz, T. J., and Kutas, M. (2003). Sounds, words, sentences: age-related changes across levels of language processing. *Psychology and aging*, 18(4):858–72.

Ferrandez, A. M., Hugueville, L., Lehéricy, S., Poline, J. B., Marsault, C., and Pouthas, V. (2003). Basal ganglia and supplementary motor area subtend duration perception: an fMRI study. *NeuroImage*, 19(4):1532–44.

Ferris, S. H. and Farlow, M. (2013). Language impairment in Alzheimer's disease and benefits of acetylcholinesterase inhibitors. *Clinical interventions in aging*, 8:1007–14.

Fiez, J. A., Tranel, D., Seager-Frerichs, D., and Damasio, H. (2006). Specific reading and phonological processing deficits are associated with damage to the left frontal operculum. *Cortex; a journal devoted to the study of the nervous system and behavior*, 42(4):624–43.

Fletcher, P. D., Downey, L. E., Agustus, J. L., Hailstone, J. C., Tyndall, M. H., Cifelli, A., Schott, J. M., Warrington, E. K., and Warren, J. D. (2013a). Agnosia for accents in primary progressive aphasia. *Neuropsychologia*, 51(9):1709–15.

Fletcher, P. D., Downey, L. E., Golden, H. L., Clark, C. N., Slattery, C. F., Paterson, R. W., Schott, J. M., Rohrer, J. D., Rossor, M. N., and Warren, J. D. (2015). Auditory hedonic phenotypes in dementia: A behavioural and neuroanatomical analysis. *Cortex*, 67:95–105.

Fletcher, P. D., Downey, L. E., Witoonpanich, P., and Warren, J. D. (2013b). The brain basis of musicophilia: evidence from frontotemporal lobar degeneration. *Frontiers in psychology*, 4:347.

Fodero-Tavoletti, M. T., Furumoto, S., Taylor, L., McLean, C. A., Mulligan, R. S., Birchall, I., Harada, R., Masters, C. L., Yanai, K., Kudo, Y., Rowe, C. C., Okamura, N., and Villemagne, V. L. (2014). Assessing THK523 selectivity for tau deposits in Alzheimer's disease and non-Alzheimer's disease tauopathies. *Alzheimer's research & therapy*, 6(1):11.

Foxe, D., Leyton, C. E., Hodges, J. R., Burrell, J. R., Irish, M., and Piguet, O. (2016). The neural correlates of auditory and visuospatial span in logopenic progressive aphasia and Alzheimer's disease. *Cortex*, 83:39–50.

Foxe, D. G., Irish, M., Hodges, J. R., and Piguet, O. (2013). Verbal and visuospatial span in logopenic progressive aphasia and Alzheimer's disease. *Journal of the International Neuropsychological Society : JINS*, 19(3):247–53.

Foxton, J. M., Dean, J. L., Gee, R., Peretz, I., and Griffiths, T. D. (2004). Characterization of deficits in pitch perception underlying 'tone deafness'. *Brain : a journal of neurology*, 127(Pt 4):801–10.

Foxton, J. M., Talcott, J. B., Witton, C., Brace, H., McIntyre, F., and Griffiths, T. D. (2003). Reading skills are related to global, but not local, acoustic pattern perception. *Nature neuroscience*, 6(4):343–4.

Gainotti, G., Barbier, A., and Marra, C. (2003). Slowly progressive defect in recognition of familiar people in a patient with right anterior temporal atrophy. *Brain : a journal of neurology*, 126(Pt 4):792–803.

Gefen, T., Gasho, K., Rademaker, A., Lalehzari, M., Weintraub, S., Rogalski, E., Wieneke, C., Bigio, E., Geula, C., and Mesulam, M.-M. (2012). Clinically concordant variations of Alzheimer pathology in aphasic versus amnestic dementia. *Brain : a journal of neurology*, 135(Pt 5):1554–65.

Gefen, T., Wieneke, C., Martersteck, A., Whitney, K., Weintraub, S., Mesulam, M.-M., and Rogalski, E. (2013). Naming vs knowing faces in primary progressive aphasia: a tale of 2 hemispheres. *Neurology*, 81(7):658–64.

Geiser, E., Zaehle, T., Jancke, L., and Meyer, M. (2008). The neural correlate of speech rhythm as evidenced by metrical speech processing. *Journal of cognitive neuroscience*, 20(3):541–52.

Gerloff, C., Corwell, B., Chen, R., Hallett, M., and Cohen, L. G. (1997). Stimulation over the human supplementary motor area interferes with the organization of future elements in complex motor sequences. *Brain : a journal of neurology*, pages 1587–602.

Geschwind, N. and Levitsky, W. (1968). Human brain: left-right asymmetries in temporal speech region. *Science (New York, N.Y.)*, 161(3837):186–7.

Giannini, L. A., Irwin, D. J., McMillan, C. T., Ash, S., Rascovsky, K., Wolk, D. A., Van Deerlin, V. M., Lee, E. B., Trojanowski, J. Q., and Grossman, M. (2017). Clinical marker for Alzheimer disease pathology in logopenic primary progressive aphasia. *Neurology*, 88(24):2276–2284.

Gil-Navarro, S., Lladó, A., Rami, L., Castellví, M., Bosch, B., Bargalló, N., Lomeña, F., Reñé, R., Montagut, N., Antonell, A., Molinuevo, J. L., and Sánchez-Valle, R. (2013). Neuroimaging and biochemical markers in the three variants of primary progressive aphasia. *Dementia and geriatric cognitive disorders*, 35(1-2):106–17.

Gillebert, C. R., Schaeverbeke, J., Bastin, C., Neyens, V., Bruffaerts, R., De Weer, A.-S., Seghers, A., Sunaert, S., Van Laere, K., Versijpt,

J., Vandenbulcke, M., Salmon, E., Todd, J. T., Orban, G. A., and Vandenberghe, R. (2015). 3D Shape Perception in Posterior Cortical Atrophy: A Visual Neuroscience Perspective. *The Journal of neuroscience : the official journal of the Society for Neuroscience*, 35(37):12673–92.

Giraud, A.-L. and Poeppel, D. (2012). Cortical oscillations and speech processing: emerging computational principles and operations. *Nature Neuroscience*, 15(4):511–517.

Gliebus, G., Bigio, E. H., Gasho, K., Mishra, M., Caplan, D., Mesulam, M.-M., and Geula, C. (2010). Asymmetric TDP-43 distribution in primary progressive aphasia with progranulin mutation. *Neurology*, 74(20):1607–10.

Golden, H. L., Clark, C. N., Nicholas, J. M., Cohen, M. H., Slattery, C. F., Paterson, R. W., Foulkes, A. J., Schott, J. M., Mummery, C. J., Crutch, S. J., and Warren, J. D. (2016). Music Perception in Dementia. *Journal of Alzheimer's Disease*, 55(3):933–949.

Goll, J. C., Crutch, S. J., Loo, J. H. Y., Rohrer, J. D., Frost, C., Bamiou, D. E., and Warren, J. D. (2010). Non-verbal sound processing in the primary progressive aphasias. *Brain*, 133:272–285.

Goll, J. C., Kim, L. G., Hailstone, J. C., Lehmann, M., Buckley, A., Crutch, S. J., and Warren, J. D. (2011). Auditory object cognition in dementia. *Neuropsychologia*, 49(9):2755–65.

Gordon, B. A., Zacks, J. M., Blazey, T., Benzinger, T. L. S., Morris, J. C., Fagan, A. M., Holtzman, D. M., and Balota, D. A. (2015). Task-evoked fMRI changes in attention networks are associated with preclinical Alzheimer's disease biomarkers. *Neurobiology of aging*, 36(5):1771–9.

Gorno-Tempini, M. L., Brambati, S. M., Ginex, V., Ogar, J., Dronkers, N. F., Marcone, A., Perani, D., Garibotto, V., Cappa, S. F., and Miller, B. L. (2008). The logopenic/phonological variant of primary progressive aphasia. *Neurology*, 71(16):1227–34.

Gorno-Tempini, M. L., Dronkers, N. F., Rankin, K. P., Ogar, J. M., Phengrasamy, L., Rosen, H. J., Johnson, J. K., Weiner, M. W., and Miller, B. L. (2004a). Cognition and anatomy in three variants of primary progressive aphasia. *Annals of neurology*, 55(3):335–46.

Gorno-Tempini, M. L., Hillis, a. E., Weintraub, S., Kertesz, a., Mendez, M., Cappa, S. F., Ogar, J. M., Rohrer, J. D., Black, S., Boeve,

B. F., Manes, F., Dronkers, N. F., Vandenberghe, R., Rascovsky, K., Patterson, K., Miller, B. L., Knopman, D. S., Hodges, J. R., Mesulam, M. M., and Grossman, M. (2011). Classification of primary progressive aphasia and its variants. *Neurology*, 76:1–10.

Gorno-Tempini, M. L., Murray, R. C., Rankin, K. P., Weiner, M. W., and Miller, B. L. (2004b). Clinical, cognitive and anatomical evolution from nonfluent progressive aphasia to corticobasal syndrome: a case report. *Neurocase*, 10(6):426–36.

Grahn, J. A. and Brett, M. (2007). Rhythm and beat perception in motor areas of the brain. *Journal of cognitive neuroscience*, 19(5):893–906.

Grahn, J. A. and Rowe, J. B. (2013). Finding and feeling the musical beat: striatal dissociations between detection and prediction of regularity. *Cerebral cortex (New York, N.Y. : 1991)*, 23(4):913–21.

Griffiths, T. D. (2008). Tone deafness: a model complex cortical phenotype. *Clinical medicine (London, England)*, 8(6):592–5.

Griffiths, T. D., Johnsrude, I., Dean, J. L., and Green, G. G. (1999). A common neural substrate for the analysis of pitch and duration pattern in segmented sound? *Neuroreport*, 10(18):3825–30.

Griffiths, T. D., Rees, A., Witton, C., Cross, P. M., Shakir, R. A., and Green, G. G. (1997). Spatial and temporal auditory processing deficits following right hemisphere infarction. A psychophysical study. *Brain : a journal of neurology*, 120 (Pt 5:785–94.

Griffiths, T. D. and Warren, J. D. (2002). The planum temporale as a computational hub. *Trends in neurosciences*, 25(7):348–53.

Grindrod, C. M., Garnett, E. O., Malyutina, S., and den Ouden, D. B. (2014). Effects of representational distance between meanings on the neural correlates of semantic ambiguity. *Brain and language*, 139:23–35.

Grossman, M. (2010). Primary progressive aphasia: clinicopathological correlations. *Nature reviews. Neurology*, 6(2):88–97.

Grossman, M. (2012). The non-fluent/agrammatic variant of primary progressive aphasia. *The Lancet Neurology*, 11(6):545–555.

Grossman, M. and Ash, S. (2004). Primary Progressive Aphasia: A Review. *Neurocase*, 10(1):3–18.

Grossman, M., Mickanin, J., Onishi, K., Hughes, E., D'Esposito, M., Ding, X.-S., Alavi, A., and Reivich, M. (1996). Progressive Nonfluent Aphasia: Language, Cognitive, and PET Measures Contrasted with Probable Alzheimer's Disease. *Journal of Cognitive Neuroscience*, 8(2):135–154.

Grothe, M., Heinsen, H., and Teipel, S. J. (2012). Atrophy of the cholinergic basal forebrain over the adult age range and in early stages of Alzheimer's disease. *Biological Psychiatry*, 71(9):805–813.

Grothe, M. J., Schuster, C., Bauer, F., Heinsen, H., Prudlo, J., and Teipel, S. J. (2014). Atrophy of the cholinergic basal forebrain in dementia with Lewy bodies and Alzheimer's disease dementia. *Journal of neurology*, 261(10):1939–48.

Grover, V. P. B., Tognarelli, J. M., Crossey, M. M. E., Cox, I. J., Taylor-Robinson, S. D., and McPhail, M. J. W. (2015). Magnetic Resonance Imaging: Principles and Techniques: Lessons for Clinicians. *Journal of clinical and experimental hepatology*, 5(3):246–55.

Grube, M., Bruffaerts, R., Schaeverbeke, J., Neyens, V., De Weer, A.-S., Seghers, A., Bergmans, B., Dries, E., Griffiths, T. D., and Vandenberghe, R. (2016). Core auditory processing deficits in primary progressive aphasia. *Brain*, 139(6):1817–1829.

Grube, M., Cooper, F. E., Chinnery, P. F., and Griffiths, T. D. (2010). Dissociation of duration-based and beat-based auditory timing in cerebellar degeneration. *Proceedings of the National Academy of Sciences of the United States of America*, 107(25):11597–601.

Grube, M., Cooper, F. E., and Griffiths, T. D. (2013). Auditory temporal-regularity processing correlates with language and literacy skill in early adulthood. *Cognitive neuroscience*, 4(3-4):225–30.

Grube, M., Cooper, F. E., Kumar, S., Kelly, T., and Griffiths, T. D. (2014). Exploring the role of auditory analysis in atypical compared to typical language development. *Hearing Research*, 308:129–140.

Grube, M. and Griffiths, T. D. (2009). Metricality-enhanced temporal encoding and the subjective perception of rhythmic sequences. *Cortex; a journal devoted to the study of the nervous system and behavior*, 45(1):72–9.

Grube, M., Kumar, S., Cooper, F. E., Turton, S., and Griffiths, T. D. (2012). Auditory sequence analysis and phonological skill. *Proceedings. Biological sciences*, 279(1746):4496–504.

Guenther, F. H. and Hickok, G. (2015). Role of the auditory system in speech production. In *Handbook of clinical neurology*, volume 129, pages 161–175.

Hailstone, J. C., Ridgway, G. R., Bartlett, J. W., Goll, J. C., Buckley, A. H., Crutch, S. J., and Warren, J. D. (2011). Voice processing in dementia: a neuropsychological and neuroanatomical analysis. *Brain : a journal of neurology*, 134(Pt 9):2535–47.

Hall, B., Mak, E., Cervenka, S., Aigbirhio, F. I., Rowe, J. B., and O'Brien, J. T. (2017). In vivo tau PET imaging in dementia: Pathophysiology, radiotracer quantification, and a systematic review of clinical findings. *Ageing Research Reviews*, 36:50–63.

Hall, H., Reyes, S., Landeck, N., Bye, C., Leanza, G., Double, K., Thompson, L., Halliday, G., and Kirik, D. (2014). Hippocampal Lewy pathology and cholinergic dysfunction are associated with dementia in Parkinson's disease. *Brain : a journal of neurology*.

Hallanger, A. E. and Wainer, B. H. (1988). Ascending projections from the pedunculopontine tegmental nucleus and the adjacent mesopontine tegmentum in the rat. *The Journal of comparative neurology*, 274(4):483–515.

Harada, R., Okamura, N., Furumoto, S., Furukawa, K., Ishiki, A., Tomita, N., Tago, T., Hiraoka, K., Watanuki, S., Shidahara, M., Miyake, M., Ishikawa, Y., Matsuda, R., Inami, A., Yoshikawa, T., Funaki, Y., Iwata, R., Tashiro, M., Yanai, K., Arai, H., and Kudo, Y. (2016). 18F-THK5351: A Novel PET Radiotracer for Imaging Neurofibrillary Pathology in Alzheimer Disease. *Journal of nuclear medicine : official publication, Society of Nuclear Medicine*, 57(2):208–14.

Hardy, C. J., Agustus, J. L., Marshall, C. R., Clark, C. N., Russell, L. L., Brotherhood, E. V., Bond, R. L., Fiford, C. M., Ondobaka, S., Thomas, D. L., Crutch, S. J., Rohrer, J. D., and Warren, J. D. (2017a). Functional neuroanatomy of speech signal decoding in primary progressive aphasias. *Neurobiology of Aging*.

Hardy, C. J. D., Agustus, J. L., Marshall, C. R., Clark, C. N., Russell, L. L., Bond, R. L., Brotherhood, E. V., Thomas, D. L., Crutch, S. J., Rohrer, J. D., and Warren, J. D. (2017b). Behavioural and neuroanatomical correlates of auditory speech analysis in primary progressive aphasias. *Alzheimer's Research & Therapy*, 9(1):53.

Harris, J. M., Gall, C., Thompson, J. C., Richardson, A. M. T., Neary, D., du Plessis, D., Pal, P., Mann, D. M. A., Snowden, J. S., and Jones, M. (2013). Classification and pathology of primary progressive aphasia. *Neurology*, 81(21):1832–1839.

Henry, M. L., Wilson, S. M., Babiak, M. C., Mandelli, M. L., Beeson, P. M., Miller, Z. A., and Gorno-Tempini, M. L. (2015). Phonological Processing in Primary Progressive Aphasia. *Journal of cognitive neuroscience*, pages 1–13.

Herdener, M., Lehmann, C., Esposito, F., di Salle, F., Federspiel, A., Bach, D. R., Scheffler, K., and Seifritz, E. (2009). Brain responses to auditory and visual stimulus offset: Shared representations of temporal edges. *Human Brain Mapping*, 30(3):725–733.

Hickok, G. (2009). The functional neuroanatomy of language. *Physics of Life Reviews*, 6(3):121–143.

Hickok, G. and Poeppel, D. (2015). Neural basis of speech perception. *Handbook of clinical neurology*, 129:149–60.

Hirano, S., Shinotoh, H., Kobayashi, T., Tsuboi, Y., Wszolek, Z. K., Aotsuka, A., Tanaka, N., Ota, T., Fukushi, K., Tanada, S., and Irie, T. (2006). Brain acetylcholinesterase activity in FTDP-17 studied by PET. *Neurology*, 66(8):1276–7.

Hirano, S., Shinotoh, H., Shimada, H., Aotsuka, A., Tanaka, N., Ota, T., Sato, K., Ito, H., Kuwabara, S., Fukushi, K., Irie, T., and Suhara, T. (2010). Cholinergic imaging in corticobasal syndrome, progressive supranuclear palsy and frontotemporal dementia. *Brain : a journal of neurology*, 133(Pt 7):2058–68.

Hodges, J. R., Mitchell, J., Dawson, K., Spillantini, M. G., Xuereb, J. H., McMonagle, P., Nestor, P. J., and Patterson, K. (2010). Semantic dementia: demography, familial factors and survival in a consecutive series of 100 cases. *Brain : a journal of neurology*, 133(Pt 1):300–6.

Hodges, J. R. and Patterson, K. (2007). Semantic dementia: a unique clinicopathological syndrome. *The Lancet. Neurology*, 6(11):1004–14.

Hodges, J. R., Patterson, K., Oxbury, S., and Funnell, E. (1992). Semantic dementia. Progressive fluent aphasia with temporal lobe atrophy. *Brain : a journal of neurology*, 115 (Pt 6:1783–806.

Hsieh, S., Hornberger, M., Piguet, O., and Hodges, J. R. (2011). Neural basis of music knowledge: evidence from the dementias. *Brain : a journal of neurology*, 134(Pt 9):2523–34.

Hsieh, S., Hornberger, M., Piguet, O., and Hodges, J. R. (2012). Brain correlates of musical and facial emotion recognition: evidence from the dementias. *Neuropsychologia*, 50(8):1814–22.

Hung, J., Bauer, A., Grossman, M., Hamilton, R. H., Coslett, H. B., and Reilly, J. (2017). Semantic Feature Training in Combination with Transcranial Direct Current Stimulation (tDCS) for Progressive Anomia. *Frontiers in Human Neuroscience*, 11:253.

Hutsler, J. J. and Gazzaniga, M. S. (1991). Acetylcholinesterase staining in human auditory and language cortices: regional variation of structural features. *Cerebral cortex (New York, N.Y. : 1991)*, 6(2):260–70.

Hyman, B. T., Phelps, C. H., Beach, T. G., Bigio, E. H., Cairns, N. J., Carrillo, M. C., Dickson, D. W., Duyckaerts, C., Frosch, M. P., Masliah, E., Mirra, S. S., Nelson, P. T., Schneider, J. A., Thal, D. R., Thies, B., Trojanowski, J. Q., Vinters, H. V., and Montine, T. J. (2012). National Institute on Aging-Alzheimer's Association guidelines for the neuropathologic assessment of Alzheimer's disease. *Alzheimer's & dementia : the journal of the Alzheimer's Association*, 8(1):1–13.

Iaccarino, L., Crespi, C., Della Rosa, P. A., Catricalà, E., Guidi, L., Marcone, A., Tagliavini, F., Magnani, G., Cappa, S. F., and Perani, D. (2015). The Semantic Variant of Primary Progressive Aphasia: Clinical and Neuroimaging Evidence in Single Subjects. *PLOS ONE*, 10(3):e0120197.

Ikonomovic, M. D., Abrahamson, E. E., Price, J. C., Mathis, C. A., and Klunk, W. E. (2016). [F-18]AV-1451 positron emission tomography retention in choroid plexus: More than "off-target" binding. *Annals of neurology*, 80(2):307–8.

Iqbal, K., Liu, F., and Gong, C.-X. (2015). Tau and neurodegenerative disease: the story so far. *Nature Publishing Group*, 12.

Irie, T., Fukushi, K., Namba, H., Iyo, M., Tamagami, H., Nagatsuka, S., and Ikota, N. (1996). Brain acetylcholinesterase activity: validation of a PET tracer in a rat model of Alzheimer's disease. *Journal of nuclear medicine : official publication, Society of Nuclear Medicine*, 37(4):649–55.

Ishiki, A., Harada, R., Okamura, N., Tomita, N., Rowe, C. C., Villemagne, V. L., Yanai, K., Kudo, Y., Arai, H., Furumoto, S., Tashiro, M., and Furukawa, K. (2017). Tau imaging with

[¹⁸ F]THK-5351 in progressive supranuclear palsy. *European Journal of Neurology*, 24(1):130–136.

Jackson, R. L., Hoffman, P., Pobric, G., and Lambon Ralph, M. A. (2016). The Semantic Network at Work and Rest: Differential Connectivity of Anterior Temporal Lobe Subregions. *The Journal of neuroscience : the official journal of the Society for Neuroscience*, 36(5):1490–501.

Jefferies, E. and Lambon Ralph, M. A. (2006). Semantic impairment in stroke aphasia versus semantic dementia: a case-series comparison. *Brain*, 129(8):2132–2147.

Jentschke, S., Koelsch, S., and Friederici, A. D. (2005). Investigating the Relationship of Music and Language in Children: Influences of Musical Training and Language Impairment. *Annals of the New York Academy of Sciences*, 1060(1):231–242.

Johnson, J. K., Diehl, J., Mendez, M. F., Neuhaus, J., Shapira, J. S., Forman, M., Chute, D. J., Roberson, E. D., Pace-Savitsky, C., Neumann, M., Chow, T. W., Rosen, H. J., Forstl, H., Kurz, A., and Miller, B. L. (2005). Frontotemporal lobar degeneration: demographic characteristics of 353 patients. *Archives of neurology*, 62(6):925–30.

Johnson, K. A., Schultz, A., Betensky, R. A., Becker, J. A., Sepulcre, J., Rentz, D., Mormino, E., Chhatwal, J., Amariglio, R., Papp, K., Marshall, G., Albers, M., Mauro, S., Pepin, L., Alverio, J., Judge, K., Philiossaint, M., Shoup, T., Yokell, D., Dickerson, B., Gomez-Isla, T., Hyman, B., Vasdev, N., and Sperling, R. (2016). Tau positron emission tomographic imaging in aging and early Alzheimer disease. *Annals of neurology*, 79(1):110–9.

Josephs, K. A., Dickson, D. W., Murray, M. E., Senjem, M. L., Parisi, J. E., Petersen, R. C., Jack, C. R., and Whitwell, J. L. (2013a). Quantitative neurofibrillary tangle density and brain volumetric MRI analyses in Alzheimer's disease presenting as logopenic progressive aphasia. *Brain and language*, 127(2):127–34.

Josephs, K. A., Duffy, J. R., Strand, E. A., Machulda, M. M., Senjem, M. L., Lowe, V. J., Jack, C. R., and Whitwell, J. L. (2013b). Syndromes dominated by apraxia of speech show distinct characteristics from agrammatic PPA. *Neurology*, 81(4):337–345.

Josephs, K. A., Duffy, J. R., Strand, E. A., Machulda, M. M., Senjem, M. L., Master, A. V., Lowe, V. J., Jack, C. R., and Whitwell, J. L. (2012). Characterizing a neurodegenerative syndrome: primary

progressive apraxia of speech. *Brain : a journal of neurology*, 135(Pt 5):1522–36.

Josephs, K. A., Duffy, J. R., Strand, E. A., Whitwell, J. L., Layton, K. F., Parisi, J. E., Hauser, M. F., Witte, R. J., Boeve, B. F., Knopman, D. S., Dickson, D. W., Jack, C. R., and Petersen, R. C. (2006a). Clinicopathological and imaging correlates of progressive aphasia and apraxia of speech. *Brain : a journal of neurology*, 129(Pt 6):1385–98.

Josephs, K. A., Duffy, J. R., Strand, E. A., Whitwell, J. L., Layton, K. F., Parisi, J. E., Hauser, M. F., Witte, R. J., Boeve, B. F., Knopman, D. S., Dickson, D. W., Jack, C. R., and Petersen, R. C. (2006b). Clinicopathological and imaging correlates of progressive aphasia and apraxia of speech. *Brain : a journal of neurology*, 129(Pt 6):1385–98.

Josephs, K. A., Stroh, A., Dugger, B., and Dickson, D. W. (2009). Evaluation of subcortical pathology and clinical correlations in FTLD-U subtypes. *Acta neuropathologica*, 118(3):349–58.

Kasashima, S. and Oda, Y. (2003). Cholinergic neuronal loss in the basal forebrain and mesopontine tegmentum of progressive supranuclear palsy and corticobasal degeneration. *Acta neuropathologica*, 105(2):117–24.

Kerbler, G. M., Fripp, J., Rowe, C. C., Villemagne, V. L., Salvado, O., Rose, S., and Coulson, E. J. (2015). Basal forebrain atrophy correlates with amyloid β burden in Alzheimer's disease. *NeuroImage. Clinical*, 7:105–13.

Kertesz, A., Morlog, D., Light, M., Blair, M., Davidson, W., Jesso, S., and Brashear, R. (2008). Galantamine in frontotemporal dementia and primary progressive aphasia. *Dementia and geriatric cognitive disorders*, 25(2):178–85.

Kertesz, A. and Munoz, D. (2004). Relationship between frontotemporal dementia and corticobasal degeneration/progressive supranuclear palsy. *Dementia and geriatric cognitive disorders*, 17(4):282–6.

Keuleers, E., Brysbaert, M., and New, B. (2010). SUBTLEX-NL: a new measure for Dutch word frequency based on film subtitles. *Behavior research methods*, 42(3):643–50.

Kikuchi, A., Okamura, N., Hasegawa, T., Harada, R., Watanuki, S., Funaki, Y., Hiraoka, K., Baba, T., Sugeno, N., Oshima, R., Yoshida, S., Kobayashi, J., Ezura, M., Kobayashi, M., Tano, O., Mugikura, S.,

Iwata, R., Ishiki, A., Furukawa, K., Arai, H., Furumoto, S., Tashiro, M., Yanai, K., Kudo, Y., Takeda, A., and Aoki, M. (2016). In vivo visualization of tau deposits in corticobasal syndrome by 18 F-THK5351 PET. *Neurology*, 87(22):2309–2316.

Kilimann, I., Grothe, M., Heinsen, H., Alho, E. J. L., Grinberg, L., Amaro, E., Dos Santos, G. A. B., da Silva, R. E., Mitchell, A. J., Frisoni, G. B., Bokde, A. L. W., Fellgiebel, A., Filippi, M., Hampel, H., Klöppel, S., and Teipel, S. J. (2014). Subregional basal forebrain atrophy in Alzheimer's disease: a multicenter study. *Journal of Alzheimer's disease : JAD*, 40(3):687–700.

Kivisaari, S. L., Tyler, L. K., Monsch, A. U., and Taylor, K. I. (2012). Medial perirhinal cortex disambiguates confusable objects. *Brain : a journal of neurology*, 135(Pt 12):3757–69.

Klunk, W. E., Engler, H., Nordberg, A., Wang, Y., Blomqvist, G., Holt, D. P., Bergström, M., Savitcheva, I., Huang, G. F., Estrada, S., Ausén, B., Debnath, M. L., Barletta, J., Price, J. C., Sandell, J., Lopresti, B. J., Wall, A., Koivisto, P., Antoni, G., Mathis, C. a., and Långström, B. (2004). Imaging Brain Amyloid in Alzheimer's Disease with Pittsburgh Compound-B. *Annals of Neurology*, 55:306–319.

Koeppe, R. a., Frey, K. a., Snyder, S. E., Meyer, P., Kilbourn, M. R., and Kuhl, D. E. (1999). Kinetic modeling of N-[11C]methylpiperidin-4-yl propionate: alternatives for analysis of an irreversible positron emission tomography trace for measurement of acetylcholinesterase activity in human brain. *Journal of cerebral blood flow and metabolism : official journal of the International Society of Cerebral Blood Flow and Metabolism*, 19:1150–1163.

Kuhl, D. E., Koeppe, R. a., Minoshima, S., Snyder, S. E., Ficaro, E. P., Foster, N. L., Frey, K. a., and Kilbourn, M. R. (1999). In vivo mapping of cerebral acetylcholinesterase activity in aging and Alzheimer's disease. *Neurology*, 52:691–699.

Kumar, S., Joseph, S., Gander, P. E., Barascud, N., Halpern, A. R., and Griffiths, T. D. (2016). A Brain System for Auditory Working Memory. *Journal of Neuroscience*, 36(16):4492–4505.

Kumfor, F., Hutchings, R., Irish, M., Hodges, J. R., Rhodes, G., Palermo, R., and Piguet, O. (2015). Do I know you? Examining face and object memory in frontotemporal dementia. *Neuropsychologia*, 71:101–111.

Kumfor, F., Landin-Romero, R., Devenney, E., Hutchings, R., Grasso, R., Hodges, J. R., and Piguet, O. (2016). On the right side? A longitudinal study of left- versus right-lateralized semantic dementia. *Brain : a journal of neurology*, 139(Pt 3):986–98.

Kumral, E., Ozdemirkiran, T., and Alper, Y. (2004). Strokes in the subinsular territory: clinical, topographical, and etiological patterns. *Neurology*, 63(12):2429–32.

Lameka, K., Farwell, M. D., and Ichise, M. (2016). Positron Emission Tomography. In *Handb Clin Neurol.*, pages 209–227.

Lang, W., Obrig, H., Lindinger, G., Cheyne, D., and Deecke, L. (1990). Supplementary motor area activation while tapping bimanually different rhythms in musicians. *Experimental brain research*, 79(3):504–14.

Lejeune, H., Maquet, P., Bonnet, M., Casini, L., Ferrara, A., Macar, F., Pouthas, V., Timsit-Berthier, M., and Vidal, F. (1997). The basic pattern of activation in motor and sensory temporal tasks: positron emission tomography data. *Neuroscience letters*, 235(1-2):21–4.

Levitt, H. (1971). Transformed up-down methods in psychoacoustics. *The Journal of the Acoustical Society of America*, 49(2):Suppl 2:467+.

Lewis, P. A. and Miall, R. C. (2003). Distinct systems for automatic and cognitively controlled time measurement: evidence from neuroimaging. *Current opinion in neurobiology*, 13(2):250–5.

Leyton, C. E., Savage, S., Irish, M., Schubert, S., Piguet, O., Ballard, K. J., and Hodges, J. R. (2014). Verbal repetition in primary progressive aphasia and Alzheimer's disease. *Journal of Alzheimer's disease : JAD*, 41(2):575–85.

Leyton, C. E., Villemagne, V. L., Savage, S., Pike, K. E., Ballard, K. J., Piguet, O., Burrell, J. R., Rowe, C. C., and Hodges, J. R. (2011). Subtypes of progressive aphasia: application of the International Consensus Criteria and validation using β-amyloid imaging. *Brain : a journal of neurology*, 134(Pt 10):3030–43.

Li, X., Kumar, Y., Zempel, H., Mandelkow, E.-M., Biernat, J., and Mandelkow, E. (2011). Novel diffusion barrier for axonal retention of Tau in neurons and its failure in neurodegeneration. *The EMBO journal*, 30(23):4825–37.

Liuzzi, A. G., Bruffaerts, R., Dupont, P., Adamczuk, K., Peeters, R., De Deyne, S., Storms, G., and Vandenberghe, R. (2015). Left perirhinal cortex codes for similarity in meaning between written words: Comparison with auditory word input. *Neuropsychologia*, 76:4–16.

Liuzzi, A. G., Bruffaerts, R., Peeters, R., Adamczuk, K., Keuleers, E., De Deyne, S., Storms, G., Dupont, P., and Vandenberghe, R. (2017). Cross-modal representation of spoken and written word meaning in left pars triangularis. *NeuroImage*, 150:292–307.

Logan, J., Fowler, J. S., Volkow, N. D., Wang, G. J., Ding, Y. S., and Alexoff, D. L. (1996). Distribution volume ratios without blood sampling from graphical analysis of PET data. *Journal of cerebral blood flow and metabolism : official journal of the International Society of Cerebral Blood Flow and Metabolism*, 16:834–840.

Lowe, V. J., Curran, G., Fang, P., Liesinger, A. M., Josephs, K. A., Parisi, J. E., Kantarci, K., Boeve, B. F., Pandey, M. K., Bruinsma, T., Knopman, D. S., Jones, D. T., Petrucelli, L., Cook, C. N., Graff-Radford, N. R., Dickson, D. W., Petersen, R. C., Jack, C. R., and Murray, M. E. (2016). An autoradiographic evaluation of AV-1451 Tau PET in dementia. *Acta neuropathologica communications*, 4(1):58.

Maas, T., Eidenmüller, J., and Brandt, R. (2000). Interaction of tau with the neural membrane cortex is regulated by phosphorylation at sites that are modified in paired helical filaments. *The Journal of biological chemistry*, 275(21):15733–40.

Mackenzie, I. R. A., Neumann, M., Baborie, A., Sampathu, D. M., Du Plessis, D., Jaros, E., Perry, R. H., Trojanowski, J. Q., Mann, D. M. A., and Lee, V. M. Y. (2011). A harmonized classification system for FTLD-TDP pathology. *Acta neuropathologica*, 122(1):111–3.

Mandelli, M. L., Caverzasi, E., Binney, R. J., Henry, M. L., Lobach, I., Block, N., Amirbekian, B., Dronkers, N., Miller, B. L., Henry, R. G., and Gorno-Tempini, M. L. (2014). Frontal white matter tracts sustaining speech production in primary progressive aphasia. *The Journal of neuroscience : the official journal of the Society for Neuroscience*, 34(29):9754–67.

Mandelli, M. L., Vilaplana, E., Brown, J. A., Hubbard, H. I., Binney, R. J., Attygalle, S., Santos-Santos, M. A., Miller, Z. A., Pakvasa, M., Henry, M. L., Rosen, H. J., Henry, R. G., Rabinovici, G. D., Miller, B. L., Seeley, W. W., and Gorno-Tempini, M. L. (2016). Healthy

brain connectivity predicts atrophy progression in non-fluent variant of primary progressive aphasia. *Brain*, 139(10):2778–2791.

Mandelli, M. L., Vitali, P., Santos, M., Henry, M., Gola, K., Rosenberg, L., Dronkers, N., Miller, B., Seeley, W. W., and Gorno-Tempini, M. L. (2015). Two insular regions are differentially involved in behavioral variant FTD and nonfluent/agrammatic variant PPA. *Cortex; a journal devoted to the study of the nervous system and behavior*, 74:149–157.

Marchant, J. L. and Driver, J. (2013). Visual and Audiovisual Effects of Isochronous Timing on Visual Perception and Brain Activity. *Cerebral Cortex*, 23(6):1290–1298.

Marcotte, K., Graham, N., Fraser, K., Meltzer, J., Tang-Wai, D., Chow, T., Freedman, M., Leonard, C., Black, S., and Rochon, E. (2017). White Matter Disruption and Connected Speech in Non-Fluent and Semantic Variants of Primary Progressive Aphasia. *Dementia and Geriatric Cognitive Disorders Extra*, 7(1):52–73.

Mariën, P., Mampaey, E., Vervaet, A., Saerens, J., and De Deyn, P. P. (1998). Normative data for the Boston naming test in native Dutch-speaking Belgian elderly. *Brain and language*, 65(3):447–67.

Marquié, M., Normandin, M. D., Vanderburg, C. R., Costantino, I. M., Bien, E. A., Rycyna, L. G., Klunk, W. E., Mathis, C. A., Ikonomovic, M. D., Debnath, M. L., Vasdev, N., Dickerson, B. C., Gomperts, S. N., Growdon, J. H., Johnson, K. A., Frosch, M. P., Hyman, B. T., and Gómez-Isla, T. (2015). Validating novel tau positron emission tomography tracer [F-18]-AV-1451 (T807) on postmortem brain tissue. *Annals of Neurology*, 78(5):787–800.

Marsh, E. B. and Hillis, A. E. (2006). Recovery from aphasia following brain injury: the role of reorganization. In *Progress in brain research*, volume 157, pages 143–156.

Martersteck, A., Murphy, C., Rademaker, A., Wieneke, C., Weintraub, S., Chen, K., Mesulam, M.-M., and Rogalski, E. (2015). Is in vivo amyloid distribution asymmetric in primary progressive aphasia? *Annals of neurology*.

Maruta, C., Makhmood, S., Downey, L. E., Golden, H. L., Fletcher, P. D., Witoonpanich, P., Rohrer, J. D., and Warren, J. D. (2014). Delayed auditory feedback simulates features of nonfluent primary progressive aphasia. *Journal of the Neurological Sciences*, 347(1-2):345–348.

Maruyama, M., Shimada, H., Suhara, T., Shinotoh, H., Ji, B., Maeda, J., Zhang, M.-R., Trojanowski, J., Lee, V.-Y., Ono, M., Masamoto, K., Takano, H., Sahara, N., Iwata, N., Okamura, N., Furumoto, S., Kudo, Y., Chang, Q., Saido, T., Takashima, A., Lewis, J., Jang, M.-K., Aoki, I., Ito, H., and Higuchi, M. (2013). Imaging of Tau Pathology in a Tauopathy Mouse Model and in Alzheimer Patients Compared to Normal Controls. *Neuron*, 79(6):1094–1108.

Matias-Guiu, J. A., Cabrera-Martín, M. N., Matías-Guiu, J., and Carreras, J. L. (2017). FDG-PET/CT or MRI for the Diagnosis of Primary Progressive Aphasia? *AJNR. American journal of neuroradiology*, 38(9):E63.

Matias-Guiu, J. a., Cabrera-Martín, M. N., Moreno-Ramos, T., García-Ramos, R., Porta-Etessam, J., Carreras, J. L., and Matías-Guiu, J. (2014). Clinical course of primary progressive aphasia: clinical and FDG-PET patterns. *Journal of Neurology*, 262:570–577.

Matías-Guiu, J. A., Cabrera-Martín, M. N., Moreno-Ramos, T., Valles-Salgado, M., Fernandez-Matarrubia, M., Carreras, J. L., and Matías-Guiu, J. (2015a). Amyloid and FDG-PET study of logopenic primary progressive aphasia: evidence for the existence of two subtypes. *Journal of neurology*, 262(6):1463–72.

Matías-Guiu, J. A., Cabrera-Martín, M. N., Pérez-Castejón, M. J., Moreno-Ramos, T., Rodríguez-Rey, C., García-Ramos, R., Ortega-Candil, A., Fernandez-Matarrubia, M., Oreja-Guevara, C., Matías-Guiu, J., and Carreras, J. L. (2015b). Visual and statistical analysis of 18F-FDG PET in primary progressive aphasia. *European Journal of Nuclear Medicine and Molecular Imaging*, 42(6):916–927.

Mazere, J., Lamare, F., Fernandez, P., Allard, M., and Mayo, W. (2016). 123I-iodobenzovesamicol SPECT Imaging of Cholinergic Systems in Dementia with Lewy Bodies. *J Nucl Med*, pages 123–129.

McConathey, E. M., White, N. C., Gervits, F., Ash, S., Coslett, H. B., Grossman, M., and Hamilton, R. H. (2017). Baseline Performance Predicts tDCS-Mediated Improvements in Language Symptoms in Primary Progressive Aphasia. *Frontiers in Human Neuroscience*, 11:347.

Mendez, M. F. (2009). Frontotemporal dementia: therapeutic interventions. *Frontiers of neurology and neuroscience*, 24:168–78.

Menon, V., Levitin, D. J., Smith, B. K., Lembke, A., Krasnow, B. D., Glazer, D., Glover, G. H., and McAdams, S. (2002). Neural correlates of timbre change in harmonic sounds. *NeuroImage*, 17(4):1742–54.

Mesulam, M. (2013a). Primary progressive aphasia: A dementia of the language network. *Dementia & neuropsychologia*, 7(1):2–9.

Mesulam, M., Wieneke, C., Rogalski, E., Cobia, D., Thompson, C., and Weintraub, S. (2009). Quantitative template for subtyping primary progressive aphasia. *Archives of neurology*, 66(12):1545–51.

Mesulam, M. M. (1982). Slowly progressive aphasia without generalized dementia. *Annals of neurology*, 11(6):592–8.

Mesulam, M. M. (1987). Primary progressive aphasia–differentiation from Alzheimer's disease. *Annals of neurology*, 22(4):533–4.

Mesulam, M.-M. (2013b). Cholinergic circuitry of the human nucleus basalis and its fate in Alzheimer's disease. *The Journal of comparative neurology*, 521(18):4124–44.

Mesulam, M.-M., Rogalski, E. J., Wieneke, C., Hurley, R. S., Geula, C., Bigio, E. H., Thompson, C. K., and Weintraub, S. (2014a). Primary progressive aphasia and the evolving neurology of the language network. *Nature Reviews Neurology*, 10(10):554–569.

Mesulam, M.-M., Weintraub, S., Rogalski, E. J., Wieneke, C., Geula, C., and Bigio, E. H. (2014b). Asymmetry and heterogeneity of Alzheimer's and frontotemporal pathology in primary progressive aphasia. *Brain : a journal of neurology*, 137(Pt 4):1176–92.

Mesulam, M.-M., Wieneke, C., Hurley, R., Rademaker, A., Thompson, C. K., Weintraub, S., and Rogalski, E. J. (2013). Words and objects at the tip of the left temporal lobe in primary progressive aphasia. *Brain : a journal of neurology*, 136(Pt 2):601–18.

Mesulam, M.-M., Wieneke, C., Thompson, C., Rogalski, E., and Weintraub, S. (2012). Quantitative classification of primary progressive aphasia at early and mild impairment stages. *Brain : a journal of neurology*, 135(Pt 5):1537–53.

Meyer, M., Alter, K., Friederici, A. D., Lohmann, G., and von Cramon, D. Y. (2002). FMRI reveals brain regions mediating slow prosodic modulations in spoken sentences. *Human Brain Mapping*, 17(2):73–88.

Midorikawa, A., Kumfor, F., Leyton, C. E., Foxe, D., Landin-Romero, R., Hodges, J. R., and Piguet, O. (2017). Characterisation of "Positive" Behaviours in Primary Progressive Aphasias. *Dementia and Geriatric Cognitive Disorders*, 44(3-4):119–128.

Mintun, M. a., Larossa, G. N., Sheline, Y. I., Dence, C. S., Lee, S. Y., MacH, R. H., Klunk, W. E., Mathis, C. a., Dekosky, S. T., and Morris, J. C. (2006). [11C]PIB in a nondemented population: Potential antecedent marker of Alzheimer disease. *Neurology*, 67:446–452.

Mion, M., Patterson, K., Acosta-Cabronero, J., Pengas, G., Izquierdo-Garcia, D., Hong, Y. T., Fryer, T. D., Williams, G. B., Hodges, J. R., and Nestor, P. J. (2010). What the left and right anterior fusiform gyri tell us about semantic memory. *Brain : a journal of neurology*, 133(11):3256–68.

Mirra, S. S., Heyman, A., McKeel, D., Sumi, S. M., Crain, B. J., Brownlee, L. M., Vogel, F. S., Hughes, J. P., van Belle, G., and Berg, L. (1991). The Consortium to Establish a Registry for Alzheimer's Disease (CERAD). Part II. Standardization of the neuropathologic assessment of Alzheimer's disease. *Neurology*, 41(4):479–86.

Molenberghs, P., Gillebert, C. R., Schoofs, H., Dupont, P., Peeters, R., and Vandenberghe, R. (2009). Lesion neuroanatomy of the Sustained Attention to Response task. *Neuropsychologia*, 47(13):2866–2875.

Morillon, B., Kell, C. A., and Giraud, A.-L. (2009). Three Stages and Four Neural Systems in Time Estimation. *Journal of Neuroscience*, 29(47).

Mufson, E. J., Counts, S. E., Perez, S. E., and Ginsberg, S. D. (2008). Cholinergic system during the progression of Alzheimer's disease: therapeutic implications. *Expert Review of Neurotherapeutics*, 8(11):1703–1718.

Müller-Gärtner, H. W., Links, J. M., Prince, J. L., Bryan, R. N., McVeigh, E., Leal, J. P., Davatzikos, C., and Frost, J. J. (1992). Measurement of radiotracer concentration in brain gray matter using positron emission tomography: MRI-based correction for partial volume effects. *Journal of cerebral blood flow and metabolism : official journal of the International Society of Cerebral Blood Flow and Metabolism*, 12(4):571–83.

Mummery, C. J., Patterson, K., Price, C. J., Ashburner, J., Frackowiak, R. S., and Hodges, J. R. (2000). A voxel-based morphometry study of

semantic dementia: relationship between temporal lobe atrophy and semantic memory. *Annals of neurology*, 47(1):36–45.

Nasrallah, I. M., Chen, Y. J., Hsieh, M.-K., Philips, J. S., Ternes, K., Stockbower, G., Sheline, Y., McMillan, C. T., Grossman, M., and Wolk, D. A. (2017). ¹⁸ F-Flortaucipir PET-MRI correlations in non-amnestic and amnestic variants of Alzheimer Disease. *Journal of Nuclear Medicine*, page jnumed.117.194282.

Neary, D., Snowden, J. S., Gustafson, L., Passant, U., Stuss, D., Black, S., Freedman, M., Kertesz, A., Robert, P. H., Albert, M., Boone, K., Miller, B. L., Cummings, J., and Benson, D. F. (1998). Frontotemporal lobar degeneration: a consensus on clinical diagnostic criteria. *Neurology*, 51(6):1546–54.

Nelissen, N., Pazzaglia, M., Vandenbulcke, M., Sunaert, S., Fannes, K., Dupont, P., Aglioti, S. M., and Vandenberghe, R. (2010). Gesture discrimination in primary progressive aphasia: the intersection between gesture and language processing pathways. *The Journal of neuroscience : the official journal of the Society for Neuroscience*, 30(18):6334–6341.

Nelissen, N., Vandenbulcke, M., Fannes, K., Verbruggen, A., Peeters, R., Dupont, P., Van Laere, K., Bormans, G., and Vandenberghe, R. (2007). A?? amyloid deposition in the language system and how the brain responds. *Brain*, 130:2055–2069.

Nenadic, I., Gaser, C., Volz, H.-P., Rammsayer, T., Häger, F., and Sauer, H. (2003). Processing of temporal information and the basal ganglia: new evidence from fMRI. *Experimental Brain Research*, 148(2):238–246.

Neumann, M., Sampathu, D. M., Kwong, L. K., Truax, A. C., Micsenyi, M. C., Chou, T. T., Bruce, J., Schuck, T., Grossman, M., Clark, C. M., McCluskey, L. F., Miller, B. L., Masliah, E., Mackenzie, I. R., Feldman, H., Feiden, W., Kretzschmar, H. A., Trojanowski, J. Q., and Lee, V. M.-Y. (2006). Ubiquitinated TDP-43 in frontotemporal lobar degeneration and amyotrophic lateral sclerosis. *Science (New York, N.Y.)*, 314(5796):130–3.

Ng, K. P., Pascoal, T. A., Mathotaarachchi, S., Therriault, J., Kang, M. S., Shin, M., Guiot, M.-C., Guo, Q., Harada, R., Comley, R. A., Massarweh, G., Soucy, J.-P., Okamura, N., Gauthier, S., and Rosa-Neto, P. (2017). Monoamine oxidase B inhibitor, selegiline, reduces 18F-THK5351 uptake in the human brain. *Alzheimer's Research & Therapy*, 9(1):25.

Nixon, P., Lazarova, J., Hodinott-Hill, I., Gough, P., and Passingham, R. (2004). The Inferior Frontal Gyrus and Phonological Processing: An Investigation using rTMS. *Journal of Cognitive Neuroscience*, 16(2):289–300.

Nordberg, A., Ballard, C., Bullock, R., Darreh-Shori, T., and Somogyi, M. (2013). A review of butyrylcholinesterase as a therapeutic target in the treatment of Alzheimer's disease. *The primary care companion for CNS disorders*, 15(2).

Odawara, T., Shiozaki, K., Iseki, E., Hino, H., and Kosaka, K. (2003). Alterations of muscarinic acetylcholine receptors in atypical Pick's disease without Pick bodies. *Journal of neurology, neurosurgery, and psychiatry*, 74(7):965–7.

Ogar, J. M., Dronkers, N. F., Brambati, S. M., Miller, B. L., and Gorno-Tempini, M. L. (2007). Progressive Nonfluent Aphasia and Its Characteristic Motor Speech Deficits. *Alzheimer Disease & Associated Disorders*, 21(4):S23–S30.

Omar, R., Henley, S. M. D., Bartlett, J. W., Hailstone, J. C., Gordon, E., Sauter, D. A., Frost, C., Scott, S. K., and Warren, J. D. (2011). The structural neuroanatomy of music emotion recognition: evidence from frontotemporal lobar degeneration. *NeuroImage*, 56(3):1814–21.

Ono, K., Nakamura, A., Yoshiyama, K., Kinkori, T., Bundo, M., Kato, T., and Ito, K. (2011). The effect of musical experience on hemispheric lateralization in musical feature processing. *Neuroscience Letters*, 496(2):141–145.

Ossenkoppele, R., Jansen, W. J., Rabinovici, G. D., Knol, D. L., van der Flier, W. M., van Berckel, B. N. M., Scheltens, P., Visser, P. J., Verfaillie, S. C. J., Zwan, M. D., Adriaanse, S. M., Lammertsma, A. A., Barkhof, F., Jagust, W. J., Miller, B. L., Rosen, H. J., Landau, S. M., Villemagne, V. L., Rowe, C. C., Lee, D. Y., Na, D. L., Seo, S. W., Sarazin, M., Roe, C. M., Sabri, O., Barthel, H., Koglin, N., Hodges, J., Leyton, C. E., Vandenberghe, R., van Laere, K., Drzezga, A., Forster, S., Grimmer, T., Sánchez-Juan, P., Carril, J. M., Mok, V., Camus, V., Klunk, W. E., Cohen, A. D., Meyer, P. T., Hellwig, S., Newberg, A., Frederiksen, K. S., Fleisher, A. S., Mintun, M. A., Wolk, D. A., Nordberg, A., Rinne, J. O., Chételat, G., Lleo, A., Blesa, R., Fortea, J., Madsen, K., Rodrigue, K. M., and Brooks, D. J. (2015). Prevalence of amyloid PET positivity in dementia syndromes: a meta-analysis. *JAMA*, 313(19):1939–49.

Ossenkoppele, R., Schonhaut, D. R., Schöll, M., Lockhart, S. N., Ayakta, N., Baker, S. L., O'Neil, J. P., Janabi, M., Lazaris, A., Cantwell, A., Vogel, J., Santos, M., Miller, Z. A., Bettcher, B. M., Vossel, K. A., Kramer, J. H., Gorno-Tempini, M. L., Miller, B. L., Jagust, W. J., and Rabinovici, G. D. (2016). Tau PET patterns mirror clinical and neuroanatomical variability in Alzheimer's disease. *Brain : a journal of neurology*, 139(Pt 5):1551–67.

Overath, T., Kumar, S., Stewart, L., von Kriegstein, K., Cusack, R., Rees, A., and Griffiths, T. D. (2010). Cortical mechanisms for the segregation and representation of acoustic textures. *The Journal of neuroscience : the official journal of the Society for Neuroscience*, 30(6):2070–6.

Overath, T., Kumar, S., von Kriegstein, K., and Griffiths, T. D. (2008). Encoding of spectral correlation over time in auditory cortex. *The Journal of neuroscience : the official journal of the Society for Neuroscience*, 28(49):13268–73.

Özdemir, E., Norton, A., and Schlaug, G. (2006). Shared and distinct neural correlates of singing and speaking. *NeuroImage*, 33(2):628–635.

Passamonti, L., V?zquez Rodr?guez, P., Hong, Y. T., Allinson, K. S. J., Williamson, D., Borchert, R. J., Sami, S., Cope, T. E., Bevan-Jones, W. R., Jones, P. S., Arnold, R., Surendranathan, A., Mak, E., Su, L., Fryer, T. D., Aigbirhio, F. I., O?Brien, J. T., and Rowe, J. B. (2017). 18 F-AV-1451 positron emission tomography in Alzheimer?s disease and progressive supranuclear palsy. *Brain*, 140(3):781–791.

Pastor, M., Macaluso, E., Day, B., and Frackowiak, R. (2006). The neural basis of temporal auditory discrimination. *NeuroImage*, 30(2):512–520.

Patterson, R. D., Uppenkamp, S., Johnsrude, I. S., and Griffiths, T. D. (2002). The processing of temporal pitch and melody information in auditory cortex. *Neuron*, 36(4):767–76.

Pepeu, G. and Grazia Giovannini, M. (2017). The fate of the brain cholinergic neurons in neurodegenerative diseases. *Brain Research*, 1670:173–184.

Phillips, J. S., Das, S. R., McMillan, C. T., Irwin, D. J., Roll, E. E., Da Re, F., Nasrallah, I. M., Wolk, D. A., and Grossman, M. (2017). Tau PET imaging predicts cognition in atypical variants of Alzheimer's disease. *Human Brain Mapping*.

Platel, H., Price, C., Baron, J. C., Wise, R., Lambert, J., Frackowiak, R. S., Lechevalier, B., and Eustache, F. (1997). The structural components of music perception. A functional anatomical study. *Brain : a journal of neurology*, 120 (Pt 2:229–43.

Poeppel, D. (2003). The analysis of speech in different temporal integration windows: cerebral lateralization as 'asymmetric sampling in time'. *Speech Communication*, 41(1):245–255.

Poldrack, R. A., Baker, C. I., Durnez, J., Gorgolewski, K. J., Matthews, P. M., Munafò, M. R., Nichols, T. E., Poline, J.-B., Vul, E., and Yarkoni, T. (2017). Scanning the horizon: towards transparent and reproducible neuroimaging research. *Nature Reviews Neuroscience*, 18(2):115–126.

Poldrack, R. A., Temple, E., Protopapas, A., Nagarajan, S., Tallal, P., Merzenich, M., and Gabrieli, J. D. (2001). Relations between the neural bases of dynamic auditory processing and phonological processing: evidence from fMRI. *Journal of cognitive neuroscience*, 13(5):687–97.

Poldrack, R. A., Wagner, A. D., Prull, M. W., Desmond, J. E., Glover, G. H., and Gabrieli, J. D. (1999). Functional Specialization for Semantic and Phonological Processing in the Left Inferior Prefrontal Cortex. *NeuroImage*, 10(1):15–35.

Poline, J. B., Worsley, K. J., Evans, a. C., and Friston, K. J. (1997). Combining spatial extent and peak intensity to test for activations in functional imaging. *NeuroImage*, 5(5):83–96.

Price, J. L. and Morris, J. C. (1999). Tangles and plaques in nondemented aging and "preclinical" Alzheimer's disease. *Annals of neurology*, 45(3):358–68.

Procter, A. W., Qurne, M., and Francis, P. T. (1999). Neurochemical features of frontotemporal dementia. *Dementia and geriatric cognitive disorders*, 10:80–4.

Rabinovici, G. D., Jagust, W. J., Furst, A. J., Ogar, J. M., Racine, C. A., Mormino, E. C., O'Neil, J. P., Lal, R. A., Dronkers, N. F., Miller, B. L., and Gorno-Tempini, M. L. (2008). Abeta amyloid and glucose metabolism in three variants of primary progressive aphasia. *Annals of neurology*, 64(4):388–401.

Rao, S. M., Mayer, A. R., and Harrington, D. L. (2001). The evolution of brain activation during temporal processing. *Nature neuroscience*, 4(3):317–23.

Reiterer, S., Erb, M., Grodd, W., and Wildgruber, D. (2008). Cerebral Processing of Timbre and Loudness: fMRI Evidence for a Contribution of Broca's Area to Basic Auditory Discrimination. *Brain Imaging and Behavior*, 2(1):1–10.

Ridgway, G. R., Omar, R., Ourselin, S., Hill, D. L., Warren, J. D., Fox, N. C., Henley, S. M. D., Rohrer, J. D., Scahill, R. I., Warren, J. D., and Fox, N. C. (2009). Issues with threshold masking in voxel-based morphometry of atrophied brains. *NeuroImage*, 44(1):99–111.

Robson, H., Grube, M., Lambon Ralph, M. A., Griffiths, T. D., and Sage, K. (2013). Fundamental deficits of auditory perception in Wernicke's aphasia. *Cortex; a journal devoted to the study of the nervous system and behavior*, 49(7):1808–22.

Rogalski, E., Cobia, D., Harrison, T. M., Wieneke, C., Thompson, C. K., Weintraub, S., and Mesulam, M.-M. (2011a). Anatomy of Language Impairments in Primary Progressive Aphasia. *Journal of Neuroscience*, 31(9):3344–3350.

Rogalski, E., Cobia, D., Harrison, T. M., Wieneke, C., Weintraub, S., and Mesulam, M.-M. (2011b). Progression of language decline and cortical atrophy in subtypes of primary progressive aphasia. *Neurology*, 76(21):1804–10.

Rohrer, J. D., Caso, F., Mahoney, C., Henry, M., Rosen, H. J., Rabinovici, G., Rossor, M. N., Miller, B., Warren, J. D., Fox, N. C., Ridgway, G. R., and Gorno-Tempini, M. L. (2013). Patterns of longitudinal brain atrophy in the logopenic variant of primary progressive aphasia. *Brain and language*, 127(2):121–6.

Rohrer, J. D., Ridgway, G. R., Crutch, S. J., Hailstone, J., Goll, J. C., Clarkson, M. J., Mead, S., Beck, J., Mummery, C., Ourselin, S., Warrington, E. K., Rossor, M. N., and Warren, J. D. (2010a). Progressive logopenic/phonological aphasia: erosion of the language network. *NeuroImage*, 49(1):984–93.

Rohrer, J. D., Rossor, M. N., and Warren, J. D. (2010b). Syndromes of nonfluent primary progressive aphasia: A clinical and neurolinguistic analysis. *Neurology*, 75(7):603–610.

Rohrer, J. D., Sauter, D., Scott, S., Rossor, M. N., and Warren, J. D. (2012). Receptive prosody in nonfluent primary progressive aphasias. *Cortex; a journal devoted to the study of the nervous system and behavior*, 48(3):308–16.

Rohrer, J. D., Warren, J. D., Barnes, J., Mead, S., Beck, J., Pepple, T., Boyes, R., Omar, R., Collinge, J., Stevens, J. M., Warrington, E. K., Rossor, M. N., and Fox, N. C. (2008). Mapping the progression of progranulin-associated frontotemporal lobar degeneration. *Nature Clinical Practice Neurology*, 4(8):455–460.

Rorden, C., Karnath, H.-O., and Bonilha, L. (2007). Improving lesion-symptom mapping. *Journal of cognitive neuroscience*, 19(7):1081–8.

Rosen, H. J., Gorno-Tempini, M. L., Goldman, W. P., Perry, R. J., Schuff, N., Weiner, M., Feiwell, R., Kramer, J. H., and Miller, B. L. (2002). Patterns of brain atrophy in frontotemporal dementia and semantic dementia. *Neurology*, 58:198–208.

Rousset, O., Rahmim, A., Alavi, A., and Zaidi, H. (2007). Partial Volume Correction Strategies in PET. *PET Clinics*, 2:235–249.

Sabri, O., Sabbagh, M. N., Seibyl, J., Barthel, H., Akatsu, H., Ouchi, Y., Senda, K., Murayama, S., Ishii, K., Takao, M., Beach, T. G., Rowe, C. C., Leverenz, J. B., Ghetti, B., Ironside, J. W., Catafau, A. M., Stephens, A. W., Mueller, A., Koglin, N., Hoffmann, A., Roth, K., Reininger, C., and Schulz-Schaeffer, W. J. (2015). Florbetaben PET imaging to detect amyloid beta plaques in Alzheimer's disease: phase 3 study. *Alzheimer's & dementia : the journal of the Alzheimer's Association*, 11(8):964–74.

Sajjadi, S. A., Patterson, K., Arnold, R. J., Watson, P. C., and Nestor, P. J. (2012). Primary progressive aphasia: a tale of two syndromes and the rest. *Neurology*, 78(21):1670–7.

Sajjadi, S. A., Patterson, K., and Nestor, P. J. (2014). Logopenic, mixed, or Alzheimer-related aphasia? *Neurology*, 82(13):1127–1131.

Sajjadi, S. A., Sheikh-Bahaei, N., Cross, J., Gillard, J. H., Scoffings, D., and Nestor, P. J. (2017). Can MRI Visual Assessment Differentiate the Variants of Primary-Progressive Aphasia? *AJNR. American journal of neuroradiology*, 38(5):954–960.

Salinas, C. A., Searle, G. E., and Gunn, R. N. (2015). The simplified reference tissue model: model assumption violations and their impact

on binding potential. *Journal of cerebral blood flow and metabolism : official journal of the International Society of Cerebral Blood Flow and Metabolism*, 35(2):304–11.

Savaskan, N. E. and Nitsch, R. (2001). Molecules involved in reactive sprouting in the hippocampus. *Reviews in the neurosciences*, 12(3):195–215.

Schaeverbeke, J., Evenepoel, C., Bruffaerts, R., Van Laere, K., Bormans, G., Dries, E., Tousseyn, T., Nelissen, N., Peeters, R., Vandenbulcke, M., Dupont, P., and Vandenberghe, R. (2017). Cholinergic depletion and basal forebrain volume in primary progressive aphasia. *NeuroImage: Clinical*, 13:271–279.

Schegg, K. M., Harrington, L. S., Neilsen, S., Zweig, R. M., and Peacock, J. H. (1992). Soluble and membrane-bound forms of brain acetylcholinesterase in Alzheimer's disease. *Neurobiology of aging*, 13(6):697–704.

Schliebs, R. and Arendt, T. (2011). The cholinergic system in aging and neuronal degeneration. *Behavioural Brain Research*, 221(2):555–563.

Schönwiesner, M. and Zatorre, R. J. (2009). Spectro-temporal modulation transfer function of single voxels in the human auditory cortex measured with high-resolution fMRI. *Proceedings of the National Academy of Sciences of the United States of America*, 106(34):14611–6.

Schubotz, R. I. and von Cramon, D. Y. (2001). Interval and ordinal properties of sequences are associated with distinct premotor areas. *Cerebral cortex (New York, N.Y. : 1991)*, 11(3):210–22.

Scott, S. K. and Wise, R. J. S. (2004). The functional neuroanatomy of prelexical processing in speech perception. *Cognition*, 92(1-2):13–45.

Selden, N. R., Gitelman, D. R., Salamon-Murayama, N., Parrish, T. B., and Mesulam, M. M. (1998). Trajectories of cholinergic pathways within the cerebral hemispheres of the human brain. *Brain : a journal of neurology*, 121 (Pt 1:2249–57.

Shafto, M. A., Burke, D. M., Stamatakis, E. A., Tam, P. P., and Tyler, L. K. (2007). On the Tip-of-the-Tongue: Neural Correlates of Increased Word-finding Failures in Normal Aging. *Journal of Cognitive Neuroscience*, 19(12):2060–2070.

Shafto, M. A. and Tyler, L. K. (2014). Language in the aging brain: The network dynamics of cognitive decline and preservation. *Science*, 346(6209):583–587.

Shannon, R. V., Zeng, F. G., Kamath, V., Wygonski, J., and Ekelid, M. (1995). Speech recognition with primarily temporal cues. *Science (New York, N.Y.)*, 270(5234):303–4.

Shiller, D. M., Gracco, V. L., Rvachew, S., Dong, W., and Greenough, W. (2010). Auditory-Motor Learning during Speech Production in 9-11-Year-Old Children. *PLoS ONE*, 5(9):e12975.

Shimada, H., Hirano, S., Shinotoh, H., Aotsuka, a., Sato, K., Tanaka, N., Ota, T., Asahina, M., Fukushi, K., Kuwabara, S., Hattori, T., Suhara, T., and Irie, T. (2009). Mapping of brain acetylcholinesterase alterations in Lewy body disease by PET. *Neurology*, 73(17590861):273–278.

Shinotoh, H. (2007). [Imaging of brain acetylcholinesterase activity in dementias and extrapyramidal disorders]. *Clinical neurology*, 47(11):822–5.

Shinotoh, H., Namba, H., Yamaguchi, M., Fukushi, K., Nagatsuka, S., Iyo, M., Asahina, M., Hattori, T., Tanada, S., and Irie, T. (1999). Positron emission tomographic measurement of acetylcholinesterase activity reveals differential loss of ascending cholinergic systems in Parkinson's disease and progressive supranuclear palsy. *Annals of neurology*, 46(1):62–9.

Silveyra, M.-X., García-Ayllón, M.-S., de Barreda, E. G., Small, D. H., Martínez, S., Avila, J., and Sáez-Valero, J. (2012). Altered expression of brain acetylcholinesterase in FTDP-17 human tau transgenic mice. *Neurobiology of aging*, 33(3):624.e23–34.

Simić, G., Mrzljak, L., Fucić, A., Winblad, B., Lovrić, H., and Kostović, I. (1999). Nucleus subputaminalis (Ayala): the still disregarded magnocellular component of the basal forebrain may be human specific and connected with the cortical speech area. *Neuroscience*, 89(1):73–89.

Small, S. L. and Llano, D. A. (2009). Biological approaches to aphasia treatment. *Current neurology and neuroscience reports*, 9(6):443–50.

Smith, E. E. and Jonides, J. (1999). Storage and executive processes in the frontal lobes. *Science (New York, N.Y.)*, 283(5408):1657–61.

Smith, R., Schöll, M., Widner, H., van Westen, D., Svenningsson, P., Hägerström, D., Ohlsson, T., Jögi, J., Nilsson, C., and Hansson, O. (2017). In vivo retention of ¹⁸ F-AV-1451 in corticobasal syndrome. *Neurology*, 89(8):845–853.

Snyder, S. E., Tluczek, L., Jewett, D. M., Nguyen, T. B., Kuhl, D. E., and Kilbourn, M. R. (1998). Synthesis of 1-[11C]Methylpiperidin-4-yl propionate (11C]PMP) for in vivo measurements of acetylcholinesterase activity. *Nuclear Medicine and Biology*, 25(98):751–754.

Spinelli, E. G., Mandelli, M. L., Miller, Z. A., Santos-Santos, M. A., Wilson, S. M., Agosta, F., Grinberg, L. T., Huang, E. J., Trojanowski, J. Q., Meyer, M., Henry, M. L., Comi, G., Rabinovici, G., Rosen, H. J., Filippi, M., Miller, B. L., Seeley, W. W., and Gorno-Tempini, M. L. (2017). Typical and atypical pathology in primary progressive aphasia variants. *Annals of Neurology*, 81(3):430–443.

Stamatakis, E. A., Shafto, M. A., Williams, G., Tam, P., and Tyler, L. K. (2011). White matter changes and word finding failures with increasing age. *PloS one*, 6(1):e14496.

Stewart, L., Overath, T., Warren, J. D., Foxton, J. M., and Griffiths, T. D. (2008). fMRI Evidence for a Cortical Hierarchy of Pitch Pattern Processing. *PLoS ONE*, 3(1):e1470.

Sudakov, K., MacLean, P. D., Reeves, A., and Marino, R. (1971). Unit study of exteroceptive inputs to claustrocortex in awake, sitting, squirrel monkey. *Brain research*, 28(1):19–34.

Tagliavini, F., Pilleri, G., Bouras, C., and Constantinidis, J. (1984). The basal nucleus of Meynert in patients with progressive supranuclear palsy. *Neuroscience letters*, 44(1):37–42.

Talcott, J. B., Witton, C., McLean, M. F., Hansen, P. C., Rees, A., Green, G. G., and Stein, J. F. (2000). Dynamic sensory sensitivity and children's word decoding skills. *Proceedings of the National Academy of Sciences of the United States of America*, 97(6):2952–7.

Tan, R. H., Wong, S., Kril, J. J., Piguet, O., Hornberger, M., Hodges, J. R., and Halliday, G. M. (2014). Beyond the temporal pole: limbic memory circuit in the semantic variant of primary progressive aphasia. *Brain : a journal of neurology*, 137(Pt 7):2065–76.

Tanaka, Y., Miyazaki, M., and Albert, M. L. (1997). Effects of increased cholinergic activity on naming in aphasia. *Lancet (London, England)*, 350(9071):116–7.

Teichmann, M., Kas, A., Boutet, C., Ferrieux, S., Nogues, M., Samri, D., Rogan, C., Dormont, D., Dubois, B., and Migliaccio, R. (2013). Deciphering logopenic primary progressive aphasia: a clinical, imaging and biomarker investigation. *Brain*, 136(11):3474–3488.

Teipel, S., Heinsen, H., Amaro, E., Grinberg, L. T., Krause, B., and Grothe, M. (2014a). Cholinergic basal forebrain atrophy predicts amyloid burden in Alzheimer's disease. *Neurobiology of Aging*, 35(3):482–491.

Teipel, S., Raiser, T., Riedl, L., Riederer, I., Schroeter, M. L., Bisenius, S., Schneider, A., Kornhuber, J., Fliessbach, K., Spottke, A., Grothe, M. J., Prudlo, J., Kassubek, J., Ludolph, A., Landwehrmeyer, B., Straub, S., Otto, M., Danek, A., and study group, F. (2016). Atrophy and structural covariance of the cholinergic basal forebrain in primary progressive aphasia. *Cortex; a journal devoted to the study of the nervous system and behavior*, 83:124–35.

Teipel, S. J., Flatz, W., Ackl, N., Grothe, M., Kilimann, I., Bokde, A. L. W., Grinberg, L., Amaro, E., Kljajevic, V., Alho, E., Knels, C., Ebert, A., Heinsen, H., and Danek, A. (2014b). Brain atrophy in primary progressive aphasia involves the cholinergic basal forebrain and Ayala's nucleus. *Psychiatry Research - Neuroimaging*, 221(3):187–194.

Teipel, S. J., Flatz, W. H., Heinsen, H., Bokde, A. L. W., Schoenberg, S. O., Stöckel, S., Dietrich, O., Reiser, M. F., Möller, H. J., and Hampel, H. (2005). Measurement of basal forebrain atrophy in Alzheimer's disease using MRI. *Brain*, 128:2626–2644.

Teki, S., Grube, M., and Griffiths, T. D. (2011). A unified model of time perception accounts for duration-based and beat-based timing mechanisms. *Frontiers in integrative neuroscience*, 5:90.

Thal, D. R., Rüb, U., Orantes, M., and Braak, H. (2002). Phases of A beta-deposition in the human brain and its relevance for the development of AD. *Neurology*, 58:1791–1800.

Tillmann, B., Koelsch, S., Escoffier, N., Bigand, E., Lalitte, P., Friederici, A. D., and von Cramon, D. Y. (2006). Cognitive priming in sung and instrumental music: activation of inferior frontal cortex. *NeuroImage*, 31(4):1771–82.

Tomaino, C. M. (2012). Effective music therapy techniques in the treatment of nonfluent aphasia. *Annals of the New York Academy of Sciences*, 1252:312–7.

Trebbastoni, A., Raccah, R., de Lena, C., Zangen, A., and Inghilleri, M. (2013). Repetitive Deep Transcranial Magnetic Stimulation Improves Verbal Fluency and Written Language in a Patient with Primary Progressive Aphasia-Logopenic Variant (LPPA). *Brain Stimulation*, 6(4):545–553.

Tregellas, J. R., Davalos, D. B., and Rojas, D. C. (2006). Effect of task difficulty on the functional anatomy of temporal processing. *NeuroImage*, 32(1):307–315.

Tsai, R. M. and Boxer, A. L. (2014). Treatment of Frontotemporal Dementia HHS Public Access. *Curr Treat Options Neurol*, 16(11).

Tzourio-Mazoyer, N., Landeau, B., Papathanassiou, D., Crivello, F., Etard, O., Delcroix, N., Mazoyer, B., and Joliot, M. (2002). Automated anatomical labeling of activations in SPM using a macroscopic anatomical parcellation of the MNI MRI single-subject brain. *NeuroImage*, 15(1):273–89.

Ueno, T., Saito, S., Rogers, T. T., and Lambon Ralph, M. A. (2011). Lichtheim 2: synthesizing aphasia and the neural basis of language in a neurocomputational model of the dual dorsal-ventral language pathways. *Neuron*, 72(2):385–96.

Uttner, I., Mottaghy, F. M., Schreiber, H., Riecker, A., Ludolph, A. C., and Kassubek, J. (2006). Primary progressive aphasia accompanied by environmental sound agnosia: a neuropsychological, MRI and PET study. *Psychiatry research*, 146(2):191–7.

Van Langenhove, T., Leyton, C. E., Piguet, O., and Hodges, J. R. (2016). Comparing Longitudinal Behavior Changes in the Primary Progressive Aphasias. *Journal of Alzheimer's Disease*, 53(3):1033–1042.

Vandenberghe, R. (2016). Classification of the primary progressive aphasias: principles and review of progress since 2011. *Alzheimer's research & therapy*, 8(1):16.

Vandenberghe, R., Adamczuk, K., Dupont, P., Laere, K. V., and Chételat, G. (2013). Amyloid PET in clinical practice: Its place in the multidimensional space of Alzheimer's disease. *NeuroImage: Clinical*, 2:497–511.

Vandenberghe, R., Rinne, J. O., Boada, M., Katayama, S., Scheltens, P., Vellas, B., Tuchman, M., Gass, A., Fiebach, J. B., Hill, D., Lobello, K., Li, D., McRae, T., Lucas, P., Evans, I., Booth, K., Luscan, G.,

Wyman, B. T., Hua, L., Yang, L., Brashear, H. R., Black, R. S., and Bapineuzumab 3000 and 3001 Clinical Study Investigators (2016). Bapineuzumab for mild to moderate Alzheimer's disease in two global, randomized, phase 3 trials. *Alzheimer's research & therapy*, 8(1):18.

Vandenbulcke, M., Peeters, R., Van Hecke, P., and Vandenberghe, R. (2005). Anterior temporal laterality in primary progressive aphasia shifts to the right. *Annals of Neurology*, 58:362–370.

Villain, N., Chételat, G., Grassiot, B., Bourgeat, P., Jones, G., Ellis, K. a., Ames, D., Martins, R. N., Eustache, F., Salvado, O., Masters, C. L., Rowe, C. C., and Villemagne, V. L. (2012). Regional dynamics of amyloid-β deposition in healthy elderly, mild cognitive impairment and Alzheimer's disease: A voxelwise PiB-PET longitudinal study. *Brain*, 135:2126–2139.

Villemagne, V. L., Fodero-Tavoletti, M. T., Masters, C. L., and Rowe, C. C. (2015). Tau imaging: early progress and future directions. *The Lancet. Neurology*, 14(1):114–24.

Walji, A. M., Hostetler, E. D., Selnick, H., Zeng, Z., Miller, P., Bennacef, I., Salinas, C., Connolly, B., Gantert, L., Holahan, M., O'Malley, S., Purcell, M., Riffel, K., Li, J., Balsells, J., OBrien, J. A., Melquist, S., Soriano, A., Zhang, X., Ogawa, A., Xu, S., Joshi, E., Della Rocca, J., Hess, F. J., Schachter, J., Hesk, D., Schenk, D., Struyk, A., Babaoglu, K., Lohith, T. G., Wang, Y., Yang, K., Fu, J., Evelhoch, J. L., and Coleman, P. J. (2016). Discovery of 6-(Fluoro-(18)F)-3-(1H-pyrrolo[2,3-c]pyridin-1-yl)isoquinolin-5-amine ([(18)F]-MK-6240): A Positron Emission Tomography (PET) Imaging Agent for Quantification of Neurofibrillary Tangles (NFTs). *Journal of medicinal chemistry*, 59(10):4778–89.

Walker, K. M., Hall, S. E., Klein, R. M., and Phillips, D. P. (2006). Development of perceptual correlates of reading performance. *Brain Research*, 1124(1):126–141.

Wallin, A., Sjögren, M., Blennow, K., and Davidsson, P. (2003). Decreased cerebrospinal fluid acetylcholinesterase in patients with subcortical ischemic vascular dementia. *Dementia and geriatric cognitive disorders*, 16(4):200–7.

Warren, J. D., Jennings, A. R., and Griffiths, T. D. (2005). Analysis of the spectral envelope of sounds by the human brain. *NeuroImage*, 24(4):1052–7.

Warren, J. D. and Rohrer, J. D. (2009). Ravel's last illness: a unifying hypothesis. *Brain*, 132(6):e114–e114.

Warren, J. D., Uppenkamp, S., Patterson, R. D., and Griffiths, T. D. (2003). Analyzing pitch chroma and pitch height in the human brain. *Annals of the New York Academy of Sciences*, 999:212–4.

Warrington, E. K. (1975). The selective impairment of semantic memory. *The Quarterly journal of experimental psychology*, 27(4):635–57.

Weingarten, M. D., Lockwood, A. H., Hwo, S. Y., and Kirschner, M. W. (1975). A protein factor essential for microtubule assembly. *Proceedings of the National Academy of Sciences of the United States of America*, 72(5):1858–62.

Wevers, A. (2011). Localisation of pre- and postsynaptic cholinergic markers in the human brain. *Behavioural Brain Research*, 221(2):341–355.

Whitehouse, P. J., Hedreen, J. C., White, C. L., and Price, D. L. (1983). Basal forebrain neurons in the dementia of Parkinson disease. *Annals of neurology*, 13(3):243–8.

Whitwell, J. L., Duffy, J. R., Machulda, M. M., Clark, H. M., Strand, E. A., Senjem, M. L., Gunter, J. L., Spychalla, A. J., Petersen, R. C., Jack, C. R., and Josephs, K. A. (2017a). Tracking the development of agrammatic aphasia: A tensor-based morphometry study. *Cortex*, 90:138–148.

Whitwell, J. L., Duffy, J. R., Strand, E. A., Xia, R., Mandrekar, J., Machulda, M. M., Senjem, M. L., Lowe, V. J., Jack Jr., C. R., and Josephs, K. A. (2013). Distinct regional anatomic and functional correlates of neurodegenerative apraxia of speech and aphasia: An MRI and FDG-PET study. *Brain and Language*, 125(3):245–252.

Whitwell, J. L., Lowe, V. J., Tosakulwong, N., Weigand, S. D., Senjem, M. L., Schwarz, C. G., Spychalla, A. J., Petersen, R. C., Jack, C. R., and Josephs, K. A. (2017b). [¹⁸ F]AV-1451 tau positron emission tomography in progressive supranuclear palsy. *Movement Disorders*, 32(1):124–133.

Whitwell, J. L., Sampson, E. L., Watt, H. C., Harvey, R. J., Rossor, M. N., and Fox, N. C. (2005). A volumetric magnetic resonance imaging study of the amygdala in frontotemporal lobar degeneration and Alzheimer's disease. *Dementia and geriatric cognitive disorders*, 20(4):238–44.

Wilson, S. M., Dronkers, N. F., Ogar, J. M., Jang, J., Growdon, M. E., Agosta, F., Henry, M. L., Miller, B. L., and Gorno-Tempini, M. L. (2010). Neural correlates of syntactic processing in the nonfluent variant of primary progressive aphasia. *The Journal of neuroscience : the official journal of the Society for Neuroscience*, 30(50):16845–16854.

Win, K. T., Pluta, J., Yushkevich, P., Irwin, D. J., McMillan, C. T., Rascovsky, K., Wolk, D., and Grossman, M. (2017). Neural Correlates of Verbal Episodic Memory and Lexical Retrieval in Logopenic Variant Primary Progressive Aphasia. *Frontiers in Neuroscience*, 11:330.

Wingfield, A. and Grossman, M. (2006). Language and the Aging Brain: Patterns of Neural Compensation Revealed by Functional Brain Imaging. *Journal of Neurophysiology*, 96(6):2830–2839.

Witton, C., Talcott, J. B., Hansen, P. C., Richardson, A. J., Griffiths, T. D., Rees, A., Stein, J. F., and Green, G. G. (1998). Sensitivity to dynamic auditory and visual stimuli predicts nonword reading ability in both dyslexic and normal readers. *Current biology : CB*, 8(14):791–7.

Wood, P. L., Etienne, P., Lal, S., Nair, N. P., Finlayson, M. H., Gauthier, S., Palo, J., Haltia, M., Paetau, A., and Bird, E. D. (1983). A post-mortem comparison of the cortical cholinergic system in Alzheimer's disease and Pick's disease. *Journal of the neurological sciences*, 62(1-3):211–7.

Woolf, N. J., Jacobs, R. W., and Butcher, L. L. (1989). The pontomesencephalotegmental cholinergic system does not degenerate in Alzheimer's disease. *Neuroscience letters*, 96(3):277–82.

Xia, C., Makaretz, S. J., Caso, C., McGinnis, S., Gomperts, S. N., Sepulcre, J., Gomez-Isla, T., Hyman, B. T., Schultz, A., Vasdev, N., Johnson, K. A., and Dickerson, B. C. (2017). Association of In Vivo [¹⁸ F]AV-1451 Tau PET Imaging Results With Cortical Atrophy and Symptoms in Typical and Atypical Alzheimer Disease. *JAMA Neurology*, 74(4):427.

Yoon, S. Y., Kim, J.-K., An, Y.-S., and Kim, Y. W. (2015). Effect of Donepezil on Wernicke Aphasia After Bilateral Middle Cerebral Artery Infarction: Subtraction Analysis of Brain F-18 Fluorodeoxyglucose Positron Emission Tomographic Images. *Clinical neuropharmacology*, 38(4):147–50.

Zaborszky, L., Csordas, A., Mosca, K., Kim, J., Gielow, M. R., Vadasz, C., and Nadasdy, Z. (2015). Neurons in the basal forebrain project to the cortex in a complex topographic organization that reflects corticocortical connectivity patterns: an experimental study based on retrograde tracing and 3D reconstruction. *Cerebral cortex (New York, N.Y. : 1991)*, 25(1):118–37.

Zaborszky, L., Hoemke, L., Mohlberg, H., Schleicher, A., Amunts, K., and Zilles, K. (2008). Stereotaxic probabilistic maps of the magnocellular cell groups in human basal forebrain. *NeuroImage*, 42(3):1127–41.

Zaccarella, E. and Friederici, A. D. (2015). Merge in the Human Brain: A Sub-Region Based Functional Investigation in the Left Pars Opercularis. *Frontiers in psychology*, 6:1818.

Zhang, T., Mullane, P. C., Periz, G., and Wang, J. (2011). TDP-43 neurotoxicity and protein aggregation modulated by heat shock factor and insulin/IGF-1 signaling. *Human Molecular Genetics*, 20(10):1952–1965.

Curriculum vitae

Personal Details

Jolien Schaeverbeke
Nationality: Belgian
Date of birth: 07/03/1990
Place of birth: Sint-Niklaas

Research and Education

2013-2017
PhD in Biomedical Sciences
KU Leuven, Belgium
Title of the Thesis: *Primary Progressive Aphasia: a language disorder studied at the behavioral, structural and molecular imaging level.*
Laboratory for Cognitive Neurology
Promotor: *Prof. dr. Rik Vandenberghe*

2011 - 2013
Master in Biomedical Sciences-Neurosciences
University of Antwerp, Belgium
Title of the Thesis: *'Quantification of cerebral $GABA_A$ receptor density in the Fragile X mouse model by means of in situ [^{3}H]-flumazenil autoradiography'*
Laboratory of cognitive genetics (Centre of medical genetics)
Promotors:
Prof. dr. Frank Kooy and Prof. dr. Stefanie Dedeurwaerdere

2008 - 2011
Bachelor in Biomedical Sciences
University of Antwerp, Belgium
Title of the Thesis: *'Vessel reaction after implantation of a drug-eluting stent'*
Laboratory of Cardiovascular diseases
Promoter: *Prof. dr. Vicky Hoymans*

2006 - 2008
Classical Studies-Sciences
Heilige Familie, Sint-Niklaas, Belgium

2004 - 2006
Classical Studies
Heilige Familie, Sint-Niklaas, Belgium

2002 - 2004
Classical Studies
Sint-Joris instituut, Bazel, Belgium

Awards and Recognitions

2017
Postdoctoral mandate funding, Interne Fondsen KU Leuven, Belgium (PDM, target start date: 01/01/2018).
Poster prize award, Medical Radioisotopes Conference, Mechelen, Belgium
Alzheimer's Association International Conference Travel Fellowship, London, UK

2015
Alzheimer's Association International Conference Travel Fellowship, Washington D.C., USA

2008
Winner of Knack Interscholenstrijd, Belgium

2007
Winner of Knack Interscholenstrijd, Belgium

Publications

7.4 Publications in international peer-reviewed journals

**asterisk indicates shared first authorship*

1. Gille,G*, **Schaeverbeke,J***, Adamczuk,K, Vanderstichele,G, Chassaing,E, Bruffaerts,R, Neyens,V, Stoops,E, Tournoy,J, Vandenberghe,R, Poesen,K. Synaptic Markers in Cerebrospinal fluid Correlate with Gray Matter Volume Loss in the Precuneus of Cognitively Intact Older Adults, *submitted for publication.*

2. Vanderschaeghe,G, **Schaeverbeke,J**, Bruffaerts,R, Vandenberghe,R, Dierickx,K. Amnestic MCI patients' experiences after disclosure of their amyloid PET result in a research context, *under revision in Alzheimer's Research and Therapy.*

3. Vanderschaeghe,G, **Schaeverbeke,J**, Vandenberghe,R, Dierickx,K (2017). Amnestic MCI Patients' Perspectives on Volunteer Participation in a Research Context, Journal of Clinical Research and Bioethics 8(3).

4. Vandenberghe,R and **Schaeverbeke,J** (2017). Knowing your enemy: From *post mortem* scene reconstruction to real-time monitoring of the spread of tau and amyloid, Brain 140(5), 1179-1182.

5. Vanderschaeghe,G, **Schaeverbeke,J**, Vandenberghe,R, Dierickx,K (2017). Amnestic MCI patients' perspectives toward disclosure of amyloid PET results in a research context, Neuroethics 10(2), 281-297.

6. **Schaeverbeke,J**, Evenepoel,C, Bruffaerts,R, Van Laere,K, Bormans,G, Dries,E, Tousseyn,T, Nelissen,N, Peeters,R, Vandenbulcke,M, Dupont,P, Vandenberghe,R (2017). Cholinergic depletion and basal forebrain volume in primary progressive aphasia, NeuroImage Clinical 13, 271-279.

7. Grube,M*, Bruffaerts,R*, **Schaeverbeke,J***, Neyens,V, De Weer,AS, Seghers,A, Bergmans,B, Dries,E, Griffiths,TD, Vandenberghe,R (2016). Core auditory processing deficits in primary progressive, Brain 139(6), 1817-1829.

8. Adamczuk,K, **Schaeverbeke,J**, Nelissen,N, Neyens,V, Vandenbulcke,M, Goffin,K, Lilja,J, Hilven,K, Dupont,P, Van,L.K, Vandenberghe,R (2016). Amyloid imaging in cognitively normal older adults: comparison between [^{18}F]-flutemetamol and [^{11}C]-Pittsburgh compound B. European Journal of Nuclear Medicine and Molecular Imaging 43(1), 142-151.

9. Gillebert,CR *, **Schaeverbeke,J***, Bastin,C, Neyens,V, Bruffaerts,R, De Weer,AS, Seghers,A, Sunaert,S, Van,LK, Versijpt,J, Vandenbulcke,M, Salmon,E, Todd,JT, Orban,GA, Vandenberghe,R. (2015). 3D Shape Perception in Posterior Cortical Atrophy: A Visual Neuroscience Perspective. Journal of Neuroscience 35(37), 12673-12692.

10. Adamczuk,K, **Schaeverbeke,J**, Vanderstichele,HM, Lilja,J, Nelissen,N, Van Laere,K, Dupont,P, Hilven,K, Poesen,K, Vandenberghe,R (2015). Diagnostic value of cerebrospinal fluid Aβ ratios in preclinical Alzheimer's disease. Alzheimer's Research and Therapy 7(1), 75.

7.5 Published conference abstracts

1. **Schaeverbeke,J**, Adamczuk,K, Goffin,K, Bruffaerts,R, Tournoy,J, Peeters,R, Van Laere,K, Vandenberghe,R. Visual reading of amyloid-PET in MCI challenged: should we consider alternative methods ? Alzheimer's association international conference, July 16-20, 2017. London, UK. Poster presentation

2. Gille,B, **Schaeverbeke,J**, Vanderstichele,H, Adamczuk,K, Demeyer,L, Francois,C, Herbst,V, Brix,B, Tournoy,J, Vandenberghe,R, Poesen,K. Synaptic markers in liquor inversely correlate with gray matter volume in cognitively healthy individuals. Alzheimer's association international conference, July 16-20, 2017. London, UK.

3. **Schaeverbeke,J**, Bruffaerts,R, Evenepoel,C, Gabel,S, Meersmans,K, Van Bouwel,K, Dries,E, Peeters,R, Van Laere,K, Vandenberghe,R. *In vivo* visualization of [^{18}F]-THK5351 binding in primary progressive aphasia. Alzheimer's association international conference, July 16-20, 2017. London, UK. Poster presentation

4. Vanderschaeghe,G, **Schaeverbeke,J**, Bruffaerts,R, Vandenberghe,R, Dierickx,K. Amnestic MCI patients' experiences after disclosure of their amyloid PET result in a research context, Alzheimer's association international conference, July 16-20, 2017. London, UK.

5. **Schaeverbeke,J**, Adamczuk,K, Goffin,K, Bruffaerts,R, Tournoy,J, Peeters,R, Van Laere,K, Vandenberghe,R. Visual reading of amyloid-PET in MCI challenged: should we consider alternative methods ? Medical Radioisotopes conference, May 11, 2017. Mechelen, Belgium. Poster presentation

6. **Schaeverbeke,J**, Gillebert,CR, Sunaert,S, Todd,JT, Orban,GA, Vandenberghe,R. 3D-shape perception deficits in diffuse Lewy body dementia and relation to gray matter volume loss, Alzheimer's and Parkinson's diseases Congress, March 29-April 2, 2017. Vienna, Austria. Poster presentation

7. Vanderschaeghe,G, Vandenberghe,R, **Schaeverbeke,J**, Dierickx,K. Involvement of Patients with Mild Cognitive Impairment on their Clinical Trial Participation: A Qualitative Empirical Study. Alzheimer's and Parkinson's diseases Congress, March 29-April 2, 2017. Vienna, Austria.

8. Van Keer,K, Abegão Pinto,L, Barbosa Breda,J, Evenepoel,C, **Schaeverbeke,J**, Stalmans,I, Vandenberghe,R, Vandewalle,E. Optical Coherence Tomograpy in Cerebral Amyloidosis. Alzheimer's and Parkinson's diseases Congress, March 29-April 2, 2017. Vienna, Austria.

9. **Schaeverbeke,J**, Gillebert,CR, Sunaert,S, Todd,JT, Van Laere,K, Orban,GA, Vandenberghe,R. Depth perception in the clinical spectrum of Alzheimer's disease. Joint meeting of the Belgian Neurological Society and Belgian Dementia Council (BeDeCo). December 10, 2016. Antwerp, Belgium. Poster presentation

10. Bruffaerts,R, **Schaeverbeke,J**, Grube,M, Neyens,V, Bergmans,B, Dries,E, Griffiths,T, Vandenberghe,R. Rhythm processing deficits in the non-fluent variant of primary progressive aphasia. Joint meeting of the Belgian Neurological Society and Belgian Dementia Council (BeDeCo). December 10, 2016. Antwerp, Belgium.

11. Van Keer,K, Evenepoel,C, **Schaeverbeke,J**, Abegão Pinto,L, Stalmans,I, Vandenberghe,R, Vandewalle,E. Optical Coherence Tomograpy in Cerebral Amyloidosis. Congress of the Academia Ophthalmologica Belgica, November 23-25, 2016. Brussels, Belgium.

12. **Schaeverbeke,J**, Bruffaerts,R, Grube,M, Neyens,V, Dries,E, Griffiths,T, Vandenberghe,R. Rhythm processing deficits in nonfluent variant primary progressive aphasia relate to atrophy of the supplementary motor area. Society for Neuroscience, November 12-16, 2016. San Diego, USA. Poster presentation

13. Bruffaerts,R, **Schaeverbeke,J**, Grube,M, Neyens,V, Bergmans,B, Dries,E, Griffiths,T, Vandenberghe,R. Rhythm processing deficits

in the non-fluent variant of primary progressive aphasia. Society for the neurobiology of language, August 17-20, 2016. London, UK.

14. **Schaeverbeke,J**, Bruffaerts,R, Grube,M, Neyens,V, Bergmans,B, Dries,E, Griffiths,T, Vandenberghe,R. Deficits in Rhythm Processing in PPA are linked to Supplementary Motor Area atrophy. International conference on frontotemporal dementias, August 31-September 2, 2016. Munich, Germany. Blitztalk and poster presentation

15. **Schaeverbeke,J**, Gillebert,CR, Sunaert,S, Todd,JT, Van Laere,K, Orban,GA, Vandenberghe,R. 3D-shape perception in amnestic MCI. Alzheimer's association international conference, July 24-28, 2016. Toronto, Canada. Poster presentation

16. Evenepoel,C, **Schaeverbeke,J**, Adamczuka,K, De Weera,A-S, Nelissen,N, Dupont,P, Van Laere,K, Vandenberghe,R. The effect of gray matter volume and amyloid load on normal cognitive performance in cognitively intact older adults. Alzheimer's association international conference, July 24-28, 2016. Toronto, Canada.

17. **Schaeverbeke,J**, Gillebert,CR, Sunaert,S, Todd,JT, Van Laere,K, Orban,GA, Vandenberghe,R. 3D-shape perception in the clinical spectrum of Alzheimer's disease. Alzheimer's association international conference, Atypical Alzheimer's Disease PIA Day Session, July 23, 2016. Toronto, Canada. Oral presentation

18. **Schaeverbeke,J**, Dupont,P, Evenepoel,C, Vandenbulcke,M, Grothe,M, Teipel,S, Bormans,G, Van Laere,K, Vandenberghe,R. In vivo characterization of basal forebrain atrophy and cholinergic denervation in primary progressive aphasia. Alzheimer's association international conference, July 18-23, 2015. Washington D.C., USA. Oral presentation

19. Adamczuk,K, **Schaeverbeke,J**, Bruffaerts,R, Nelissen,N, Neyens,V, Dupont,P, Goffin,K, Vandenbulcke,M, Van Laere,K, Poesen K, Vandenberghe,R. Comparison of three amyloid biomarkers for preclinical Alzheimer's disease. International conference on

Alzheimer's and Parkinson's diseases, March 18-22, 2015. Nice, France.

20. Adamczuk,K, **Schaeverbeke,J**, Bruffaerts,R, Nelissen,N, Neyens,V, Dupont,P, Goffin,K, Vandenbulcke,M, Van Laere,K, Poesen K, Vandenberghe,R. Amyloid biomarkers in cognitively normal older adults: comparison of [^{18}F]-flutemetamol to [^{11}C]-PIB and CSF Aβ42. Human Amyloid Imaging, January 14-16, 2016. Miami, USA.

21. Adamczuk,K, **Schaeverbeke,J**, Bruffaerts,R, Nelissen,N, Neyens,V, Dupont,P, Goffin,K, Vandenbulcke,M, Van Laere,K, Poesen K, Vandenberghe,R. Definition of preclinical Alzheimer's disease with three amyloid biomarkers. Leuven research institute for Neuroscience and Disease Seminar, December 5, 2014. Mechelen, Belgium.

22. Adamczuk,K, **Schaeverbeke,J**, Bruffaerts,R, Nelissen,N, Neyens,V, Dupont,P, Goffin,K, Vandenbulcke,M, Van Laere,K, Poesen K, Vandenberghe,R. Amyloid PET imaging in cognitively normal older adults: Comparison of [^{18}F]-flutemetamol to [^{11}C]-PIB and CSF measurements of Aβ42. World federation of Neurology Research on Aphasia, Dementia and Cognitive Disorders, November 27-30, 2014. Hong-Kong, China.

23. **Schaeverbeke,J**, Adamczuk,K, Bruffaerts,R, Nelissen,N, Neyens,V, Dupont,P, Van Laere,K, Poesen,K, Vandenberghe,R. Comparison of [^{18}F]-flutemetamol uptake and CSF measurements in cognitively intact older individuals. Alzheimer's association international conference, July 12-17, 2014. Copenhagen, Denmark. Oral presentation

24. Adamczuk,K, **Schaeverbeke,J**, Nelissen,N, Neyens,V, Dupont,P, Goffin,K, Vandenbulcke,M, Van Laere,K, Vandenberghe,R. Comparison between semi-quantitative measures and reader concordance of amyloid load based on [^{18}F]-flutemetamol versus [^{11}C]-PIB in cognitively intact older adults. Alzheimer's association international conference, July 12-17, 2014. Copenhagen, Denmark.

Appendix A

Conflict of interest statement, Personal Contribution and Acknowledgments

A.1 Conflict of interest and Personal Contribution

There are no conflicts of interest relevant to the thesis manuscript. Financial support was provided by the Inter-University Attraction Pole P6/29 (RV) and P7/11 (RV), KU Leuven OT/12/097 (RV, PD) and Programme Financing PFV 10/008 (RV, PD), Fund for Scientific Research - Flanders (FWO) G.0660.09N (RV, PD), IWT 337404 Vlaamse Impulsfinanciering voor Netwerken voor Dementie-onderzoek (VIND) (RV), Geneeskundige Stichting Koninging Elisabeth, Flanders Innovation and Entrepreneurship grant VIND. RV is a senior clinical investigator of the FWO. RB is a postdoctoral researcher of the FWO, TG received funding from the Wellcome Trust WT091681MA and MG from the People Programme (Marie Curie Actions) of the European Union's Seventh Framework Programme (FP7/2007-2013) under REA grant agreement no. 600209. Funding was also received from the Stichting Alzheimer Onderzoek #15005 and the Flemish government (Vlaams Initiatief voor

Netwerken voor Dementie Onderzoek (VIND)).

Regarding the shared first author paper described in chapter 3 of this thesis: I was actively involved in data acquisition (MRI, neuropsychological, and psychoacoustic data) and data analysis (factor analysis calculations on the psychoacoustic test data, correlations with demographical and neuropsychological data, processing the MRI scans with VBM, modified t-test calculations). I also assisted in writing the manuscript.

A.2 Acknowledgments

This booklet contains four years of my life. These four years encompass the transformation from a curious student moving from my alma mater UAntwerpen to a researcher at KU Leuven, the pater (mater ?) familias of Belgian universities. First, I would like to mention my jury members, Prof. dr. Jason Warren, Prof. dr. Mathieu Vandenbulcke, Prof. dr. Wim Van Paesschen and Dr. Tim Van Langenhove for spending time to revise and improve my thesis. I am also especially thankful to my promotor, Prof. dr. Rik Vandenberghe, who gave me the opportunity to discover clinical research in all its aspects. During these four years, your broad intellectual knowledge fostered my passion for neuroscience immensely, though at the same time also faced me with my own limits. The weekly lab meetings during which we could profoundly discuss new findings were of invaluable importance to my development as a critical researcher. Off course it was not always serious business in our lab: there were the yearly Christmas parties, during which we discovered your great sense of humour and the dinners at conferences in which you shared your passion for jazz music. I am also very grateful for providing me with several occasions to present my work at international conferences during which I could exchange thoughts with kindred-spirits. I also would like to pronounce my gratitude to Prof. dr. Patrick Dupont. I admire your unique skills to translate difficult matter into comprehensible terms. The many clarifying discussions we had, made me observe things from different perspectives. Also as a person, your life philosophy inspired me to find a healthy balance between work and life.

Reflecting now on my PhD trajectory, one can observe an analogy between my personal, scientific development and the growth cycle of microbes when they are moved to a new environment. In both cases there are lag phases, periods in which there is little visible growth as the microbes adjust to their new surroundings, and growth phases once the microbes learn how to flourish. The seemingly unproductive lag phases, although sometimes discouraging, have been necessary preludes to the following growth phases. The first months of my PhD can be classified as a lag phase as I was adapting from an environment of laboratory animal science during my Masters to research in humans. The first day I even felt like a laboratory animal myself, which has been put in a Morris water/hospital maze, while struggling to find my way in its many corridors. Thank you Veerle and Gabriella for guiding me (literally) during the first days of my PhD and giving me a warm and friendly welcome in the lab. I also had the pleasure to collaborate with

Kate, who was by that time already a senior PhD student. We worked together on the recruitment and genotyping of healthy volunteers for enrollment into a longitudinal study on preclinical Alzheimer's disease. Kate patiently learned me how to screen volunteers with an enthusiastic though professional attitude. Thank you Prof. dr. An Goris, Klara, Kelly and Ide for sharing some lab space with us and assisting with genotyping of more than 500 blood samples in the never-ending search for that one particularly rare genotype. The initial lag-phase soon turned into a growth phase once I was able to independently analyze imaging data acquired in these healthy volunteers thanks to Kate's elaborative, educative evening sessions on SPM software. The hard work resulted in my first oral presentation at the Alzheimer's Association International conference in Kopenhagen. Thank you Kate for being a major source of inspiration to me. Also, thank you Dorien for introducing me to the basic principles of neuropsychology and teach me how to perform memory tests during my first months.

I am also grateful to Veerle, Celine and Rose, to introduce me to the many different psychophysical studies performed in patients with heterogeneous underlying neurodegenerative causes. My collaboration with Veerle, Celine, Prof. dr. Guy Orban and Prof. dr. James Todd on visual neuroscience could be situated between lag and growth phase. As my own research encountered some delay in the approval status, they fostered me in a totally new field of visual neuroscience. I am very grateful for this fruitful collaboration and the honor I received to be a shared first-author on the resulting publication. I was impressed by the neat and efficient programming skills of Celine, which assisted me in developing my own scripts for future studies. Celine, thank you for sharing these skills with me.

Thanks to a side-project during my PhD on biomarker-based research in patients with mild cognitive impairment, I met Gwendolien and Eva. We discovered that we not only shared a passion for research but also had the same birth date. We joked that this would have been an inclusion criterion for Rik's studies. The three of us became experts in puzzling as many appointments as possible in one day to reduce the burden on patients. Our efforts resulted in several interesting findings also thanks to the great team work with my PhD copain Benjamin, and the CSF biomarker analyses performed in the lab of Prof. dr. Koen Poesen and Prof. dr. Jos Tournoy. I am also thankful to the neurologists who performed the lumbar punctures at the day clinic including Jan, Nicolas and many others. Thank you Gwendolien for sharing your reflective thoughts on ethical issues in science. It was always nice to discover new

perspectives of research: we learned that the opinion of patients can also be valuable to scientific study design and that there exist an unmet need in the research community on how to communicate research results in a transparent way to patients. Also thank you Prof. dr. Kris Dierickx for letting me be part of that experience.

Eva, regardless of your busy agenda, I could always count on you. I admire your endless motivation and commitment to research. You have not only wonderful skills to comfort patients during neuropsychological testing, but also had the gift to motivate me when I couldn't see the wood for the trees.

Thanks to the data acquisition by Nathalie and Mathieu and the subsequent analyses by Patrick and Charlotte, I was able to write my first paper on primary progressive aphasia. Also thank you Prof. dr. Stefan Teipel and Michel Grothe for sharing your elegantly developed basal forebrain mask. Thank you Charlotte for sharing your skills with me as a great scientist. We both got the luck to work with the newest tau PET ligands thanks to the pioneering work of Lieven, Sofie, Prof. dr. Guy Bormans and colleagues. Lieven, your thesis established the building blocks for my clinical work with tau PET ligands, thank you for that. I really enjoyed the discussions we had regarding tau tracer binding with Rik, Prof. dr. Dietmar Thal, Guy and Sofie.

I also learned how to process blood samples with the help of Carine. I never met somebody with such quick and efficient pipetting skills as Carine. With the increasing number of clinical trials, Carine could not always assist and I had to become a trained negotiator to find a nurse on the consultation to draw blood for our studies. Therefore, my sincere gratitude goes to Lydia, who was always so nice to help me out regardless of her busy schedule. Thank you Katleen, Nikita, An, Petra, and Magda for helping me as well. I would also like to mention Prof. dr. Isabelle Cleynen and Sare for their professional help with blood sample collection, processing and storage. I hope this will ultimately provide you with some interesting results as well.

During my PhD, I spent countless hours at Nuclear Medicine, which could almost be considered as my second habitat in the hospital. I learned that PET tracers can be seemingly stubborn: sometimes they failed to be synthesized, or in case they had been successfully produced the number of counts might have been too low so that Kwinten, the patient and me had to run from PET/CT to PET/MR to eventually realize we could not acquire a PET scan anymore. Though, I do not blame the PET tracer for his bad behavior, as the PET scanner could also behave pretty

nasty: it might well be that the PET scanner simply decided to take a 'day-off'. Without Kwinten's and Jef's flexibility and dedication, I would not have been able to have scanned so many patients and volunteers in a relatively short time period. The latter aspect deserves also a big thank you to Dr. Anne Sieben, Dr. Yolande Pijnenburg, Dr. Bruno Bergmans, Rik and Rose for the referral of patients.

Prof. dr. Koen Van Laere, your advise on the countless abstracts I've sent and on the new tau PET tracers was always very valuable to me. Thank you for performing a wide variety of visual reads as well. Prof. dr. Karolien Goffin, also thank you for providing your trained eye in the many visual readings sessions. Thanks to Prof. dr. Johan Nuyts and his talented PhD students Matthew and Tao, we were able to apply motion correction during some tau PET scan acquisitions. We had a lot of fun during the wizard-like set-up of the equipment itself.

Thank you Prof. dr. Michel Koole and Nathalie Mertens for fixing problems during data acquisition or storage on the PET/MR scanner. Ron, thank you for being always stand-by to set-up new MRI acquisition parameters and to creatively solve ASL processing problems. For the latter, I also thank Tom for his time spent during ASL explanations. And for the challenges encountered at MR8, I thank Ingrid, Guido, Stefan and Kris for their support.

While I definitely encountered some stressful moments, I started to appreciate during the course of my PhD that science is 'simply' a continuous process of trail and error. Eventually, by believing in yourself and keeping calm, you will always find a solution to a particular problem. If I mention the word 'problem', I should bring tribute to Latex and Matlab to mention these in the same sentence. Thank you Veerle, Gabriella, Yu, and Eshwar for sharing your creative problem solving skills. Now that we are all finishing our PhD, I started to realize I will definitely miss these moments. Good luck in your future career and hopefully we will see each other again.

Not only my PhD trajectory but also the lab underwent several lag and growth phases. Yu, we became not only colleagues but also gym buddies and together we discovered Leuven's cultural scene through several classical music concerts and performances. I would also like to thank 'the monkey lab' and Ruben, Steven and Lise for showing me the other spectrum of Leuvens cultural scene.

I had the honor to meet several talented researchers over the years: Daniella, Kim, Tatiana, Charlotte and 'the neighbors': Laura, Jan,

Francois-Laurent, Daphne, Flavio and Mansoureh. The different backgrounds intermingled to solve problems with VBM, Caret or simply made us think out of the box. I should also thank 'the monkey lab' for exchanging thoughts across disciplines with a nice cup of coffee, which was never strong enough according to Gabriella and Marcello. In the last year, the entire lab underwent a flourishing growth phase with the arrival of Karen, Tarik, Silvy and Qian. Thanks to these 'fresh' scientists, our lab became a place in which we could discuss science but also share our thoughts on other things in life during cozy lunch sessions. Eshwar, I would like to thank you for introducing me to Indian culture and the richness of Indian cuisine. Regardless of the fact that Veerle and I once burned our lips, I am very glad you told us that yoghurt ameliorates the hotness. Qian, I was pleasantly surprised by the different dimensions authentic Chinese tea can have. Thank you for giving me the opportunity to discover that. Thank you Eva, Karen, Karen Van Bouwel and Silvy for assisting me with testing our PPA patients. Not only me, but also the PPA patients appreciated the empathy and enthusiasm you've put into the acquisition of language tests. Also a big thank you to all patients who participated in my studies. I cherish many good memories of these encounters. Thanks to the positive attitude of my patients, I also had a lot of fun while actually being at work.

Regarding the language tests, I would like to thank the efforts Prof. dr. Eric Manders and the friendly staff of the UA library made in providing me with WEZT and DIAS test material. Thank you Maaike, Astrid and Eline for acquiring audiograms. Manon and Prof. dr. Tim Griffiths, I am glad we intensively collaborated and still are in close contact. Thanks to your elegantly developed auditory processing test battery, we were able to reveal auditory deficits in our patients which would otherwise be unnoticed. Manon, I am happy I could finally meet you at Society for Neuroscience in San Diego. It was nice to talk in real life instead of through Skype. Thank you for sharing your insights with me.

Prof. dr. Stefanie Dedeurwaerdere was the first to make me realize I had to start a PhD. I met Joery in her lab, and we encountered again during several AAIC meetings and the international FTD conference in Munich. Your work on FTD with Prof. dr. Sebastiaan Engelborghs and Dr. Anne Sieben made me reflect about my own work in PPA. Thank you for the nice German dinners without Sauerkraut at the FTD conference.

Regarding the booking arrangements for conferences and all the administrative tasks I had to do, I would like to thank Olivia, Elisa, Marissa, Frieda, Stefanie and Cindy for walking me through these.

Joke and Charlotte Sleurs, I had the pleasure to meet you during my PhD. I don't know if this has to do with the fact that you are both working with diffusion tensor imaging, but there was immediately a connection between us. Thank you for the ice cream moments and many reflective conversations on SPM and many more. Charlotte, I will never forget the 'perfect abs session' we did together at the gym, for which the laughing bursts did more for our abs than the session per se. I think we should just stick with 'working out' hard in the lab.

Magda, we first encountered during yoga sessions at KU Leuven and later coincidently bumped into each other again at the stroke unit of UZ Leuven. Thanks to you, I met Laura and Pedro during climbing at Sportoase and Alex and Liliana. Laura, thank you for introducing me to your funny lab members who made my lunch moments very entertaining. The hiking or running moments in the woods provided me with new inspiration, a strategy that apparently has been applied by many 'great' minds to stimulate inspiration. Igor, I am glad to have met you as part of the KU Leuven buddy program and for letting me discover the mysterious world of statistics. For this I also would like to thank Bart, in particular for reflecting on the statistics used in my first paper in front of more than 500 students.

Nina, Katja, Cateau, Brecht, Caroline, Jesse, Femke, Anne-Lore, Nils, Stephan, Stephanie, Arno, Jonas, Lina, Rida, thank you for supporting me with friendship, wisdom, and joy. Karel, Lara, Thomas, Peter-Jan and Els, thank you for providing me with enough opportunities to watch geek series together or discover the student life in Leuven.

Onder het motto 'de laatsten zullen de besten zijn', zou ik ook graag een woord van dank aan mijn familie willen laten.
Mama en papa, jullie hebben me altijd vrij gelaten en gesteund in de keuzes die ik maakte. Jullie geloofden rotsvast in mij ook op momenten dat ik soms aan mezelf twijfelde. Dankzij de open geest die jullie, maar ook moeke, peter, oma, opa en mijn nonkels en tantes me meegaven, ben ik opgegroeid tot een leergierig en nieuwsgierig persoon. Wie weet hebben het lezen van de eerste Zonnekindjes me wel beinvloed in mijn latere keuze als wetenschapper. 'Discipline is de sleutel tot succes', dat had tante Rein me een keer doorgemaild. Die discipline heb ik zeker en vast nodig gehad tijdens mijn doctoraat. Dankje peter om me dit al van kinds af aan mee te geven bij het werken in de moestuin. Ik ben blij dat je nog fier mocht vernemen dat ik een doctoraat mocht starten in Leuven. En dankje moeke om al je verstand aan je kinderen en kleinkinderen te geven, zoals je al eens grapt. Mijn drie broers, Robbe, Korneel en Zeger,

zijn ondertussen ook voorbeeldige studenten geworden. Bedankt om me met welbepaalde software uit de nood te helpen en geregeld wat kennis van onder de ivoren toren bij te brengen zoals jullie vreemde jongerentaal bijvoorbeeld. 'Cringe' zou ik zeggen.

Valentijn, mijn grootste fan, ik ben bijzonder gelukkig je ontmoet te mogen hebben. Jij hebt me altijd onvoorwaardelijk gesteund met liefde maar ook veel geduld getoond op momenten dat ik het erg druk had. Bedankt om mijn rots in de branding te zijn. Toen mijn laptopscherm de geest gaf tijdens de laatste maanden van mijn thesis, waren jij, je papa en Marta de redders in nood dankzij het externe scherm dat jullie me bezorgden. Ook bedankt aan je oma's, je zus en je mama om me te steunen met lieve woorden.

Now that I finished this PhD, this definitely does not mean the growth phase has stopped. I decided to broaden my horizon and I will from January onwards investigate pathology under the microscope. Thank you Melissa, Dietmar and Rik for providing me with this new opportunity.

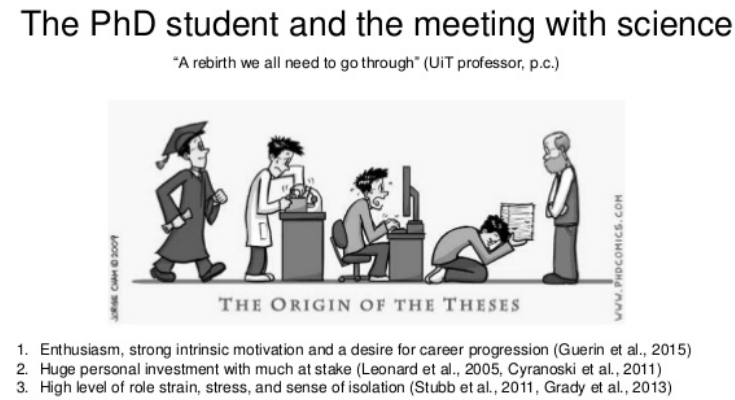


Figure A.1: The trajectory of this PhD. With thanks to Johan Maertens.

FACULTY OF MEDICINE
DEPARTMENT OF NEUROSCIENCES
LABORATORY FOR COGNITIVE NEUROLOGY
Herestraat 49, ON-2, box 1027
3000 Leuven, Belgium
jolien.schaeverbeke@kuleuven.be
http://med.kuleuven.be/lcn/